

NOTE TO USERS

This reproduction is the best copy available.

UMI[®]



uOttawa

L'Université canadienne
Canada's university

**FACULTÉ DES ÉTUDES SUPÉRIEURES
ET POSTDOCTORALES**



**FACULTY OF GRADUATE AND
POSTDOCTORAL STUDIES**

Margaret Neuspiel

AUTEUR DE LA THÈSE / AUTHOR OF THESIS

Ph.D. (Biochemistry)

GRADE / DEGREE

Department of Biochemistry

FACULTÉ, ÉCOLE, DÉPARTEMENT / FACULTY, SCHOOL, DEPARTMENT

**Mitochondrial Dynamics, Mechanisms and Meaning:
Investigations into Fusion and Fission Proteins Mitofusin 2 and MAPL**

TITRE DE LA THÈSE / TITLE OF THESIS

Heidi McBride

DIRECTEUR (DIRECTRICE) DE LA THÈSE / THESIS SUPERVISOR

CO-DIRECTEUR (CO-DIRECTRICE) DE LA THÈSE / THESIS CO-SUPERVISOR

EXAMINATEURS (EXAMINATRICES) DE LA THÈSE / THESIS EXAMINERS

Angus McQuibban

Jonathan Lee

Mary-Ellen Harper

Johnny Hgsee

Gary W. Slater

Le Doyen de la Faculté des études supérieures et postdoctorales / Dean of the Faculty of Graduate and Postdoctoral Studies

**MITOCHONDRIAL DYNAMICS, MECHANISMS AND MEANING:
INVESTIGATIONS INTO FUSION AND FISSION PROTEINS MITOFUSIN
2 AND MAPL**

by

MARGARET NEUSPIEL

A thesis submitted to the Faculty of Graduate and Postdoctoral Studies in partial fulfillment
of the requirement for the degree of

DOCTOR OF PHILOSOPHY

Department of Biochemistry, Microbiology and Immunology

University of Ottawa

Ottawa, Ontario, Canada

© Margaret Neuspiel , May 2nd, 2008



Library and
Archives Canada

Published Heritage
Branch

395 Wellington Street
Ottawa ON K1A 0N4
Canada

Bibliothèque et
Archives Canada

Direction du
Patrimoine de l'édition

395, rue Wellington
Ottawa ON K1A 0N4
Canada

Your file *Votre référence*
ISBN: 978-0-494-48409-8
Our file *Notre référence*
ISBN: 978-0-494-48409-8

NOTICE:

The author has granted a non-exclusive license allowing Library and Archives Canada to reproduce, publish, archive, preserve, conserve, communicate to the public by telecommunication or on the Internet, loan, distribute and sell theses worldwide, for commercial or non-commercial purposes, in microform, paper, electronic and/or any other formats.

The author retains copyright ownership and moral rights in this thesis. Neither the thesis nor substantial extracts from it may be printed or otherwise reproduced without the author's permission.

AVIS:

L'auteur a accordé une licence non exclusive permettant à la Bibliothèque et Archives Canada de reproduire, publier, archiver, sauvegarder, conserver, transmettre au public par télécommunication ou par l'Internet, prêter, distribuer et vendre des thèses partout dans le monde, à des fins commerciales ou autres, sur support microforme, papier, électronique et/ou autres formats.

L'auteur conserve la propriété du droit d'auteur et des droits moraux qui protègent cette thèse. Ni la thèse ni des extraits substantiels de celle-ci ne doivent être imprimés ou autrement reproduits sans son autorisation.

In compliance with the Canadian Privacy Act some supporting forms may have been removed from this thesis.

Conformément à la loi canadienne sur la protection de la vie privée, quelques formulaires secondaires ont été enlevés de cette thèse.

While these forms may be included in the document page count, their removal does not represent any loss of content from the thesis.

Bien que ces formulaires aient inclus dans la pagination, il n'y aura aucun contenu manquant.


Canada

Acknowledgements

To begin I would like to thank my supervisor Dr. Heidi McBride who has been a wonderful mentor throughout my graduate student years. Upon entering her lab she quickly became my mentor and teacher. In addition to being a dedicated scientist, her enthusiasm for cell biology was contagious and I quickly became hooked on mitochondrial dynamics. I would also like to thank the members, both past and present of the McBride lab for making my graduate years truly enjoyable. Each member of the lab has provided me with a lot of encouragement, technical assistance and friendship. A special thanks to Emelie Braschi, Vincent Soubannier and Astrid Schauss, who are taking over my project. I sleep easy at night knowing it is in good hands. Furthermore, I would like to thank my family for all their support. Both my parents, Valerie and Sherman Nelson, have been instrumental in their encouragement, support and advice along the way. To my sisters, Sarah Chaires, and Carla Cernic thanks for your encouragement. A special thanks to my sister Olivia Nelson, co-founder of the special “TechyP” club. Next, I would like to thank my husband Victor Neuspiel for his unwavering support through all of the ups and downs this doctorate degree. I would also like to thank his passion for finance and investing, without this second love, our lifestyle today would not be possible. Finally, I thank him for our son Henrik, who has made our lives more complete than I could have ever imagined. There are many other past and present members of the Heart Institute that have been instrumental in keeping me motivated during this time, including everyone on the fourth floor. Among them, are my good friends Joanne McBane and Katey Rayner. Without their support and encouragement I would not have gone to as many seminars or had nearly as much fun. I would also like to sincerely

thank REMIX Coffee house, for their hospitality, providing me with a lot of good coffee and free wireless internet.

ABSTRACT

It has recently been established that mitochondria function as an interconnected reticulum that is maintained through dynamic fission and fusion events. The research performed throughout the course of this doctoral thesis has profound impacts on cell biology, impacting mitochondrial dynamics, programmed cell death, intracellular signaling, and peroxisome biology. Research into the protein mechanisms of mitochondrial fusion and fission is presented as two distinct research aims. The first objective of this thesis investigated the mechanisms and meaning of mitochondrial fusion; specifically the role of Mitofusin 2. It is presented as a manuscript which describes Mfn2 functioning as a signaling GTPase for mitochondrial fusion, rather than a mechanoenzyme, and that activated Mfn2 protects against both cytosolic and mitochondrial apoptosis as well as inhibits Bax activation. The second objective of this doctoral thesis was the investigation into the mechanisms and meaning of mitochondrial fission; specifically the role of a novel uncharacterized protein FLJ12875 (subsequently named MAPL). The identification of MAPL and a previously unrecognized pathway for mitochondrial vesiculation as a means to segregate selected cargo into distinct transport vesicles which traffic to the peroxisome is presented. MAPL is evolutionarily conserved from plants to bacteria and is an integral mitochondrial outer membrane protein. MAPL has two transmembrane domains and a carboxy-terminal RING domain. Additionally it has an uncharacterized highly conserved middle domain positioned between the two membranes, the BAM domain (Beside A Membrane) MAPL overexpression results in a stimulation of Drp1-dependent mitochondrial fragmentation. Unexpectedly, it was found that in cells where mitochondrial fission was blocked, a pool of small (70-100 nm) vesicles enriched for MAPL and or TOM20 was observed. Convincing data are presented

documenting that this pool of vesicles generates independently of the canonical mitochondrial fission pathway. This thesis describes the identification of a novel vesicular trafficking pathway for the cell. Both the signaling capabilities of Mfn2 and the identification of Mitochondrial Derived Vesicles (MDV's), provide a new platform for investigations of mitochondrial dynamics and opens up new avenues of research into mitochondrial mechanism and meaning.

TABLE OF CONTENTS **PAGE**

1.0 INTRODUCTION.....1

1.1 **RESEARCH OUTLINE.....2**

1.2 **MITOCHONDRIA HISTORY AND FUNCTION.....2**

1.2.1 Mitochondrial Biogenesis.....6

1.2.2 Protein Import.....9

1.2.3. Mitochondrial Turnover.....11

1.2.3.1 *Autophagy*..... 15

1.2.3.2 *Mitochondrial Proteases*.....19

1.3 **MITOCHONDRIAL DYNAMICS23**

1.3.1 Mitochondrial Movement and Calcium Signaling.....24

1.3.1.1 *Microtubule Movement*.....24

1.3.1.2 *Actin Movement*.....26

1.3.1.3 *Calcium Signaling*.....28

1.3.2 Mitochondrial Fusion.....29

1.3.2.1. *Fusion Proteins*.....31

1.3.3. Mitochondrial fission.....41

1.3.3.1 *Fission and SUMOylation*.....46

1.4 **MITOCHONDRIAL DYNAMICS AND CELLULAR FUNCTION.49**

1.4.1 Mitochondria and Apoptosis..... 49

1.4.2 Mitofusin 2 Signaling and Disease.....53

1.4.2.1 *Mfn2 and Metabolism*.....55

1.4.2.2 *Mfn2 and Cell cycle*58

1.5	RESEARCH OBJECTIVES	58
1.6	REFERENCES.....	60
2.0	MANUSCRIPT #1	
	Activated mitofusin 2 signals mitochondrial fusion, interferes with Bax activation, and reduces susceptibility to radical induced depolarization.	
2.1	CHAPTER INTRODUCTION.....	84
2.2	ABSTRACT.....	85
2.3	INTRODUCTION.....	86
2.4	RESULTS.....	89
2.5	DISCUSSION.....	100
2.6	EXPERIMENTAL PROCEDURES.....	103
2.7	ACKNOWLEDGEMENTS.....	111
2.8	REFERENCES.....	112
3.0	MANUSCRIPT #2	
	Cargo-selected transport from the mitochondria to peroxisomes is mediated by vesicular carriers.	
3.1	MANUSCRIPT INTRODUCTION.....	118
3.2	ABSTRACT.....	121
3.3	RESULTS.....	122
3.4	DISCUSSION.....	128
3.5	MATERIALS AND METHODS.....	129
3.6	ACKNOWLEDGEMENTS.....	137
3.7	REFERENCES.....	138
4.0	DISCUSSIONS.....	140

4.1	MITOFUSIN 2 AND MITOCHONDRIAL FUSION.....	..140
4.1.1	Mfn2 and Signaling.....	..141
4.1.2	Apoptosis.....	..144
4.1.2.1	<i>Mfn2 and Apoptotic Pore formation...</i>	..146
4.1.2.2	<i>Mfn2 and Bax/Bak.....</i>147
4.2	MITOCHONDRIAL DERIVED VESICLES.....	...151
4.2.1	MAPL Evolution.....	...152
4.2.2	Function of the RING Domain.....	..153
4.2.3	MAPL and Mitochondrial Fission.....	.155
4.3	MAPL AND TOM20 VESICLES157
4.3.1	MAPL Delivery to the Peroxisome.....	...158
4.3.2	Fate of TOM20 Vesicles.....	..162
4.4	CONCLUSIONS.....	...164
4.5	REFERENCES.....	..167
5.0	CURRICULUM VITAE.....	170

A. APPENDIX #1

Mitofusin 2 Protects Cerebellar Granule Neurons against Injury Induced Cell Death

B. APPENDIX #2

Mitochondria: more than just a powerhouse

C. APPENDIX #3

Dissociating the dual roles of apoptosis-inducing factor in maintaining mitochondrial structure and apoptosis

LIST OF ABBREVIATIONS:

$\Delta\Psi$,	Mitochondrial membrane potential
Cyt c,	Cytochrome c
DRP1,	Dynamin related protein 1
Fzo1p,	Fuzzy Onion 1 protein
STS,	Staurosporin
Mant-GDP,	2'-(or-3')- <i>O</i> -(<i>N</i> - methylanthraniloyl)guanosine 5'-diphosphate
mtDNA,	Mitochondrial DNA
Mfn1	Mitofusin 1
Mfn2,	Mitofusin 2
TMRE,	Tetramethylrhodamine ester
IMS,	Intermembrane space
OM,	Outer membrane
ATP,	Adenosine triphosphate,
PPAR γ ,	Peroxisome-proliferator-activated receptor-gamma
PGC1,	Peroxisome-proliferator-activated receptor coactivator-1
UCP1,	Uncoupling protein 1
TOM,	Translocases of the outer membrane
TIM,	Translocases of the inner membrane
SAM,	Sorting and assembly machinery
HSP,	Heat shock protein
Lon,	Lon peptidase 1
Mdm30,	Morphology and distribution mutant 30

ER,	Endoplasmic reticulum
OPA1,	Optic Atrophy Type 1
Atg,	Autophagy-related genes
Uth1,	SUN family gene product
ABC protein,	ATP-binding cassette adenosine triphosphatases
MMP,	Mitochondrial processing peptidase
MIP,	Mitochondrial intermediate peptidase
IMP,	Inner membrane protease
Smac,	Second mitochondria-derived activator of caspases
DIABLO,	Diablo homolog (Drosophila)
AIF	Apoptosis inducing factor
Pcp1,	Protease of the inner membrane
Mgm1,	Mitochondrial genome maintenance protein 1
HSP,	Hereditary spastic paraplegia
MCL1,	Myeloid cell leukemia sequence 1
OIP106,	TRAK1 trafficking protein, kinesin binding
GRIF-1,	TRAK2 trafficking protein, kinesin binding 2
GTP,	Guanosine triphosphate
RNA,	Ribonucleic acid
mRNA,	Messenger RNA
ROS,	Reactive oxygen species
PDH,	Pyruvate dehydrogenase
PDK,	PDH kinases
Akt,	Protein kinase B

PI(3)Kinase,	Phosphatidylinositol (3) kinase
AMPK,	AMP-activated protein kinase
AMP,	Adenosine monophosphate
p53,	Tumor protein 53
CoVa,	Cytochrome oxidase subunit Va
Bcl-XL,	BCL2-like 1
Bcl-2,	B-cell lymphoma 2
GAPs,	GTPase-activating proteins
Bax,	BCL2-associated X protein
Bak,	BCL2-antagonist/killer 1
NRF1,	Nuclear respiratory factor
PIPs,	Phosphatidylinositol phosphates
Ypt11p,	Rab-type small GTPase
Myo2p,	Myosin V actin motor
Arp2/3,	Actin-Related Proteins 2 and 3
NGF,	Nerve growth factor 1
RhoA,	Ras homolog gene family member A
Miro1,	Mitochondrial Rho-1
TCA,	Trichloroacetic acid cycle
PINK1,	PTEN-Induced Kinase 1
LRRK2,	Leucine rich repeat kinase 2
MPTP,	Mitochondrial permeability transition pore
PTP,	Permeability transition pore
ANT,	Adenine nucleotide translocase

VDAC,	Voltage-dependent anion channel
rRNA,	Ribosomal RNA
tRNA,	Transfer RNA
OXPPOS,	Ooxidative phosphorylation
Tfam,	Transcription factor A
SNARE,	Soluble NEM Sensitive Adaptor Receptor
MitoPLD,	Mitochondrial PLD
PLD,	Phospholipase D
SUMO,	Small ubiquitin-related modifier
RING,	Really interesting new gene
PIAS,	Protein inhibitors of activated sTAT
CMT2A,	Charcot-Marie-Tooth type 2A
MERRF,	Myoclonic epilepsy associated with ragged-red fibers
ERK,	Extracellular signal-regulated kinases
MAPL,	Mitochondrial anchored protein ligase
BAM,	Beside a membrane

LIST OF FIGURES

- Figure 1.1 *Research objectives*
- Figure 1.2 *Mitochondrial membrane structures*
- Figure 1.3 *Overview of mitochondrial biogenesis*
- Figure 1.4 *Overview of mitochondrial import*
- Figure 1.5 *Mitochondrial turnover*
- Figure 1.6 *Mitochondrial dynamics*
- Figure 1.7 *Mitochondrial fusion steps*
- Figure 1.8 *Mitochondrial fusion proteins*
- Figure 1.9 *Mitochondrial fission proteins*
- Figure 1.10 *Mitochondrial fission and SUMOylation*
- Figure 1.11 *Mitochondrial Drp1 and Apoptosis*
- Figure 2.1 *PEG fusion assay*
- Figure 2.2 *Creation of a hydrolysis-deficient mutant of Mfn2*
- Figure 2.3 *Mitochondrial morphology and distribution of Mfn2 mutants*
- Figure 2.4 *Mfn2RasG12V stimulates mitochondrial fusion in PEG cell fusion assays*
- Figure 2.5 *Ultra-structural analysis reveals that clustered mitochondria are interconnected by novel Mfn2-containing membrane elements*
- Figure 2.6 *Activation of Mfn2 protects against STS-induced cell death.*
- Figure 2.7 *Activation of Mfn2 protects against permeability transition*
- Figure 3.1 *Bioinformatics screen*
- Figure 3.2 *Characterization of MAPL, a novel mitochondrial outer membrane protein.*

- Figure 3.3 *MAPL induces mitochondrial fragmentation and marks unique mitochondrial structures.*
- Figure 3.4 *Evidence of cargo selection within mitochondrial vesicles.*
- Figure 3.5 *Mitochondrial morphology in MAPL silenced cells*
- Figure 3.6 *Quantification of cargo selectivity and DRP1-independent vesicle formation*
- Figure 3.7 *MAPL vesicles target the peroxisomes*
- Figure 3.8 *Saturated exposures reveal low levels of MAPL within a larger sub-population of peroxisomes*
- Figure 4.1 *Mfn2 and internal signaling*
- Figure 4.2 *Mfn2 signaling and apoptosis*
- Figure 4.3 *MAPL phylogenic tree*
- Figure 4.4 *MAPL BAM domain conservation*
- Figure 4.5 *Tom20 vesicle fates*

LIST OF TABLES

Table 1.1	<i>List of proteins involved in mitochondrial motility</i>
Table 2.1	<i>Quantification of MitoFluor Red 589 uptake into mitochondria of transfected cells</i>
Table 2.2	<i>Quantification of hET oxidation within transfected cells</i>
Table 3.1	<i>Quantification of vesicle marker co-localization</i>

LIST OF VIDEOS

- Video 2.1 *PEG fusion assay shows immotile Mfn2RasG12V:CFP expressing mitochondrial cluster that signals the docking and fusion of pOCT:GFP expressing acceptor mitochondria.*
- Video 3.1 *Confocal video analysis of MAPL-CFP-positive vesicle formation in COS7 cells.*
- Video 3.2 *Confocal video analysis of mitochondrial fission.*
- Video3.3 *Confocal video analysis of a MAPL-YFP-positive vesicle fusing with a CFP-SKL-containing peroxisome*

CHAPTER 1
INTRODUCTION

1.1 RESEARCH OUTLINE

This doctoral thesis provides new molecular details for the mechanisms of both mitochondrial fission and mitochondrial fusion, as well as, the identification of a novel cell biology phenomenon. It is presented as a series of published manuscripts.

The introduction is divided into three sections, each of which is important for understanding the origins of mitochondrial fission and fusion. The first section provides some historical perspective and some molecular details regarding well known mitochondrial functions, such as, biogenesis, metabolism, and protein import. The second part of the introduction, and the focus of this doctoral thesis, originates from the unexpected observation in 1998 that the mitochondria undergo fusion events and are highly dynamic. In this section, what is known about mitochondrial dynamics; the molecular machinery, the mechanism of both fission and fusion, and some unexplained observations, are presented. The specific aim of this work is to address some of the outstanding questions of mitochondrial fusion and of mitochondrial fission (Figure 1.1) revolving around the fusion protein Mfn2, and the fission protein Drp1. The third section of the introduction focuses on the integration of mitochondrial dynamics into intracellular signaling, cellular function, and disease progression. Through this, the emerging concept of the fission and fusion proteins, and of mitochondrial dynamics as central regulators of intracellular homeostasis and cellular function, will hopefully be conveyed.

1.2 MITOCHONDRIA HISTORY AND FUNCTION

The mitochondria are an essential mammalian organelle of ancestral origin, originally derived from endosymbiotic prokaryotes roughly 1-3 billion years ago (1-3) They are generally known for their role as the energy producer in the cell, whose function is essential

Figure 1.1

Research objectives

The specific aim of this research was to address some of the outstanding questions of mitochondrial fusion and of mitochondrial fission, specifically the mechanistic actions of both, the fusion GTPase Mitofusin 2 (Mfn2), and the fission GTPase Dynamin1 (Drp1). The first specific aims of this thesis were to characterize the Mfn2 GTPase cycle and to determine the effect of nucleotide state of this protein, on mitochondrial fusion. The second aims of this thesis were to identify proteins which regulate the SUMOylation of Drp1 and to determine the effect of these proteins on mitochondrial fission.

**Research Objective #1
FUSION**

**Research Objective #2
FISSION**

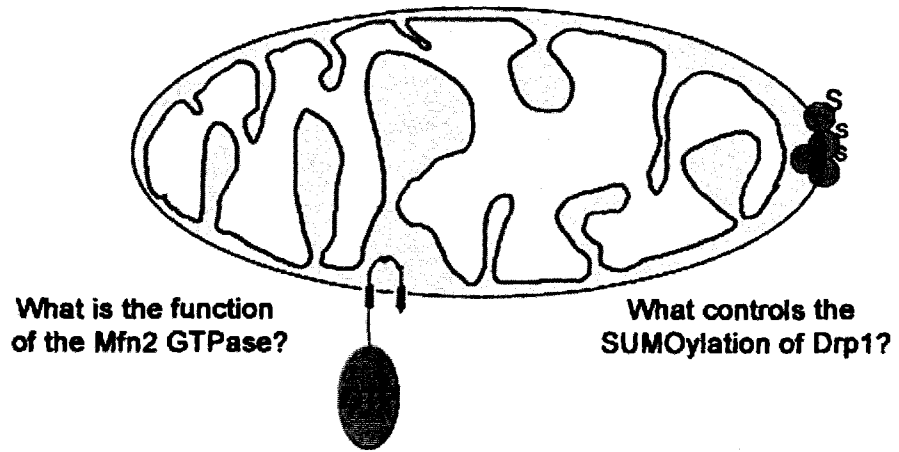


Figure 1.1

Research objectives

to sustain cellular life (4). The total mitochondria within a human individual synthesizes approximately 50 kg of ATP from ADP by oxidative phosphorylation daily (5). The mitochondria contain the enzymatic molecular machinery that governs metabolic processes such as, the trichloroacetic acid (TCA) cycle, fatty-acid oxidation, Fe-S biogenesis, and heme synthesis in which lipids, carbohydrates, and proteins are converted to ATP to sustain cellular life (6-7).

Mitochondrial number ranges from a single organelle in retina cells to hundreds of organelles in hepatocytes. Over the past decade, genetic screens in yeast have been instrumental in uncovering a diverse list of new proteins which function at the mitochondria to control their overall shape, size, movement and energy output (8-10). It has also only been in the past decade that researchers have become aware of the dynamic nature of this ancient organelle and, that they are capable of rapid change in response to a variety of different biological stimuli. For example; during differentiation of embryonic stem cells into cardiomyocytes, the mitochondrial network elongates into tubules (11), during synapse formation in hippocampal neurons the mitochondrial network undergoes increased division in order to recruit mitochondria into the neural protrusions for both increased mitochondrial number and increased mitochondrial activity(12), and in response to apoptotic triggers the mitochondria fragment their network to facilitate crista remodeling and cytochrome c release(13-15).

The mitochondria are unique, within the cell, in that they are surrounded by a double membrane system consisting of the outer mitochondrial membrane and the inner boundary membrane(4). This membrane system creates 2 highly distinct microenvironments; the intermembrane space between the 2 membranes, and the matrix in the middle of the

organelle (Figure 1.2). High levels of cardiolipin are found in the inner membrane which clearly distinguishes this bilayer from all others.

The intermembrane space can be further divided into two separated regions; the intermembrane boundary space and the crista. The intermembrane boundary space is the narrow stretch of space between the outer and inner membranes including protein mediated contact sites. Invaginations of the inner boundary membrane result in the formation of crista folds where much of the ATP synthesis takes place. The crista form relatively long tubules as well as, folds which emanate into the matrix (16) (Figure 1.2). There is less protein content in the crista than in the matrix. The crista sequesters many proteins such as, cytochrome c (essential for respiration) which once released from the mitochondria into the cytosol becomes pro-apoptotic (17-18). Detailed biochemical fractionation and cytological studies have demonstrated that the crista is a separate mitochondrial inner membrane compartment that connects to the IMS through small, relatively uniform tubular crista (16, 19). This compartment is also dynamically regulated, in that the size and shape of crista can differ within the same cell, ranging from short to long and from flat and lamellar to tubular (19).

The electron transport protein complexes of oxidative phosphorylation are embedded within the inner membrane (Figure 1.2). This is a protein rich membrane and contains the abundant respiratory complexes, as well as, a large number of gated channel-forming proteins, including some 49 different metabolite transporter proteins (20-21). Briefly, pyruvate generated from carbohydrates during glycolysis and fatty acids produced from triglycerides are transported into the mitochondrial matrix and converted to acetyl CoA, this then drives the citric acid cycle in which NADH and FADH, substrates for oxidative phosphorylation are generated. NADH and FADH generate electrons which are transported

Figure 1.2

Mitochondrial membrane structures

Mitochondrial architecture and membrane structure. The mitochondria consist of two membranes; the outer membrane and the inner membrane. The outer membrane houses many of the mitochondrial import proteins, apoptotic proteins as well as some of the fission and fusion proteins. This unique membrane system creates 2 highly distinct microenvironments; the intermembrane space between the 2 membranes, and the matrix in the middle of the organelle. The intermembrane space can be further divided into two separated regions; the intermembrane boundary space and the crista. The intermembrane boundary space is the narrow stretch of space between the outer and inner membranes including protein mediated contact sites. Invaginations of the inner boundary membrane result in the formation of crista folds where much of the ATP synthesis takes place. The matrix of the organelle contains the mtDNA nucleoids and is the site of mtDNA transcription/translation.

Mitochondrial Structure

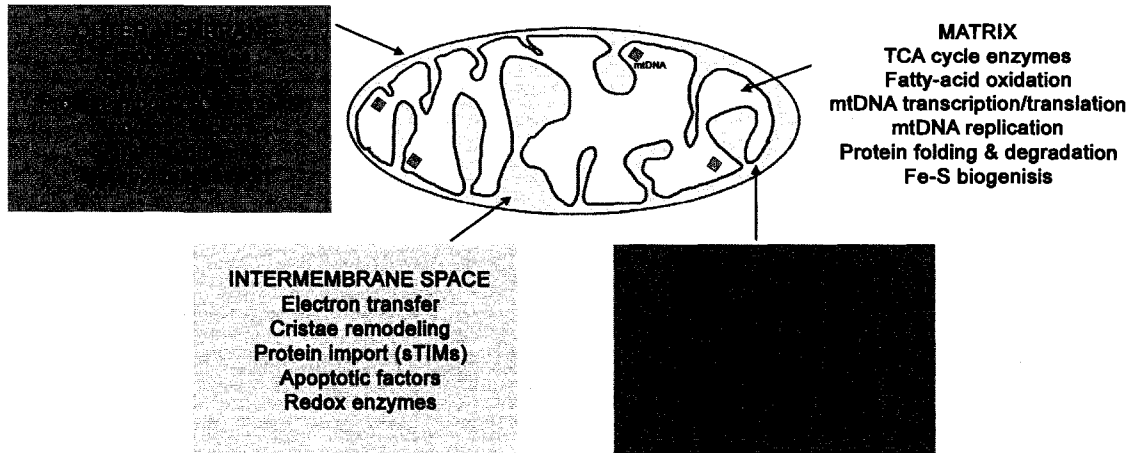


Figure 1.2

Mitochondrial membrane structures

through the electron transport chain (22). This results in the generation of protons which are then pumped from the matrix across the mitochondrial inner membrane through respiratory complexes: I, III, and IV (22). This action establishes a proton gradient between the matrix and the inner membrane which is used to drive the F_1F_0 ATPase, generating ATP and a resting membrane potential ($\Delta\psi$) (7, 23).

The matrix houses the mitochondrial nucleoids, which contain the mitochondrial DNA (mtDNA) (Figure 1.2). The maintenance of mtDNA is essential for mitochondrial respiration, biogenesis and cell viability. Two distinct genetic systems encode mitochondrial proteins: mtDNA and nuclear DNA and are thought to be of separate evolutionary origin. mtDNA is a small 16.6 kb circle of double stranded DNA derived from the circular genomes of ancient bacteria. The human mitochondrial DNA contains 16,569 base pairs (24), which encode 37 genes: 13 respiratory chain polypeptides of the respiratory complexes I, III, IV, and V (only complex II is solely composed of proteins encoded by nuclear genes), 22 for transfer RNA (tRNA) and one for each of the small and large subunits of ribosomal RNA (rRNA) (23, 25). The remainder of mitochondrial proteins are encoded by nuclear DNA and are transported to the mitochondria and function either on the cytosolic face of the outer membrane, as integral outer membrane proteins, in the inner membrane space as integral proteins of the inner membrane, or finally residing in the matrix.

The mitochondria also contain the so called “mitochondrial permeability transition pore” (MPTP), a non-selective protein channel which forms at contact sites between the inner and outer membranes. This is the pore through which membrane potential is dissipated (permeability transition) as a result of a variety of stresses both apoptotic and non apoptotic. When $\Delta\psi$ is lost, protons and molecules are able to freely flow across the inner mitochondrial membrane resulting in decreased ATP synthesis, Ca^{2+} release and increased

ROS production and accumulation, all of which cause mitochondrial swelling, dysfunction and rupture (26). The exact structure of the MPTP is still controversial, however, it is generally considered that several proteins of both membranes come together to form the pore, including adenine nucleotide translocase (ANT), and the outer membrane voltage-dependent anion channel (VDAC) (27, 28). Furthermore, the Bcl-2 apoptotic proteins seem to regulate pore opening during apoptosis through unknown mechanisms (26).

1.2.1 MITOCHONDRIAL BIOGENESIS

Mitochondrial biogenesis can be loosely defined as the making and growth of new mitochondria. Current understanding of biogenesis is that it is under the control of a variety of transcriptional regulation pathways mostly responding to metabolic demand. The control of mitochondrial function depends on the regulated control of two cellular genomes. The expression of two distinct sets of genes must be coordinated during biogenesis, making nuclear to mitochondrial and mitochondrial to nuclear communication an essential element of cell survival. (Figure 1.3) The mitochondria respond to the changes within the cellular environment often through new biogenesis to control damage caused by mutations in mtDNA, potentially leading to oxidative phosphorylation (OXPHOS) subunits that cannot fold properly, compromising mitochondrial function (29, 30).

Mitochondrial to nuclear communication is thought to occur at two levels; the first involves nuclear signaling pathways which have been described over the past 20 years. In this transcription factor mediated method of mitochondrial biogenesis, the mitochondria undergo new import of mitochondrial proteins and recruitment mitochondrial associated proteins and lipids to facilitate new growth. Transcription factors or co-activators regulate

Figure 1.3

Overview of mitochondrial biogenesis

Mitochondrial biogenesis signals and/or mitochondrial dysfunction (hypoxia, increased ROS, mutation/deletions in mtDNA resulting in a loss of membrane potential and a loss of ATP synthesis) are communicated to the nucleus through signaling pathways resulting in the transcriptional up regulation of mitochondrial biogenesis genes. Protein synthesis and import into the mitochondria in addition to mtDNA transcription/translation results in new mitochondrial growth and increased mitochondrial mass.

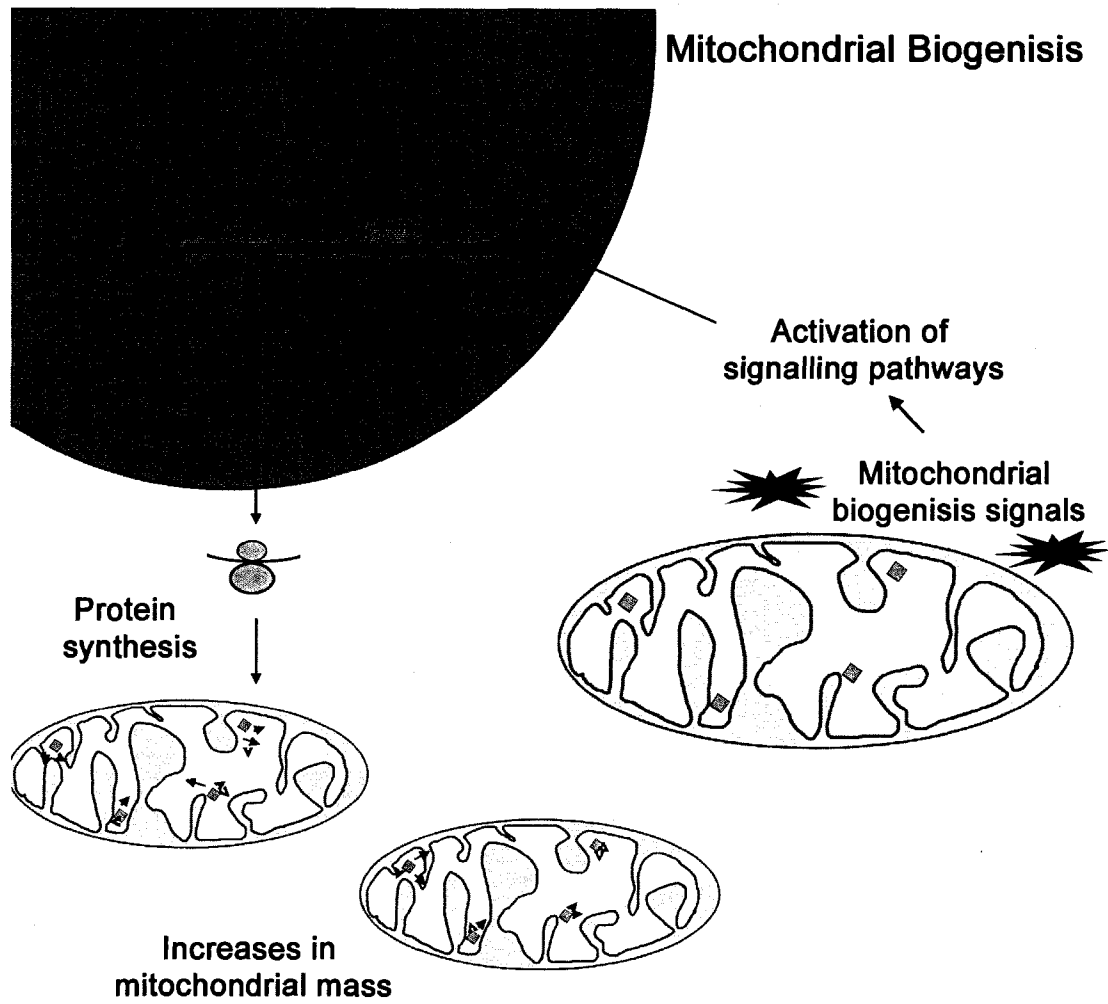


Figure 1.3

Overview of Mitochondrial biogenesis

both mitochondrial and nuclear gene expression in response to, for example changes in environmental temperatures (Figure 1.3) (31), external stimuli such as changes in caloric intake (32), exercise (33-34), or changes in the levels of certain hormones such as thyroxine (21, 35-36). The second type of mitochondrial- nuclear communication observed is the so called “retrograde regulation” which is the cellular responses associated with changes in the functional state of the mitochondria itself (4, 37). An example of this is the mitochondrial stress response, whereby, the mitochondria lose function in response to a loss of electrochemical potential (uncoupling), of OXPHOS protein damage (38) or through the accumulation of unfolded proteins in the organelle (39). (Figure 1.3) Recently, a genome-wide RNAi- screen, for genes that signal the mitochondrial unfolded protein response (UPRmt) in *C. elegans*, identified that *clpp-1*, a mitochondrial matrix protease homologous to bacterial ClpP, is involved in the UPRmt. This work also found that in animals with reduced activity of *clpp-1*, the UPRmt was attenuated suggesting that eukaryotes utilize component(s) from the protomitochondrial symbiont to signal the UPR(mt) (40). The ability of the mitochondria to respond to these stressors enables this ancient organelle to recover from stress and prevent damage of the entire network.

During biogenesis, several factors have been identified such as sequence-specific transcription factors, co-activators, and hormones which function upstream of transcriptional activators (21,41-42). For example, mitochondrial transcription factor A (Tfam), which stimulates the transcription of mtDNA into a polygenic transcript (43) and is processed into 14 tRNAs, 12 mRNAs, and two rRNAs, is itself activated by the transcription factor nuclear respiratory factor 1 (NRF1) (42). The regulation of protein expression for nuclear encoded mitochondrial proteins cannot be accounted for through the action of only these factors above. It is, therefore, now known that mitochondrial biogenesis involves the integration of

multiple transcriptional regulatory pathways which control the expression of both nuclear and mitochondrial genes in a tissue- and stimulus-specific ways (21). One of the most studied is that of the peroxisome-proliferator-activated receptor coactivator-1 (PGC-1). It has been considered to be the universal regulatory system for mitochondrial biogenesis in vertebrates. It was first discovered as an interacting partner of the nuclear receptor PPAR γ in brown adipose tissue (31).

PGC-1 α acts on mitochondrial biogenesis in two ways. Firstly, it regulates the transcriptional activation of many nuclear encoded mitochondrial proteins, including those required for protein import (44). PGC-1 α activates the family of PPAR nuclear receptor which are transcription regulators, where for example; PPAR α , stimulates mitochondrial fatty-acid oxidation and oxidative phosphorylation (45) and PPAR γ , induces expression of uncoupling protein 1 (UCP1), a mitochondrial transporter involved in thermogenesis in brown adipose tissue (31). Secondly, PGC-1 α regulates mitochondrial biogenesis as it is also a co-activator for non-nuclear receptor transcription factors for non-mitochondrial proteins involved in energy metabolism (46-48).

The complex regulatory control that PGC-1 α exerts over a family of coregulators and a large collection of target genes enables distinct and diverse patterns of the regulation of mitochondrial biogenesis in different tissues and during different stages of development. PGC-1 α itself is also differentially induced in specific tissues in response to environmental cues. For example; PGC-1 α is induced in response to cold exposure in brown adipose tissue(31). Furthermore, overexpression of PGC-1 α in tissue culture cells results in the activation of many genes involved in mitochondrial function, such as respiration, oxidative metabolism, and uptake and utilization of energy substrates (44).

1.2.2 PROTEIN IMPORT

In order for mitochondria to function, they require that these nuclear encoded mitochondrial proteins translated on ribosomes in the cytosol be delivered post translationally to the mitochondrial surface by cytosolic chaperones for import into the organelle. These proteins are synthesized as precursor proteins, which differ from the mature form of the protein in that they are in an unfolded conformation and associated with chaperones, which maintain them in a translocation-competent conformation (49). A complex system of protein import consisting of the transporter of outer membrane (TOM), and transporter of inner membrane, (TIM) machinery and processing (mitochondrial proteases) ensures the proper targeting of mitochondrial proteins (Figure 1.4). The sorting signals of nuclear encoded mitochondrial pre-proteins are removed by specific processing peptidases present within different subcompartments of mitochondria and the resulting proteins are often inserted into the lipid bilayers and or assembled with cofactors and other proteins to form macromolecular complexes (49). There are three types of sorting signals known for mitochondrial proteins; the presequences sorting signals, the internal targeting sequence, and the signal anchor sequence. The cleavable pre-sequence consists of about 10–80 hydrophobic amino acids with the potential to form amphipathic helices with one hydrophobic and one positively charged face (49-50). These positively charged extensions function as targeting signals for the import receptors and direct the preproteins across both outer and inner membranes (51-52).

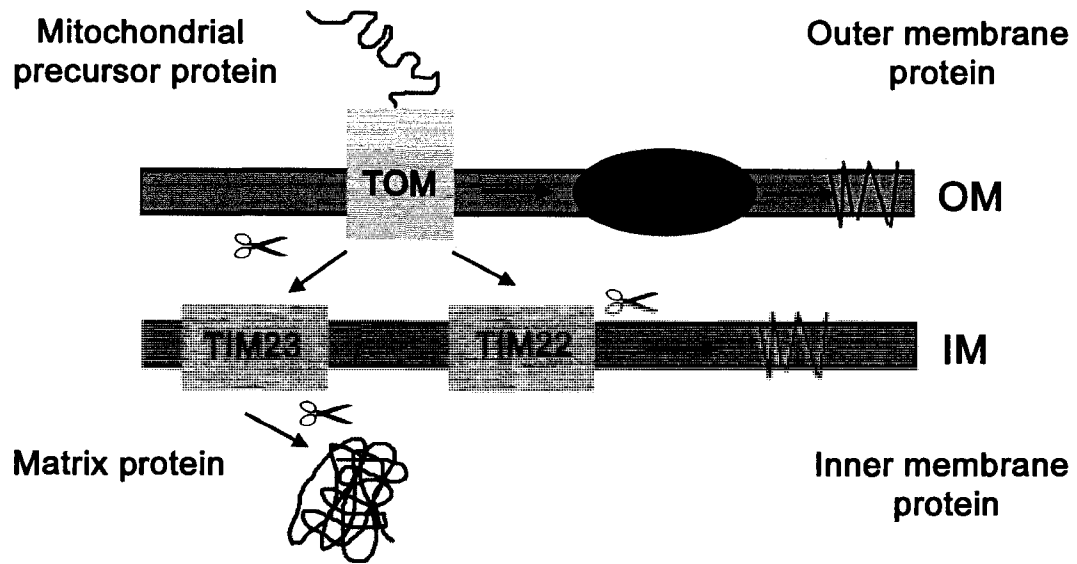
Internal targeting sequences are found in proteins that span the membrane several times. The precise nature of these signals remains unclear. These include all outer membrane proteins along with many intermembrane space and inner membrane proteins. These precursors are synthesized without cleavable extensions (52). They have the same primary

Figure 1.4

Overview of mitochondrial import

The precursor form of a mitochondrial protein, containing the targeting signal (red) enters the TOM (translocase of the outer membrane) complex for entry into the mitochondria. Once inside various compartments of the mitochondria, proteases of the intermembrane space and matrix remove the mitochondrial targeting sequences. The TOM complex consists of the receptor subunits Tom70, Tom22, and Tom20 and the membrane-embedded subunits Tom40, Tom7, Tom6, and Tom5. The pre-proteins destined for the matrix enter the TIM23 complex in the inner membrane for translocation across the inner membrane. The TIM23 complex consists of Tim 21, Tim50, Tim17, Tim44, Tim16, Tim14, Hsp70, and Mge1. The pre-proteins destined for the outer membrane utilize the SAM (Sorting and assembly) complex for membrane insertion. Pre-proteins are translocated across the outer membrane by the TOM complex and then bound by small Tim proteins in the intermembrane space and inserted and assembled in the membrane by the SAM complex. Pre-proteins destined for inner membrane insertion utilize the TIM22 inner membrane protein complex. Tim22 is aided by Tim54 and Tim18 for the delta-psi dependent, insert of proteins into the inner membrane.

Mitochondrial Protein Import



structure as the mature protein, but a conformation which is different from the mature protein. Finally, the signal anchor sequence targets proteins to the outer membrane and the transmembrane domain functions as the targeting sequence.

Protein translocase complexes exist in both the outer and inner membranes and function either to allow protein translocation through the membrane into a sub-mitochondrial compartments or function to integrate proteins with transmembrane domains into either the outer or inner membranes. (Figure 1.4) Translocases of the outer membrane are called TOM proteins and function to act as entry points for all cytosolically synthesized mitochondrial precursor proteins (21, 53). Typically, TOM receptors bind to precursor proteins or the molecular chaperones which deliver precursor proteins to the outer membrane (54) and these proteins transit through the Tom40 channel (55). The TOM channel is a cation specific high conductance channel with a pore size diameter of 21Å. Of the TOM receptor family, three have been characterized; TOM70: Binds to internal targeting peptides and acts as a docking point for cytosolic chaperones, TOM20: Binds presequences, TOM22: Binds both presequences and internal targeting peptides.

Outer membrane proteins, such as porin, which possess a more complicated topology with multiple β -barrel proteins require the action of the outer membrane sorting and assembly machinery (SAM complex described below). Precursors of these proteins, first are imported through the TOM complex to the intermembrane space side (56). Next the small Tim proteins of the intermembrane space (57-58) pass the precursor proteins to the SAM in the outer membrane for assembly into the membrane.

Precursor proteins which contain a typical amino-terminal mitochondrial targeting signal become engaged with the TIM23 receptor complex of the inner membrane (59). The presequence translocase23 (TIM23) is localized to the mitochondrial inner membrane and

acts as a pore forming protein which binds precursor proteins with its N-terminal (Figure 1.4) (60-61). TIM23 acts a translocator for preproteins destined for the mitochondrial matrix, the inner mitochondrial membrane as well as for the intermembrane space (61). Precursor proteins with an internal targeting signal (often more hydrophobic) instead utilize the TIM22 complex, which binds preproteins exclusively bound for the inner mitochondrial membrane (62-63). These proteins are chaperoned across the hydrophilic intermembrane space by the hexameric small Tim family (18). Additionally, TIM50 is bound to TIM23 at the inner mitochondrial side and found to bind presequences. TIM44 is bound on the matrix side and found binding to mtHsp70. Protein import into the matrix requires that proteins must be unfolded in order to transit through the protein translocase channels(58). Following import, the pre-sequence is proteolytically cleaved by the processing proteases. The matrix contains its own protein folding chaperones, such as, the evolutionarily conserved Hsp70 and Hsp60/10 (Chaperonin 60/10), (59, 64). Other molecular chaperones and proteases involved in protein maturation are also found in the matrix and inner membrane and include ClpP, Lon, Yme1, DnaJ, and Hsp78 (49). These proteins are often dual functional in that they are responsible for the folding of newly imported proteins, but they are also critical components in mitochondrial quality control (49). For example, levels of these proteins are increased following increased cellular temperatures(“heat-shock”) or other global mitochondrial stresses (49).

1.2.3 MITOCHONDRIAL TURNOVER

Mitochondria possess the ability to regulate their own biogenesis and their protein levels through gene transcription, as described above. Conversely, they also are capable of regulating their own mass and protein levels through regulated turnover and degradation of

both entire mitochondria and individual proteins (Figure 1.5). The ability to eliminate proteins which are synthesized in excess, proteins which are improperly assembled, and proteins with abnormal conformation is fundamental for the survival of the mitochondria. If internal protein damage accumulates, the metabolic outputs of individual mitochondria would become compromised. Additionally, the ability to eliminate whole damaged organelles is also fundamental for the health and survival of the organelle. If damage accumulates from external stress, such as nutrient deprivation or excess free radical accumulation, the functional outputs of the mitochondria would also be compromised. It is known that the turnover of damaged mitochondria and mitochondrial proteins can be removed by both the ubiquitin proteosomal and vacuolar/lysosomal (autophagic) degradation pathways, as well as, proteolytic activity of cytosolic and mitochondrial proteases, which together, provide regulated continuous turnover of damaged proteins and organelles.(Figure 1.5) (65-66). The balance between mitochondrial biogenesis and mitochondrial turnover governs the health, integrity and metabolic outputs of the network and is often reflective of the overall physiology of the cell.

There is evidence that ubiquitin mediated proteolysis of mitochondrial content is an important mechanism and pathway of removal of damaged mitochondria. It has been reported that in reticulocytes during maturation the proteolysis of the mitochondria is ubiquitin-dependent (67), and that, ubiquitin-dependent proteolysis is implicated in the recognition and selective elimination of paternal mitochondria and mitochondrial DNA (mtDNA) after fertilization in mammals (66, 68). These studies provided the first evidence for the role of the ubiquitin proteosomal degradation system in the control of mammalian mitochondrial inheritance (66, 68). Furthermore, it had already been shown that in alpha-

factor-arrested yeast cells the turnover of Fzo1 (yeast mitochondrial fusion protein, introduced below) was ubiquitin-and-proteasome dependent (69).

Mitochondrial protein turnover is complicated by the recent discovery of yet another uncharacterized pathway of selective protein removal (70) Surprisingly, during vegetative growth in yeast cells, it was found that Fzo1 degradation occurred along a novel proteolytic pathway not involving ubiquitylation, vacuolar hydrolases, or 26S proteasomes (Figure 1.5). These conflicting results were the first to demonstrate the existence of two distinct proteolytic pathways for the turnover of an individual mitochondrial outer membrane protein in yeast cells (69-71).

During a G1 arrest induced by alpha factor mating pheromone in yeast, Fzo1 protein levels were down regulated (69). Fzo1 was stabilized upon inhibition of the ubiquitin proteosomal pathway; however, the deletion of Mdm30 did not stabilize Fzo1 levels post alpha factor treatment. Mdm30 is a peripheral mitochondrial outer membrane F-box-containing protein. F-box containing proteins are present in subunits of some E3 ubiquitin ligases and are often required for the conjugation step between substrate and ubiquitin. Members of this family are often components of the SCF (Skp Cdc53/Cullin F-box) E3 ubiquitin ligase, and function to target proteins to the proteasome for ubiquitin mediated degradation (72). These results demonstrate proteosomal dependent turnover of Fzo1 during the G1 arrest of the cell cycle. During this arrest, the mitochondrial network, consistent with a loss of Fzo1, underwent fragmentation (69).

Conversely, during vegetative growth in yeast, Fzo1p stability is regulated by Mdm30. Surprisingly, the turnover of Fzo1p, by an unknown proteasome-independent pathway, requires Mdm30 (69). Interestingly, Mdm30p seems to be required for mitochondrial fusion. Yeast cells expressing Mdm30p with and F-box mutation have

Figure 1.5

Mitochondrial turnover

Mitochondria can be degraded through three known mechanisms; apoptosis, mitophagy and proteosomal turnover. Mitochondria, under conditions of starvation or sub-lethal damage, can undergo mitophagy to remove and recycle damaged mitochondria. If the damage is above an autophagic threshold, the mitochondria can be removed through regulated apoptosis. Mitochondrial fragments and mitochondrial proteins can be processed by the ubiquitin proteosomal degradation machinery. This pathway requires the action of mitochondrial proteases to degrade mitochondrial proteins. An unknown pathway not involving the proteasome and or the autophagic pathway has also been reported in yeast.

accumulated levels of Fzo1p as would be expected, however they also contain fragmented mitochondria (71). Excess levels of Fzo1p protein indicate that Mdm30p is required for the turnover of Fzo1p, however, the surprising result that, in the absence of a functional F-box, the mitochondria can not fuse suggests that Mdm30p is an integral component of the fission fusion pathway. Constitutive Fzo1p turnover in vegetative growing cells does not require known ubiquitin or proteasome machinery, suggesting that Mdm30p-mediated degradation can occur independently of the proteasome (70, 73). Inhibition of proteosomal processing through either, *pre1-1* cells (mutation in a proteolytic subunit of the 20S core particle) or *cim5-1* cells (mutation in an ATPase subunit of the 19S regulatory complex) or through deletion of Ump1 (proteosomal assembly factor), did not interfere with the turnover of Fzo1 (70).

The turnover of Fzo1p, through a proteosomal independent pathway, suggests that mitochondrial outer membrane proteins, or perhaps more specifically, fusion proteins are regulated through a pathway distinct from other mitochondrial proteins. Mitophagy was investigated, as this pathway is the only other known mechanism of mitochondrial protein degradation. In yeast cells, vacuolar degradation is responsible for the general removal of mitochondrial proteins following treatment with rapamycin (induces autophagic conditions) (74). Yeast *pep4* mutant cells lack active vacuolar peptidases and do not degrade proteins. Surprisingly, Fzo1 levels were not stabilized in these cells with defective vacuolar degradation.

As discussed above, the levels of Fzo1 and Mfn2 are critical for maintaining mitochondrial and cellular homeostasis. Studies investigating the regulated turnover of Fzo1 provide a good example of the complexities of the mitochondria. Very little is known about the mechanisms of selective mitochondrial protein turnover and of the stability of the

mitochondrial proteome. It is currently not understood how mitochondrial outer membrane proteins are processed for degradation, and the molecular details regarding the turnover of intermembrane space and matrix proteins are only beginning to be elucidated.

1.2.3.1 AUTOPHAGY

It was initially believed that the turnover of mitochondrial proteins was through non-selective lysosomal mediated autophagy of the whole organelle. These studies conducted in yeast, under conditions of starvations, were the first to demonstrate autophagy of the mitochondria (Figure 1.5) (75). Most mitochondrial proteins are stable for ~3.5 days in mammalian cells, however, some proteins such as g-aminolevulinase synthase are stable for only ~20-80 min (76-78). It is now believed that lysosomal autophagy of mitochondria therefore cannot explain the differences in turnover rates of various proteins (79).

Furthermore, the vacuolar/lysosomal pathway is estimated to account for, at most, 25-30% of mitochondrial catabolism (80). However, there have also been a number of reports of mitochondria within vesicles with multiple membrane boundaries (known as autophagic bodies and/or autophagosomes). Initial studies in rat hepatocytes (81), erythroid cells in mammals (82), and in yeast cells, provided examples to demonstrate that whole mitochondria are degraded through mitophagy.

Autophagy is a highly regulated process whose role is becoming more and more apparent in the maintenance of cellular and mitochondrial homeostasis. It has recently been found that autophagy has essential roles in differentiation and development and in response to stress (83). Autophagy is initiated during amino acid deprivation and has been associated with neurodegenerative diseases, cancer, and myopathies (84). Autophagy occurs when parts of the cytoplasm and intracellular organelles are sequestered within characteristic

double- or multi-membraned autophagic vacuoles (named autophagosomes) (Figure 1.5). These autophagosomes are delivered to the lysosome for degradation for the turnover and recycling of selected proteins and whole organelles. (85-86). The process of autophagy can specifically target separate organelles, such as the mitochondria in mitophagy and the endoplasmic reticulum (ER) in reticulophagy. It is generally accepted that these organelles are specifically targeted for elimination when either their numbers are in excess or they are damaged (87). Autophagy was first understood as a response to starvation, in that, it is a process by which cells adapt their metabolic signaling to initiate catabolism of macromolecules. Catabolism generates metabolic substrates as a stress response for the cell to provide substrates for protein synthesis. In addition to starvation, high levels of ROS which oxidize lipids, proteins and DNA pose a damaging threat to the integrity of the cell. There are various defense mechanisms to combat oxidative damage, such as up-regulation of antioxidants, removal of specific proteins by the ubiquitin–proteasome system (88), and removal of damaged proteins and organelles by autophagy (89).

There is also increasing evidence that mitophagy can occur as a response to elevated reactive oxygen species (83, 90). For example; in aged cells, autophagic pathways are compromised and under normal growth conditions, high levels of oxidized proteins can accumulate (89, 91-94). Oxidized proteins have also been found to accumulate in age related disorders such as Alzheimer’s disease (95), and diabetes mellitus (96), where there is also a decrease in autophagy.

Mitophagy occurs in response to various stimuli, both in yeast and in mammalian cells. Mitophagy was also observed in yeast cells which contained a temperature-sensitive mutant of the mitochondrial proton ATPase, under anaerobic conditions and at restrictive temperature (97). In this study, it was found that impairing the mitochondrial electrochemical

transmembrane potential resulted in the induction of mitophagy. Furthermore, they found that mitochondrial damage-induced autophagy resulted in the preferential degradation of impaired mitochondria before leading to cell death (97). It was these studies which first suggested that autophagy can function either as a process of mitochondrial quality control, or as whole cell response when cells reach a threshold of damaged mitochondria.

In mammals, mitophagy was reported in rat hepatocytes exposed to nutrient starvation or to photodamage (83). It has since been found that when autophagic survival mechanisms fail, death programs are activated in response to oxidative stress. It is now accepted that autophagy has a dual role leading to cell death when survival mechanisms are overwhelmed (87, 98, 99).

Autophagy is initiated under starvation conditions and the isolation membrane sequesters cellular material to be degraded into double membrane vesicles called autophagosomes. The isolation membranes are thought to be derived from the endoplasmic reticulum and the edges of the membranes fuse with each other to form a closed double-membrane structure. Finally, the outer membrane of the autophagosome fuses with a lysosome and its content is degraded by lysosomal hydrolases. Over the past few years genetic studies in yeast have been instrumental in uncovering some of the protein machinery involved in the regulation of this process. To date, 28 Autophagy-related genes (Atg) have been identified and most of them have a function during this survival process. (100-102). Subsequent biochemical studies in mammalian systems have provided some molecular definition to these processes however very little mechanistic details are known. For example scientists still are not clear as to where the lipid for the isolation membrane comes from. Some have suggested an involvement of the mitochondria in providing the phospholipids source for this membrane, however, these studies are not conclusive. Interestingly, one of the

Atg proteins, Atg9 is an integral mitochondrial outer membrane protein, which cycles between the mitochondria and the pre-autophagosomal structure (103). Atg9 is required for isolation membrane formation and it is hypothesized by this group that it functions as a lipid carrier protein for autophagic vesicle formation (104).

It is proposed, that whole de-energised and damaged mitochondria are somehow recognized, captured and digested by the vacuole / lysosome for autophagy (105). However, very little is known as to the roles of the Atg proteins in recognizing damaged mitochondria, or of the mitochondrial signals which mark them for mitophagy. Interestingly, a newly identified protein in yeast of the mitochondrial outer membrane Uth1p was found to be essential for the progression of mitophagy (74). When Uth1p null yeast cells were treated with rapamycin and/or nutrient deprivation, mitophagy was suppressed by ~ 50%, whereas, autophagy of cytoplasmic proteins occurred normally. This finding is very intriguing, in that, it suggests alternate protein mechanism or additional pathways for autophagic turnover of mitochondrial content (74). The mammalian orthologue of this protein is unknown.

An open question in mitochondrial biology is that of turnover, more specifically, how mitochondria are specifically selected for autophagy? It has been suggested that under certain circumstances in mammalian cells, loss of membrane potential plays a role for mitophagy initiation (106). It has also been proposed that mitochondria with mutated DNA are less prone to be degraded by mitophagy than healthy mitochondria. Studies in cardiac myocytes led to the observation that the majority of autophagocytosed mitochondria were small and relatively free from the hallmark features of oxidative damage. It was hypothesized that mitochondria with mutated mtDNA generate less ROS, and therefore, are exposed to less damaging free radicals over time (107). It has also been suggested that large mitochondria do not undergo mitophagy as readily as small mitochondria due to their size,

and, as such, accumulate more damage over time (108). Subsequently, the enlarged mitochondria have fewer chances of undergoing mitophagy which further promotes oxidative damage. This cycle of growth and damage results in populations of mitochondria which cannot be selectively degraded whose function compromises that of the whole cell (108). Since mitochondrial homeostasis is such an important component of cellular survival, it is not surprising that the organelle would develop alternative mechanisms to regulate its turnover. Recently, it has been reported that, during lens and erythroid differentiation, mitochondrial degradation is independent of autophagy. In *Atg5*^{-/-} mice in the lens and erythroid cells autophagy is inhibited, however, the mitochondria still underwent degradation, suggesting an alternative pathway for turnover. However, this result could also indicate that alternative *Atg5* pathways exist within these cells for mitophagy (109). In order to understand the functional significance of the mitochondrial involvement during autophagy, and alternative pathways of mitochondrial turnover, further investigations of the protein mechanisms of selected turnover must be performed.

1.2.3.2 MITOCHONDRIAL PROTEASES

The mitochondria contain a number of proteases which exert essential housekeeping functions and control critical steps during mitochondrial biogenesis (110) and are responsible for the selective degradation of a number of mitochondrial proteins. Mitochondrial proteases can be assigned to three functional classes (1) processing peptidases, which cleave off mitochondrial targeting sequences of nuclearly encoded proteins and process mitochondrial proteins with regulatory functions (2). ATP-dependent proteases, which either act as processing peptidases with regulatory functions or as quality-control enzymes degrading

non-native polypeptides to peptides and (3) oligopeptidases, which degrade these peptides and mitochondrial targeting sequences to amino acids (110).

The ATP-dependent proteases and mitochondrial oligopeptidases degrade proteins and polypeptides into peptides, and subsequently into amino acids, to ensure the quality control of mitochondrial proteins in different sub compartments (80, 111). Peptides derived from mitochondrial proteins in both mammalian cells and in yeast cells have been documented to be released from the mitochondria into the cytoplasm (112-113). Currently, two pathways for 6-20 amino acid peptide export in yeast have been identified (113). The mitochondrial ABC protein (ATP-binding cassette adenosine triphosphatases) Mdl1, is an intracellular peptide transporter localized in the inner membrane of yeast mitochondria. It functions to export peptides ranging from 600-2100 daltons generated from proteolysis by the m-AAA protease complex across the inner membrane from the matrix to the intermembrane space. Peptides generated through i-AAA protease complex activity were also exported from the mitochondria; however Mdl1 activity was not required, suggesting two pathways of peptide export. This study demonstrated that mitochondrial intermembrane space and matrix peptides can be exported to the cytoplasm. This study, however, only examined the export of peptides generated from AAA protease activity, it did not examine the export of peptides generated from other mitochondrial proteases. In a recent elegant study (111), the proteolysis of newly synthesized and pre-existing mitochondrial proteins, as well as characterized peptides exported from the mitochondria, was analyzed by mass spectrometry. This work resulted in the identification of 270 peptides that are exported in an ATP- and temperature-dependent manner. The peptides originate from 51 mitochondrial and nuclear encoded proteins, which are localized mainly in the matrix and inner membrane (111). This study provided many important findings, perhaps the most significant result is

that only one peptide released corresponded to an outer membrane protein. Of the released peptides, 40% corresponded to inner membrane proteins, 46% to proteins of the matrix space, and 10% as not determined. Proteins of the outer membrane and intermembrane space represented 2%, respectively (111). These results are indicative of alternative mechanisms for outer membrane protein export and turnover. Currently, very little is known regarding the turnover of integral outer membrane proteins.

The processing peptidases efficiently remove the sorting signals of nuclear encoded proteins (114). Most notably known MMP, mitochondrial processing peptidase, is a conserved heterodimeric metallopeptidase cleaves sorting signals in the matrix (115-117). Additionally, some proteins, once in the matrix, are further processed by MIP, the mitochondrial intermediate peptidase (118). MIP is a monomeric metallopeptidase which removes peptides from preproteins post MMP processing and functions in their maturation (118-120). IMP inner membrane protease, whose active site functions in the intermembrane space, mediates the maturation of intermediate forms of nuclear encoded proteins generated by MPP in the matrix space (121-122), such as, precursor forms of Smac/DIABLO (123). In addition to these above proteases involved in protein import and processing, additional processing peptidases exist within the mitochondria and directly effect mitochondrial function. For example, the yeast rhomboid protease of the inner membrane Pcp1 involved in fusion (124-126), cleaves a component of the yeast fusion machinery, Mgm1 (discussed in more detail below). Pcp1 cleavage occurs post MMP processing and the removal of the mitochondrial targeting sequence (124).

The family of ATP dependent proteases have been identified in various mitochondrial compartments, and have two main functions; protein quality control and proteolytic control of the regulatory steps during mitochondrial biogenesis (127). They are known to degrade

proteins to peptides. The Lon protease (or PIM1 protease in yeast) is localized in the mitochondrial matrix (128-130). Its functions include quality control during conditions of stress, such as oxidative damage (131). Lon proteases recognizes misfolded and or damaged proteins and prevents their accumulation by facilitating complete proteolysis. Functions of this protease have also been linked to mitochondrial biogenesis, in that deletion of *PIM1* gene causes the destabilization of the mitochondrial genome, impairs mitochondrial gene expression, and results in respiratory deficiency (128-129, 132) A second type of ATP dependent protease is ClpP, which acts under cellular stress a similar fashion as the Lon protease suggesting overlapping functions in protein quality control (39). ClpP is also present in the matrix of mammalian mitochondria (133).

A third class of ATP-dependent proteases is the AAA proteases, which are present within the inner membrane of mitochondria and expose their catalytic sites, either to the matrix or the intermembrane space (134). The *m*-AAA protease, is active on the matrix side, and *i*-AAA protease, is active on the intermembrane side. AAA proteases have been identified in all mitochondrial subcompartments, except the outer membrane, and complementation studies in yeast have revealed a functional conservation of *m*- and *i*-AAA proteases from yeast to mammals (110, 135-137). These conserved proteolytic proteases function in quality control of mitochondrial inner membrane proteins, mediate peptide dislocation from the mitochondria, and act as processing enzymes, control ribosome assembly, mitochondrial protein synthesis, and mitochondrial fusion (110).

The functions and substrates of these proteases are only partially understood (80). It is known, however, that many of these enzymes have importance in human disease, such as Hereditary Spastic Paraplegia (138). For example, human mitochondria contain two *m*-AAA protease subunits, Afg3l2 and paraplegin (see below). Nonsense mutations in paraplegin are

causative for an autosomal recessive form of hereditary spastic paraplegia (HSP) (138).

Other diseases related to altered proteosomal function are Idiopathic Torsion Dystonia (139-140), Friedreich's Ataxia (141-142) and Batten's disease (143).

Proteins of the intermembrane space and matrix once processed by the AAA proteases have been found to be degraded by the ubiquitin-proteasome system (69-70, 134). Intriguingly, only two proteins of the outer membrane have been found to be degraded by the ubiquitin proteosomal system; MCL1 an anti-apoptotic protein of the outer membrane and Fzo1 the fusion protein of the outer membrane in yeast. This raises an interesting question as to how integral membrane proteins are excised from the mitochondria and how they are degraded?

1.3 MITOCHONDRIAL DYNAMICS

The mitochondria are highly dynamic within the cell and function, not as individual organelles but, as a complex system of mitochondrial networks. The mitochondria, within the networks, exhibit frequent motility, fission and fusion events. Their shape and structure are maintained by the regulation of these fission and fusion events, and mitochondrial shape is reflective of cell type and metabolic demand (Figure 1.6) For example, mitochondria are often arranged along the myofibrils in skeletal muscle, are coiled around the flagella in sperm and form long filamentous networks in fibroblast cells. The dynamic nature of the mitochondria, and its tightly regulated functional outputs, highlight the relationship between mitochondrial morphology and metabolic function and the relationship between mitochondrial morphology and cellular function.

Figure 1.6

Mitochondrial Dynamics

Mitochondrial morphology is regulated by the antagonistic forces of fission and fusion. Cos-7 cells, incubated with 50 nM of the delta psi sensitive dye, tetramethyl rhodamine ester (TMRE) display typical mitochondrial morphologies. Stimulating mitochondrial fusion and or inhibiting mitochondrial fission, results in an interconnected fused network of mitochondria within the cell. Conversely, inhibiting mitochondrial fusion and or stimulating mitochondrial fission, results in a fragmented network of individual mitochondria. Images were obtained using a wide field fluorescent microscope.

Mitochondrial morphology is regulated by the balance between fission and fusion

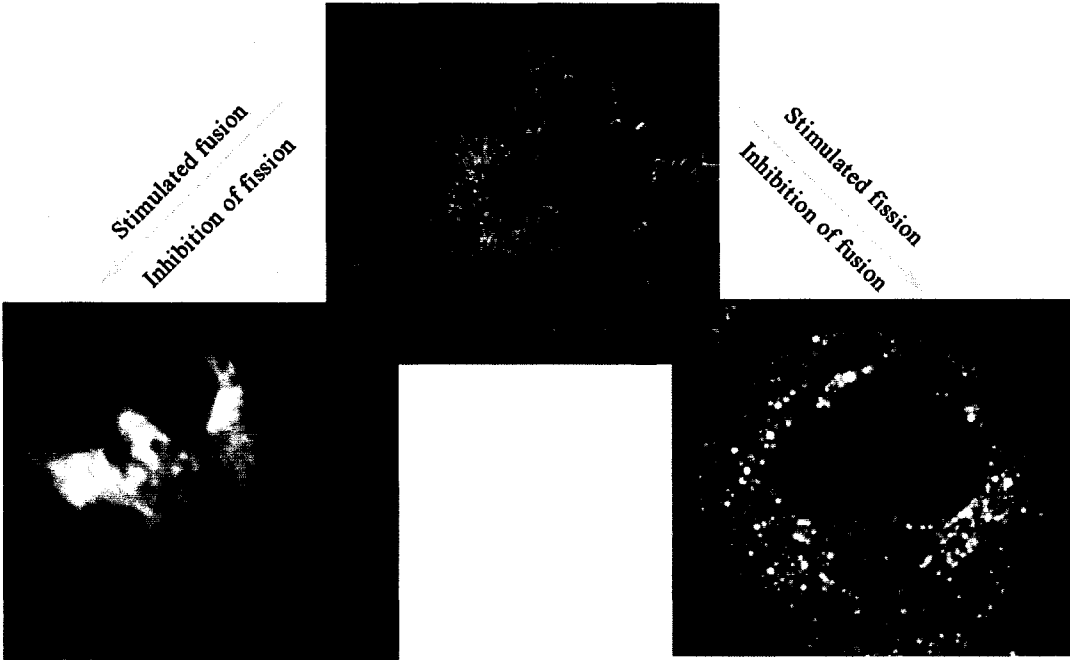


Figure 1.6

Mitochondrial Dynamics

1.3.1 MITOCHONDRIAL MOVEMENT AND CALCIUM SIGNALLING

It is known that interactions between the cytoskeleton and the mitochondria impact the respiratory capacity, fusion, fission, inheritance in yeast, as well as, the localization of mitochondria at sites of high energy demand. Interactions with the cytoskeleton also influence the ability of mitochondria to regulate metabolites and reactive oxygen species, biogenesis and calcium homeostasis (144). Mitochondria also use different cytoskeletal networks and different mechanisms to control their movement and morphology within cells. In the cell, the cytoskeleton is composed of three main types of filamentous systems: microfilaments, microtubules, and intermediate filaments. (144). Briefly, microfilaments consist of monomeric actin (G-actin), short helical actin filaments (F-actin), and polarized actin polymers which contain distinct plus and minus ends forming actin bundles and cables. Microtubules are polarized cylindrical polymers made up of tubulin monomers and are much more rigid than actin filaments. They extend their network throughout the cytoplasm and are a major component of the mitotic spindle and are essential for intracellular transport and cell motility. Finally, intermediate filaments consist of different types of monomers that are expressed in a tissue-specific manner and polymerize into nonpolar filaments. There are three major classes of intermediate filaments: keratins in epithelial cells, neurofilaments in neurons and vimentins in fibroblasts or the vimentin-like desmin in muscle cells. Intermediate filaments are less dynamic and more resilient than microfilaments or microtubules and provide more mechanical strength to the cell (144).

1.3.1.1 MICROTUBULE MOVEMENT

During microtubule-dependent mitochondrial movement, the microtubule-based motor proteins dynein and kinesin drive mitochondrial movement to the minus and plus ends of microtubules, respectively. The longest form of mitochondrial movement occurs in the

axons of neurons, this movement is motor based and the mitochondria travel along polarized parallel arrays of microtubules. The anterograde transport of the mitochondria occurs when the mitochondria translocates from the cell body to the distal portions of the axons, whereas, retrograde movement occurs when the mitochondria translocate in the opposite direction towards the cell body. The coordination of these movements facilitates the enrichment of mitochondria at sites of neuronal high energy demand. For example, mitochondria are often found to be in high numbers at the synapse, active growth cones and branches, nodes of Ranvier, distal initial segments, myelination boundaries and sites of axonal protein synthesis (145). In neurons, two kinesins; kinesin -1 (KIF5B) and kinesin-3 (KIF1B) are responsible for anterograde mitochondrial movement (146). Additionally, dynein inhibition also disrupts mitochondrial distribution in the axon, implicating dynein in retrograde mitochondrial movement (147-148). It has also been suggested that there exists a functional interdependence between Kinesin-1 and dynein. For example in *Drosophila*, inhibition of kinesin-1 inhibits anterograde and retrograde movement and causes a depletion of mitochondria in the axons (149-150).

The activity of the motor proteins on the mitochondria is facilitated by mitochondrial specific adaptor proteins; Milton-Miro, syntabulin and dynactin, which bind to the cargo-binding domain of the motors. The regulations and mechanism of the interactions between the adaptor proteins and the mitochondria are not well characterized. Some of the best characterized, thus far are Milton and Miro, two adaptor proteins which link the mitochondria to Kinesin-1. These were both identified using genetic screens in *Drosophila*, designed to identify genes required for eyesight (151-152). Milton is a Kinesin heavy chain binding protein which can co-immunoprecipitate and bind to the C-terminal cargo binding domain of Kinesin-1 (153-154). Miro, on the other hand, does not bind Kinesin-1 but co-

immunoprecipitates with Milton and is required for the interaction between Milton and Kinesin-1 (153). It is an integral outer membrane mitochondrial protein with a Rho-like GTPase domain (155).

The levels and activities of these adaptor proteins are critical for mitochondrial function. Mutation of, either Miro or Milton in *Drosophila*, abolishes anterograde mitochondrial axonal transport, and depletes mitochondria in the axon and synapse which are otherwise normally formed. (144). Conversely, the overexpression of the mammalian homologues of Milton OIP106 and GRIF-1 (aka TRAK1 and TRAK2), also produces disrupted mitochondrial localization (144, 154).

Interestingly, mitochondrial movement and shape have also recently been found to be important in the migration of the lymphocytes (156). In this work, it is demonstrated that mitochondria specifically concentrate at the uropod during lymphocyte migration by a process involving rearrangements of their shape. More specifically, mitochondrial fission facilitates relocation of the organelle and promotes lymphocyte chemotaxis, whereas, mitochondrial fusion inhibits both processes (156). These findings provide evidence linking mitochondrial dynamics and movement, suggesting that mitochondria redistribution is required to regulate the motors of migrating cells.

1.3.1.2 ACTIN MOVEMENT

Actin based mitochondrial movement is best characterized in budding yeast during cell division. Yeast mitochondria undergo anterograde movement towards the bud tip along polarized actin cables. Mitochondrial movement from mother to daughter requires actin cables, the mitochore, (a mitochondrial protein complex which links the mitochondria to actin cables) and the Arp2/3 complex. The Arp2/3 complex is known as the force generator

PROTEINS IMPLICATED IN MOTILITY		
PROTEIN	LOCATION	FUNCTION
Mdm10	OMM	Links to mtDNA nucleoids, required for movement, also involved in protein import and assembly.
Mdm12	OMM	Links to mtDNA nucleoids, required for movement.
MMM1	Outer and IMM	Links to mtDNA nucleoids, required for movement
Arp2/3 complex	Peripheral	Complex to initiate the polymerization of actin for mitochondrial motility.
Jsn1p	Peripheral	Pumilo repeats that bind RNA. Recruits Arp2/3.
Myo2p	Peripheral	Myosin motor required for retention of mitos in the bud, binds Ypt11p and Mmr1p.
Ypt11p	Peripheral	Regulatory small Rab GTPase required for retention of mitos within the yeast bud.
Mmr1p	Peripheral	Myo2p-dependent inheritance of mitochondria in the budding yeast
Synaptojanin 2A	Peripheral	Inositol 5'-phosphatase which binds to OMM protein, OMP25. Maintenance of intracellular distribution of mitochondria. Targeted to mitochondria via a PDZ domain-mediated interaction
Mitofin	IMM	Critical organizer of mitochondrial cristae morphology.
mDial / Diaphanous	Cytosolic	Formin family effector of RhoA involved in actin polymerization. Arrests mitochondrial motility.
Milton	Peripheral	Contains coiled coil domains, function in kinesin-mediated transport of mitochondria to nerve terminals. Interacts with miro for KHC mediated anterograde transport.
OIP106/ Grif-1	Peripheral	Member of milton family with long coiled coils. Associates with Kif5a and Kif5b.
Gem1 / Miro/ dMiro	OMM	Contains two EF hands, and two Rho-like GTPase domains, required for motility, function of domains unknown. Interacts with Milton for KHC mediated anterograde transport.
Kif1b/kinesin-1	Peripheral	Primary kinesin to move mitochondria in the anterograde direction.
Kinesin Binding Protein	Peripheral	Regulates mitochondria localization by interaction with a kinesin-like protein Kif1b.
Kif5c	Peripheral	kinesin to move mitochondria in the anterograde direction
kinectin 120	Peripheral	Links kinesin to mitochondria.
syntabulin	Peripheral	Mediated anterograde transport of mitochondria along neuronal processes.
tau	Peripheral	Involved in intracellular transport, links to kinesin. GSK-3beta phosphorylation required for mitochondrial transport. Implications in Alzheimer's disease.
KLP67A	Peripheral	Mitotic kinesin that may direct mitochondria to the spindle pole.
dynein	Peripheral	Microtubule motor for retrograde transport of mitochondria.
APLIP1 / JIP-1	Peripheral	Kinesin binding adaptor protein, adaptor for JNK.

Black: *S. cerevisiae*, Red: *H. sapiens*, Blue: *D. melanogaster*

Table 1.1 Mitochondrial motility proteins

Table illustrating the known mitochondrial motility proteins. Adapted from appendix 2.

for the mitochondria (157). In this study, it was shown, that if the actin cables are destabilized or if the mitochore is mutated, all mitochondrial movements were blocked. Interestingly, mutation within the Arp2/3 complex only inhibited anterograde, but not retrograde movements. This study provided evidence, that during mitochondrial inheritance, anterograde movement is responsible for the movement of mitochondria from the mother to the bud, and that retrograde movement is responsible for retaining the mitochondria in the mother. It was concluded that the mitochondria must interact with actin cables for both anterograde and retrograde movement, however, only Arp2/3 mediated force generation is required only for anterograde movement (157).

Three integral mitochondrial outer membrane proteins are required to facilitate the association of mitochondria with actin bundles. These proteins were also identified using genetic screens designed to identify defective mitochondrial movement. The complex consists of maintenance of mitochondrial morphology (Mmm)1p (158), mitochondrial distribution and morphology (Mdm)10p and Mdm12p (159-160). Deletion of any one of the three components leads to defects in mitochondrial morphology, inhibition of retrograde and anterograde mitochondrial motility, inhibition of mitochondrial actin binding activity, and high rates of mitochondrial DNA loss resulting in impaired mitochondrial respiratory activity (161). These studies demonstrate that the mitochondria undergo motor-independent, actin-dependent movement during inheritance in budding yeast and that these movements are regulated by different metabolic stimuli.

The relationship between mitochondrial motility, morphology and function is a complex issue which raises many open ended questions. For example, the role of actin motility in mammalian mitochondrial movement has not been established. The relationship between these different activities must be elucidated to properly understand the integration of

the mitochondria into the homeostasis of the cell. What regulates the specific motility mechanisms controlling mitochondrial distribution, and morphology and how are these mechanisms regulated in different cell types and in different regions within a cell are important questions to be addressed? How do two mitochondria know how to move toward each other for fusion? And conversely, how do two mitochondria know how to move apart to facilitate the fission event. It is intuitive that the mechanisms regulating microtubule and actin based mitochondrial movement must be highly integrated into those that regulate both fission/fusion and mitochondrial signaling. It is therefore, surprising, that these two lines of research are generally studied independently. Future studies into the mechanisms of fission and fusion will undoubtedly identify regulatory roles, for mitochondrial motility factors.

1.3.1.3 CALCIUM SIGNALLING

Mitochondria have additional essential cellular functions regulating levels of intracellular calcium. The mitochondria respond to different calcium levels within the cell resulting in diverse functional outcomes of the organelle. They can act as calcium sinks, sequestering these ions upon their release from endoplasmic reticulum (ER) and/ or following increased Ca^{2+} uptake across the plasma membrane (162). This is functionally demonstrated in cardiomyocytes during cellular Ca^{2+} spikes required for contraction. The mitochondrial Ca^{2+} concentrations oscillate in response to the contractile Ca^{2+} waves within the cell (163). Conversely, the mitochondria can also release their Ca^{2+} to increase the local concentrations within the cytosol or in specific subcellular regions. (164). The mitochondria also perform a general Ca^{2+} buffering role for the cell, whereby, they often are found in different localized areas within the cytoplasm to facilitate rapid Ca^{2+} uptake. For example, in pancreatic acinar cells, populations of mitochondria are often found near the

plasma membrane to buffer the local influx of Ca^{2+} . Localized increases in mitochondrial Ca^{2+} facilitate insulin signaling and release (165). In these same cells, a separate population of mitochondria are localized in close proximity to the nucleus to prevent the cell from the damaging effects of rapid increases of Ca^{2+} levels (165).

This ability of the mitochondria to actively participate in the uptake and release of intracellular Ca^{2+} and the regulation of Ca^{2+} signaling, is dependent on their relative position within the cell, as well as, their proximity to the endoplasmic reticulum (166). The mitochondrial Ca^{2+} uniporter has low affinity for Ca^{2+} , and as such, juxtaposition to the ER, is required for the production of microdomains of high Ca^{2+} concentration.

The mitochondria also respond functionally to different levels of Ca^{2+} within the organelle. Ca^{2+} uptake is required for the proper functioning of a number of metabolic enzymes and metabolite carriers (162, 167). The mitochondria can also signal for increased proliferation through the release of internal Ca^{2+} into the cytoplasm (164). Mitochondrial Ca^{2+} signaling can also induce apoptosis (168). Mitochondrial dynamics, motility, fission and fusion directly influence the propagation of Ca^{2+} waves and Ca^{2+} signaling. High-speed mitochondrial Ca^{2+} imaging revealed that if the mitochondrial network was fragmented, the propagation of intra-mitochondrial Ca^{2+} waves was blocked (169). Interestingly, this effect seems to be dependent on fission molecules and the mechanisms of this dynamic relationship have not yet been elucidated. Furthermore, the relationship between Ca^{2+} binding proteins, Ca^{2+} and the morphology response is unclear.

1.3.2 MITOCHONDRIAL FUSION

It had been assumed that the mitochondrial population would undergo fission events for mitochondrial biogenesis, but it was not anticipated that these organelles were capable of

fusion events. It was only in 1998, that the first documented fusion phenotype was observed. Since this time, the field of mitochondrial dynamics has emerged, which has significantly expanded our understanding of mitochondrial biology. We now know, that the mitochondria readily undergo fusion events, which are highly regulated by outer and inner membrane mitochondrial GTPase's, ATP levels and cellular metabolic demands. The investigation into the complex mechanisms of fusion represented the first half of this doctoral thesis.

The process of mitochondrial fusion requires the co-ordination of many complex steps between two or more mitochondria within the cytoplasm. The so called “acceptor” and “donor” mitochondria respond to intracellular fusion requirements and communicate via unknown signaling mechanisms to coordinate mitochondrial fusion. (Figure 1.7) In order to relay the fusion signal, the mitochondria must recruit motility factors, form associations with the microtubule network, and assemble fusion pore protein complexes on both the outer and inner membranes of each mitochondrion. The donor mitochondrion migrates through the cytoplasm towards the acceptor mitochondria where the protein machinery (on each opposing mitochondria) coordinates docking and tethering events. The fusion site is formed when four sets of membranes (two outer and two inner) are in close opposition, separating four distinct microenvironments (two intermembrane space and two matrix's). Complete mitochondrial fusion results when both the outer and inner membranes have fused to form one mitochondria with a continuous matrix. Studies investigating mitochondrial fusion in vitro, have revealed that inner and outer membrane fusion are distinct mechanistic processes, both, however, require guanosine 5'-triphosphate (GTP) hydrolysis (170-172). For example, in vitro studies in yeast revealed that in low GTP concentrations outer membrane but not inner membrane fusion occurs and that the addition of a GTP regenerating system allows for complete fusion to occur. The loss of mitochondrial membrane potential has been shown to

Figure 1.7

Mitochondrial fusion steps

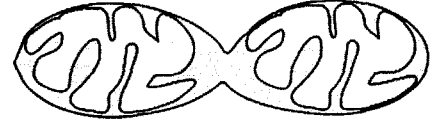
Cartoon schematic illustrating the steps required for mitochondrial fusion. In order for mitochondrial fusion to occur many events must happen. First one mitochondrial must send out a fusion signal to neighboring mitochondrial to initiate the fusion reaction. Next fusion proteins must be recruited to, or assembled into micro domains on the mitochondrial surface for fusion. Next the mitochondria need to engage motility factors to bring the two opposing outer membranes into close opposition. Next the two mitochondria must tether by unknown factors. A fusion pore must form on the outer membrane to fuse the two opposing membranes. Next the two opposing inner membranes must also tether and form a fusion pore. Complete mitochondrial fusion results when four sets of membranes fuse forming a single continuous matrix.

Mitochondrial Fusion required steps

1. Recruitment of components to microdomains on mitochondrial surface.



2. Mitochondrial motility.



3. Mitochondrial tethering, factors?



4. Fusion machinery and fusion pore formation.

5. Inner membrane tethering machinery.



6. Inner membrane pore formation.

7. Structural rearrangements of cristae.

Figure 1.7

Mitochondrial fusion steps

block mitochondrial fusion (173), and interestingly, in mammalian cells treated with CCCP (H⁺ ionophore) or valinomycin (K⁺ ionophore) inner membrane but not outer membrane fusion is blocked (174). This is hypothesized to occur through dissipation of the membrane potential (170, 174). In contrast, yeast cells, *in vitro*, treated with CCCP, show a complete block of outer membrane fusion (172). These studies highlight some of the complexities involved in fusing four sets of lipid bilayers and illustrate some of the differences between the mammalian and yeast systems.

If mitochondrial fusion is inhibited, the process of ongoing fission results in a fragmented mitochondrial network (Figure 1.6). Defects in fusion result in the delayed growth of mammalian cells due to a low respiratory capacity which is speculated to be the result of incomplete mtDNA complementation and nucleoid loss. As such, these small mitochondria could either lack mtDNA or contain mutated mtDNA with dysfunctional electron transport chains, leading to compromised oxygen consumption. Furthermore, it remains an open question as to how mitochondrial genomes are lost in the absence of fusion. Mice deficient in mitochondrial fusion die in mid gestation; mutations in components of the fusion pathway have also been implicated in the pathology of certain neurodegenerative diseases such as peripheral neuropathy, Charcot-Marie-Tooth Disease subtype 2A and in autosomal dominant optic atrophy.

1.3.2.1. FUSION PROTEINS

Most intracellular fusion events are mediated by families of SNARE proteins (Soluble NEM Sensitive Adaptor Receptor), Rab GTPase's and Rab effector proteins and fusogenic lipids, such as phosphatidic acid, and the interaction of these provide the initial segregation and tethering between membranes of different vesicle compartments (175-176).

The regulations of these different interactions ensure that only the correct pairs of membranes can proceed to fusion. To date, none of the known Rab GTPase's, Rab effector proteins or SNAREs have been found to be involved in the regulation of mitochondria fusion. An open question in the field of mitochondrial fusion is that of the identity of the protein machinery, and whether mitochondrial fusion proteins, function in an analogous fashion similar to the SNARE proteins? If so, they would pull mitochondrial membranes into close opposition, providing sufficient force to overcome the intrinsic forces of repulsion between opposing membranes (177). Interestingly, Mitochondrial PLD (MitoPLD), an ancestral member of the phospholipase D (PLD) superfamily of lipid-modifying enzymes has recently been found to be required for mitochondrial fusion (178-179). MitoPLD promotes trans mitochondrial membrane tethering in a Mitofusin (see below) dependent manner (178). It functions by hydrolysing cardiolipin to generate phosphatidic acid, a fusogenic lipid. An unresolved question in this discovery, is that cardiolipin resides in the inner membrane and MitoPLD is on the cytoplasmic face of the outer membrane. This finding suggests that mitochondria utilize analogous protein machinery to facilitate mitochondrial fusion.

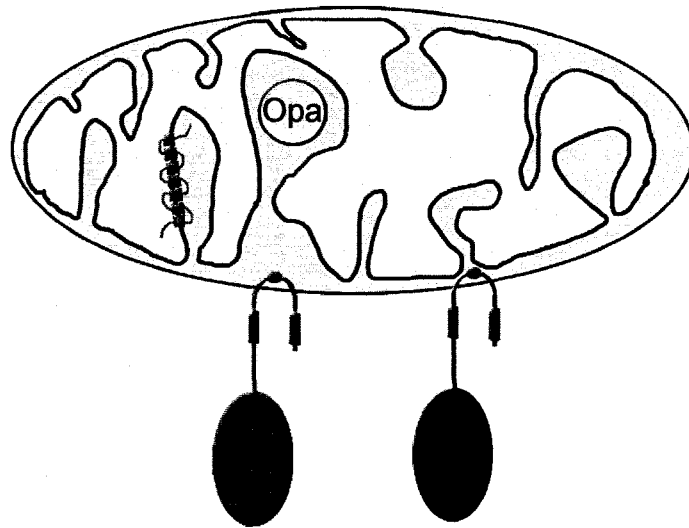
Mitochondrial fusion in mammalian cells is regulated in part, by three highly conserved essential GTPases; two of the Mitofusin family, Mitofusin 1 and Mitofusin 2 (Fzo1p in yeast) and OPA1 (Mgm1p in yeast) (170-171, 180-185) (Figure 1.8). The mitochondrial GTPase Fzo1p, of yeast *Saccharomyces Cereviscae* and *Drosophila Melanogaster*, is an outer membrane protein, first identified in *Drosophila* screens searching for genes causing male sterility, and was found to play an essential role in mitochondrial fusion (180). Mitochondria, during sperm formation, aggregate and fuse into large, multilayered structures resembling a slice of onion. In this particular mutant, the mitochondria in spermatid cells could not form this structure and instead had a “fuzzy onion

Figure 1.8

Mitochondrial fusion proteins

A) Cartoon schematic illustrating the mammalian mitochondrial fusion proteins and their yeast orthologues. Mitofusin 1 and 2 are shown with the GTPase domains, and coiled coiled domains exposed to the cytosol. The intermembrane space loop is illustrated between the two transmembrane domains. PARL, a serine rhomboid protease of the inner membrane space is illustrated in pink with its 7 transmembrane domains. OPA1, the GTPase of the intermembrane space is shown in yellow deep within a crista fold. B) Table illustrating the known mitochondrial fusion proteins. *S. cerevisiae*, *H. sapiens*, *D. melanogaster* proteins in black, red and blue respectively.

A



B

PROTEINS IMPLICATED IN FUSION		
PROTEIN	LOCATION	FUNCTION
Fzo1p / Mfn1 / Fzo	OMM	Dynamin family of GTPases, contains 2 heptad repeats required for tethering and fusion.
Mfn2 / HSG / dMfn	OMM	Dynamin family of GTPases, shown to also exhibit regulatory properties, 60% identical to Mfn1. Mutations found in CMT2A.
Mgm1p / Opa1	IMS and IMM	Dynamin like GTPase, coiled coils. 8 splice variants in human, cleavage patterns upon import are complex. Opa1 mutations found in DOA. Required for fusion and cristae structure. Mgm1p binds Fzo1p in complex with Ugo1p.
Rbd1p/cp1p/Mdm37 / PARL	IMM	Rhomboid family of 7 transmembrane IMM serine protease. PARL is processed upon import. Rbd1p cleaves Mgm1p in yeast.
Ugo1p	OMM	Contains a carrier Motif, and is part of complex with Fzo1p and Mgm1p. Human orthologue unknown.
Mdm30p	Peripheral	F-Box motif. Involved in mitochondrial protein degradation

Black: *S. cerevisiae*, Red: *H. sapiens*, Blue: *D. melanogaster*

Figure 1.8

Mitochondrial fusion proteins

appearance". Fzo1 was then cloned and identified to be a mitochondrial integral outer membrane, GTP-binding protein. When fusion is blocked in yeast cells lacking Fzo1p, mitochondrial fission continues and the phenotype observed is of fragmented mitochondria, which ultimately lose their ability to segregate mtDNA. The human genome contains 2 isoforms of Fzo1p, which appear to have arisen from a gene duplication event. The proteins encoded by these genes are Mitofusin1 (Mfn1) and Mitofusin2 (Mfn2) (171, 180-182). The reason for the gene duplication of Fzo1 in higher organisms remains unknown. Mammalian mitofusins, Mfn1 and Mfn2 are large integral GTPase's of the mitochondrial outer membrane which contain two coiled-coil domains (heptad repeats HR1 and HR2), a GTPase domain and two transmembrane domains (186). The majority of these proteins, including the N-terminus, GTPase domain, HR1, and the C-terminus-proximal HR2, are exposed to the cytosol. Both transmembrane domains are separated by a small highly conserved intermembrane space loop of two to three amino acids (186) (Figure 1.8).

Both Mfn1 and Mfn2 are highly homologous with 60% identity at the amino acid level. Mfn1^{-/-} and Mfn2^{-/-} mice die during embryonic development, highlighting the importance of these proteins and mitochondrial dynamics during development (187). Mouse embryonic fibroblasts (MEF), derived from these embryos, have defects in mitochondrial fusion and show altered mitochondrial morphology and MEF cells derived from the double knockout ^{-/-} Mfn1/Mfn2 mice (lacking both mitofusins) have a complete block in fusion and multiple intracellular dysfunctions (187). Mfn2 and Mfn1 can form homo- and hetero-oligomers in-cis and in-trans and one of either Mfn1 or Mfn2 is required on opposing mitochondria to facilitate fusion (187). Interestingly, in vitro studies have demonstrated that Mfn1 forms homooligomeric complexes in trans with greater efficiency than Mfn2 (188). These studies also found that the heptad repeat domains of Mfn1 form a 95-° A-long

antiparallel coiled-coil structure through intermolecular interactions (189). Specific point mutations within this conserved c-terminal region of Mfn1 attenuate mitochondrial fusion, and it was therefore suggested that in vivo, this coiled coil structure is a functionally relevant fusion intermediate, which represents opposing mitochondria tethered in *trans* (189). The same in *trans* interactions have been reported in yeast cells demonstrating that in vitro studies of temperature sensitive Fzo1 at non-permissive temperatures are defective for outer membrane fusion (172). This study is also consistent with the mammalian Mfn1 *trans* pairing studies, in that heteroallelic reactions of *fzo1ts* and wild-type mitochondria failed to fuse outer membranes (172). These findings demonstrate the critical role that this protein plays in the fusion reaction and that both opposing mitochondria must be fusion competent in order for fusion to proceed.

Both Mfn1 and Mfn2 were assumed to be of the dynamin family of GTPases and as members of this family of mechanoenzymes, it was thought that the mitofusins exert their fusogenic action through the hydrolysis of GTP to GDP. Conversely, the regulatory family of signaling GTPases, such as, the RAB GTPases exert their action through nucleotide exchange and binding of GTP rather than hydrolysis of GTP to GDP. In this GTP bound form, these regulatory GTPase's are active for intracellular signaling (190). The Fzo1 protein and the mitofusins are considered to be of the dynamin family of GTPases, however they do not contain all of the evolutionary conserved domains that other family members possess (177). They lack easily identifiable middle regions and GEDs domains but possess, like the other family members, a GTPase domain and regions that form intermolecular coiled-coil structures (177). Their large mass and their structural properties make the proteins unique within the family of GTPases (191). It is however, also assumed that like other dynamins, they function through self –assembly (177).

Studies investigating the nucleotide binding and hydrolysis properties of Mfn1 have been performed, it was found that Mfn1 binds nucleotide with low affinity and shows high rates of hydrolysis for GTP, consistent with its evolutionary relationship to the dynamin family of GTPase (188). Similar studies had not been performed for Mfn2. My studies were designed to investigate the nucleotide binding, exchange and hydrolysis properties of this protein.

This investigation was divided into two specific research objectives #1 *Since Mfn2 represents an atypical class of GTPase, it needed to be determined what type of GTPase it was, either, mechano or regulatory. It was hypothesized that, by creating point mutations within the p-loop of the nucleotide binding pocket, the affinity for nucleotide would be altered and the properties of this GTPase domain would be determined.* To this effect, if Mfn2 stimulates fusion when bound to GTP, this would demonstrate that it is indeed a regulatory GTPase (active when bound to GTP) as opposed to a mechanoenzyme GTPase (active upon GTP hydrolysis).

The second research objective #2 *It was further hypothesized that stimulated fusion, would delay the onset of apoptosis, and that active GTP bound Mfn2 would inhibit the mitochondrial death pathway.* (see below) The investigations into the mechanisms and functions of Mfn2 for fusion and apoptosis represented the first half of my doctoral studies. The research findings are presented as a manuscript in chapter 2 of this thesis.

A third mitochondrial protein that is essential for mitochondrial fusion is Optic Atrophy 1 (OPA1), an intermembrane space dynamin-related GTPase (yeast homolog Mgm1) (183, 185, 192) (Figure 1.8). Mutations within OPA1 cause autosomal dominant optic atrophy type I (185). RNA interference of Opa1 induces mitochondrial fragmentation and the resulting mitochondrial contain aberrant inner membrane structures. OPA1 functions

together with Mfn1 but not Mfn2 to promote fusion (193). Deletion of Opa1, causes vesiculation of the inner membrane and cells lacking Opa1 are highly susceptible to apoptotic death, indicating the importance of maintaining inner membrane morphology for mitochondrial viability. Both OPA1 and Mgm1 are essential proteins for the maintenance of mitochondrial crista structure. Detailed electron microscopy studies using immunodecoration of both proteins found that they are enriched along the crista (Figure 1.8) (192, 194). Downregulation of OPA1 by siRNA results in wide crista junctions and the crista become disorganized. Conversely, overexpression of OPA1 results in narrow crista and crista junctions (195).

Alternative splicing of OPA1 results in eight different isoforms, each of which is subsequently processed to form several isoforms with distinct molecular sizes. Single variants of OPA1 are found as several processed forms; however the proteolytic processing and functional significance these distinct forms remain largely unknown. There are differences between the yeast and mammalian systems in the regulation of this inner membrane space GTPase, and these differences highlight some of the complexities between these two systems.

The yeast Mgm1 is essential for maintaining mitochondrial DNA and inner membrane structures in yeast (196). Mgm1 was found to interact indirectly in a complex with Fzo1 through the yeast protein Ugo1 and is involved in mitochondrial fusion (196-197). Ugo1 is an outer membrane protein and the cytoplasmic domain of Ugo1 directly interacts with Fzo1, whereas, its intermembrane space domain binds Mgm1 (Figure 1.8). The interaction between Fzo1 and Ugo1 is essential for maintaining mitochondrial shape, maintenance of mitochondrial DNA, and fusion of mitochondria. Interestingly, the GTPase domain of Fzo1 is not required for the interaction with Ugo1 (197). The mammalian

orthologue of Ugo1, has not yet been identified, and the field of mitochondrial dynamics is anxious for its discovery.

Mgm1 exists in two forms as well: the large isoform (l-Mgm1) and the small isoform (s-Mgm1). l-Mgm1, alone is sufficient for mitochondrial fusion, however the levels are reduced (198). The presence of both l-Mgm1 and s-Mgm1 are required for efficient levels of mitochondrial fusion (124). The l-Mgm1 isoform is the mitochondrial processing peptidase (MPP)-processed mature form after protein import. L-Mgm1 can then be cleaved by the inner membrane rhomboid protease Pcp1 to generate s-Mgm1. More specifically, Mgm1 is translocated into the mitochondria through outer membrane translocase complexes and the TIM23 complex of the inner membrane for import (49). During import the matrix metalloprotease removes the N-terminal presequence (as described above). Mgm1 contains two hydrophobic regions that are important for determining the ratio of long to short Mgm1. This first region, may function as a stop transfer sequence resulting in mgm1 being imbedded into the inner membrane. This results in the formation of l-Mgm1. Alternatively, with the help of an ATP-dependent Hsp70 motor, Mgm1 may translocate further into the matrix. Once in the matrix, Pcp1 has access to its cleavage site within the second hydrophobic region of Mgm1 (199), resulting in the formation of s-Mgm1. s-Mgm1 has lost its transmembrane domain, but remains closely associated with the inner membrane. The degree of proteolytic processing of Mgm1 depends on relative ATP levels. l-Mgm1p is when ATP is low, whereas, high levels of ATP favor the formation of s-Mgm1p. It has been suggested that the ATP dependence on proteolytic processing is directly related to less efficient Hsp70 driven import (199).

Pcp1 is a member of the conserved family of membrane-embedded serine proteases, whose catalytic residues lie within the hydrophobic, membrane spanning domains (Figure

1.8). Rhomboid proteases cleave membrane anchored proteins within transmembrane segments to generate soluble, biologically active protein fragments. Pcp1 processing of Mgm1 greatly effects mitochondrial dynamics since both the short and long forms of mgm1 are essential for fusion. Interestingly, Mgm1 cleavage by Pcp1 was found to depend on mitochondrial Hsp70 and the cellular ATP levels. Loss of Pcp1 function reduces fusion but does not block it completely. This result is consistent with the above finding that l-Mgm1 alone can support attenuated fusion as well (124-126). It has been suggested that Pcp1 functions as an energy sensor regulating mitochondrial fusion, controlling the segregation of damaged organelles from the network of intact mitochondria.

In mammalian cells, however, OPA1 processing is more complex and the identity of proteases responsible for regulated OPA1 cleavage less clear. OPA1 cleavage, like Mgm1, however, reflects the energy level in mitochondria and can be regulated by the membrane potential across the IM (200). Opa1 contains a bipartite mitochondrial targeting signal: a matrix-targeting signal (MTS) followed by a transmembrane domain. The N-terminal MTS is removed by MPP in the matrix during import to form the mature L-OPA1 isoform. Similarly to the yeast l-Mgm1, L-OPA1 is further processed to form the short isoforms S-Opa1. The L-isoform of Opa1 has mitochondrial fusion stimulating activity, which is lost once proteolytic processing to be the S-isoforms has occurred. Increased L-OPA1 proteolytic processing results in the stimulation of mitochondrial fragmentation, whereas conversely, inhibition of the processing resulted in increased mitochondrial tubular networks. Furthermore, the loss of membrane potential and or apoptotic stimuli triggered Opa1 cleavage and mitochondrial fragmentation. Loss of membrane potential triggers the conversion of OPA1 isoforms into smaller isoforms accompanied by a simultaneous

fragmentation of mitochondria. Proteolysis of OPA1 is also observed in patients and in various model systems of human disorders associated with mitochondrial dysfunction .

The regulated cleavage of OPA1 in mammalian cells is an issue of high controversy, as both PARL (presenilin-associated rhomboid-like), a mitochondrial rhomboid protease, and paraplegin, a subunit of the *m*-AAA protease, have both been proposed to be involved in cleaving OPA1. There is also evidence to suggest that alternate spliced products may influence the efficiency of proteolytic processing.

The PARL protease is the obvious candidate for OPA1 cleavage since it is the mammalian orthologue of yeast Pcp1, can directly interact with OPA1 and can functionally replace pcp1 in yeast cells (124-125, 195). Deletion of *Parl* in *Drosophila* leads to fragmented mitochondria. Additionally, PARL is a critical regulator of OPA1-dependent cristea remodeling during apoptosis resulting in the accumulation of a soluble form of OPA1 in the intermembrane space. Significantly, deletion of PARL does not impair the processing or function of OPA1, suggesting the involvement of different mitochondrial proteases. PARL activity is also regulated by phosphorylation and this post-translational modification affects mitochondrial shape, however it is not yet known whether the phosphorylation of PARL modulates Opa1 cleavage (201) Other groups have observed that PARL is not required for OPA1 processing. For example, studies in mice have found that deletion of *Parl* does not have an obvious effect on mitochondrial morphology. Additionally, the cleavage of OPA1 has recently been linked to the hetero-oligomeric *m*-AAA protease which is a metalloprotease of the inner membrane. Paraplegin, a subunit of the *m*-AAA protease, when downregulated has been implicated in OPA1 processing. Interestingly, paraplegin-deficient mouse models contain aberrant mitochondria, and the deletion of paraplegin is causative for axonal degeneration in hereditary spastic paraplegia .

It has since been hypothesized that the impaired processing of OPA1 and mitochondrial dysfunction are causative in this disease. It has also been suggested that both PARL and paraplegin are required for OPA1 processing, however, the specific activity of each protease varies dependent on cell type. This controversy also indicates that it is likely that other factors are involved in the regulation of OPA1 cleavage. Some of the most convincing evidence has come from recent work in which the i-AAA protease Yme1L was shown to be responsible for the cleavage to form the short form of OPA1 (202-203). In yeast cells, a newly identified protein of the inter membrane space Ups1, which associates with the inner membrane has been found to be essential for Mgm1 processing, only when cells are grown in fermentable carbon sources (204). The mechanism of action is yet to be elucidated; however, this finding indicates a degree of metabolic regulation of this process.

Interestingly, the human orthologue of Ups1, PRELI can functionally replace Ups1 in yeast cells. Similar studies have not yet been performed in mammalian cells to investigate the contribution of PRELI to OPA1 cleavage, however, it will be important to understand the functional significance of this newly identified protein on mitochondrial dynamics, fusion and its contribution to the apoptotic program.

Currently, most of the mammalian proteins discovered for mitochondrial fusion have followed the initial yeast discovery screens, which have identified all of the proteins known thus far. This approach proved to be useful for mammalian cell biologists, however, it is also limited in its breadth. An example highlighting the complex differences between these two systems is that of Mgm1 and OPA1 processing. Yeast Mgm1 processing, is not a perfect model system to study mammalian OPA1 cleavage. Evidence suggests that the mitochondria respond differently to cellular stress and metabolic demand in these two systems, and the regulation of Mgm1/OPA1 processing is not analogous. In mammalian cells, dissipation of

membrane potential results in OPA1 processing to the short form, in yeast however, this loss inhibits Mgm1 processing (200, 205). This difference could be attributed to the functional roles of OPA1 during apoptosis, which differ from Mgm1? Future studies investigating the mechanisms and regulation of OPA1/Mgm1 processing will undoubtedly shed light on these questions.

1.3.3. MITOCHONDRIAL FISSION

Mitochondrial fission, in addition to steady state dynamics, can be triggered by a variety of cellular stresses; two of which are the loss of mitochondrial membrane potential and apoptotic stimuli. Mitochondria have been observed to become more tubular in the G1 phase and S phase during mitosis in fibroblasts and osteosarcoma cells. During G2 to M, they are observed to fragment in a Drp1 dependent fashion. Critical to all fission events is the action of the peripherally associated dynamin related GTPase Drp1, mutations in the GTP binding or in GTPase activity, lead to highly elongated filamentous mitochondria structures (206-207). Drp1 is a member of the dynamin superfamily of multimeric large GTPases (208), with the most characterized being dynamin, known for oligomeric scission of endocytic vesicles from the plasma membrane. Cytosolic Drp1 is recruited to fission sites on the outer membrane, where it forms drp1 collars which wrap around the mitochondria (Figure 1.9). Hydrolysis of GTP to GDP is thought to provide the energy for scission. The targeting and self-assembly of DRP1 into punctate foci on the mitochondria may be facilitated by the actin cytoskeleton and/or by microtubules. Disruption of both the actin cytoskeleton and inactivation of the microtubule dynein/dynactin complex disrupts Drp1

targeting (209-210). The molecular mechanisms of this targeting, however is not currently understood.

Dnm1 and Drp1 function for fission in a similar fashion, although subtle differences between these two proteins exist. For example, time-lapse imaging of Dnm1 localization in yeast cells indicated that Dnm1 is targeted to the mitochondrial membrane, in a rate-limiting, stochastic manner, but the majority of Dnm1 is found as self-assembled structures, however, only a subset of these Dnm1-associated sites undergo fission (211-212). Conversely, Drp1 is mainly a cytosolic protein with diffuse localization and not self assembled. A small fraction of Drp1 is recruited to mitochondrial membranes into discrete puncta (206, 213). Only a small fraction, of Drp1 puncta defines a fission site, whereas the majority of the sites of Drp1 recruitment do not undergo fission. The molecular mechanisms of Drp1 recruitment, self-assembly and activity on the membrane for fission, is a highly studied question. As the details of these events are being uncovered, the role of post-translational modification is becoming apparent. Studies investigating the self assembly properties of Dnm1 and Drp1 have revealed difference between the yeast and mammalian systems as well. It is assumed that Dnm1/Drp1 functions through self-assembly into oligomeric spirals for fission of mitochondrial membranes in an analogous fashion to that of Dynamin and scission of endocytic vesicles (212, 214). Some evidence exists to support this assumption; however, in mammalian cells additional factors are clearly required.

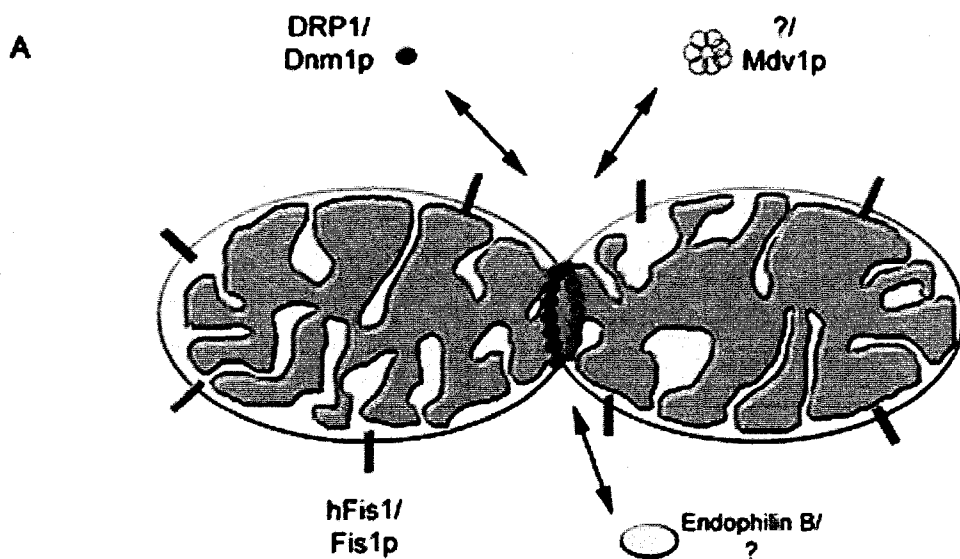
Hydrodynamic and cross-linking experiments have shown that Drp1 dimers or tetramers are required for self assembly. In the nucleotide-free or GDP-bound state, DRPs form curved filaments, whereas, in the GTP-bound state, DRPs form spiral-like helical structures and both helical DRP structures as well as GTP hydrolysis are believed to be responsible for Drp1 function (212-213). Dnm1 has been found to form spirals in yeast cells,

and studies characterizing the exact dimensions have provided insight into the mechanisms of fission (212). Dnm1 spirals form a larger diameter than dynamin spirals (~109 nm versus ~50 nm). This diameter is surprisingly the exact diameter of mitochondrial constriction sites found in vivo (~109 nm) (212). Dnm1 self-assembly into spirals can also constrict artificial liposomes in vitro and form tubules, with a diameter similar to mitochondrial constriction sites. Similar studies of the self assembly properties of Drp1, however, have revealed a more complex system. In vitro Drp1 experiments found that Drp1 self assembles and forms spirals, however, to a lesser extent and with less efficiency than Dnm1. Also, Drp1 spirals are smaller (~30-50 nm) than Dnm1 spirals (213).

Drp1 does not act alone; it is often found to interact with Fis1 along the same genetic pathway. Fis1 a 16KDa integral outer membrane protein localized at fission sites (Figure 1.9). Studies in *S. cerevisiae* have been fundamental for the initial discovery of these proteins and have laid the foundation for current studies in mammalian cells. In yeast cells, three essential fission proteins have been discovered; Dnm1 (mammalian orthologue DRP1, Fis1 (mammalian orthologue Fis1), and Mdv1 (215-218) (Figure 1.9). Dnm1 and Fis1 are both highly conserved, and it is considered that the basic mechanism of mitochondrial division is analogous in yeast and mammalian cells. The structural or functional orthologue of Mdv1 has not yet been found, and like the fusion proteins above, its discovery is highly anticipated. Mdv1 is an 80-KDa protein which mediates protein-protein interaction with Fis1 and Dnm1 (Figure 1.9) (215-216, 219). Fis1, is required for targeting of fission proteins Dnm1, Mdv1 (220). In the absence of Fis1, targeting of Dnm1 and Mdv1 to mitochondria is compromised. It has been suggested that Fis1 is the membrane receptor for these proteins. In support of this hypothesis, Fis1 and Mdv1 have been found to interact, however the same is not true for Fis1 and Dnm1. It is therefore thought that Fis1-dependent targeting of Dnm1 to

Figure 1.9 *Mitochondrial fission proteins*

A) Cartoon schematic illustrating the mammalian mitochondrial fission proteins and their yeast orthologues. Cytosolic Drp1 is recruited to the outer membrane for mitochondrial constriction. Fis1 is evenly distributed along the outer membrane and participates with Drp1, Mdv1 (in yeast) and endophilin B1 for fission. B) Table illustrating the known mitochondrial fission proteins. *S. cerevisiae*, *H. sapiens*, *D. melanogaster* proteins in black, red and blue respectively.



B

PROTEINS IMPLICATED IN FISSION		
PROTEIN	LOCATION	FUNCTION
Dnm1p / DRP1 / Dlp1	Peripheral	GTPase, mechanoenzyme. Dnm1p is recruited through Mdv1p/Fis1p complex. Oligomerizes to form rings that constrict around the mitochondria. Also required for fission and cristae remodeling during apoptotic stimuli.
Fis1p / hFis1	OMM	TPR repeats, implicated in the control of Drp1 recruitment and activation of fission complexes.
Mdv1p	Peripheral	WD40 Repeats, adaptor linking Fis1p with Dnm1p and regulates Dnm1p self-assembly.
Caf4	Peripheral	WD40 Repeats, component of the mitochondrial fission machinery and recruits Dnm1p to mitochondria.
Endophilin B1	Peripheral	Contains BAR membrane binding domain, binds Bax. Loss of Endophilin leads to outer membrane tubules without apparent inner membrane.
SUMO1	Peripheral	Ubiquitin-like modifying enzyme that covalently and reversibly modifies DRP1, stimulates fission.
GDAP1	OMM	Required for fission, function unknown. Contains GST domains. Mutations found in CMT4A.
Mtp18	IMM	Involved in fission of the mitochondrial IMM. Mtp18 activity is regulated by phosphatidylinositol 3-kinase activity.
Dap3	Matrix	Involved in mitochondrial fission post apoptotic signal. Contains a GTPase domain which is essential for fission
Rab32	Peripheral	Regulatory GTPase, participates in both mitochondrial anchoring of PKA and mitochondrial dynamics.

Black: *S. cerevisiae*, Red: *H. sapiens*, Blue: *D. melanogaster*

Figure 1.9

Mitochondrial fission proteins

mitochondria requires an interaction between Fis1 and Mdv1(220). In yeast cells lacking functional *dnm1*, *mdv1*, and *fis1*, mitochondrial division is inhibited, resulting in the formation of elaborate net-like structures (207, 215-217, 221-222).

In mammalian cells, recruitment of Drp1 to the mitochondrial membrane does not follow that same pattern as yeast cells. Surprisingly, changes in the levels of hFis1, either through overexpression or siRNA, do not effect the targeting of Drp1 to mitochondrial membranes (223-225). Also, hFis1 and Drp1 *in vivo* have not been found to directly interact. It is assumed that these two proteins function together in a complex for fission, similar to the yeast system. Interactions through co-immunoprecipitations between the two proteins can be detected when they are both purified and chemically cross-linked (226). Again, the mammalian functional counterpart of Mdv1, has not been found and it is believed that this missing link will provide some molecular definition to the Drp1 recruitment complex.

These two proteins mediate recruitment of other fission protein such as; endophilin B1 (227), and GDAP1, ganglioside-induced differentiation associated protein 1 (228) (Figure 1.9). Endophilin B1 acts downstream of Drp1 and Fis1, however the mechanisms of action remain unknown (227).

Endophilin B1 is a member of the endophilin family of fatty acid acyl transferases and these proteins self-assemble forming filaments which remodel membranes. Endophilin A, co-assembles with dynamin at the plasma membrane to promote endocytosis (229). Endophilin B1, like other endophilins possesses an N-BAR domain, which is thought to induce membrane curvature (230-231). Loss of endophilin B1 results in increased interconnectivity between mitochondria, consistent with decreased fission (227). GDAP1, is an integral protein of the mitochondrial outer membrane, and is involved in mitochondrial fission, since depletion of this protein results in an increase in mitochondrial tubules and a

decrease in fission (228). Overexpression of GDAP1 in cells results in fragmented mitochondria. Interestingly, mutations of these proteins have also been found in patients with Charcot-Marie-Tooth disease (232). Detailed characterization of these proteins and their mechanistic function for fission need to be investigated, to provide insight into the regulation of recruitment, self assembly and post-translation modification of Drp1.

Studies in *C. elegans* and human cells have revealed that mitochondrial inner membrane constriction can occur independently of outer membrane fission in the absence of Drp1 or endophilin B1 function (39, 72, 208, 227). Additionally, in yeast cells, inner membrane constriction was also observed in the absence of functional Dnm1, and outer membrane fission. These findings suggest the existence of distinct inner membrane fission machinery (233-234). A very interesting hypothesis has been proposed, which speculated the involvement of OPA1 in regulating inner membrane fission (235-236). OPA1 may provide the molecular link between both fusion and fission machinery. It has often been suggested that fission regulates fusion, and that fusion regulates fission, and that these processes are not mutually exclusive. Since OPA1 has important molecular functions regulating crista morphology, it is fitting that it would regulate inner membrane constrictions. However, it is also thought that this notion of OPA1 constricting inner membranes through a dynamin like mechanism is unlikely since only the long form of OPA1 is integrated into the inner membrane (237).

Obviously, extensive studies of these proteins and of the mechanisms of inner membrane fission need to be performed to fully understand whether or not there exists separate inner membrane division machinery, and whether there are coordinating mechanisms of outer and inner membrane fission.

The details of how these above mentioned proteins contribute to the maintenance of both outer and inner membrane architecture, the recruitment of motility factors as well as mediating fission and fusion events, are largely unknown. However, they illustrate the fact that membrane dynamics as well as crista formation are not spontaneous events, and are highly active, regulated processes.

1.3.3.1 FISSION AND SUMOYLATION

Fission and Drp1 GTPase activity, have also recently been shown to be differentially regulated by post-translational modification via phosphorylation, ubiquitination and SUMOylation (225, 238-242). Drp1 is specifically phosphorylated by mitosis-promoting factor (MPF, Cdk1/cyclin B), a modification found to be essential for stimulating mitochondrial fragmentation during mitosis (238). It is also negatively regulated by Protein Kinase A, (PKA) a cAMP-dependent protein kinase-dependent phosphorylation within the GED domain (239). MARCH5 (MITOL) a ubiquitin E3 ligase negatively regulates mitochondrial fission through ubiquitination of Drp1 and as, would be expected, this ubiquitination promotes proteosomal mediated degradation (240-241). Previous studies in our lab have provided evidence for the role of SUMOylation in regulating Drp1 levels on the mitochondria and mitochondrial morphology (Figure 1.10) (225, 242). Overexpression of SUMO (small ubiquitin-related modifier) in mammalian cells or compromised MARCH5 function, result in fragmented mitochondria (240, 242), suggesting that SUMOylation and ubiquitination regulate mitochondrial fission by modulating levels of Drp1. It is interesting to note that this degree of regulation and post translational modification has not been observed in yeast systems.

Overexpression of SUMO1 or depletion of SENP5 (SUMO protease) by siRNA leads to fragmented mitochondria and these results demonstrate that SUMO modification results in fragmented mitochondria, suggesting that this reversible highly transient modification is essential for maintaining the balance between fission and fusion (Figure 1.10) (243). SUMO (small ubiquitin-related modifier) was identified as a reversible post-translational protein modifier about ten years ago. In the past ten years, hundreds of SUMO substrates have been identified and most of them are nuclear. Modification by SUMO can alter protein localization, activity and stability. SUMO proteins are ~10kDa in size and their 3D structure is similar to ubiquitin (244-245). In most SUMOylation events the conjugation of SUMO to substrate is monomeric, although some cases of polySUMOylation have been documented although the function is unknown. SUMO proteins are ubiquitously expressed in eukaryotes. A single SUMO gene exists in, *C. elegans* and *Drosophila melanogaster*. The human genome, however, has evolved four distinct SUMO proteins; SUMO1 to SUMO4. SUMO2 and SUMO3 are 97% identical, however, they are only 50% identical to SUMO1. SUMO1 and SUMO2/3, have distinct functions as they are selectively conjugated to different substrates (246). All SUMO proteins are found in an immature conjugation incompetent form and must be proteolytically processed to the mature form prior to conjugation. SUMO4 is the only SUMO protein which is not known to be processed into its mature form and as such has not been found to conjugate to any substrates.

The process of modification is similar to ubiquitination, in that it involves an enzymatic cascade utilizing an E1 activating enzyme, an E2 conjugating enzyme and an E3 ligase (246). Briefly, the E1 enzyme (AOS1-UBA2) in an ATP dependent reaction forms a high energy thioester bond with the C-terminal Gly residue of SUMO and the AOS1-UBA2. The E1 and the E2 (UBC9) enzymes then interact and SUMO is transferred to the E2

Figure 1.10 *SUMOylation and Mitochondrial Morphology*

The SUMOylation cycle of Drp1 is illustrated. Increased SUMOylation of Drp1 through the action of an unknown SUMO E3 ligase results in increased mitochondrial fission, whereas de-SUMOylation of Drp1 by the SUMO protease SENP5 results in decreased fission.

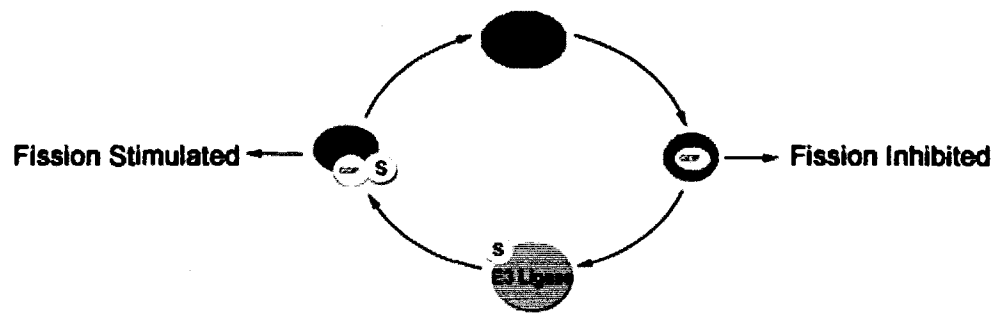


Figure 1.10 *SUMOylation and Mitochondrial Morphology*

forming a thioester linkage between the catalytic cysteine residue of UBC9 and the c-terminal carboxy group of SUMO. In the third step of SUMOylation, an isopeptide bond is formed between the C-terminal glycine residue of SUMO and a lysine residue in the substrate (246). The SUMO E3 ligase enzyme aids in this step as it provides the substrate specificity and catalyzes the transfer of SUMO from UBC9 to a substrate. There are three known classes of SUMO E3 ligases with the most characterized being those with an essential SP-RING domain. This RING domain is predicted to resemble the RING domain of ubiquitin E3 ligases. It is suggested that these E3 SUMO ligases function through binding the substrate and UBC9 directly, functioning as a platform to position the substrate and UBC9 in an optimal position for SUMO transfer. Members of this share a conserved SP-RING domain and a ~400 a.a N-terminal domain. Members of this type of E3 ligase include the PIAS family members (Siz1 and Siz2 in yeast (247, 248) and PIAS1, PIAS3 and the splice variants PIAS α , PIAS β and PIAS in mammalian cells) (249-252). These were initially identified for their ability to repress the transcription factor sTAT3 (PIAS: protein inhibitors of activated sTAT). The second type of SUMO E3 ligase is the nuclear pore protein RanBP2 (253). RanBP2 is vertebrate specific and does not mimic the action of a protein in the ubiquitination cascade. The catalytic domain of RanBP2 is natively unfolded and exerts its catalytic activity through folding around Ubc9 (254). Currently no known endogenous targets of RanBP2 are known, however *in vitro*, it SUMOylates proteins such as HDAC4, Sp100 and PML, but not its known binding partner RanGAP1 (253, 255-256). The third type of SUMO E3 ligase known is the human Polycomb group member Pc2 (257). These proteins are large multimeric complexes that are involved in gene silencing. These proteins were originally identified in *Drosophila melanogaster*, as protein required for stable and heritable repression of several genes. It is not known how Pc2 facilitates SUMOylation of

substrate proteins, however overexpression of Pc2 results in increased SUMOylation of ctBP (transcriptional co-repressor) (257-258).

Since increased expression of SUMO in tissue culture cells resulted in increased mitochondrial fission and, since DRP1 was found to co-localize with SUMO-YFP on mitochondrial membranes (242), it was hypothesized that a SUMO E3 ligase should function at the mitochondria.

Thus my third research objective #3; *To investigate the mechanisms of post-translational modification of Drp1 on the mitochondria, and to investigate the role of this modification on dynamics.*

This research focus led to identification and characterization of a novel protein involved in mitochondrial fission. This work is presented in chapter 3 as a published manuscript.

1.4 MITOCHONDRIAL DYNAMICS AND CELLULAR FUNCTION

1.4.1 MITOCHONDRIA AND APOPTOSIS

Apoptosis is a critical cellular phenomenon in which a cell undergoes programmed cell death, either, through extracellular death receptor signaling or through intracellular stressors. Apoptosis is essential for such things as embryonic development, tissue homeostasis and immune responses. Disruptions in the apoptotic signaling cascades can result in numerous proliferative and/or degenerative disorders including cancer, autoimmune diseases, and neurodegenerative diseases, to name a few. The mitochondria are also known to play an important role during cell death, as they sequester critical regulators of the apoptotic cascade such as cytochrome c and apoptosis inducing factor (AIF). During apoptosis, it has recently been observed that the mitochondrial membranes undergo dramatic remodeling events including fragmentation, cristea remodeling, and outer membrane

permeabilization (15, 259-260). There is a growing list of proteins which translocate to the mitochondria in a highly synchronized fashion, in addition to those that are systematically released from the mitochondrial intermembrane space and crista. The apoptotic factors which are sequentially released post cytochrome c release, then facilitate the formation of the apoptosome and initiation of the caspase cleavage cascade (15, 223, 259, 261).

Two classical apoptosis signaling cascades have been characterized in mammalian cells; the extrinsic receptor pathway and the mitochondrial pathway. The extrinsic pathway, is activated through binding of ligands to cell membrane receptors, such as Fas, TNF or the TRAIL receptors. Upon ligand binding, the receptors oligomerize, which triggers the recruitment of adaptor proteins and procaspases 8 and 10, to the receptor complex. The procaspases are activated and amplify the apoptosis signaling cascade through the caspase cascade in which downstream effector caspases like caspase 3 or 7 are activated (260). Within both of these pathways, diverse upstream signaling cascades emerge on the mitochondria to facilitate remodeling and death. These are still not well understood at the molecular level. What is known, however, is that upstream molecules (for example BH3-only proteins) respond to apoptotic stimuli and subsequently activate the multi-domain pro-apoptotic proteins. The requirement for fission, the role of Drp1, and the mechanism underlying membrane permeabilization of the outer membrane are not well understood. Permeabilization of the mitochondrial outer membrane, loss of potential and fragmentation of the network leads to the release of apoptogenic factors such as cytochrome c, Smac/Diablo, Omi/HtrA, endonuclease G, and AIF (262). Permeabilization is mediated in part by the recruitment and activation of the pro-apoptotic protein Bax, which forms a heterodimer with Bak, both of which are multi-domain pro-apoptotic Bcl-2 family proteins (263). This family of proteins contains both pro-apoptotic and anti-apoptotic proteins which have

between one and four BH domains (BH1-4). The pro-apoptotic BH3-only proteins respond to death signals and translocate to the mitochondria, where they activate the multi-domain pro-apoptotic proteins Bax and Bak (263). Both Drp1 and Fis1 are essential for the efficient execution of the mitochondrial death program. Expression of the dominant negative mutant of Drp1 (DrpK38E) blocks mitochondrial fission under stress conditions and delays the onset of apoptosis (264). Similarly loss of Fis1p blocks the recruitment and activation of Bax (264). It had also recently been shown that the overexpression of both Mitofusin proteins together resulted in delay in the onset of apoptosis and cytochrome c release.

Small amounts of cytochrome c reside near the boundary membrane and during the onset of apoptosis, can escape from the mitochondria. Since the majority of cytochrome c is sequestered deep within the cristea folds, the inner membranes must remodel and cristea junctions must open prior to the release of cytochrome c into the cytoplasm. This release has also been shown to occur prior to mitochondrial fragmentation (265). Electron tomography studies have characterized cristea remodeling events as, the widening of the narrow tubular junctions and, by the fusion of individual cristea. These morphological changes during apoptosis allow for the translocation of cytochrome c from the cristea folds to the IMS, for subsequent release to the cytosol. (266-267).

In an elegant study using fluorescence recovery after photobleaching, it was demonstrated, during apoptosis YFP-Drp1 undergoes a transition from rapid recycling to stable membrane association (Figure 1.11) (225). Drp1 was found to rapidly cycle on and off of the membranes and that this property was characteristic of the early stages of apoptosis where the mitochondria were undergoing fission events. Furthermore, this Drp1 recycling, occurs independently of Bax/Bak. Post Bax recruitment to the mitochondrial membranes, but before the loss of mitochondrial membrane potential, it was found that YFP-Drp1 becomes

Figure 1.11

Mitochondrial Drp1 and Apoptosis

Cartoon schematic illustrating the SUMO dependent, Bax/Bak dependent transition from rapid membrane recycling to stable membrane association of Drp1 during apoptosis. Drp1 puncta shown in red, SUMO in yellow and small blue dots illustrate released cytochrome c.

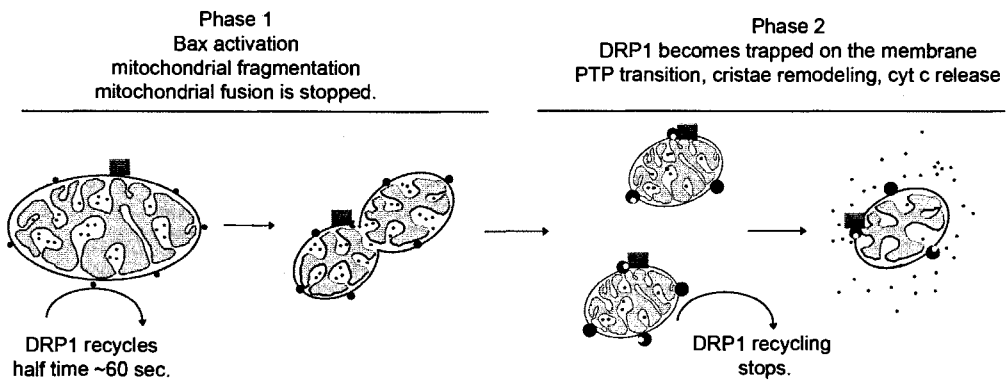


Figure 1.11

Mitochondrial Drp1 and Apoptosis

locked on the membrane (Figure 1.11). Unlike the rapid recycling, this membrane associated pool of Drp1 is dependent on the presence of Bax/Bak. Interestingly, the transition to stable membrane association occurs independently of hFis1 and independently of mitochondrial fragmentation. This study further demonstrated that the change in Drp1 recycling occurred concomitantly with the SUMOylation of Drp1 (225).

Using a mitochondrial matrix-targeted photoactivatable green fluorescent protein quantifying organelle fusion, it was found that during apoptosis, Mfn1 dependent mitochondrial fusion is blocked independently of caspase activation, and that this block occurs during Bax recruitment to the mitochondrial outer membrane (268). Interestingly, some OPA1 is co-released from the mitochondria with cytochrome c. This group then used RNA interference of OPA1 and observed structural changes in the mitochondrial crista and increased fragmentation thought to occur by a block in fusion. During apoptosis they found that OPA1 loss accelerated the rate of cytochrome c release. They hypothesize from their results that an initial mitochondrial leak of OPA1 leads to crista structural alterations which allow for the release of previously sequestered proteins. And that OPA1 depletion (though OPA1 release from the mitochondria) causes a block in mitochondrial fusion, which results in a dramatic increase of mitochondrial fragmentation seen during apoptosis (265).

Conversely, the over-expression of Opa1 in cells deficient for Mfn1 and Mfn2, had a protective effect, against a variety of apoptotic triggers. Although these cells had defective mitochondrial fusion, the protective effect observed by the overexpression of Opa1, suggests that it has dual functions in both fusion and apoptosis (237). Additionally, the protective effect of Opa1 did not interfere with the activation of Bax/Bak, instead, it was found that overexpression of Opa1 had a stabilizing effect on the diameter of the tubular junctions and prevented the mobilization of the sequestered pool of cytochrome c. They further

demonstrated that the tightness of the cristea junctions could be correlated to the oligomerization of two forms of Opa1 (soluble, intermembrane space s-Opa1 and an integral inner membrane l-Opa1) (237). Since Opa1 genetically interacts with Mfn1 for fusion, and that this relationship is distinct from its molecular role in maintaining tubular cristea junctions, it has been suggested that Opa1 has genetically and molecularly distinct functions in mitochondrial fusion and in cristae remodeling during apoptosis (237).

1.4.2 MFN2, SIGNALLING AND DISEASE

In addition to ATP synthesis and apoptosis, the mitochondria have recently been shown to have additional functions regulating cellular homeostasis through thermogenesis, calcium and iron homeostasis and intracellular signaling (appendix 2)(4). Mitochondrial damage and dysfunction have also been identified as important factors in the development of a host of diseases. A common theme linking mitochondrial dysfunction and disease is the accumulation of reactive oxygen species and cellular damage due to oxidative stress. Mitochondrial associated ROS damage has been linked to diseases such as schizophrenia, bipolar disorder, dementia, Alzheimer's disease, Parkinson's disease, epilepsy, strokes, heart disease, retinitis pigmentosa, and diabetes (269-270). Mutations in mitochondrial DNA can also be inherited, causing genetic disorders such as dominant optic atrophy, Friedreich's ataxia, hereditary spastic paraplegia, and Wilson's disease (271).

It is now becoming apparent that the mitochondria are positioned in the cell as a central regulator of diverse processes through a highly complex and largely undescribed signaling network (4). The emerging role of mitochondrial dynamics and the morphology regulatory proteins in mediating intracellular signaling cascades is highlighted as well as the

critical role of the mitochondria in cellular signaling cascades, metabolism, cell cycle control, development, the antiviral response and cell death. (appendix 2) (4).

Mitochondrial dysfunction is emerging as a mitigating factor in the development and progression of neurodegenerative diseases. It is thought that deficiencies in energy supply, free radical generation, Ca^{2+} buffering and or control of apoptosis, are all implicated in the degeneration of the nervous system. Emerging evidence highlights the sensitivity of neurons to mutations in genes encoding mitochondrial proteins. Mutations in morphology genes such as *Opal*, and *Mfn2*, are causative in certain neurodegenerative diseases and indicate that mitochondrial dynamics are especially important for the long-term maintenance of the nervous system (185, 272). For example, analysis of the mutations that cause CMT2A has revealed that the disease causing point mutations are concentrated near and in the GTPase domain, and in the C-terminal domain of *Mfn2* and effect mitochondrial oxidative phosphorylation (273). As another example, Parkinson disease resulting from dysfunction and loss of dopaminergic neurons highlights the importance of the mitochondria in disease progression. It is known that the death of dopamine neurons causes Parkinson's disease; however, it was not known what causes the death of these cells until recently. Numerous groups have demonstrated that the mitochondria play a common and central role in neurodegeneration, injury, plasticity and function in Parkinson's disease (274). Several causative Parkinson's disease genes, DJ-1, Parkin, LRRK2, and PINK1 have been at least partially localized or recruited to mitochondria, and impact their function. Furthermore, the role of PINK1 and Parkin, in regulating mitochondrial function and morphology has recently, been elucidated in *Drosophila* (274). The removal of the *Drosophila* PINK1 homologue, resulted in cristea fragmentation, male sterility, and apoptotic muscle degeneration. Removal of Parkin, resulted in similar phenotypes. These effects could be

rescued by the expression of human PINK1 or Parkin, demonstrating that these two proteins function in the same pathway, with pink1 functioning upstream of parkin. This discovery of PINK1 and Parkin, in regulating mitochondrial function, highlights the importance of mitochondrial dysfunction as a central mechanism of Parkinson's disease pathogenesis (4, 274).

The understanding of the molecular signals that govern mitochondrial morphology changes and apoptosis in neurons is therefore of critical importance. More specifically, elucidating the role of Mfn2 in response to acute neuronal injury is therefore crucial for understanding disease progression and for the development of novel therapeutic strategies. Due to the importance of Mfn2 in fusion, as well as its importance in the nervous system, in collaboration with Arezu Jahani-Asl and Ruth Slack of the neuroscience program at the Ottawa Health Research Institute, it was asked whether Mfn2 is involved in the regulation of acute injury using cerebellar granule neurons (appendix 1). Two specific questions were investigated whether Mfn2 could protect neurons against different mechanisms of injury? And whether this protection resulted from increased mitochondrial fusion and shifting the morphological equilibrium or through an additional role for Mfn2 that is distinct from the stimulation of mitochondrial fusion?

1.4.2.1 MFN2 AND METABOLISM

One of the best studied examples of mitochondrial signaling is that of mitochondrial proliferation. Staining of mitochondria is often used as a diagnostic tool when investigating mitochondrial disorders. Ragged-red fibers are often found in skeletal muscle, these correspond to increases in mitochondrial staining due to proliferation and increases in mitochondrial mass (29). For example, patients with MERRF (myoclonic epilepsy

associated with ragged-red fibers) syndrome have mutations within the tRNA of the mitochondria, this leads to decreased respiratory output due to OXPHOS defects (275-276). These defects are signaled back to the nucleus, and it is assumed that in response to low ATP levels the nucleus signals for increased mitochondrial proliferation. The detailed mechanisms of this signaling pathway however have not been elucidated (3). Mitochondrial proliferation is also found to occur in exercise-conditioned skeletal muscle (277) and in adipose tissue in response to cold exposure (278). These two examples clearly document that the mitochondria communicate their metabolic state with the nucleus in a feedback mechanism to direct their function and proliferation.

How the mitochondria mediate this communication, is an open question within the field of cell biology? Since the mitochondria are a self-contained organelle surrounded by two membranes, one of which is impermeable (inner membrane) except for gated protein channels, the ability of signaling molecules to communicate back and forth between the nucleus, is complex and intriguing to say the least. It has been suggested that signaling is mediated by; changes in metabolite and or ion flow in and out of the mitochondria (e.g., calcium signaling), or through changes in mitochondrial dynamics (altered fission / fusion) (4). The connections between morphology and nuclear signaling are intriguing and it has recently become known that the mitochondria are capable of dynamically responding to different environmental cues as detailed above. What is not yet known, however are the protein connections mediating the cause and effect.

One significant hypothesis of my doctoral thesis research was that Mfn2 somehow was capable of sensing a requirement for fusion and/or relaying a fusion signal to other mitochondria. Before two mitochondria are tethered through Mfn1 trans-coiled coil interactions, many steps must first occur. Each individual mitochondrion, within the

network, must be able to be cognitive of its internal environment (levels of ROS, mtDNA integrity, protein folding, metabolic outputs and respiratory capacity). If it requires a fusion event, it must be able to then communicate its status to the other mitochondria within the cell and with the nucleus. The donor mitochondria must then be capable of responding to this fusion signal, relay it internally, recruit motility factors, and move directly towards the acceptor mitochondria. Once in close opposition, the fusion complex /fusion pore must be assembled to resolve the membrane for complete content mixing. It was hypothesized that Mfn2, in a distinct role from Mfn1, facilitated this intracellular communication through its GTPase domain. This hypothesis followed on the first one of this study; that Mfn2 was a regulatory GTPase, active for fusion in the GTP bound form. Mfn2 in an active state would signal for fusion. Additionally, it was also hypothesized that the highly conserved intermembrane space loop of Mfn2 is critical for communication between the two membranes.

Interestingly, other studies were simultaneously suggesting a similar function for Mfn2, in mitochondrial to nuclear communication. In skeletal muscles post exercise, the levels of Mfn2 were found to increase during increased energy expenditure (279), during proliferation (279), and following cold exposure in a PGC-1 α responsive manner(280). It was also found that the mitochondria responded to different Mfn2 levels. Ectopic up regulation of Mfn2 increased expression of OXPHOS subunits, increased glucose oxidation, and increased deltapasi. Conversely, if Mfn2 levels are decreased, the cells responded by increasing glucose uptake for glycolysis (273). In support of this metabolic effect, Mfn2 protein and mRNA levels are reduced in skeletal muscle from obese patients and also in Zucker obese rat model (273, 281). Interestingly, Mfn2 has not been directly linked to the metabolic machineries themselves indicating that this effect is specific to the loss of the

fusion protein, rather than to defective fusion, (since stimulated mitochondrial fission does not interfere with metabolism). These data suggest that Mfn2 has a role in metabolic signaling that is distinct from its role in fusion (4).

1.4.2.2 MFN2 AND CELL CYCLE

Fzo1p in yeast was shown to be actively degraded by a proteasome dependent process during mating, in response to G-protein coupled receptor signaling initiated by the yeast α -mating factor (69). The selective degradation of Fzo1p indicated that it is intimately linked within the signaling cascades which initiate cell cycle and mating transitions in yeast. In the mammalian system, overexpression of Mfn2 has been implicated in inducing a cell cycle arrest at the G1 to S transition through Ras GTPase inhibition (282). Following typical epidermal growth factor signaling, ligand binding and receptor activation leads to Ras recruitment and activation. This leads to ERK phosphorylation at the plasma membrane which initiates a phosphorylation cascade of downstream effectors modulating cell cycle progression (282). Mfn2 overexpression inhibits the ERK phosphorylation cascade, and is believed to be linked to the cell cycle arrest. Reduced proliferation as a result of Mfn2 overexpression remained even when Mfn2 was not targeted to the mitochondria. These data further suggest that Mfn2 has specific signaling capabilities following receptor/ligand binding which are distinct from its role in mitochondrial fusion (4, 283).

1.5 RESEARCH OBJECTIVES

The complex mechanisms regulating mitochondrial morphology and the integration of signaling cascades with these events are largely unknown. The objectives of my doctoral thesis were to uncover the regulatory mechanisms of mitochondrial dynamics, examining both fusion and fission mechanisms. Two research projects are presented

#1 My first research project was to determine what the nucleotide properties of Mfn2 were and what type of GTPase Mfn2 is; mechano or regulatory?. Furthermore, it was hypothesized that if mitochondrial fusion could be stimulated through Mfn2 mutation, increased fusion would result in protection against apoptotic triggers. It was hypothesized that this delay would occur through either an inability to fragment the mitochondrial network and or through a protective signaling pathway mediated by activated Mfn2.

#2 Secondly investigations into the mechanism of fission and the post-translation modification of Drp1 led to the identification of a novel protein MAPL (Mitochondrial Anchored Protein Ligase) and the discovery of a new phenomenon of mitochondria in cell biology.

1.6 REFERENCES:

1. O'Brien, T.W. 2003. Properties of human mitochondrial ribosomes. *IUBMB Life* 55:505-513.
2. Spees, J.L., S.D. Olson, M.J. Whitney, and D.J. Prockop. 2006. Mitochondrial transfer between cells can rescue aerobic respiration. *Proc Natl Acad Sci U S A* 103:1283-1288.
3. Wallace, D.C. 2005. A mitochondrial paradigm of metabolic and degenerative diseases, aging, and cancer: a dawn for evolutionary medicine. *Annu Rev Genet* 39:359-407.
4. McBride, H.M., M. Neuspiel, and S. Wasiak. 2006. Mitochondria: more than just a powerhouse. *Curr Biol* 16:R551-560.
5. Westermann, B. 2007. Focus on mitochondria: introducing a new series in Trends in Cell Biology. *Trends Cell Biol*.
6. Chance, B., H. Sies, and A. Boveris. 1979. Hydroperoxide metabolism in mammalian organs. *Physiol Rev* 59:527-605.
7. Saraste, M. 1999. Oxidative phosphorylation at the fin de siecle. *Science* 283:1488-1493.
8. Hermann, G.J., and J.S. Shaw. 1998. Mitochondrial dynamics in yeast. *Annu. Rev. Cell Dev. Biol.* 14:265-303.
9. Dimmer, K.S., S. Fritz, F. Fuchs, M. Messerschmitt, N. Weinbach, W. Neupert, and B. Westermann. 2002. Genetic Basis of Mitochondrial Function and Morphology in *Saccharomyces cerevisiae*. *Mol Biol Cell* 13:847-853.
10. Scott, S.V., A. Cassidy-Stone, S.L. Meeusen, and J. Nunnari. 2003. Staying in aerobic shape: how the structural integrity of mitochondria and mitochondrial DNA is maintained. *Curr Opin Cell Biol* 15:482-488.
11. Chung, S., P.P. Dzeja, R.S. Faustino, C. Perez-Terzic, A. Behfar, and A. Terzic. 2007. Mitochondrial oxidative metabolism is required for the cardiac differentiation of stem cells. *Nat Clin Pract Cardiovasc Med* 4 Suppl 1:S60-67.
12. Li, Z., K. Okamoto, Y. Hayashi, and M. Sheng. 2004. The importance of dendritic mitochondria in the morphogenesis and plasticity of spines and synapses. *Cell* 119:873-887.
13. Karbowski, M., Y.J. Lee, B. Gaume, S.Y. Jeong, S. Frank, A. Nechushtan, A. Santel, M. Fuller, C.L. Smith, and R.J. Youle. 2002. Spatial and temporal association of Bax with mitochondrial fission sites, Drp1, and Mfn2 during apoptosis. *J Cell Biol* 159:931-938.

14. Youle, R.J., and M. Karbowski. 2005. Mitochondrial fission in apoptosis. *Nat Rev Mol Cell Biol* 6:657-663.
15. Breckenridge, D.G., M. Stojanovic, R.C. Marcellus, and G.C. Shore. 2003. Caspase cleavage product of BAP31 induces mitochondrial fission through endoplasmic reticulum calcium signals, enhancing cytochrome c release to the cytosol. *J Cell Biol* 160:1115-1127.
16. Frey, T.G., and C.A. Mannella. 2000. The internal structure of mitochondria. *Trends Biochem. Sci.* 25:319-324.
17. Koehler, C.M., K.N. Beverly, and E.P. Leverich. 2006. Redox pathways of the mitochondrion. *Antioxid Redox Signal* 8:813-822.
18. Webb, C.T., M.A. Gorman, M. Lazarou, M.T. Ryan, and J.M. Gulbis. 2006. Crystal structure of the mitochondrial chaperone TIM9.10 reveals a six-bladed alpha-propeller. *Mol Cell* 21:123-133.
19. Mannella, C.A. 2006. Structure and dynamics of the mitochondrial inner membrane cristae. *Biochim Biophys Acta* 1763:542-548.
20. Arco, A.D., and J. Satrustegui. 2005. New mitochondrial carriers: an overview. *Cell Mol Life Sci* 62:2204-2227.
21. Ryan, M.T., and N.J. Hoogenraad. 2007. Mitochondrial-nuclear communications. *Annu Rev Biochem* 76:701-722.
22. Brookes, P.S., Y. Yoon, J.L. Robotham, M.W. Anders, and S.S. Sheu. 2004. Calcium, ATP, and ROS: a mitochondrial love-hate triangle. *Am J Physiol Cell Physiol* 287:C817-833.
23. Wallace, D.C. 1999. Mitochondrial diseases in man and mouse. *Science* 283:1482-1488.
24. Legros, F., F. Malka, P. Frachon, A. Lombes, and M. Rojo. 2004. Organization and dynamics of human mitochondrial DNA. *J Cell Sci* 117:2653-2662. Epub 2004 May 2611.
25. Wallace, D.C. 1992. Diseases of the mitochondrial DNA. *Annu Rev Biochem* 61:1175-1212.
26. Ranger, A.M., B.A. Malynn, and S.J. Korsmeyer. 2001. Mouse models of cell death. *Nat Genet* 28:113-118.
27. Crompton, M. 1999. The mitochondrial permeability transition pore and its role in cell death. *Biochem J* 341 (Pt 2):233-249.

28. Haworth, R.A., and D.R. Hunter. 1979. The Ca²⁺-induced membrane transition in mitochondria. II. Nature of the Ca²⁺ trigger site. *Arch Biochem Biophys* 195:460-467.
29. Shoubridge, E.A. 1994. Mitochondrial DNA diseases: histological and cellular studies. *J Bioenerg Biomembr* 26:301-310.
30. Butow, R.A., and E.M. Bahassi. 1999. Adaptive thermogenesis: orchestrating mitochondrial biogenesis. *Curr Biol* 9:R767-769.
31. Puigserver, P., Z. Wu, C.W. Park, R. Graves, M. Wright, and B.M. Spiegelman. 1998. A cold-inducible coactivator of nuclear receptors linked to adaptive thermogenesis. *Cell* 92:829-839.
32. Yoon, J.C., P. Puigserver, G. Chen, J. Donovan, Z. Wu, J. Rhee, G. Adelmant, J. Stafford, C.R. Kahn, D.K. Granner, C.B. Newgard, and B.M. Spiegelman. 2001. Control of hepatic gluconeogenesis through the transcriptional coactivator PGC-1. *Nature* 413:131-138.
33. Baar, K., A.R. Wende, T.E. Jones, M. Marison, L.A. Nolte, M. Chen, D.P. Kelly, and J.O. Holloszy. 2002. Adaptations of skeletal muscle to exercise: rapid increase in the transcriptional coactivator PGC-1. *Faseb J* 16:1879-1886.
34. Norrbom, J., C.J. Sundberg, H. Ameln, W.E. Kraus, E. Jansson, and T. Gustafsson. 2004. PGC-1alpha mRNA expression is influenced by metabolic perturbation in exercising human skeletal muscle. *J Appl Physiol* 96:189-194.
35. Houten, S.M., and J. Auwerx. 2004. PGC-1alpha: turbocharging mitochondria. *Cell* 119:5-7.
36. Wu, Z., P. Puigserver, U. Andersson, C. Zhang, G. Adelmant, V. Mootha, A. Troy, S. Cinti, B. Lowell, R.C. Scarpulla, and B.M. Spiegelman. 1999. Mechanisms controlling mitochondrial biogenesis and respiration through the thermogenic coactivator PGC-1. *Cell* 98:115-124.
37. Liu, Z., and R.A. Butow. 1999. A transcriptional switch in the expression of yeast tricarboxylic acid cycle genes in response to a reduction or loss of respiratory function. *Mol Cell Biol* 19:6720-6728.
38. Amuthan, G., G. Biswas, H.K. Ananadatheerthavarada, C. Vijayasathy, H.M. Shephard, and N.G. Avadhani. 2002. Mitochondrial stress-induced calcium signaling, phenotypic changes and invasive behavior in human lung carcinoma A549 cells. *Oncogene* 21:7839-7849.
39. Zhao, Q., J. Wang, I.V. Levichkin, S. Stasinopoulos, M.T. Ryan, and N.J. Hoogenraad. 2002. A mitochondrial specific stress response in mammalian cells. *Embo J* 21:4411-4419.

40. Haynes, C.M., K. Petrova, C. Benedetti, Y. Yang, and D. Ron. 2007. ClpP mediates activation of a mitochondrial unfolded protein response in *C. elegans*. *Dev Cell* 13:467-480.
41. Butow, R.A., and N.G. Avadhani. 2004. Mitochondrial signaling: the retrograde response. *Mol Cell* 14:1-15.
42. Kelly, D.P., and R.C. Scarpulla. 2004. Transcriptional regulatory circuits controlling mitochondrial biogenesis and function. *Genes Dev* 18:357-368.
43. Garesse, R., and C.G. Vallejo. 2001. Animal mitochondrial biogenesis and function: a regulatory cross-talk between two genomes. *Gene* 263:1-16.
44. Mootha, V.K., C.M. Lindgren, K.F. Eriksson, A. Subramanian, S. Sihag, J. Lehar, P. Puigserver, E. Carlsson, M. Ridderstrale, E. Laurila, N. Houstis, M.J. Daly, N. Patterson, J.P. Mesirov, T.R. Golub, P. Tamayo, B. Spiegelman, E.S. Lander, J.N. Hirschhorn, D. Altshuler, and L.C. Groop. 2003. PGC-1alpha-responsive genes involved in oxidative phosphorylation are coordinately downregulated in human diabetes. *Nat Genet* 34:267-273.
45. Vega, R.B., J.M. Huss, and D.P. Kelly. 2000. The coactivator PGC-1 cooperates with peroxisome proliferator-activated receptor alpha in transcriptional control of nuclear genes encoding mitochondrial fatty acid oxidation enzymes. *Mol Cell Biol* 20:1868-1876.
46. Finck, B.N., J.J. Lehman, P.M. Barger, and D.P. Kelly. 2002. Regulatory networks controlling mitochondrial energy production in the developing, hypertrophied, and diabetic heart. *Cold Spring Harb Symp Quant Biol* 67:371-382.
47. Lin, J., C. Handschin, and B.M. Spiegelman. 2005. Metabolic control through the PGC-1 family of transcription coactivators. *Cell Metab* 1:361-370.
48. Puigserver, P., and B.M. Spiegelman. 2003. Peroxisome proliferator-activated receptor-gamma coactivator 1 alpha (PGC-1 alpha): transcriptional coactivator and metabolic regulator. *Endocr Rev* 24:78-90.
49. Neupert, W., and J.M. Herrmann. 2007. Translocation of proteins into mitochondria. *Annu Rev Biochem* 76:723-749.
50. Lister, R., M.W. Murcha, and J. Whelan. 2003. The Mitochondrial Protein Import Machinery of Plants (MPIMP) database. *Nucleic Acids Res* 31:325-327.
51. Schatz, G., and B. Dobberstein. 1996. Common principles of protein translocation across membranes. *Science* 271:1519-1526.
52. Pfanner, N., and A. Geissler. 2001. Versatility of the mitochondrial protein import machinery. *Nat Rev Mol Cell Biol* 2:339-349.

53. Hoogenraad, N.J., L.A. Ward, and M.T. Ryan. 2002. Import and assembly of proteins into mitochondria of mammalian cells. *Biochim Biophys Acta* 1592:97-105.
54. Young, J.C., N.J. Hoogenraad, and F.U. Hartl. 2003. Molecular chaperones Hsp90 and Hsp70 deliver preproteins to the mitochondrial import receptor Tom70. *Cell* 112:41-50.
55. Hill, K., K. Model, M.T. Ryan, K. Dietmeier, F. Martin, R. Wagner, and N. Pfanner. 1998. Tom40 forms the hydrophilic channel of the mitochondrial import pore for preproteins [see comment]. *Nature* 395:516-521.
56. Model, K., C. Meisinger, T. Prinz, N. Wiedemann, K.N. Truscott, N. Pfanner, and M.T. Ryan. 2001. Multistep assembly of the protein import channel of the mitochondrial outer membrane. *Nat Struct Biol* 8:361-370.
57. Hoppins, S.C., and F.E. Nargang. 2004. The Tim8-Tim13 complex of *Neurospora crassa* functions in the assembly of proteins into both mitochondrial membranes. *J Biol Chem* 279:12396-12405.
58. Wiedemann, N., A.E. Frazier, and N. Pfanner. 2004. The protein import machinery of mitochondria. *J Biol Chem* 279:14473-14476.
59. Voos, W., and K. Rottgers. 2002. Molecular chaperones as essential mediators of mitochondrial biogenesis. *Biochim Biophys Acta* 1592:51-62.
60. Jensen, R.E., and A.E. Johnson. 2001. Opening the door to mitochondrial protein import. *Nat Struct Biol* 8:1008-1010.
61. Truscott, K.N., P. Kovermann, A. Geissler, A. Merlin, M. Meijer, A.J. Driessen, J. Rassow, N. Pfanner, and R. Wagner. 2001. A presequence- and voltage-sensitive channel of the mitochondrial preprotein translocase formed by Tim23. *Nat Struct Biol* 8:1074-1082.
62. Sirrenberg, C., M.F. Bauer, B. Guiard, W. Neupert, and M. Brunner. 1996. Import of carrier proteins into the mitochondrial inner membrane mediated by Tim22. *Nature* 384:582-585.
63. Kovermann, P., K.N. Truscott, B. Guiard, P. Rehling, N.B. Sepuri, H. Muller, R.E. Jensen, R. Wagner, and N. Pfanner. 2002. Tim22, the essential core of the mitochondrial protein insertion complex, forms a voltage-activated and signal-gated channel. *Mol Cell* 9:363-373.
64. Martinus, R.D., M.T. Ryan, D.J. Naylor, S.M. Herd, N.J. Hoogenraad, and P.B. Hoj. 1995. Role of chaperones in the biogenesis and maintenance of the mitochondrion. *Faseb J* 9:371-378.
65. Dubiel, W., and S.M. Rapoport. 1989. ATP-dependent proteolysis of mitochondria of reticulocytes. *Revis Biol Celular* 21:505-521.

66. Sutovsky, P., R.D. Moreno, J. Ramalho-Santos, T. Dominko, C. Simerly, and G. Schatten. 1999. Ubiquitin tag for sperm mitochondria. *Nature* 402:371-372.
67. Rapoport, S., W. Dubiel, and M. Muller. 1985. Proteolysis of mitochondria in reticulocytes during maturation is ubiquitin-dependent and is accompanied by a high rate of ATP hydrolysis. *FEBS Lett* 180:249-252.
68. Sutovsky, P., R.D. Moreno, J. Ramalho-Santos, T. Dominko, C. Simerly, and G. Schatten. 2000. Ubiquitinated sperm mitochondria, selective proteolysis, and the regulation of mitochondrial inheritance in mammalian embryos. *Biol Reprod* 63:582-590.
69. Neutzner, A., and R.J. Youle. 2005. Instability of the mitofusin Fzo1 regulates mitochondrial morphology during the mating response of the yeast *Saccharomyces cerevisiae*. *J Biol Chem* 280:18598-18603.
70. Escobar-Henriques, M., B. Westermann, and T. Langer. 2006. Regulation of mitochondrial fusion by the F-box protein Mdm30 involves proteasome-independent turnover of Fzo1. *J Cell Biol* 173:645-650.
71. Fritz, S., N. Weinbach, and B. Westermann. 2003. Mdm30 is an F-box protein required for maintenance of fusion-competent mitochondria in yeast. *Mol Biol Cell* 14:2303-2313.
72. Petroski, M.D., and R.J. Deshaies. 2005. In vitro reconstitution of SCF substrate ubiquitination with purified proteins. *Methods Enzymol* 398:143-158.
73. Durr, M., M. Escobar-Henriques, S. Merz, S. Geimer, T. Langer, and B. Westermann. 2006. Nonredundant roles of mitochondria-associated F-box proteins Mfb1 and Mdm30 in maintenance of mitochondrial morphology in yeast. *Mol Biol Cell* 17:3745-3755.
74. Kissova, I., M. Deffieu, S. Manon, and N. Camougrand. 2004. Uth1p is involved in the autophagic degradation of mitochondria. *J Biol Chem* 279:39068-39074.
75. Takeshige, K., M. Baba, S. Tsuboi, T. Noda, and Y. Ohsumi. 1992. Autophagy in yeast demonstrated with proteinase-deficient mutants and conditions for its induction. *J Cell Biol* 119:301-311.
76. Russell, S.M., R.J. Burgess, and R.J. Mayer. 1980. Protein degradation in rat liver during post-natal development. *Biochem J* 192:321-330.
77. Russell, S.M., R.J. Burgess, and R.J. Mayer. 1982. Protein degradation in rat liver. Evidence for populations of protein degradation rates in cellular organelles. *Biochim Biophys Acta* 714:34-45.
78. Dice, J.F., and A.L. Goldberg. 1975. Relationship between in vivo degradative rates and isoelectric points of proteins. *Proc Natl Acad Sci U S A* 72:3893-3897.

79. Lipsky, N.G., and P.L. Pedersen. 1981. Mitochondrial turnover in animal cells. Half-lives of mitochondria and mitochondrial subfractions of rat liver based on [14C]bicarbonate incorporation. *J Biol Chem* 256:8652-8657.
80. Bota, D.A., and K.J. Davies. 2001. Protein degradation in mitochondria: implications for oxidative stress, aging and disease: a novel etiological classification of mitochondrial proteolytic disorders. *Mitochondrion* 1:33-49.
81. Mortimore, G.E., G. Miotto, R. Venerando, and M. Kadowaki. 1996. Autophagy. *Subcell Biochem* 27:93-135.
82. Takano-Ohmuro, H., M. Mukaida, E. Kominami, and K. Morioka. 2000. Autophagy in embryonic erythroid cells: its role in maturation. *Eur J Cell Biol* 79:759-764.
83. Scherz-Shouval, R., and Z. Elazar. 2007. ROS, mitochondria and the regulation of autophagy. *Trends Cell Biol* 17:422-427.
84. Maiuri, M.C., E. Zalckvar, A. Kimchi, and G. Kroemer. 2007. Self-eating and self-killing: crosstalk between autophagy and apoptosis. *Nat Rev Mol Cell Biol* 8:741-752.
85. Ohsumi, Y. 2001. Molecular dissection of autophagy: two ubiquitin-like systems. *Nat Rev Mol Cell Biol* 2:211-216.
86. Klionsky, D.J., and S.D. Emr. 2000. Autophagy as a regulated pathway of cellular degradation. *Science* 290:1717-1721.
87. Shintani, T., and D.J. Klionsky. 2004. Autophagy in health and disease: a double-edged sword. *Science* 306:990-995.
88. Grune, T., K. Merker, G. Sandig, and K.J. Davies. 2003. Selective degradation of oxidatively modified protein substrates by the proteasome. *Biochem Biophys Res Commun* 305:709-718.
89. Kiffin, R., U. Bandyopadhyay, and A.M. Cuervo. 2006. Oxidative stress and autophagy. *Antioxid Redox Signal* 8:152-162.
90. Lemasters, J.J. 2005. Selective mitochondrial autophagy, or mitophagy, as a targeted defense against oxidative stress, mitochondrial dysfunction, and aging. *Rejuvenation Res* 8:3-5.
91. Terman, A., and U.T. Brunk. 1998. Lipofuscin: mechanisms of formation and increase with age. *Apmis* 106:265-276.
92. Donati, A., G. Cavallini, C. Paradiso, S. Vittorini, M. Pollera, Z. Gori, and E. Bergamini. 2001. Age-related changes in the regulation of autophagic proteolysis in rat isolated hepatocytes. *J Gerontol A Biol Sci Med Sci* 56:B288-293.

93. Rubinsztein, D.C. 2006. The roles of intracellular protein-degradation pathways in neurodegeneration. *Nature* 443:780-786.
94. Cuervo, A.M., and J.F. Dice. 2000. Age-related decline in chaperone-mediated autophagy. *J Biol Chem* 275:31505-31513.
95. Cataldo, A.M., D.J. Hamilton, J.L. Barnett, P.A. Paskevich, and R.A. Nixon. 1996. Properties of the endosomal-lysosomal system in the human central nervous system: disturbances mark most neurons in populations at risk to degenerate in Alzheimer's disease. *J Neurosci* 16:186-199.
96. Sooparb, S., S.R. Price, J. Shaoguang, and H.A. Franch. 2004. Suppression of chaperone-mediated autophagy in the renal cortex during acute diabetes mellitus. *Kidney Int* 65:2135-2144.
97. Priault, M., B. Salin, J. Schaeffer, F.M. Vallette, J.P. di Rago, and J.C. Martinou. 2005. Impairing the bioenergetic status and the biogenesis of mitochondria triggers mitophagy in yeast. *Cell Death Differ* 12:1613-1621.
98. Gozuacik, D., and A. Kimchi. 2007. Autophagy and cell death. *Curr Top Dev Biol* 78:217-245.
99. Codogno, P., and A.J. Meijer. 2005. Autophagy and signaling: their role in cell survival and cell death. *Cell Death Differ* 12 Suppl 2:1509-1518.
100. Thumm, M., R. Egner, B. Koch, M. Schlumpberger, M. Straub, M. Veenhuis, and D.H. Wolf. 1994. Isolation of autophagocytosis mutants of *Saccharomyces cerevisiae*. *FEBS Lett* 349:275-280.
101. Mizushima, N., Y. Ohsumi, and T. Yoshimori. 2002. Autophagosome formation in mammalian cells. *Cell Struct Funct* 27:421-429.
102. Kawamata, T., Y. Kamada, K. Suzuki, N. Kuboshima, H. Akimatsu, S. Ota, M. Ohsumi, and Y. Ohsumi. 2005. Characterization of a novel autophagy-specific gene, ATG29. *Biochem Biophys Res Commun* 338:1884-1889.
103. Reggiori, F., K.A. Tucker, P.E. Stromhaug, and D.J. Klionsky. 2004. The Atg1-Atg13 complex regulates Atg9 and Atg23 retrieval transport from the pre-autophagosomal structure. *Dev Cell* 6:79-90.
104. Reggiori, F., T. Shintani, U. Nair, and D.J. Klionsky. 2005. Atg9 cycles between mitochondria and the pre-autophagosomal structure in yeasts. *Autophagy* 1:101-109.
105. Nair, U., and D.J. Klionsky. 2005. Molecular mechanisms and regulation of specific and nonspecific autophagy pathways in yeast. *J Biol Chem* 280:41785-41788.
106. Mijaljica, D., M. Prescott, and R.J. Devenish. 2007. Different fates of mitochondria: alternative ways for degradation? *Autophagy* 3:4-9.

107. de Grey, A.D. 2000. The reductive hotspot hypothesis: an update. *Arch Biochem Biophys* 373:295-301.
108. Coleman, R., M. Silbermann, D. Gershon, and A.Z. Reznick. 1987. Giant mitochondria in the myocardium of aging and endurance-trained mice. *Gerontology* 33:34-39.
109. Matsui, M., A. Yamamoto, A. Kuma, Y. Ohsumi, and N. Mizushima. 2006. Organelle degradation during the lens and erythroid differentiation is independent of autophagy. *Biochem Biophys Res Commun* 339:485-489.
110. Koppen, M., and T. Langer. 2007. Protein degradation within mitochondria: versatile activities of AAA proteases and other peptidases. *Crit Rev Biochem Mol Biol* 42:221-242.
111. Augustin, S., M. Nolden, S. Muller, O. Hardt, I. Arnold, and T. Langer. 2005. Characterization of peptides released from mitochondria: evidence for constant proteolysis and peptide efflux. *J Biol Chem* 280:2691-2699.
112. Loveland, B., C.R. Wang, H. Yonekawa, E. Hermel, and K.F. Lindahl. 1990. Maternally transmitted histocompatibility antigen of mice: a hydrophobic peptide of a mitochondrially encoded protein. *Cell* 60:971-980.
113. Young, L., K. Leonhard, T. Tatsuta, J. Trowsdale, and T. Langer. 2001. Role of the ABC transporter Mdl1 in peptide export from mitochondria. *Science* 291:2135-2138.
114. Gakh, O., P. Cavadini, and G. Isaya. 2002. Mitochondrial processing peptidases. *Biochim Biophys Acta* 1592:63-77.
115. Hawlitschek, G., H. Schneider, B. Schmidt, M. Tropschug, F.U. Hartl, and W. Neupert. 1988. Mitochondrial protein import: identification of processing peptidase and of PEP, a processing enhancing protein. *Cell* 53:795-806.
116. Yang, M., R.E. Jensen, M.P. Yaffe, W. Oppliger, and G. Schatz. 1988. Import of proteins into yeast mitochondria: the purified matrix processing protease contains two subunits which are encoded by the nuclear MAS1 and MAS2 genes. *Embo J* 7:3857-3862.
117. Ou, W.J., A. Ito, H. Okazaki, and T. Omura. 1989. Purification and characterization of a processing protease from rat liver mitochondria. *Embo J* 8:2605-2612.
118. Kalousek, F., G. Isaya, and L.E. Rosenberg. 1992. Rat liver mitochondrial intermediate peptidase (MIP): purification and initial characterization. *Embo J* 11:2803-2809.
119. Isaya, G., F. Kalousek, W.A. Fenton, and L.E. Rosenberg. 1991. Cleavage of precursors by the mitochondrial processing peptidase requires a compatible mature protein or an intermediate octapeptide. *J Cell Biol* 113:65-76.

120. Isaya, G., F. Kalousek, and L.E. Rosenberg. 1992. Sequence analysis of rat mitochondrial intermediate peptidase: similarity to zinc metallopeptidases and to a putative yeast homologue. *Proc Natl Acad Sci U S A* 89:8317-8321.
121. Daum, G., S.M. Gasser, and G. Schatz. 1982. Import of proteins into mitochondria. Energy-dependent, two-step processing of the intermembrane space enzyme cytochrome b2 by isolated yeast mitochondria. *J Biol Chem* 257:13075-13080.
122. Nunnari, J., T.D. Fox, and P. Walter. 1993. A mitochondrial protease with two catalytic subunits of nonoverlapping specificities. *Science* 262:1997-2004.
123. Burri, L., Y. Strahm, C.J. Hawkins, I.E. Gentle, M.A. Puryer, A. Verhagen, B. Callus, D. Vaux, and T. Lithgow. 2005. Mature DIABLO/Smac is produced by the IMP protease complex on the mitochondrial inner membrane. *Mol Biol Cell* 16:2926-2933.
124. Herlan, M., F. Vogel, C. Bornhovd, W. Neupert, and A.S. Reichert. 2003. Processing of Mgm1 by the rhomboid-type protease Pcp1 is required for maintenance of mitochondrial morphology and of mitochondrial DNA. *J Biol Chem* 278:27781-27788.
125. McQuibban, G.A., S. Saurya, and M. Freeman. 2003. Mitochondrial membrane remodelling regulated by a conserved rhomboid protease. *Nature* 423:537-541.
126. Sesaki, H., S.M. Southard, A.E. Hobbs, and R.E. Jensen. 2003. Cells lacking Pcp1p/Ugo2p, a rhomboid-like protease required for Mgm1p processing, lose mtDNA and mitochondrial structure in a Dnm1p-dependent manner, but remain competent for mitochondrial fusion. *Biochem Biophys Res Commun* 308:276-283.
127. Van Dyck, L., and T. Langer. 1999. ATP-dependent proteases controlling mitochondrial function in the yeast *Saccharomyces cerevisiae*. *Cell Mol Life Sci* 56:825-842.
128. Suzuki, C.K., K. Suda, N. Wang, and G. Schatz. 1994. Requirement for the yeast gene LON in intramitochondrial proteolysis and maintenance of respiration. *Science* 264:891.
129. Van Dyck, L., D.A. Pearce, and F. Sherman. 1994. PIM1 encodes a mitochondrial ATP-dependent protease that is required for mitochondrial function in the yeast *Saccharomyces cerevisiae*. *J Biol Chem* 269:238-242.
130. Wang, N., M.R. Maurizi, L. Emmert-Buck, and M.M. Gottesman. 1994. Synthesis, processing, and localization of human Lon protease. *J Biol Chem* 269:29308-29313.
131. Bota, D.A., and K.J. Davies. 2002. Lon protease preferentially degrades oxidized mitochondrial aconitase by an ATP-stimulated mechanism. *Nat Cell Biol* 4:674-680.

132. van Dyck, L., W. Neupert, and T. Langer. 1998. The ATP-dependent PIM1 protease is required for the expression of intron-containing genes in mitochondria. *Genes Dev* 12:1515-1524.
133. Santagata, S., D. Bhattacharyya, F.H. Wang, N. Singha, A. Hodtsev, and E. Spanopoulou. 1999. Molecular cloning and characterization of a mouse homolog of bacterial ClpX, a novel mammalian class II member of the Hsp100/Clp chaperone family. *J Biol Chem* 274:16311-16319.
134. Langer, T. 2000. AAA proteases: cellular machines for degrading membrane proteins. *Trends Biochem Sci* 25:247-251.
135. Shah, Z.H., G.A. Hakkaart, B. Arku, L. de Jong, H. van der Spek, L.A. Grivell, and H.T. Jacobs. 2000. The human homologue of the yeast mitochondrial AAA metalloprotease Yme1p complements a yeast yme1 disruptant. *FEBS Lett* 478:267-270.
136. Atorino, L., L. Silvestri, M. Koppen, L. Cassina, A. Ballabio, R. Marconi, T. Langer, and G. Casari. 2003. Loss of m-AAA protease in mitochondria causes complex I deficiency and increased sensitivity to oxidative stress in hereditary spastic paraplegia. *J Cell Biol* 163:777-787.
137. Nolden, M., S. Ehses, M. Koppen, A. Bernacchia, E.I. Rugarli, and T. Langer. 2005. The m-AAA protease defective in hereditary spastic paraplegia controls ribosome assembly in mitochondria. *Cell* 123:277-289.
138. Casari, G., M. De Fusco, S. Ciarmatori, M. Zeviani, M. Mora, P. Fernandez, G. De Michele, A. Filla, S. Coccozza, R. Marconi, A. Durr, B. Fontaine, and A. Ballabio. 1998. Spastic paraplegia and OXPHOS impairment caused by mutations in paraplegin, a nuclear-encoded mitochondrial metalloprotease. *Cell* 93:973-983.
139. Banfi, S., M.T. Bassi, G. Andolfi, A. Marchitello, S. Zanotta, A. Ballabio, G. Casari, and B. Franco. 1999. Identification and characterization of AFG3L2, a novel paraplegin-related gene. *Genomics* 59:51-58.
140. Ozelius, L.J., C.E. Page, C. Klein, J.W. Hewett, M. Mineta, J. Leung, C. Shalish, S.B. Bressman, D. de Leon, M.F. Brin, S. Fahn, D.P. Corey, and X.O. Breakefield. 1999. The TOR1A (DYT1) gene family and its role in early onset torsion dystonia. *Genomics* 62:377-384.
141. Koutnikova, H., V. Campuzano, and M. Koenig. 1998. Maturation of wild-type and mutated frataxin by the mitochondrial processing peptidase. *Hum Mol Genet* 7:1485-1489.
142. Branda, S.S., P. Cavadini, J. Adamec, F. Kalousek, F. Taroni, and G. Isaya. 1999. Yeast and human frataxin are processed to mature form in two sequential steps by the mitochondrial processing peptidase. *J Biol Chem* 274:22763-22769.

143. Tanner, A.J., and J.F. Dice. 1996. Batten disease and mitochondrial pathways of proteolysis. *Biochem Mol Med* 57:1-9.
144. Boldogh, I.R., and L.A. Pon. 2007. Mitochondria on the move. *Trends Cell Biol* 17:502-510.
145. Hollenbeck, P.J., and W.M. Saxton. 2005. The axonal transport of mitochondria. *J Cell Sci* 118:5411-5419.
146. Hirokawa, N., and R. Takemura. 2005. Molecular motors and mechanisms of directional transport in neurons. *Nat Rev Neurosci* 6:201-214.
147. Martin, M., S.J. Iyadurai, A. Gassman, J.G. Gindhart, Jr., T.S. Hays, and W.M. Saxton. 1999. Cytoplasmic dynein, the dynactin complex, and kinesin are interdependent and essential for fast axonal transport. *Mol Biol Cell* 10:3717-3728.
148. Waterman-Storer, C.M., S.B. Karki, S.A. Kuznetsov, J.S. Tabb, D.G. Weiss, G.M. Langford, and E.L. Holzbaaur. 1997. The interaction between cytoplasmic dynein and dynactin is required for fast axonal transport. *Proc Natl Acad Sci U S A* 94:12180-12185.
149. Pilling, A.D., D. Horiuchi, C.M. Lively, and W.M. Saxton. 2006. Kinesin-1 and Dynein are the primary motors for fast transport of mitochondria in *Drosophila* motor axons. *Mol Biol Cell* 17:2057-2068.
150. Ligon, L.A., M. Tokito, J.M. Finklestein, F.E. Grossman, and E.L. Holzbaaur. 2004. A direct interaction between cytoplasmic dynein and kinesin I may coordinate motor activity. *J Biol Chem* 279:19201-19208.
151. Guo, X., G.T. Macleod, A. Wellington, F. Hu, S. Panchumarthi, M. Schoenfield, L. Marin, M.P. Charlton, H.L. Atwood, and K.E. Zinsmaier. 2005. The GTPase dMiro is required for axonal transport of mitochondria to *Drosophila* synapses. *Neuron* 47:379-393.
152. Stowers, R.S., L.J. Megeath, J. Gorska-Andrzejak, I.A. Meinertzhagen, and T.L. Schwarz. 2002. Axonal transport of mitochondria to synapses depends on milton, a novel *Drosophila* protein. *Neuron* 36:1063-1077.
153. Glater, E.E., L.J. Megeath, R.S. Stowers, and T.L. Schwarz. 2006. Axonal transport of mitochondria requires milton to recruit kinesin heavy chain and is light chain independent. *J Cell Biol* 173:545-557.
154. Brickley, K., M.J. Smith, M. Beck, and F.A. Stephenson. 2005. GRIF-1 and OIP106, members of a novel gene family of coiled-coil domain proteins: association in vivo and in vitro with kinesin. *J Biol Chem* 280:14723-14732.
155. Fransson, A., A. Ruusala, and P. Aspenstrom. 2003. Atypical Rho GTPases have roles in mitochondrial homeostasis and apoptosis. *J Biol Chem* 278:6495-6502.

156. Campello, S., R.A. Lacalle, M. Bettella, S. Manes, L. Scorrano, and A. Viola. 2006. Orchestration of lymphocyte chemotaxis by mitochondrial dynamics. *J Exp Med* 203:2879-2886.
157. Fehrenbacher, K.L., H.C. Yang, A.C. Gay, T.M. Huckaba, and L.A. Pon. 2004. Live cell imaging of mitochondrial movement along actin cables in budding yeast. *Curr Biol* 14:1996-2004.
158. Burgess, S.M., M. Delannoy, and R.E. Jensen. 1994. MMM1 encodes a mitochondrial outer membrane protein essential for establishing and maintaining the structure of yeast mitochondria. *J Cell Biol* 126:1375-1391.
159. Sogo, L.F., and M.P. Yaffe. 1994. Regulation of mitochondrial morphology and inheritance by Mdm10p, a protein of the mitochondrial outer membrane. *J Cell Biol* 126:1361-1373.
160. Berger, K.H., L.F. Sogo, and M.P. Yaffe. 1997. Mdm12p, a component required for mitochondrial inheritance that is conserved between budding and fission yeast. *J Cell Biol* 136:545-553.
161. Boldogh, I.R., and L.A. Pon. 2006. Interactions of mitochondria with the actin cytoskeleton. *Biochim Biophys Acta* 1763:450-462.
162. Rizzuto, R., and T. Pozzan. 2006. Microdomains of intracellular Ca²⁺: molecular determinants and functional consequences. *Physiol Rev* 86:369-408.
163. Robert, V., M.L. Massimino, V. Tosello, R. Marsault, M. Cantini, V. Sorrentino, and T. Pozzan. 2001. Alteration in calcium handling at the subcellular level in mdx myotubes. *J Biol Chem* 276:4647-4651.
164. Ojuka, E.O., T.E. Jones, D.H. Han, M. Chen, and J.O. Holloszy. 2003. Raising Ca²⁺ in L6 myotubes mimics effects of exercise on mitochondrial biogenesis in muscle. *Faseb J* 17:675-681.
165. Park, M.K., M.C. Ashby, G. Erdemli, O.H. Petersen, and A.V. Tepikin. 2001. Perinuclear, perigranular and sub-plasmalemmal mitochondria have distinct functions in the regulation of cellular calcium transport. *Embo J* 20:1863-1874.
166. Yi, M., D. Weaver, and G. Hajnoczky. 2004. Control of mitochondrial motility and distribution by the calcium signal: a homeostatic circuit. *J Cell Biol* 167:661-672.
167. Palmieri, L., B. Pardo, F.M. Lasorsa, A. del Arco, K. Kobayashi, M. Iijima, M.J. Runswick, J.E. Walker, T. Saheki, J. Satrustegui, and F. Palmieri. 2001. Citrin and aralar1 are Ca(2+)-stimulated aspartate/glutamate transporters in mitochondria. *Embo J* 20:5060-5069.
168. Smaili, S.S., Y.T. Hsu, R.J. Youle, and J.T. Russell. 2000. Mitochondria in Ca²⁺ signaling and apoptosis. *J Bioenerg Biomembr* 32:35-46.

169. Szabadkai, G., A.M. Simoni, M. Chami, M.R. Wieckowski, R.J. Youle, and R. Rizzuto. 2004. Drp-1-dependent division of the mitochondrial network blocks intraorganellar Ca²⁺ waves and protects against Ca²⁺-mediated apoptosis. *Mol Cell* 16:59-68.
170. Ishihara, N., A. Jofuku, Y. Eura, and K. Mihara. 2003. Regulation of mitochondrial morphology by membrane potential, and DRP1-dependent division and FZO1-dependent fusion reaction in mammalian cells. *Biochem Biophys Res Commun* 301:891-898.
171. Legros, F., A. Lombes, P. Frachon, and M. Rojo. 2002. Mitochondrial fusion in human cells is efficient, requires the inner membrane potential, and is mediated by mitofusins. *Mol Biol Cell* 13:4343-4354.
172. Meeusen, S., J.M. McCaffery, and J. Nunnari. 2004. Mitochondrial fusion intermediates revealed in vitro. *Science* 305:1747-1752.
173. Mattenberger, Y., D.I. James, and J.C. Martinou. 2003. Fusion of mitochondria in mammalian cells is dependent on the mitochondrial inner membrane potential and independent of microtubules or actin. *FEBS Lett* 538:53-59.
174. Malka, F., O. Guillery, C. Cifuentes-Diaz, E. Guillou, P. Belenguer, A. Lombes, and M. Rojo. 2005. Separate fusion of outer and inner mitochondrial membranes. *EMBO Rep* 6:853-859.
175. Sollner, T., M.K. Bennett, S.W. Whiteheart, R.H. Scheller, and J.E. Rothman. 1993. A protein assembly-disassembly pathway in vitro that may correspond to sequential steps of synaptic vesicle docking, activation, and fusion. *Cell* 75:409-418.
176. Bonifacino, J.S., and B.S. Glick. 2004. The mechanisms of vesicle budding and fusion. *Cell* 116:153-166.
177. Hoppins, S., L. Lackner, and J. Nunnari. 2007. The machines that divide and fuse mitochondria. *Annu Rev Biochem* 76:751-780.
178. Choi, S.Y., P. Huang, G.M. Jenkins, D.C. Chan, J. Schiller, and M.A. Frohman. 2006. A common lipid links Mfn-mediated mitochondrial fusion and SNARE-regulated exocytosis. *Nat Cell Biol* 8:1255-1262.
179. Vitale, N., A.S. Caumont, S. Chasserot-Golaz, G. Du, S. Wu, V.A. Sciorra, A.J. Morris, M.A. Frohman, and M.F. Bader. 2001. Phospholipase D1: a key factor for the exocytotic machinery in neuroendocrine cells. *Embo J* 20:2424-2434.
180. Hales, K.G., and M.T. Fuller. 1997. Developmentally regulated mitochondrial fusion mediated by a conserved, novel, predicted GTPase. *Cell* 90:121-129.
181. Santel, A., and M.T. Fuller. 2001. Control of mitochondrial morphology by a human mitofusin. *J. Cell Sci.* 114:867-874.

182. Santel, A., S. Frank, B. Gaume, M. Herrler, R.J. Youle, and M.T. Fuller. 2003. Mitofusin-1 protein is a generally expressed mediator of mitochondrial fusion in mammalian cells. *J Cell Sci* 116:2763-2774.
183. Guan, K., L. Farh, T.K. Marshall, and R.J. Deschenes. 1993. Normal mitochondrial structure and genome maintenance in yeast requires the dynamin-like product of the MGM1 gene. *Curr Genet* 24:141-148.
184. Olichon, A., L.J. Emorine, E. Descoins, L. Pelloquin, L. Bricchese, N. Gas, E. Guillou, C. Delettre, A. Valette, C.P. Hamel, B. Ducommun, G. Lenaers, and P. Belenguer. 2002. The human dynamin-related protein OPA1 is anchored to the mitochondrial inner membrane facing the inter-membrane space. *FEBS Lett* 523:171-176.
185. Alexander, C., M. Votruba, U.E. Pesch, D.L. Thiselton, S. Mayer, A. Moore, M. Rodriguez, U. Kellner, B. Leo-Kottler, G. Auburger, S.S. Bhattacharya, and B. Wissinger. 2000. OPA1, encoding a dynamin-related GTPase, is mutated in autosomal dominant optic atrophy linked to chromosome 3q28. *Nat. Genet.* 26:211-215.
186. Rojo, M., F. Legros, D. Chateau, and A. Lombes. 2002. Membrane topology and mitochondrial targeting of mitofusins, ubiquitous mammalian homologs of the transmembrane GTPase Fzo. *J Cell Sci* 115:1663-1674.
187. Chen, H., S.A. Detmer, A.J. Ewald, E.E. Griffin, S.E. Fraser, and D.C. Chan. 2003. Mitofusins Mfn1 and Mfn2 coordinately regulate mitochondrial fusion and are essential for embryonic development. *J Cell Biol* 160:189-200.
188. Ishihara, N., Y. Eura, and K. Mihara. 2004. Mitofusin 1 and 2 play distinct roles in mitochondrial fusion reactions via GTPase activity. *J Cell Sci* 117:6535-6546. Epub 2004 Nov 6530.
189. Koshihara, T., S.A. Detmer, J.T. Kaiser, H. Chen, J.M. McCaffery, and D.C. Chan. 2004. Structural basis of mitochondrial tethering by mitofusin complexes. *Science* 305:858-862.
190. Rybin, V., O. Ullrich, M. Rubino, K. Alexandrov, I. Simon, M.C. Seabra, R. Goody, and M. Zerial. 1996. GTPase activity of rab5 acts as a timer for endocytic membrane fusion. *Nature* 383:266-269.
191. Song, B.D., and S.L. Schmid. 2003. A molecular motor or a regulator? Dynamin's in a class of its own. *Biochemistry* 42:1369-1376.
192. Wong, E.D., J.A. Wagner, S.W. Gorsich, J.M. McCaffery, J.M. Shaw, and J. Nunnari. 2000. The dynamin-related GTPase, Mgm1p, is an intermembrane space protein required for maintenance of fusion competent mitochondria. *J. Cell Biol.* 151:341-352.

193. Cipolat, S., O. Martins de Brito, B. Dal Zilio, and L. Scorrano. 2004. OPA1 requires mitofusin 1 to promote mitochondrial fusion. *Proc Natl Acad Sci U S A* 101:15927-15932. Epub 12004 Oct 15927.
194. Olichon, A., L. Baricault, N. Gas, E. Guillou, A. Valette, P. Belenguer, and G. Lenaers. 2003. Loss of OPA1 perturbs the mitochondrial inner membrane structure and integrity, leading to cytochrome c release and apoptosis. *J Biol Chem* 278:7743-7746.
195. Scorrano, L. 2007. Multiple functions of mitochondria-shaping proteins. *Novartis Found Symp* 287:47-55; discussion 55-49.
196. Wong, E.D., J.A. Wagner, S.V. Scott, V. Okreglak, T.J. Holewinski, A. Cassidy-Stone, and J. Nunnari. 2003. The intramitochondrial dynamin-related GTPase, Mgm1p, is a component of a protein complex that mediates mitochondrial fusion. *J Cell Biol* 160:303-311.
197. Sesaki, H., and R.E. Jensen. 2004. Ugo1p links the Fzo1p and Mgm1p GTPases for mitochondrial fusion. *J Biol Chem* 14:14.
198. Sesaki, H., S.M. Southard, M.P. Yaffe, and R.E. Jensen. 2003. Mgm1p, a dynamin-related GTPase, is essential for fusion of the mitochondrial outer membrane. *Mol Biol Cell* 14:2342-2356.
199. Herlan, M., C. Bornhovd, K. Hell, W. Neupert, and A.S. Reichert. 2004. Alternative topogenesis of Mgm1 and mitochondrial morphology depend on ATP and a functional import motor. *J Cell Biol* 165:167-173. Epub 2004 Apr 2004.
200. Duvezin-Caubet, S., R. Jagasia, J. Wagener, S. Hofmann, A. Trifunovic, A. Hansson, A. Chomyn, M.F. Bauer, G. Attardi, N.G. Larsson, W. Neupert, and A.S. Reichert. 2006. Proteolytic processing of OPA1 links mitochondrial dysfunction to alterations in mitochondrial morphology. *J Biol Chem* 281:37972-37979.
201. Jeyaraju, D.V., L. Xu, M.C. Letellier, S. Bandaru, R. Zunino, E.A. Berg, H.M. McBride, and L. Pellegrini. 2006. Phosphorylation and cleavage of presenilin-associated rhomboid-like protein (PARL) promotes changes in mitochondrial morphology. *Proc Natl Acad Sci U S A* 103:18562-18567.
202. Song, Z., H. Chen, M. Fiket, C. Alexander, and D.C. Chan. 2007. OPA1 processing controls mitochondrial fusion and is regulated by mRNA splicing, membrane potential, and Yme1L. *J Cell Biol* 178:749-755.
203. Griparic, L., T. Kanazawa, and A.M. van der Bliek. 2007. Regulation of the mitochondrial dynamin-like protein Opa1 by proteolytic cleavage. *J Cell Biol* 178:757-764.

204. Sesaki, H., C.D. Dunn, M. Iijima, K.A. Shepard, M.P. Yaffe, C.E. Machamer, and R.E. Jensen. 2006. Ups1p, a conserved intermembrane space protein, regulates mitochondrial shape and alternative topogenesis of Mgm1p. *J Cell Biol* 173:651-658.
205. Ishihara, N., Y. Fujita, T. Oka, and K. Mihara. 2006. Regulation of mitochondrial morphology through proteolytic cleavage of OPA1. *Embo J* 25:2966-2977.
206. Smirnova, E., L. Griparic, D.L. Shurland, and A.M. van Der Blik. 2001. Dynamin-related protein drp1 is required for mitochondrial division in mammalian cells. *Mol Biol Cell* 12:2245-2256.
207. Bleazard, W., J.M. McCaffery, E.J. King, S. Bale, A. Mozdy, Q. Tieu, J. Nunnari, and J.M. Shaw. 1999. The dynamin-related GTPase Dnm1 regulates mitochondrial fission in yeast. *Nature Cell Biol.* 1:298 - 304.
208. Labrousse, A.M., M.D. Zappaterra, D.A. Rube, and A.M. van der Blik. 1999. C. elegans dynamin-related protein DRP-1 controls severing of the mitochondrial outer membrane. *Mol. Cell.* 4:815-826.
209. De Vos, K.J., V.J. Allan, A.J. Grierson, and M.P. Sheetz. 2005. Mitochondrial function and actin regulate dynamin-related protein 1-dependent mitochondrial fission. *Curr Biol* 15:678-683.
210. Varadi, A., L.I. Johnson-Cadwell, V. Cirulli, Y. Yoon, V.J. Allan, and G.A. Rutter. 2004. Cytoplasmic dynein regulates the subcellular distribution of mitochondria by controlling the recruitment of the fission factor dynamin-related protein-1. *J Cell Sci* 117:4389-4400. Epub 2004 Aug 4310.
211. Fukushima, N.H., E. Brisch, B.R. Keegan, W. Bleazard, and J.M. Shaw. 2001. The GTPase effector domain sequence of the Dnm1p GTPase regulates self-assembly and controls a rate-limiting step in mitochondrial fission. *Mol Biol Cell* 12:2756-2766.
212. Ingerman, E., E.M. Perkins, M. Marino, J.A. Mears, J.M. McCaffery, J.E. Hinshaw, and J. Nunnari. 2005. Dnm1 forms spirals that are structurally tailored to fit mitochondria. *J Cell Biol* 170:1021-1027.
213. Zhang, P., and J.E. Hinshaw. 2001. Three-dimensional reconstruction of dynamin in the constricted state. *Nat Cell Biol* 3:922-926.
214. Danino, D., and J.E. Hinshaw. 2001. Dynamin family of mechanoenzymes. *Curr Opin Cell Biol* 13:454-460.
215. Tieu, Q., V. Okreglak, K. Naylor, and J. Nunnari. 2002. The WD repeat protein, Mdv1p, functions as a molecular adaptor by interacting with Dnm1p and Fis1p during mitochondrial fission. *J Cell Biol* 158:445-452.
216. Cerveny, K.L., J.M. McCaffery, and R.E. Jensen. 2001. Division of mitochondria requires a novel DMN1-interacting protein, Net2p. *Mol Biol Cell* 12:309-321.

217. Mozdy, A.D., J.M. McCaffery, and J.M. Shaw. 2000. Dnm1p GTPase-mediated mitochondrial fission is a multi-step process requiring the novel integral membrane component Fis1p. *J Cell Biol.* 151:367-380.
218. Fekkes, P., K.A. Shepard, and M.P. Yaffe. 2000. Gag3p, an outer membrane protein required for fission of mitochondrial tubules. *J. Cell Biol.* 151:333-340.
219. Cerveny, K.L., and R.E. Jensen. 2003. The WD-repeats of Net2p interact with Dnm1p and Fis1p to regulate division of mitochondria. *Mol Biol Cell* 14:4126-4139. Epub 2003 Jul 4111.
220. Griffin, E.E., J. Graumann, and D.C. Chan. 2005. The WD40 protein Caf4p is a component of the mitochondrial fission machinery and recruits Dnm1p to mitochondria. *J Cell Biol* 170:237-248.
221. Otsuga, D., B.R. Keegan, E. Brisch, J.W. Thatcher, G.J. Hermann, W. Bleazard, and J.M. Shaw. 1998. The dynamin-related GTPase, Dnm1p, controls mitochondrial morphology in yeast. *J. Cell Biol.* 143:333-349.
222. Sesaki, H., and R.E. Jensen. 1999. Division versus Fusion: Dnm1p and Fzo1p Antagonistically Regulate Mitochondrial Shape. *J Cell Biol* 147:699-706.
223. Lee, Y.J., S.Y. Jeong, M. Karbowski, C.L. Smith, and R.J. Youle. 2004. Roles of the mammalian mitochondrial fission and fusion mediators Fis1, Drp1, and Opa1 in apoptosis. *Mol Biol Cell* 15:5001-5011. Epub 2004 Sep 5008.
224. Jofuku, A., N. Ishihara, and K. Mihara. 2005. Analysis of functional domains of rat mitochondrial Fis1, the mitochondrial fission-stimulating protein. *Biochem Biophys Res Commun* 333:650-659.
225. Wasiak, S., R. Zunino, and H.M. McBride. 2007. Bax/Bak promote sumoylation of DRP1 and its stable association with mitochondria during apoptotic cell death. *J Cell Biol* 177:439-450.
226. Yoon, Y., E.W. Krueger, B.J. Oswald, and M.A. McNiven. 2003. The mitochondrial protein hFis1 regulates mitochondrial fission in mammalian cells through an interaction with the dynamin-like protein DLP1. *Mol Cell Biol* 23:5409-5420.
227. Karbowski, M., S.Y. Jeong, and R.J. Youle. 2004. Endophilin B1 is required for the maintenance of mitochondrial morphology. *J Cell Biol* 166:1027-1039.
228. Niemann, A., M. Ruegg, V. La Padula, A. Schenone, and U. Suter. 2005. Ganglioside-induced differentiation associated protein 1 is a regulator of the mitochondrial network: new implications for Charcot-Marie-Tooth disease. *J Cell Biol* 170:1067-1078.

229. Farsad, K., N. Ringstad, K. Takei, S.R. Floyd, K. Rose, and P. De Camilli. 2001. Generation of high curvature membranes mediated by direct endophilin bilayer interactions. *J Cell Biol* 155:193-200. Epub 2001 Oct 2015.
230. Gallop, J.L., C.C. Jao, H.M. Kent, P.J. Butler, P.R. Evans, R. Langen, and H.T. McMahon. 2006. Mechanism of endophilin N-BAR domain-mediated membrane curvature. *Embo J* 25:2898-2910.
231. Peter, B.J., H.M. Kent, I.G. Mills, Y. Vallis, P.J. Butler, P.R. Evans, and H.T. McMahon. 2004. BAR domains as sensors of membrane curvature: the amphiphysin BAR structure. *Science* 303:495-499. Epub 2003 Nov 2026.
232. Kijima, K., C. Numakura, H. Izumino, K. Umetsu, A. Nezu, T. Shiiki, M. Ogawa, Y. Ishizaki, T. Kitamura, Y. Shozawa, and K. Hayasaka. 2005. Mitochondrial GTPase mitofusin 2 mutation in Charcot-Marie-Tooth neuropathy type 2A. *Hum Genet* 116:23-27. Epub 2004 Nov 2011.
233. Legesse-Miller, A., R.H. Massol, and T. Kirchhausen. 2003. Constriction and dnm1p recruitment are distinct processes in mitochondrial fission. *Mol Biol Cell* 14:1953-1963.
234. Jakobs, S., N. Martini, A.C. Schauss, A. Egner, B. Westermann, and S.W. Hell. 2003. Spatial and temporal dynamics of budding yeast mitochondria lacking the division component Fis1p. *J Cell Sci* 116:2005-2014.
235. Cipolat, S., T. Rudka, D. Hartmann, V. Costa, L. Serneels, K. Craessaerts, K. Metzger, C. Frezza, W. Annaert, L. D'Adamio, C. Derks, T. Dejaegere, L. Pellegrini, R. D'Hooge, L. Scorrano, and B. De Strooper. 2006. Mitochondrial rhomboid PARL regulates cytochrome c release during apoptosis via OPA1-dependent cristae remodeling. *Cell* 126:163-175.
236. Pellegrini, L., and L. Scorrano. 2007. A cut short to death: Parl and Opa1 in the regulation of mitochondrial morphology and apoptosis. *Cell Death Differ* 14:1275-1284.
237. Frezza, C., S. Cipolat, O. Martins de Brito, M. Micaroni, G.V. Beznoussenko, T. Rudka, D. Bartoli, R.S. Polishuck, N.N. Danial, B. De Strooper, and L. Scorrano. 2006. OPA1 controls apoptotic cristae remodeling independently from mitochondrial fusion. *Cell* 126:177-189.
238. Taguchi, N., N. Ishihara, A. Jofuku, T. Oka, and K. Mihara. 2007. Mitotic phosphorylation of dynamin-related GTPase Drp1 participates in mitochondrial fission. *J Biol Chem* 282:11521-11529.
239. Chang, C.R., and C. Blackstone. 2007. Cyclic AMP-dependent protein kinase phosphorylation of Drp1 regulates its GTPase activity and mitochondrial morphology. *J Biol Chem* 282:21583-21587.

240. Yonashiro, R., S. Ishido, S. Kyo, T. Fukuda, E. Goto, Y. Matsuki, M. Ohmura-Hoshino, K. Sada, H. Hotta, H. Yamamura, R. Inatome, and S. Yanagi. 2006. A novel mitochondrial ubiquitin ligase plays a critical role in mitochondrial dynamics. *Embo J* 25:3618-3626.
241. Nakamura, N., Y. Kimura, M. Tokuda, S. Honda, and S. Hirose. 2006. MARCH-V is a novel mitofusin 2- and Drp1-binding protein able to change mitochondrial morphology. *EMBO Rep* 7:1019-1022.
242. Harder, Z., R. Zunino, and H. McBride. 2004. Sumo1 conjugates mitochondrial substrates and participates in mitochondrial fission. *Curr. Biol.* 14:340-345.
243. Zunino, R., A. Schauss, P. Rippstein, M. Andrade-Navarro, and H.M. McBride. 2007. The SUMO protease SENP5 is required to maintain mitochondrial morphology and function. *J Cell Sci* 120:1178-1188.
244. Bayer, P., A. Arndt, S. Metzger, R. Mahajan, F. Melchior, R. Jaenicke, and J. Becker. 1998. Structure determination of the small ubiquitin-related modifier SUMO-1. *J Mol Biol* 280:275-286.
245. Bernier-Villamor, V., D.A. Sampson, M.J. Matunis, and C.D. Lima. 2002. Structural basis for E2-mediated SUMO conjugation revealed by a complex between ubiquitin-conjugating enzyme Ubc9 and RanGAP1. *Cell* 108:345-356.
246. Muller, S., C. Hoege, G. Pyrowolakis, and S. Jentsch. 2001. SUMO, ubiquitin's mysterious cousin. *Nat Rev Mol Cell Biol* 2:202-210.
247. Johnson, E.S., and A.A. Gupta. 2001. An E3-like factor that promotes SUMO conjugation to the yeast septins. *Cell* 106:735-744.
248. Takahashi, Y., T. Kahyo, E.A. Toh, H. Yasuda, and Y. Kikuchi. 2001. Yeast Ull1/Siz1 is a novel SUMO1/Smt3 ligase for septin components and functions as an adaptor between conjugating enzyme and substrates. *J Biol Chem* 276:48973-48977. Epub 42001 Sep 48927.
249. Kahyo, T., T. Nishida, and H. Yasuda. 2001. Involvement of PIAS1 in the sumoylation of tumor suppressor p53. *Mol Cell* 8:713-718.
250. Schmidt, D., and S. Muller. 2002. Members of the PIAS family act as SUMO ligases for c-Jun and p53 and repress p53 activity. *Proc Natl Acad Sci U S A* 99:2872-2877.
251. Nishida, T., and H. Yasuda. 2002. PIAS1 and PIASxalpha function as SUMO-E3 ligases toward androgen receptor and repress androgen receptor-dependent transcription. *J Biol Chem* 277:41311-41317.
252. Sachdev, S., L. Bruhn, H. Sieber, A. Pichler, F. Melchior, and R. Grosschedl. 2001. PIASy, a nuclear matrix-associated SUMO E3 ligase, represses LEF1 activity by sequestration into nuclear bodies. *Genes Dev* 15:3088-3103.

253. Pichler, A., A. Gast, J.S. Seeler, A. Dejean, and F. Melchior. 2002. The nucleoporin RanBP2 has SUMO1 E3 ligase activity. *Cell* 108:109-120.
254. Pichler, A., P. Knipscheer, H. Saitoh, T.K. Sixma, and F. Melchior. 2004. The RanBP2 SUMO E3 ligase is neither HECT- nor RING-type. *Nat Struct Mol Biol* 11:984-991.
255. Tatham, M.H., S. Kim, E. Jaffray, J. Song, Y. Chen, and R.T. Hay. 2005. Unique binding interactions among Ubc9, SUMO and RanBP2 reveal a mechanism for SUMO paralog selection. *Nat Struct Mol Biol* 12:67-74.
256. Kirsh, O., J.S. Seeler, A. Pichler, A. Gast, S. Muller, E. Miska, M. Mathieu, A. Harel-Bellan, T. Kouzarides, F. Melchior, and A. Dejean. 2002. The SUMO E3 ligase RanBP2 promotes modification of the HDAC4 deacetylase. *Embo J* 21:2682-2691.
257. Kagey, M.H., T.A. Melhuish, and D. Wotton. 2003. The polycomb protein Pc2 is a SUMO E3. *Cell* 113:127-137.
258. Kagey, M.H., T.A. Melhuish, S.E. Powers, and D. Wotton. 2005. Multiple activities contribute to Pc2 E3 function. *Embo J* 24:108-119.
259. Frank, S., B. Gaume, E.S. Bergmann-Leitner, W.W. Leitner, E.G. Robert, F. Catez, C.L. Smith, and R.J. Youle. 2001. The role of dynamin-related protein 1, a mediator of mitochondrial fission, in apoptosis. *Dev Cell* 1:515-525.
260. Zamzami, N., and G. Kroemer. 2001. The mitochondrion in apoptosis: how Pandora's box opens. *Nat Rev Mol Cell Biol* 2:67-71.
261. James, D.I., P.A. Parone, Y. Mattenberger, and J.C. Martinou. 2003. hFis1, a novel component of the mammalian mitochondrial fission machinery. *J Biol Chem* 278:36373-36379.
262. Kinnally, K.W., and B. Antonsson. 2007. A tale of two mitochondrial channels, MAC and PTP, in apoptosis. *Apoptosis* 12:857-868.
263. Heath-Engel, H.M., and G.C. Shore. 2006. Regulated targeting of Bax and Bak to intracellular membranes during apoptosis. *Cell Death Differ* 13:1277-1280.
264. Stojanovski, D., O.S. Koutsopoulos, K. Okamoto, and M.T. Ryan. 2004. Levels of human Fis1 at the mitochondrial outer membrane regulate mitochondrial morphology. *J Cell Sci* 117:1201-1210.
265. Arnoult, D., A. Grodet, Y.J. Lee, J. Estaquier, and C. Blackstone. 2005. Release of OPA1 during apoptosis participates in the rapid and complete release of cytochrome c and subsequent mitochondrial fragmentation. *J Biol Chem* 280:35742-35750.

266. Scorrano, L., M. Ashiya, K. Buttle, S. Weiler, S.A. Oakes, C.A. Mannella, and S.J. Korsmeyer. 2002. A Distinct Pathway Remodels Mitochondrial Cristae and Mobilizes Cytochrome c during Apoptosis. *Dev Cell* 2:55-67.
267. Germain, M., J.P. Mathai, H.M. McBride, and G.C. Shore. 2005. Endoplasmic reticulum BIK initiates DRP1-regulated remodelling of mitochondrial cristae during apoptosis. *EMBO J* 24:1546-1556.
268. Karbowski, M., D. Arnoult, H. Chen, D.C. Chan, C.L. Smith, and R.J. Youle. 2004. Quantitation of mitochondrial dynamics by photolabeling of individual organelles shows that mitochondrial fusion is blocked during the Bax activation phase of apoptosis. *J Cell Biol* 164:493-499. Epub 2004 Feb 2009.
269. Pieczenik, S.R., and J. Neustadt. 2007. Mitochondrial dysfunction and molecular pathways of disease. *Exp Mol Pathol* 83:84-92.
270. Schapira, A.H. 2006. Mitochondrial disease. *Lancet* 368:70-82.
271. Chinnery, P.F., and E.A. Schon. 2003. Mitochondria. *J Neurol Neurosurg Psychiatry* 74:1188-1199.
272. Bach, D., D. Naon, S. Pich, F.X. Soriano, N. Vega, J. Rieusset, M. Laville, C. Guillet, Y. Boirie, H. Wallberg-Henriksson, M. Manco, M. Calvani, M. Castagneto, M. Palacin, G. Mingrone, J.R. Zierath, H. Vidal, and A. Zorzano. 2005. Expression of Mfn2, the Charcot-Marie-Tooth neuropathy type 2A gene, in human skeletal muscle: effects of type 2 diabetes, obesity, weight loss, and the regulatory role of tumor necrosis factor alpha and interleukin-6. *Diabetes* 54:2685-2693.
273. Pich, S., D. Bach, P. Briones, M. Liesa, M. Camps, X. Testar, M. Palacin, and A. Zorzano. 2005. The Charcot-Marie-Tooth type 2A gene product, Mfn2, up-regulates fuel oxidation through expression of OXPHOS system. *Hum Mol Genet* 14:1405-1415. Epub 2005 Apr 1413.
274. Clark, I.E., M.W. Dodson, C. Jiang, J.H. Cao, J.R. Huh, J.H. Seol, S.J. Yoo, B.A. Hay, and M. Guo. 2006. Drosophila pink1 is required for mitochondrial function and interacts genetically with parkin. *Nature* 441:1162-1166.
275. Heddi, A., P. Lestienne, D.C. Wallace, and G. Stepien. 1993. Mitochondrial DNA expression in mitochondrial myopathies and coordinated expression of nuclear genes involved in ATP production. *J Biol Chem* 268:12156-12163.
276. Heddi, A., G. Stepien, P.J. Benke, and D.C. Wallace. 1999. Coordinate induction of energy gene expression in tissues of mitochondrial disease patients. *J Biol Chem* 274:22968-22976.
277. Hood, D.A., I. Irrcher, V. Ljubcic, and A.M. Joseph. 2006. Coordination of metabolic plasticity in skeletal muscle. *J Exp Biol* 209:2265-2275.

278. Scarpulla, R.C. 2002. Transcriptional activators and coactivators in the nuclear control of mitochondrial function in mammalian cells. *Gene* 286:81-89.
279. Cartoni, R., B. Leger, M.B. Hock, M. Praz, A. Crettenand, S. Pich, J.L. Ziltener, F. Luthi, O. Deriaz, A. Zorzano, C. Gobelet, A. Kralli, and A.P. Russell. 2005. Mitofusins 1/2 and ERRalpha expression are increased in human skeletal muscle after physical exercise. *J Physiol* 567:349-358. Epub 2005 Jun 2016.
280. Soriano, F.X., M. Liesa, D. Bach, D.C. Chan, M. Palacin, and A. Zorzano. 2006. Evidence for a mitochondrial regulatory pathway defined by peroxisome proliferator-activated receptor-gamma coactivator-1 alpha, estrogen-related receptor-alpha, and mitofusin 2. *Diabetes* 55:1783-1791.
281. Bach, D., S. Pich, F.X. Soriano, N. Vega, B. Baumgartner, J. Oriola, J.R. Dagaard, J. Lloberas, M. Camps, J.R. Zierath, R. Rabasa-Lhoret, H. Wallberg-Henriksson, M. Laville, M. Palacin, H. Vidal, F. Rivera, M. Brand, and A. Zorzano. 2003. Mitofusin-2 determines mitochondrial network architecture and mitochondrial metabolism. A novel regulatory mechanism altered in obesity. *J Biol Chem* 278:17190-17197.
282. Chen, K.H., X. Guo, D. Ma, Y. Guo, Q. Li, D. Yang, P. Li, X. Qiu, S. Wen, R.P. Xiao, and J. Tang. 2004. Dysregulation of HSG triggers vascular proliferative disorders. *Nat Cell Biol* 6:872-883. Epub 2004 Aug 2022.
283. Honda, S., and S. Hirose. 2003. Stage-specific enhanced expression of mitochondrial fusion and fission factors during spermatogenesis in rat testis. *Biochem Biophys Res Commun* 311:424-432.

CHAPTER 2 ~ Manuscript #1

Activated mitofusin 2 signals mitochondrial fusion, interferes with Bax activation, and reduces susceptibility to radical induced depolarization.

2.1 CHAPTER INTRODUCTION

The research presented as a manuscript in chapter 2 represents the first half of my doctoral research. I am the first author of this work published in the *Journal of Biological Chemistry* entitled “Activated mitofusin 2 signals mitochondrial fusion, interferes with Bax activation, and reduces susceptibility to radical induced depolarization” Margaret Neuspiel, Rodolfo Zunino, Sandhya Gangaraju, Peter Rippstein and Heidi McBride.

This work required the generation of a rabbit polyclonal Mfn2 antibody, the development of a series of Mfn2 mutants, a fluorescence microscopy based PEG whole cell mitochondrial fusion assay (figure 2.1), and a free radical induced terminal depolarization assay. With the exception of the generation of some of the Mfn2 mutants, I generated the remainder of the tools during the initial period of this doctorate thesis.

A technician in the laboratory of Dr. McBride, Rodolfo Zunino, is responsible for the nucleotide assays represented in figure 2.2 of this thesis. A former master’s student in the laboratory, Sandhya Gangaraju, is responsible for some of the preliminary data behind this current manuscript. Peter Rippstein, is responsible for the processing of all samples for electron microscopy.

Figure 2.1

Whole cell mitochondrial fusion assay

Cartoon schematic illustrating the whole cell mitochondria PEG fusion assay. Cos-7 cells transfected with either matrix targeted pOCT-DsRED or pOCT-GFP or pOCT-DsRED + Mfn2-CFP (and mutants) are collected by trypsinization and re-seeded together onto coverslips for 24 hours. Cells are treated with cycloheximide for 2 hours to stop new protein synthesis, prior to the addition of PEG for 60 seconds. Once whole cell fusion has occurred, the heterokaryons are imaged on a time course to determine the extent of DsRED and GFP mixing within heterokaryons.

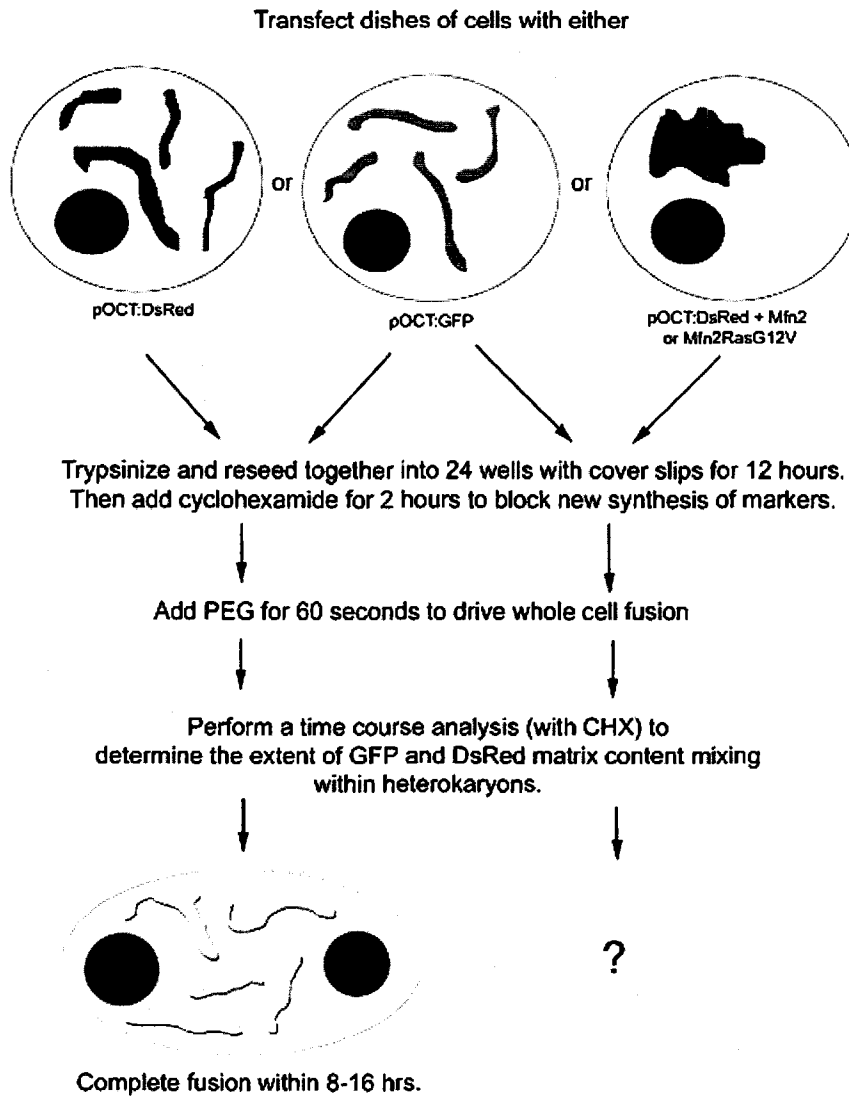


Figure 2.1

Whole cell mitochondrial fusion assay

2.2 ABSTRACT

Mitochondrial fusion in higher eukaryotes requires at least two essential GTPases, Mitofusin1 and Mitofusin2. We have created an activated mutant of Mfn2, which shows increased rates of nucleotide exchange and decreased rates of hydrolysis relative to wild type Mfn2. Mitochondrial fusion is dramatically stimulated within heterokaryons expressing this mutant, demonstrating that hydrolysis is not requisite for the fusion event, and supporting a role for Mfn2 as a signalling GTPase. Although steady state mitochondrial fusion required the conserved intermembrane space tryptophan residue, this requirement was overcome within the context of the hydrolysis deficient mutant. Furthermore, the punctate localization of Mfn2 is lost in the dominant active mutants, indicating that these sites are functionally controlled by changes in the nucleotide state of Mfn2. Upon staurosporin stimulated cell death, activated Bax is recruited to the Mfn2 containing puncta, however Bax activation and cytochrome c release are inhibited in the presence of the dominant active mutants of Mfn2. The dominant active form of Mfn2 also protected the mitochondria against free radical induced permeability transition. In contrast to staurosporin induced outer membrane permeability transition, pore opening induced through the introduction of free radicals was dependent upon the conserved intermembrane space residue. This is the first evidence that Mfn2 is a signalling GTPase regulating mitochondrial fusion, and that the nucleotide dependent activation of Mfn2 concomitantly protects the organelle from permeability transition. The data provides new insights into the critical relationship between mitochondrial membrane dynamics and programmed cell death.

2.3 INTRODUCTION

The mitochondria sit at the crossroad of hundreds of chemical reactions that are essential for the life and death of a cell. The dynamic behaviour of these organelles has only just begun to be examined and the implications of steady state fission, fusion, motility and cristae remodelling events in the control of the mitochondrial activity are not yet known. Studies in different model organisms are addressing this question by investigating the molecular mechanisms that govern mitochondrial dynamics in order to gain insights into the physiological triggers and consequences of these events. Mitochondrial fusion in mammalian cells requires at least two essential outer membrane GTPases, Mitofusin 1 (Mfn1) and Mitofusin 2 (Mfn2) (1-6). These proteins span the outer membrane twice and in addition to their amino terminal GTPase domain, they have two conserved hydrophobic heptad repeats, HR1 and HR2 that are exposed to the cytosol (2, 7). The second HR2 domain of Mfn1 has been shown to facilitate mitochondrial tethering and the crystal structure of the purified HR2 domain demonstrates that it can form a 100 Angstrom antiparallel structure that could bind in *trans* to bridge mitochondria (7). Another important region of Mfns is their short, 2-3 amino acid intermembrane space loop, which contains a highly conserved tryptophan residue. In yeast, this region of the protein is required for mitochondrial fusion, and has been shown to anchor Fzo1p to sites of membrane contact between the inner and outer membrane (8). Although Mfn1 and Mfn2 are 60% identical, recent evidence with both *in vitro* mitochondrial docking assays and in rescue experiments of Mfn1 knock out cells has shown that Mfn1 appears to play a more direct role in mitochondrial docking (7, 9), and that it functions in co-operation with the intermembrane space dynamin like GTPase Opa1 (autosomal dominant optical atrophy 1) (10). The role of

Mfn2 in mitochondrial fusion has remained elusive, although it is clearly required for fusion and can be found in heterodimeric complexes with Mfn1. Recent studies have shown that the nucleotide binding and hydrolysis properties of the two Mfn proteins are distinct (9), consistent with the idea that the two GTPases regulate different steps along the fusion pathway (5). These steps may include the processes that drive mitochondrial motility, tethering, assembly of a fusion pore to facilitate lipid bilayer mixing and eventually leading to inner mitochondrial membrane fusion. Given the complexity of these molecular requirements, the Mfn proteins do not act alone, and studies in yeast have identified a number of additional proteins required for mitochondrial fusion, including the outer membrane protein, Ugo1p (11-13), the inner membrane serine protease Rbd1p (14-16), an F-box containing protein Mdm30p (17), along with other candidates like Mdm35p, Mdm34p, Mdm39p (18).

One of the outstanding questions in the field of mitochondrial dynamics remains the physiological importance of mitochondrial fission and fusion under steady state conditions. Knock outs of either Mfn1 or Mfn2 are embryonic lethal (6), demonstrating an essential role of mitochondrial fusion for viability. In addition, mutations within the Mfn2 gene have been found in patients suffering from Charcot-Marie-Tooth neuropathy Type 2A, and 6 out of 7 of these mutations were found within the conserved GTPase region (19, 20). Interestingly, evidence that Mfn2 may exhibit intracellular signalling activity has come from one study that identified the rat Mfn2 (called hyperplasia suppressor gene *HSG*) as an important anti-proliferative protein, which interferes with the Ras pathway and blocks signalling from growth factor receptors at the plasma membrane (21). Although the mechanism for this

inhibition is unknown, these findings suggest that Mfn2 and/or the morphological state of the mitochondria are highly integrated into cellular signalling cascades.

Another example of how the mitochondrial morphology is integrated into cellular signalling events is the growing evidence for a role of mitochondrial dynamics in the progression of apoptosis. For example, two of the proteins required for mitochondrial fission, Fis1p and DRP1 are also essential for programmed cell death (22-25). Fis1p knock down by siRNA blocks recruitment and activation of Bax at the surface of mitochondria following a death stimuli, indicating an essential role for this small integral membrane protein in apoptosis (25). Similarly, although loss of DRP1 does not dramatically interfere with Bax activation, cytochrome c release is partially inhibited and mitochondrial fission is blocked in these cells (25, 26). In addition, siRNA knock down of Opa1, a protein required for mitochondrial fusion, results in fragmented mitochondria, which are highly sensitized to loss of electrochemical potential and cytochrome c release (25, 27). In contrast, overexpression of the two mitofusin proteins together provided some protection against different apoptotic stimuli (28). These recent data highlight the dual roles of mitochondrial GTPases in the regulation of both mitochondrial dynamics and the mitochondrial contribution to programmed cell death.

Given the increasing evidence that Mfn1 plays a direct role in mitochondrial tethering (5, 9), we have specifically investigated the function of Mfn2 in the process of mitochondrial fusion and further examined how the GTPase activity of Mfn2 might contribute to the regulation of programmed cell death.

2.4 RESULTS

2.4.1 Creation of a hydrolysis deficient mutant of Mfn2.

In order to determine whether nucleotide hydrolysis of Mfn2 was essential for mitochondrial fusion, we constructed a RasG12V mutant. Our purpose in designing the mutant was to maintain nucleotide binding and exchange properties of Mfn2 and yet reduce the intrinsic rate of nucleotide hydrolysis. Therefore we replaced the residues within the P-loop with those from the activated Ras G12V (29-31) by substituting amino acids GRTSNGKS with GAVGVGKS (the consensus for GTP binding is **GxxxxGKS** (32)). We first compared the nucleotide exchange properties of this mutation (Mfn2_{RasG12V}) with wild type Mfn2 and controls by using crude extracts from cells transfected with CFP fusion proteins. COS7 cells were transfected with either matrix targeted CFP (negative control), wild type Mfn2:CFP, Mfn2_{RasG12V}:CFP or Rab5:CFP as a positive control. Rab5 is the best characterized of the Rab GTPases, and is known to regulate early endosome fusion (33). Regulatory GTPases of the Ras family are all characterized by their low intrinsic rates of hydrolysis and high nucleotide affinities, which results in stable nucleotide states that require accessory proteins for their activity. Given the evidence that Mfn2 exhibits low rates of nucleotide hydrolysis and high affinity (9), it is relevant to use Rab5 as a positive control in these assays. Following transfection with CFP tagged constructs, the cells were harvested, broken, and the mitochondrial enriched heavy membrane fractions were incubated with the environment-sensitive non-hydrolysable GTP analogue, *N*-methylantraniloyl 5'-guanylyl-beta,gamma-imidotriphosphate (Mant-GMP-PNP) (34, 35). Increased Mant-nucleotide fluorescence is a direct measurement of nucleotide exchange. As expected, untransfected

Figure 2.2

Creation of a hydrolysis-deficient mutant of Mfn2

A. Mant GMP-PNP binding of cell extracts either untransfected (Utf), or transfected with pOCT:CFP (negative control), Mfn2:CFP, Mfn2_{RasG12V}:CFP or Rab5:CFP (positive control). Incubations performed at 37°C for 1 and 10 minutes were analyzed in the fluorimeter (see Experimental Procedures). Competition with unlabelled GTP was performed for the 10 minute time point only, as indicated. All values obtained were normalized for total protein concentration and for expression levels of CFP tagged proteins and expressed as fluorescence arbitrary units (AU). These results are representative of 4 independent experiments. P values (unpaired t-test) show insignificant differences when comparing untransfected, pOCT:CFP and Mfn2:CFP. P values demonstrate a significant increase between Mfn2:CFP and Mfn2_{RasG12V}:CFP (p=0.013), but the values between Mfn2_{RasG12V}:CFP and Rab5:CFP are insignificant (p=0.347). B. Mant GMP-PNP binding to GST tagged proteins purified from COS7 cells transfected with either GST, Mfn2:GST or Mfn2_{RasG12V}:GST. Incubations performed at 37°C for 15 minutes were analyzed in the fluorimeter and the values were expressed as arbitrary units of fluorescence per µg GST protein. Competition in the presence of cold GTP is shown in black. The data presented is representative of 3 independent experiments. P values are less than 0.05 when comparing GST with GST:Mfn2 (p=0.019), and also when comparing GST:Mfn2 and GST:Mfn2_{RasG12V} (p=0.016) demonstrating that they represent statistically significant differences. There was no statistical significance to the differences observed between GST:Mfn2_{RasG12V} and GST:Rab5 (p=0.404). C. Purified Mfn2:His6, Mfn2_{RasG12V}:His6 and Rab5:GST were loaded with GTP[γ32P] and the amount of radiolabelled phosphate remaining bound per nmole of protein over time was quantified. Each point was collected in triplicate, and the data are representative of 4 individual experiments. D. Western blot analysis of the purification of proteins used in the hydrolysis experiments indicates the initial levels of expression relative to the endogenous Mfn2 (arrows). Control, LacZ:His6 transfected cell extracts are shown in lane 1, and transfections of Mfn2:His6 (lane2) and Mfn2_{RasG12V}:His6 (lane 3) reveal at least a 10 fold increased expression over endogenous protein. Eluates of tagged, purified proteins are shown in lane 4 (LacZ control), lane 5 (Mfn2:His6) and lane 6 (Mfn2_{RasG12V}:His6).

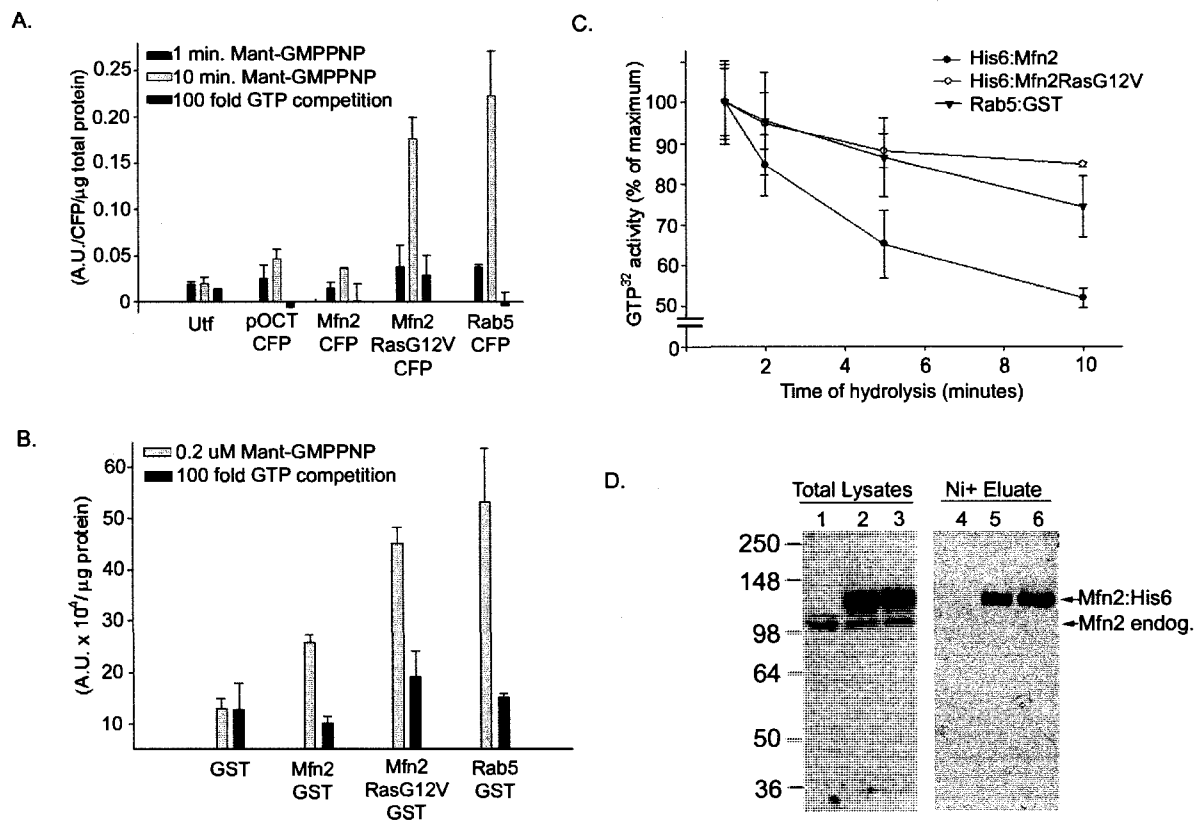


Figure 2.2

Creation of a hydrolysis-deficient mutant of Mfn2

cells, or cells transfected with the matrix CFP control plasmid, bind a constant level of Mant-GMP-PNP due to the endogenous GTPases present in the extracts. Interestingly, overexpression of Mfn2:CFP did not significantly alter the basal amount of nucleotide binding in the heavy membrane fraction (Fig. 2.2A). Overexpression of Rab5 provided a ~4 fold increase in Mant GMP-PNP binding within the first 10 minutes after incubation at 37 degrees (Fig. 2.2 A). This signal is specific since addition of unlabeled GTP competes for the binding. Notably, although transfection of Mfn2:CFP had no effect on basal nucleotide binding in this assay, transfection of Mfn2_{RasG12V}:CFP demonstrated a significant increase in nucleotide binding (Fig. 2.2A). We next isolated Mfn2_{RasG12V}:GST or Mfn2:GST from transfected mammalian cells using glutathione sepharose beads. We employed a quantitative GST enzyme assay with 1 chloro-2,4 dinitro-benzene as substrate and determined that the total amount of GST fusion proteins purified in order to normalize per mole of purified protein (Fig. 2.2B). GST tagged protein was purified from transfected cell lysates and, as in total cell lysates, the nucleotide binding experiments demonstrate a ~2 fold increase in activity of Mfn2_{RasG12V}:GST relative to the wild type protein (Fig. 2.2B). In addition, the stimulated exchange activity of the Mfn2_{RasG12V} mutant reached levels similar to those obtained with molar equivalents of recombinant Rab5:GST (Fig. 2.2B). Although we could detect no significant differences in nucleotide binding to Mfn2:CFP within whole cell extracts (Fig. 2.2A), the GST purified Mfn2 did demonstrate nucleotide binding/exchange relative to the GST control (Fig. 2.2B). These biochemical data indicate that purified Mfn2 has extremely low rates of nucleotide exchange, consistent with high affinity binding. These data are consistent with published data that have also shown much stronger binding of Mfn2 to nucleotide relative to Mfn1 (9). Our data now shows that

mutations within the P-Loop of Mfn2 increase nucleotide exchange relative to the wild type protein, thereby bringing the rates closer to the intrinsic rates observed for the Rab GTPases.

We next examined the intrinsic rates of GTP[γ 32] hydrolysis using the established filter based assay quantifying the release of the labelled tertiary phosphate from the GTP bound protein purified from transfected COS7 cells (Fig. 2.2D) (36). Purified His6:Mfn2 hydrolysed 7.33×10^{-3} mmol GTP/mmol protein/min, which is approximately 4 times faster than the rates obtained for molar equivalents of bacterial expressed Rab5 protein (1.55×10^{-3} mmol GTP/mmol protein/min) (Fig. 2.2C). Although part of this signal may be due to complete loss/exchange of nucleotide rather than nucleotide hydrolysis, we consider this to be negligible since the rates of exchange for wild type Mfn2 are lower than Rab5 (Fig. 2.2A and B). The rates of GTP hydrolysis we have determined for Rab5 are similar to previously calculated rates of 2×10^{-3} /min (36, 37), further demonstrating the validity of the assay. Although the mutant Mfn2 exhibited increased rates of nucleotide exchange, His6:Mfn2_{RasG12V} demonstrated significantly reduced levels of hydrolysis (2.08×10^{-3} /min) relative to the wild type protein (7.33×10^{-3} /min) (Fig. 2.2C). Although we cannot exclude the contribution of trace levels of co-purifying GTPases, GTP exchange factors or GTPase activating proteins in the Mfn2 purification from cell extracts, our data clearly demonstrate that specific mutations in Mfn2 alter the nucleotide binding and hydrolysis properties of the purified protein.

2.4.2 Mfn2 is localized to specific subdomains along mitochondrial tubules in a nucleotide dependent manner.

We examined the cellular consequences of the GTPase mutant by transfecting Cos7 cells with either wild type Mfn2:CFP, GTPase mutant Mfn2_{RasG12V}:CFP, or a truncation mutant completely lacking the GTPase domain Mfn2₍₄₃₀₋₇₅₇₎CFP. Transfection of Cos7 cells with the wild type Mfn2 resulted in increased interconnectivity among the mitochondrial reticulum (Fig. 2.3), which upon high levels of expression appears as a cluster (1, 2, 4). As previously reported (38), Mfn2:CFP was localized in puncta along the mitochondrial tubules. Transfection of the GTPase mutant Mfn2_{RasG12V}:CFP resulted in the clustering of mitochondria, which appeared to be fused even at the lowest levels of detectable expression (Fig. 2.3). Importantly, unlike Mfn2:CFP, Mfn2_{RasG12V}:CFP was evenly distributed along the surface of these clusters (Fig. 2.3). In contrast, transfection of the Mfn2₍₄₃₀₋₇₅₇₎CFP mutant resulted in mitochondria visibly fragmented into small, spherical units which cluster together in a stable manner (Fig. 2.3 and data not shown), similar to those found in the Mfn1 GTPase truncation mutant (7). These phenotypes are specific to Mfn2 since transfection of another mitochondrial outer membrane protein, Tom7 (24), did not cause significant mitochondrial clustering (Fig. 2.3). In addition, these phenotypes were not affected by the presence of the CFP tag since transfection of untagged constructs gave similar results (data not shown). We considered that the assembly of the Mfn2 puncta may depend upon the conserved IMS residues. Mammalian Mfn2 contains only 2 to 3 amino acids separating the two transmembrane domains, one of which is a highly conserved tryptophan residue that we replaced with a proline residue (Mfn2_{W631P}). This proline residue is naturally occurring within the IMS loop in *Drosophila melanogaster* Fzo, indicating that this substitution should

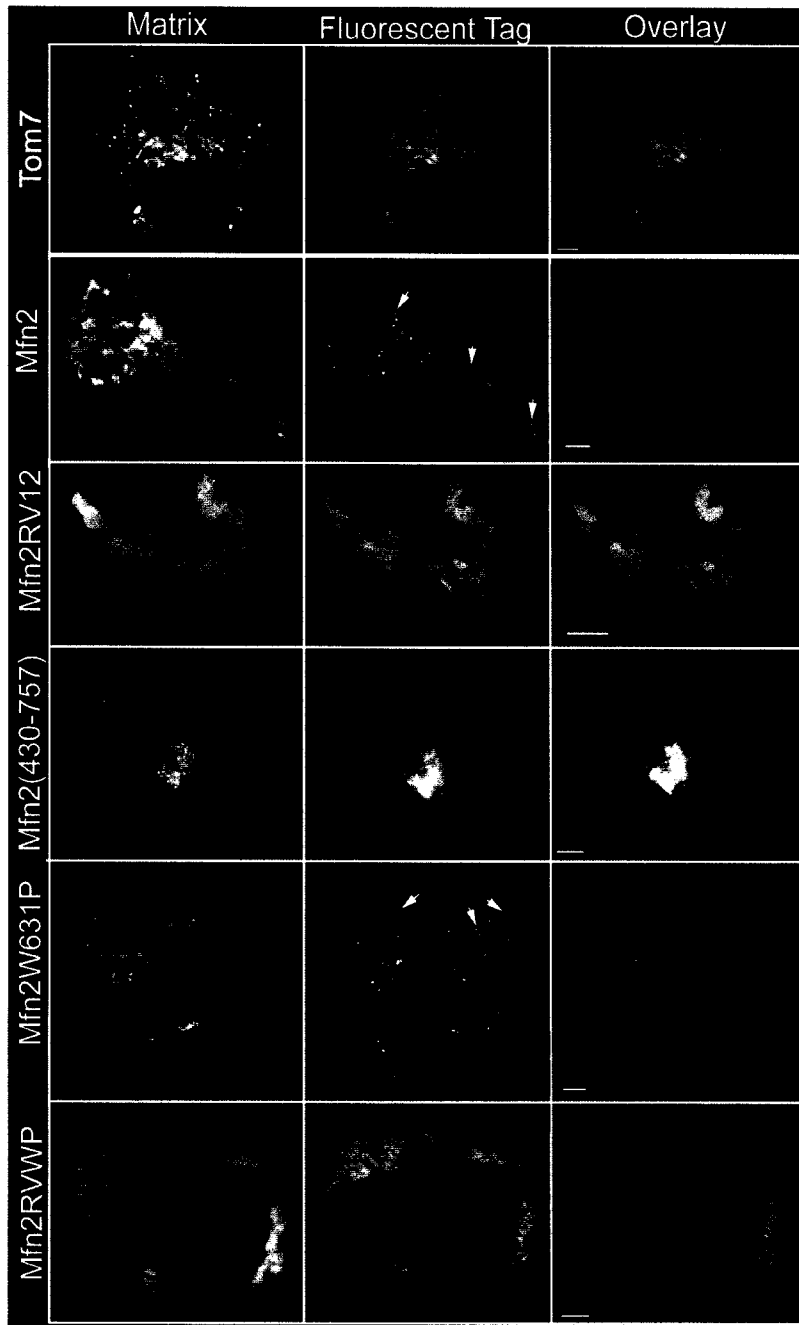


Figure 2.3 *Mitochondrial morphology and distribution of Mfn2 mutants*

Figure 2.3 *Mitochondrial morphology and distribution of Mfn2 mutants*

COS7 cells were co-transfected with pOCT:YFP (left panels) and the CFP tagged constructs indicated (middle panels). As a control Tom7:GFP was co-transfected with pOCT:DsRed2 (top panels). Images were taken from living cells 16 hours after transfection. In the overlay, the matrix marker is shown in red and FP fusion proteins in green. Note the punctate appearance of Mfn2:CFP and Mfn2_{W631P}:CFP (arrows) compared to the smooth distribution of Mfn2_{RasG12V}:CFP and Mfn2_{RVWP}:CFP. Scale bars are 1 μ m.

not alter the topology of Mfn2. Mfn2_{W631P}:CFP remains sharply localized in distinct foci, however the tubular morphology of the mitochondria is reduced, and the organelles eventually fragment (Fig. 2.2). Creation of a double mutant where both the Mfn2_{RasG12V} and Mfn2_{W631P} mutations are present (Mfn2_{RVWP}:CFP) also resulted in a loss of Mfn2 puncta, indicating that the punctate localization does not depend upon the conserved IMS residues, rather it is determined by the nucleotide state (Fig. 2.3). Video analysis showed that the Mfn2:CFP puncta remained highly immotile and were not observed at sites of mitochondrial fusion, nor did they significantly colocalize with the cytoskeleton (actin filaments or microtubules), and they did not accumulate at sites of ER/mitochondrial contact (data not shown).

To ensure that the clustered mitochondria within cells transfected with Mfn2 and mutants maintained their electrochemical potential, we quantified the total fluorescence intensity within cells loaded with a $\Delta\Psi$ dependent dye and scored the results in a distribution profile as shown in Table 2.1. In untransfected cells, the fluorescence intensity was between 1 and 3×10^6 arbitrary units in 90% of the cells examined. Transfection of Mfn2_{W631P} showed some loss in total dye uptake, with 61% of the cells examined exhibiting fluorescent units of less than 1×10^6 AU. Transfection of the other constructs did not show significant loss in potential, but showed a broader distribution profile than untransfected cells, with many transfected cells exhibiting fluorescence units higher than normal. For example, transfection of Mfn2, Mfn2_{RasG12V} or Mfn2_{RVWP} showed 15-20% of cells having greater than 4×10^6 AU fluorescent units. These data demonstrate that electrochemical potential is maintained, with a slight reduction in cells transfected with Mfn2_{W631P}.

Distribution profile of intensities of $\Delta\Psi$ -Dependent Dye Uptake (as % of total cells)							
Fluorescence A.U. $\times 10^6$	UTF	Mfn2:CFP	Mfn2 _{RasG12V} :CFP	Mfn2 _{W631P} :CFP	Mfn2 _{RVWP} :CFP	Mfn2 ₍₄₃₀₇₅₇₎ :CFP	Drp1K38E:CFP
<1	4.8	19	9	61.1	14.3	16.7	6.3
1 to 2	57.1	28.6	25	33.3	38.1	33.3	18.8
2 to 3	33.3	28.6	25	5.6	9.5	38.9	37.5
3 to 4	4.8	9.5	19	0	23.8	11.1	37.5
>4	0	15	22	0	15	0	0

Table 2.1: *Quantification of MitofluorRed589 uptake into mitochondria of transfected cells.*

2.4.3 PEG induced cell fusion demonstrates that Mfn2_{RasG12V} is a dominant active mutant.

In order to directly assess the fusion competence of mitochondria in cells expressing these proteins, we employed a well characterized assay that induces fusion between whole cells transfected with different matrix marker proteins (4-6). Mitochondria from heterokaryons transfected with marker proteins alone fused completely within 8-12 hours (Fig. 2.4, top left panels) (4-6). Mitochondria from donor cells expressing Mfn2:CFP also fused with acceptor mitochondria within a similar time course (Fig. 2.4, middle left n=29), however approximately 20% of the heterokaryons expressing Mfn2:CFP scored complete content mixing within 2 hours. Strikingly, fusion between mitochondria expressing Mfn2_{RasG12V}:CFP with acceptor GFP organelles occurred within 30 minutes after the addition of PEG in >90% of the observed cell fusions (Fig. 2.4, bottom left, n=20). Video analysis of the PEG fusion assay shows that the Mfn2_{RasG12V}:CFP cluster remains immobile whereas the GFP containing acceptor mitochondria are motile within the heterokaryon (Supplemental Video 2.1). This efficient fusion between mitochondria was highly significant since the migration of mitochondria from one cell into another is a slow process in mammalian cells. In control experiments very few mitochondria within the heterokaryon had migrated across the cell boundary in the first hour (Fig 2.4). In contrast, the rapid and/or directed migration of the GFP expressing mitochondria towards the Mfn2_{RasG12V}:CFP expressing DsRed mitochondria allowed complete fusion of all mitochondria to occur within 30 minutes. This indicates that the presence of Mfn2_{RasG12V} within one population of mitochondria initiates a cascade of events that lead to highly efficient mitochondrial fusion.

Figure 2.4

Mfn2RasG12V stimulates mitochondrial fusion in PEG cell fusion assays

COS7 cells transfected with pOCT:GFP or pOCT:DsRed2 and Mfn2:CFP constructs (as indicated) were seeded together for 12 hours and 50% PEG 5000 was added for 60 seconds following a 2 hour pre-incubation with cyclohexamide. Images of both fluorophores were taken from live cells after 1 hour and 8 hours. The overlay of the pOCT:GFP (green) and pOCT:DsRed (red) is shown for each time point. Mitochondrial fusion is indicated by GFP and DsRed matrix content mixing, which appears yellow in the image. Scale bars are 1 μ m.

Video 2.1 Mfn2_{RasG12V}:CFP PEG fusion assay

This video documents the immobility of the Mfn2_{RasG12V}:CFP induced mitochondrial cluster expressing pOCT:DsRed, and shows the pOCT:GFP expressing mitochondria from the acceptor cell within the heterokaryon docked around the perimeter of the Mfn2_{RasG12V} cluster. These GFP containing mitochondria are already fusing among themselves and are more motile than the DsRed containing cluster since they have migrated through the heterokaryon in order to dock and fuse into the cluster. Within this video they are seen to still have mobility, however once they have docked and fused, the GFP mitochondria also lose motility since they also become trapped. Video was taken 20 minutes after the addition of PEG (see Experimental Procedures) by excitation at 589 nm to excite pOCT:DsRed (shown red) and 488 nm to excite the pOCT:GFP (shown green). Imaging of each fluorophore was separated by 3 msec for the monochromator to switch wavelengths and there were 2 second delays between frames. 100 frames are shown, played back at 10 frames per second. Scale bar on still image is 1 micron

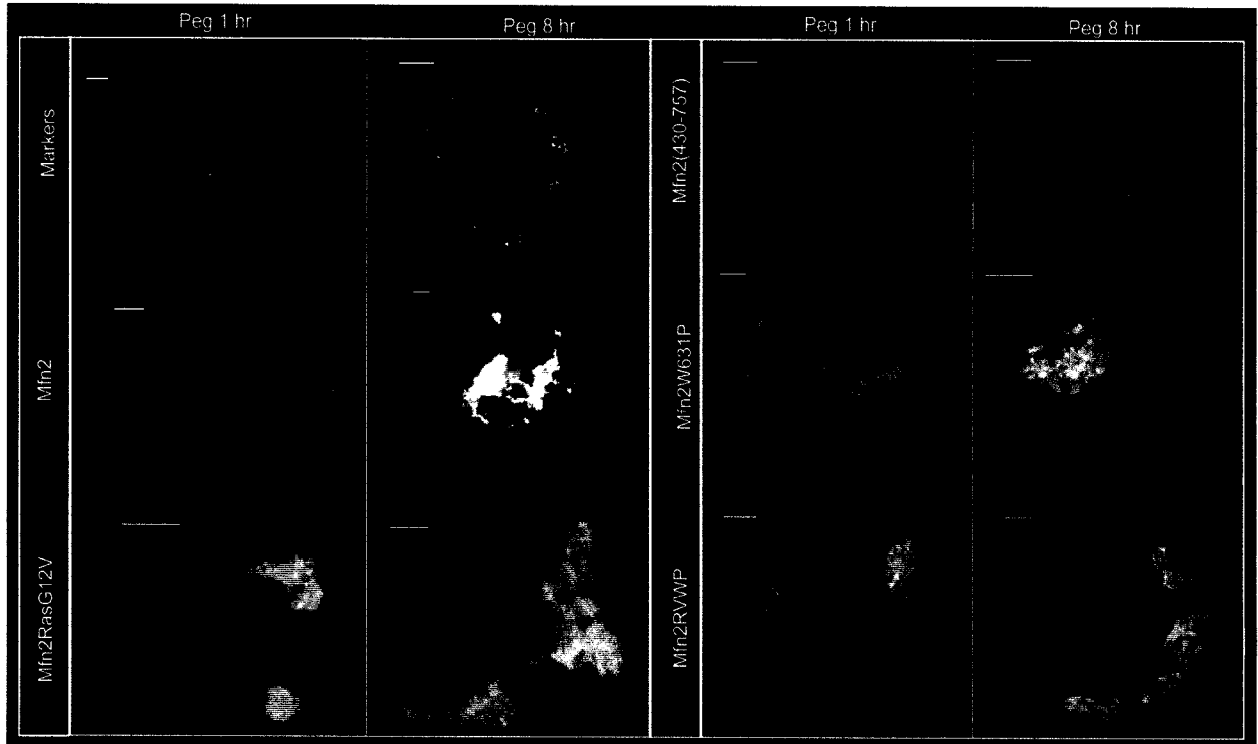


Figure 2.4

Mfn2RasG12V stimulates mitochondrial fusion in PEG cell fusion assays

Therefore, we consider the Mfn2_{RasG12V} to be the first characterized dominant active, GTPase deficient mutant that stimulates mitochondrial fusion.

The Mfn2₍₄₃₀₋₇₅₇₎CFP construct completely inhibited the fusion, confirming the requirement for the GTPase domain (Fig. 2.4, upper right). In addition to a role in contact site formation, previous studies with yeast Fzo1p have demonstrated the requirement for the IMS loop of Fzo1p for mitochondrial fusion (8). Consistent with this, fusion was inhibited between mitochondria containing Mfn2_{W631P}:CFP and acceptor GFP containing mitochondria. Surprisingly, the inhibition of mitochondrial fusion conferred by the Mfn2_{W631P} mutation (Fig. 2.4, middle right) was rescued by the Mfn2_{RasG12V} mutation within the double mutant (Fig. 2.4, bottom right), indicating that the conserved IMS domain is not directly required for the fusion event, but likely plays a more regulatory role in the activation of Mfn2.

2.4.4 Fused mitochondria are interconnected by novel membrane elements.

Ultrastructural analysis revealed that the mitochondria do not fuse into a single organelle, but instead they are interconnected through unusual membranous networks (Fig. 2.5 A). The fused clusters in Mfn2_{RasG12V} transfected cells were qualitatively similar to the wild type (Fig. 2.5 A), indicating that the end point of the fused mitochondrial reticulum is similar, even though the PEG fusion assay demonstrated that kinetics of the fusion event are different (Fig. 2.4). Analysis of Mfn2_{W631P} transfected cells did not reveal any interconnecting membranes between the clustered organelles. Notably, some of the mitochondria in the Mfn2_{W631P} transfected cells appeared to “unravel”, with membranous material emanating beyond the clear boundaries of the outer membrane (Fig. 2.5 A). This

Figure 2.5

Ultra-structural analysis reveals that clustered mitochondria are interconnected by novel Mfn2-containing membrane elements

A. Representative images taken at high magnification are shown from cells expressing the constructs indicated. Mitochondria from untransfected cells are also shown for comparison (upper left panel). **B.** Immuno-electron micrographs using anti-FP antibodies to label mitochondrial clusters expressing the activated Mfn2_{RasG12V}:CFP and Mfn2_{RVWP}:CFP, as indicated.

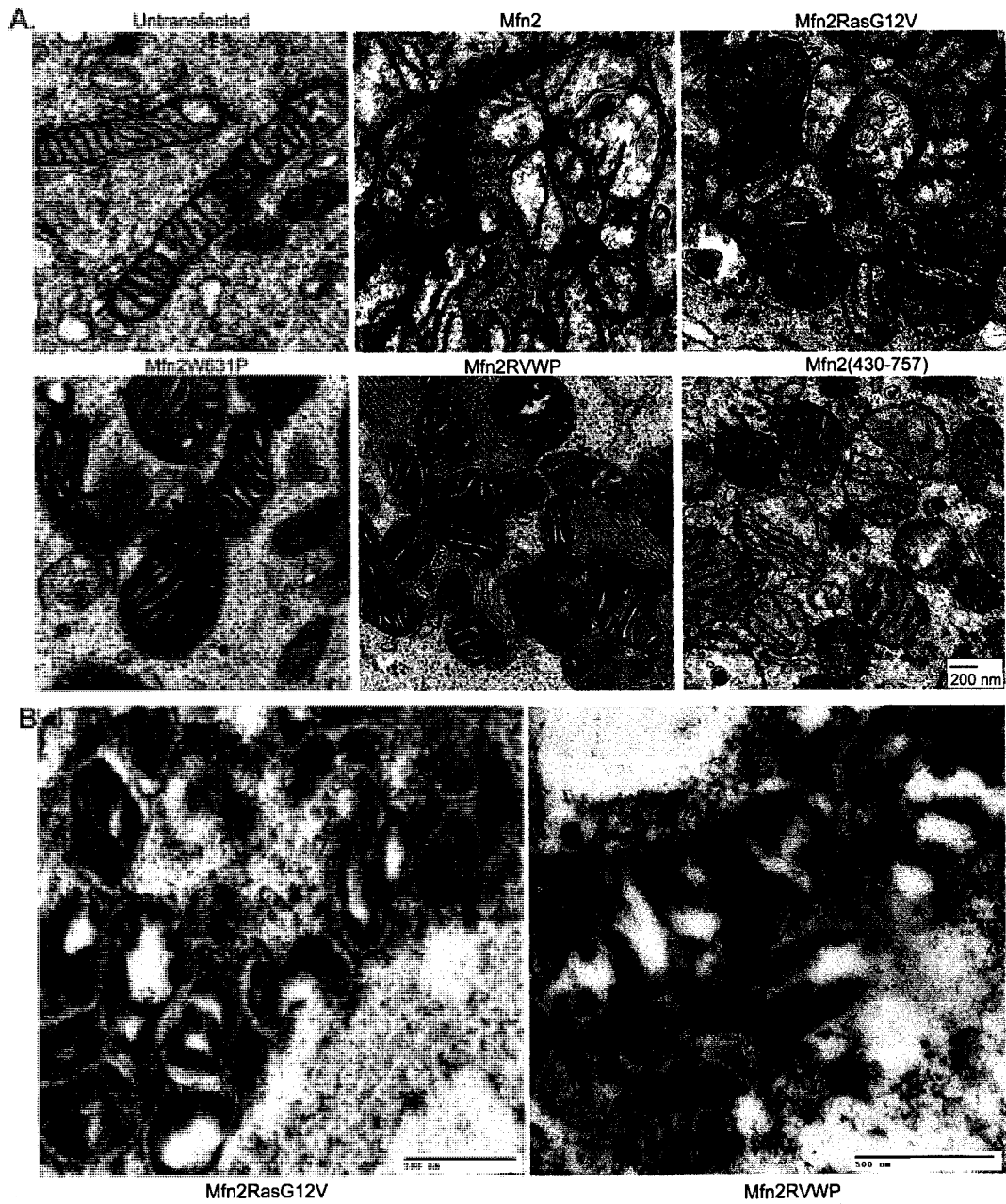


Figure 2.5

Ultra-structural analysis reveals that clustered mitochondria are interconnected by novel Mfn2-containing membrane elements

may be due to loss of contact site formation (8), leading to aberrant membrane architecture.

Mitochondria in cells expressing Mfn2_{RVWP}:CFP contained stacks of parallel membranes and extensive membrane whorls that were interconnected throughout the cluster.

Immunolabelling of the fused mitochondrial clusters indicates that the Mfn2 protein is found within the interconnecting membranes, demonstrating that these membranes are derived, at least in part, from the outer mitochondrial membrane (Fig. 2.5 B). Regardless of this massive alteration in membrane architecture, the cristae and electron dense matrix compartments appeared normal, consistent with their ability to maintain electrochemical potential (Table 2.1) and stimulate mitochondrial fusion (Fig. 2.4). Mitochondria within cells expressing Mfn2₍₄₃₀₋₇₅₇₎CFP were docked together within a cluster, consistent with the proposed tethering function of the HR2 domain (7). However there was no fused membrane material between the mitochondria (Fig. 2.5 A), demonstrating that the fused membranes do not arise simply due to non-specific mitochondrial clustering.

2.4.5 Activated Mfn2 represses Bax activation, cytochrome c release and permeability transition.

Given the increasing involvement of dynamic changes in mitochondrial morphology during the progression of apoptosis, we next examined the specific consequence of Mfn2 activation on the mitochondrial response to two different types of stimuli. Stimulation of programmed death by STS treatment resulted in the efficient recruitment and activation of Bax to the mitochondria, as revealed by an antibody that specifically recognizes the conformationally active form of Bax (39). As expected (40, 41), the amount of Bax activation correlated with the amount of cytochrome c release (~50% by 3 hours, Fig. 2.6 A

and 5B, n=379). As a negative control, we transfected cells with DRP1(K38E) (42-44), which has been shown to block mitochondrial fission and inhibit cytochrome c release from mitochondria (26, 45). As expected, only 3% of these cells showed cytochrome c release after 3 hours of STS treatment, with ~10% of cells showing Bax activation (n=66). By 5 hours of treatment, this level of Bax activation increased without a release of cytochrome c (data not shown), as has been previously reported within cells transfected with DRP1(K38A) (38). Transfection of Mfn2:CFP showed a reduction of STS induced Bax activation and cytochrome c release (Fig. 2.6 A), with only ~35% of cells showing susceptibility to STS treatment (Fig. 2.6 B, n=92). Interestingly, in the 35% of STS sensitive cells, many of the Mfn2:CFP containing puncta colocalized with activated Bax (insets Fig. 2.6 A).

Mfn2_{RasG12V}:CFP and Mfn2_{RVWP}:CFP both repressed Bax activation and cytochrome c release, where only ~20% of cells were susceptible to STS treatment (Fig. 2.6 B, n=69, 72 respectively). In contrast, the fusion incompetent Mfn2_{W631P}:CFP did not provide protection against Bax activation or cytochrome c release (Fig. 2.6 A, n=73). As with Mfn2:CFP, activated Bax often colocalized with Mfn2_{W631P}:CFP containing puncta (see insets, Fig. 2.6 A). Cells transfected with the dominant negative mutant Mfn2₍₄₆₀₋₇₅₇₎:CFP were highly sensitive to STS treatment, with 80% of cells showing complete cytochrome c release by 3 hours (Fig. 5A, n=95). Oddly, the amount of cytochrome c release in this condition (~80%) did not mirror the amount of Bax activation (~40%) which could be explained since cytochrome c was released in Mfn2₍₄₃₀₋₇₅₇₎:CFP transfected cells in a Bax independent manner, without any death stimuli (Fig. 2.6 A). As expected, transfection of the other Mfn2 constructs showed normal, mitochondrial cytochrome c staining in the absence of any death

stimuli (data not shown). Taken together, the data show that activated Mfn2 is a repressor of Bax activation and outer membrane pore formation.

Given that activated Mfn2 can provide protection against Bax activation and cytochrome c release triggered by external apoptotic stimuli, we next wanted to investigate whether Mfn2 could also protect the mitochondria from damage induced by internal metabolic stress. We therefore adapted an assay which artificially produces free radicals within the matrix of the mitochondria, thereby triggering permeability transition and PTP opening in the absence of Bax activation (46-48). This approach allowed us to damage the mitochondria from the matrix side, simulating physiological systems where mitochondrial radical loads are increased due to excessive respiratory activity or other stresses. The $\Delta\Psi$ sensitive dye tetramethyl rhodamine ester (TMRE) and its derivatives, such as MitofluorRed 589, become photoactivated upon exposure to light and subsequently produce free radicals within the matrix of the mitochondria. With the increasing accumulation of free radicals, the permeability transition pore opens and protons become equilibrated across the inner membrane (47, 48). Concomitant with the loss in $\Delta\Psi$, the potential sensitive dye is redistributed within the cell, a process observed using time lapse video microscopy. The mitochondria then regain $\Delta\Psi$, which allows the re-uptake of the potential-sensitive dye, and in time lapse appear to “flicker” until they become terminally depolarized. Four hundred images were collected over 25 minutes by exciting MitofluorRed 589 for 1000 msec, followed by a 2500 msec delay. Fig. 2.7 shows that 84% of the untransfected cells incubated with 50 nM MitofluorRed 589 reached terminal depolarization within the first frame category (frames 1-250, n=56). Mfn2:CFP expressing cells revealed a moderate, but significant protection from free radical induced damage, with a varied distribution of rates of

Figure 2.6

Activation of Mfn2 protects against STS-induced cell death

A. Transfected COS7 cells were incubated with 2 μ M STS in the presence of 10 μ M zvad-fmk and immunolabelled with anti-cytochrome c antibodies (blue) and anti-Bax antibodies (red). Representative images of cells are shown. Cytochrome c release of cells transfected with Mfn2₍₄₃₀₋₇₅₇₎CFP in the absence of death stimuli is shown in lower right panel. Insets show higher magnifications of the individual channels, as indicated. Note the co-localization of Bax with Mfn2:CFP proteins upon activation. **B.** The percentage of cells with cytochrome c release and Bax activation were scored at 3 hours post STS treatment and the data was plotted as a percentage distribution of total cells

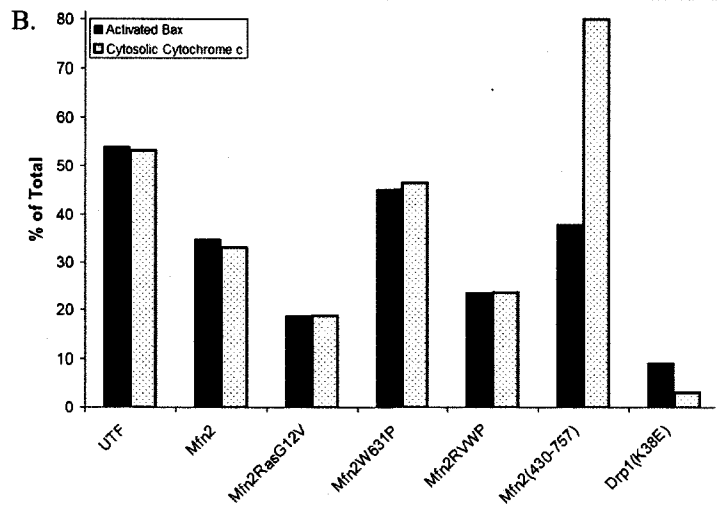
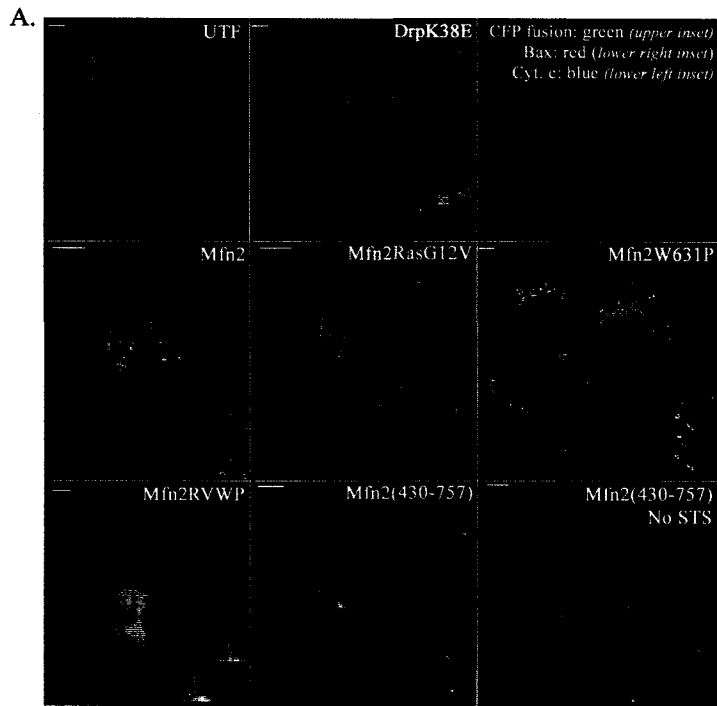


Figure 2.6

Activation of Mfn2 protects against STS-induced cell death

dye loss across the four frame categories ($p < 0.003$ Fishers exact test, $n=19$). Similar to the protection granted against STS treatment, 62% of the cells containing a fused mitochondrial reticulum induced by transfection of Mfn2_{RasG12V}:CFP were significantly protected against free radical induced damage until the fourth frame category (350-400 frames, $p < 0.001$ from Fishers exact test, $n=21$). In contrast, the mitochondria within cells expressing Mfn2_{W631P}:CFP rapidly reached their damage threshold with 92% of cells losing their dye ($n=13$) within the first frame category, consistent with their susceptibility to STS.

Unexpectedly, although the morphological phenotypes were similar between Mfn2_{RVWP}:CFP and Mfn2_{RasG12V}, and they both significantly protected mitochondria against STS treatment, the double mutant was not protected from the radical induced damage, with 78% ($n=18$) of mitochondria terminally depolarized in the first frame category. These data suggest that both the activation of Mfn2 GTPase domain and the IMS tryptophan residue are essential for PTP inhibition to occur. As expected, fragmented mitochondria expressing Mfn2₍₄₃₀₋₇₅₇₎:CFP did not affect the loss of dye in these experiments since 82% ($n=22$) of mitochondria were terminally depolarized within the first frame category. These effects are not due to differences in either Mitofluor dye loading or absolute free radical production, since fluorescent quantification of initial Mitofluor dye uptake and the radical dye hET show no differences between the transfected vs. untransfected controls (Tables 2.1 and 2.2). The specificity of this assay was further verified by creating a fused reticulum following transfection with the dominant interfering DRP1 mutant, DRP1(K38E). In contrast with the protection granted by DRP1(K38E) in terms of STS induced cytochrome c release, the fused mitochondrial reticulum within cells expressing DRP1(K38E):CFP were not protected from

Figure 2.7.

Activation of Mfn2 protects against permeability transition

COS7 cells, as indicated, were incubated with 50 nM MitoFluorRed 589, exposed to light (see Experimental Procedures) and scored for terminal depolarization. The results were converted to a percent value and plotted as a frequency distribution for each transfection condition, as indicated in the graph

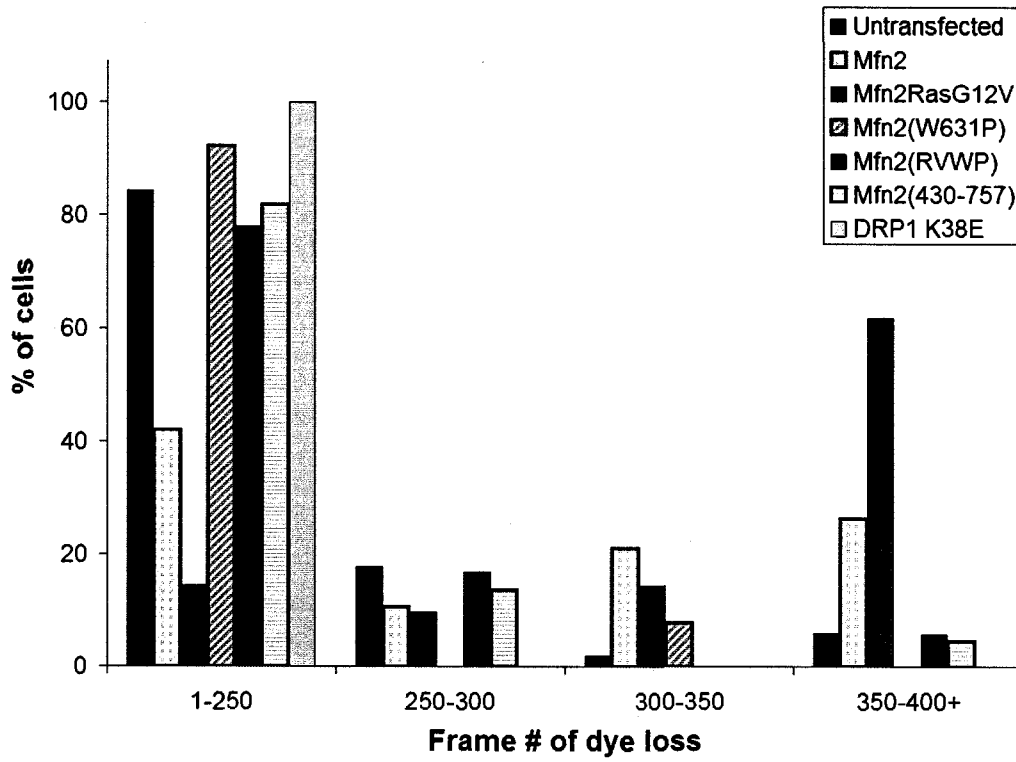


Figure 2.7.

Activation of Mfn2 protects against permeability transition

Distribution profile of steady state radical load (% of total cells)							
Fluorescence A.U. x10⁶	UTF	Mfn2:CFP	Mfn2_{RASG12V}:CFP	Mfn2_{W631P}:CFP	Mfn2_{RVWP}:CFP	Mfn2₍₄₃₀₇₅₇₎:CFP	Drp1K38E:CFP
<1	41.7	40	26.7	61.5	12.5	12	10
1 to2	25	50	40	38.5	62.5	59	34.5
2 to 3	25	10	20	0	18.8	29	24.1
>3	8.3	0	13.3	0	6.3	0	31

Table 2.2: *Quantification of hET oxidation within transfected cells*

the free radical load (Fig. 2.7, n=26), demonstrating that a fused mitochondrial morphology alone does not inhibit permeability transition.

2.5 DISCUSSION

We have shown for the first time that Mfn2 exhibits properties of a signalling GTPase capable of regulating not only mitochondrial fusion, but that its nucleotide state also plays a critical role in regulating the mitochondrial response to apoptotic and free radical induced damage. Through the creation of mutants, we have dissected the functional role of the GTPase activity and the intermembrane space domain within Mfn2. Biochemical evidence indicates that Mfn2 exhibits nucleotide properties similar to Rab5, with low intrinsic rates of hydrolysis and nucleotide exchange. These data are consistent with the recently published work showing that Mfn2 has a higher affinity to nucleotide and dramatically slower rates of hydrolysis relative to Mfn1 (9). Most importantly, we have characterized the nucleotide binding and hydrolysis properties of a mutant form of Mfn2, Mfn2_{RasG12V} and showed that this mutant has slower hydrolysis and increased nucleotide exchange when compared directly to the wild type protein (Fig.2.2). This mutant allowed us to examine the functional consequences of a GTP hydrolysis deficient, dominant active form of Mfn2. Our mutants have demonstrated a number of important findings. First, the hydrolysis deficient mutant of Mfn2 results in a dramatic stimulation of mitochondrial fusion, and the ultrastructural analysis of the fused mitochondrial clusters indicate a striking proliferation of interconnected membranes, shedding new light on the plasticity of the mitochondrial membranes. Furthermore, we have determined that the conserved tryptophan residue within the intermembrane space region of Mfn2 is not essential to form a fusion pore, but is required to activate fusion within the context of the wild type GTPase. The

mutational analysis also allowed us to determine that the punctate localization of Mfn2 (38) is regulated by the nucleotide state. The hydrolysis deficient mutants of Mfn2 that stimulate mitochondrial fusion do not readily form puncta, whereas the mutants that inhibit mitochondrial fusion are found in these foci. Finally, the activated Mfn2 constructs significantly represses Bax activation, cytochrome c release and free radical induced permeability transition. Taken together, these data reveal a role for Mfn2 as a regulator of mitochondrial fusion and as a nucleotide dependent modulator of the apoptotic response.

The PEG fusion assay demonstrates that Mfn2 is a regulatory GTPase, which when in the activated form is capable of signalling to neighbouring mitochondria to fuse in an accelerated manner. Since Mfn2_{RasG12V}:CFP is anchored within the mitochondrial outer membrane of the DsRed containing mitochondria in Fig. 2.4, it follows that Mfn2_{RasG12V} initiated cytosolic events resulting in the efficient recruitment and fusion of GFP containing mitochondria with the Mfn2_{RasG12V}:CFP/DsRed reticulum. Clearly there are a number of molecular events that contribute to this dramatic increase in fusion, including increased motility events, as well as the activation of the fusion machinery. Our data therefore indicate that Mfn2 may play a dual role, both as a direct constituent of the tethering/fusion machinery (minimally through the coiled coil domains of Mfn₄₃₀₋₇₅₇) and as a GTPase capable of initiating secondary cellular events. These secondary cellular events likely include the co-operation and/or activation of Mfn1, which has been shown to function directly with Opa1 in driving mitochondrial tethering and fusion (7, 9, 10). Evidence supporting a primary role for Mfn2 as a signalling GTPase has come from previous work demonstrating that mouse embryonic fibroblast cells lacking Mfn2 show a loss of long range motility events (6), consistent with a role for Mfn2 in regulating mitochondrial movement. Our data is also

consistent with the recently identified role for Mfn2 as a regulator of the Ras signalling pathway (21). Given that Ras signalling occurs at the plasma membrane, the ability of Mfn2 to invoke a signalling cascade would provide a mechanism for it to act upstream of events at a separate intracellular location.

What are the physiological triggers that might activate Mfn2? Since Mfn2_{W631P}:CFP results in fusion inhibition, we consider that this IMS residue is required for the stimulation of GTP nucleotide exchange in Mfn2. In this case, the GTPase domain within the Mfn2_{W631P} protein would remain in the inactive, GDP bound state locked within the puncta where fusion could not be initiated, as observed in Figs 2.3 and 2.4. Since the IMS tryptophan residue is so critical in providing protection against free radical induced permeability transition (Fig. 2.7), we speculate that internal mitochondrial signals would communicate with Mfn2 through this residue in order to initiate mitochondrial fusion in response to local free radical production and other forms of metabolic damage. Mitochondrial fusion may then buffer and rescue local radical damage by sharing scavengers and other metabolites between healthy and damaged organelles. Under physiological conditions, this novel link between mitochondrial fusion and PTP inhibition suggests a robust system to protect against accumulated cellular damage that could potentially lead to inopportune cell death. Consistent with this, mouse embryonic fibroblast cells lacking Mfn2 showed a loss in membrane potential (6), and antisense experiments to reduce Mfn2 levels in cultured myotubes demonstrated a loss in glucose oxidation, membrane potential and oxygen consumption (49).

In addition to providing protection against free radical induced permeability transition, the data demonstrate that activated Mfn2 represses STS induced Bax activation and cytochrome c release. This places a primary component of the mitochondrial fusion

machinery as a regulator of the apoptotic response. Given that the activation of Mfn2 concomitantly blocks permeability transition and activates mitochondrial fusion, it suggests that these two pathways are mutually exclusive. It has been previously shown that mitochondrial fusion events are inhibited during an apoptotic stimulus (50), consistent with our data indicating that Mfn2 must be in the inactive, GDP bound form to allow for activation of Bax. Although the mechanism by which Mfn2 might regulate Bax activation is unknown, it is possible that the punctate Mfn2 sites represent preassembled channels competent for activated Bax recruitment and outer membrane permeability transition, and upon activation of Mfn2, critical components within these microdomains may disassemble. Alternatively, the activation of Mfn2 for fusion may directly inhibit the fission machinery in order that the two events remain exclusive. Since fission precedes cytochrome c release and appears requisite for apoptosis (51, 52), any interference of activated Mfn2 with components of the fission machinery would effectively block Bax activation and cytochrome c release. Obvious candidates would be Fis1 and DRP1 since they function together in promoting mitochondrial fission and eliciting an efficient apoptotic response (22, 23, 25, 26, 45). It will be important to characterize the Mfn2 interacting proteins, those both cytosolic and mitochondrial, in order to better define the molecular events that link the GTPase cycle of Mfn2 with mitochondrial fusion and the control of permeability transition.

2.6 EXPERIMENTAL PROCEDURES:

Construct preparation and reagents.

The cDNA encoding human Mfn2 (KIAA0214) was graciously provided by Kazusa DNA Research Institute, Japan. Mitofusin2 cDNA was PCR amplified using standard protocols, for insertion into pECFP-C1 (Clontech, Palo Alto, USA) and pcDNA3.1

(Invitrogen, Burlington, Canada) with BamH1 and HindIII restriction sites. Mfn2_{RasG12V}:CFP was prepared using Quick-Change mutagenesis (Stratagene, La Jolla, USA) using pECFP-C1:Mfn2 as the template and a set of oligonucleotides designed to replace amino acids **GRTSNGKS** with **GAVGVGKS**. The restriction site Nar1 was introduced into the primers for screening purposes. The pcDNA3:GST, Mfn2:His6 and Mfn2_{RasG12V}:His6 constructs vectors for protein purification from transfected cell lysates were also prepared using subcloning techniques and all sequences used in this work were confirmed. Mfn2_{W631P}:CFP was prepared using Quick-Change mutagenesis (Stratagene, La Jolla, USA) with pECFP-C1:Mfn2 as the template and a set of oligonucleotides designed to replace the tryptophan amino acid at position 631 with a proline. The Apa1 restriction site was introduced into the primers for screening purposes. Mfn2_{R₁VWP}:CFP was prepared by isolating the DNA fragment encoding amino acids 1-431 of Mfn2_{RasG12V}:CFP by digestion with HindIII and Sal1, and subcloning this fragment containing the RasG12V mutation into the Mfn2_{W631P}:CFP construct cut with the same enzymes, thereby replacing the wild type GTPase domain of Mfn2_{W631P}:CFP with the Mfn2_{RasG12V} mutation. The cDNA encoding DsRed2 was amplified from pDsRed2-C1 (Clontech, Palo Alto, USA) using primers designed for digestion with BamH1 and Xba1 and ligation into the pcDNA3-pOCT vector (53). Tom7:GFP was gratefully obtained from Mike Ryan, La Trobe University, Melbourne Australia. Mfn2 mouse polyclonal antisera was generated against a cocktail containing both recombinantly expressed Mfn2₍₇₁₀₋₇₅₇₎:GST, and a synthetic Mfn2 NH₂-terminal peptide CNSIVTVKKNKRIIM-OH (Dalton Chemical Laboratories, Toronto, Canada), conjugated to 5 mg of maleimide activated KLH. Antisera was generated following a 56 day standard immunization protocol. Polyclonal antibodies against fluorescent proteins (anti-FP) used for

immunoEM were purchased from Clontech, Palo Alto, USA. Dihydroethidium (D23107) Molecular Probes (Eugene, USA) was utilized to determine steady state radical levels in transfected cells. Monoclonal 7H8.2C12 anti-cytochrome c antibodies were obtained from BD Biosciences, and rabbit polyclonal anti-Bax antibodies were obtained from Upstate cell signalling solutions. Alexa Flour 350 and 594 goat anti-mouse or rabbit secondary antibodies from Molecular Probes (Eugene, USA) were used for STS experiments. zVAD was obtained from Enzyme Systems Products (Aurora, Canada) and staurosporin (STS) was obtained from Sigma (Oakville, Canada).

Transfection and imaging of COS7 cells

Transfection and imaging methods were exactly as described in (53). For electrochemical potential determination cells were incubated with 50 nM MitofluorRed 589 at 37°C for 20 minutes. Whole cell images were acquired for untransfected and transfected cells by exciting at 589 nm with the CFP/YFP/DsRed triple pass filter (Chroma, Vermont). The presence of transfected CFP tagged protein was confirmed by exciting at 434 nm using the same filter set. Areas of interest were selected for each cell and total fluorescence arbitrary units were summed for each cell. The total fluorescence intensity per cell was quantified as the sum of the values of each pixel within the area of interest minus the average background signal obtained per pixel. The number of cells within each fluorescence distribution range was scored and tabulated as a percentage.

For MitofluorRed 589 (Molecular Probes, Oregon) flickering experiments, 50 nM dye was added to the chamber medium and incubated with the cells at 37°C for 20 minutes. Following equilibration of the dye, 400 images were collected by exciting at 589 nm with

the CFP/YFP/DsRed triple pass filter (Chroma, Vermont) for 1 second followed by a 2.5 second delay. The presence of transfected CFP tagged protein was confirmed as indicated above. The time series were analyzed and each frame where all mitochondrial dye was released from the whole cell was plotted.

To determine steady state radical loads, cells were incubated with 5 μ M dihydroethidium (hET) at 37°C for 20 minutes. Dihydroethidium oxidation by super oxide to ethidium was visualized by excitation at 547 nm. Whole cell imaging and fluorescence quantification for untransfected and transfected cells was performed as indicated above

Mant GMP-PNP binding assay:

COS-7 cells were transfected with pOCT:CFP, Mfn2:CFP, Mfn2_{RasG12V}:CFP, and Rab5:CFP fusion constructs. The day after transfection, the cells were harvested by trypsinization, washed with PBS, and with nucleotide binding buffer (220 mM mannitol , 68 mM sucrose, 200 mM NaCl, 2 mM MgCl₂, 0.5 mM EGTA, 2.5 mM KH₂PO₄, 10 mM HEPES, pH 7.4, 1mg/ml BSA) containing protease inhibitors. Cells were then broken in a cell cracker, and the whole lysate centrifuged at 10,000 rpm, to concentrate heavy membrane fractions. Pellets were resuspended in binding buffer and 50 μ l aliquots were mixed with Mant-GMP-PNP (1 μ M final conc., Molecular Probes, Oregon) and incubated at 37°C for different times. After incubation the aliquots were scanned for emission fluorescence of Mant-nucleotides in a QuantaMaster 6000SE (Photon Technology International, London, Canada) (excitation at 360 nm). The peak emission at 448 nm was recorded and the background fluorescence of the nucleotide alone was subtracted. Each value was also normalized for total protein concentration in the sample (determined using the DC protein

assay (Biorad)), and for the level of recombinant protein expression by measuring the CFP signal obtained in the fluorimeter upon excitation at 434 nm, emission at 477 nm.

For the purification of GST, Mfn2:GST and Mfn2_{RasG12V}:GST from transfected cell lysates, 10 cm dishes of COS7 cells were transfected using Lipofectamine 2000 (Invitrogen), and following 12 hours, were trypsinized, washed and lysed with TNE buffer (25 mM Tris-HCl, pH 7.4, 150 mM NaCl, 5mM, EDTA, 1 mM DTT, 60 µg/ml chymotrypsin, 1 µM leupeptin, 25 µg/ml antipain, 2 µg/ml aprotinin, 40 µM APMSF, 1 mM pepstatin A), containing 1 % Triton X-100 for 2 hours at 4°C. Lysates were adjusted to 40 % sucrose, and centrifuged at 70,000 rpm for 1 hour, at 4°C. Supernatants were diluted to 10 % sucrose with TNE + Triton buffer, and were incubated overnight with glutathion-sepharose beads at 4°C. Beads were washed and GST fusion proteins were eluted with 50 mM reduced glutathione in TNE buffer + 10 % sucrose. Eluted aliquots (50 µl elutions) were incubated, in duplicate, with 0.2 uM Mant-GMP-PNP for 15 min. at 37°C, and assayed for fluorescence (excitation, 360 nm; emission, 448 nm). Normalization was done by assaying the enzymatic activity of GST within each aliquot, with 1, chloro, 2, 4, di-nitro benzene (CDNB, Sigma) and glutathione as substrates, with formation of a product with absorbance at 340 nm (Amershan Biosciences), being the product formation rate proportional to the amount of GST in the aliquots. Known concentrations of bacterially purified GST was used as a standard in this assay. Bacterially expressed Rab5:GST was purified as previously described (54).

GTP³² hydrolysis assay

COS-7 cells were transfected with Mfn2:His6, Mfn2_{RasG12V}:His6, or LacZ:His6, and the following day cells were washed with PBS, harvested by scrapping and centrifuged. Cell

pellets were resuspended in a small volume of TNX solubilization buffer (50 mM Tris, pH 7.4, 150 mM NaCl, 2 % Triton X-100, 1 mM BME, 2 mM MgCl₂, protease inhibitor cocktail) and incubated for 1 hour at 4 C. Lysates were then cleared at 70,000 x g in a TLA 110 rotor, for 30 min. at 4°C, and supernatants were incubated with Nickel-NTA agarose beads, for 1.5 hour at 4°C. Beads were then centrifuged and washed 2 times with TNX buffer containing 200 μM ATP (to remove chaperones and other non-specific proteins of the lysate), followed by 2 more washes with TNX buffer containing 20 mM imidazole. Proteins were eluted with series of 100 and 200 mM imidazole in TNX buffer, and concentrations were determined by the Bio-Rad method. 10 μg of the different eluted proteins were preloaded with 1 μl of γP³² GTP (2000 Ci/mmol) in exchange buffer (50 mM Tris, pH 7.4, 100 mM NaCl, 1 % Triton X-100, 2 mM MgCl₂, 1 mM DTT) by incubating for 30 seconds at 37°C in a 140 μl volume. The reaction was then diluted 10 times to trap the nucleotide in place and begin γP³² GTP hydrolysis. From this mix, aliquots were taken, in triplicate, at different time points (0, 1, 2, 5 and 10 minutes), applied to nitrocellulose filters in a vacuum manifold, and flushed immediately with 1 ml PBS (to remove unbound nucleotide and hydrolyzed P³²). Filters were then placed in vials and assayed for P³² scintillation counting.

Electron Microscopy

COS7 cells were transfected with the appropriate cDNA in 10 cm dishes with Lipofectamine 2000 for 16 hours. Following this, fluorescence was first examined using the light microscope to ensure transfection was at least 70% prior to trypsinization and washing of the cells in PBS. The washed cells were then pelleted and fixed in 1.6% glutaraldehyde in 0.1 M NaCacodylate buffer prior to osmium tetroxide and uranyl acetate staining, spurr resin

embedding and final thin sectioning of the blocks, and the grids were stained with lead citrate. For immuno electron microscopy, the same transfection procedure was followed. Cells were trypsinized, washed in PBS, fixed in 1.6% glutaraldehyde and centrifuged at 3000 x g for 15 minutes. Cell pellets were embedded in LR white (Marivac, PQ, Canada), thin sections were cut with a Leica Ultracut E ultramicrotome, immunolabelled with polyclonal anti-FP antibodies (Clontech, Palo Alto, USA) and 10 nm gold-labelled secondary antibodies (Jackson Laboratories, Bar Harbor, USA). Cells were then counterstained with lead citrate and uranyl acetate. Digital images were taken using a JEOL 1230 TEM at 60 kV adapted with a 2K x 2K bottom mount CCD digital camera (Hamamatsu, Japan) and AMT software.

PEG Fusion Assay.

The whole cell fusion assay was performed as described (4). Given that the broad excitation spectra of DsRed overlaps with the GFP excitation wavelength, special precautions were taken to ensure the images of fused mitochondria did not include any bleed through between the channels. For this, live cells were imaged on the Olympus IX70 microscope with a 100X objective U Plan Apochromat, NA 1.35 – 0.50 objective, excited at 488 nm (GFP) and 560 nm (DsRed) with the Polychrome IV monochromator (TillPhotonics, Gräfelfing, Germany) through a FITC/Cy3/Cy5 triple pass filter (Chroma, Battelboro, USA). The emitted light was filtered through an additional Dual-View beam splitter (Optical Insights, Santa Fe, USA) equipped with two filters HQ520-20 and D600/40 to separate the GFP and DsRed emission signals, and images were captured as described above. The transfected CFP tagged protein was imaged using the CFP/YFP dual pass filter

(TillPhotonics) along with the beam splitter equipped with D465/30 and HQ535/30 filters (data not shown). The acquired images were saved as .tiff images and overlaid in Adobe Photoshop for image assembly.

2.7 ACKNOWLEDGEMENTS

This work was supported by the CIHR. S. Gangaraju was the recipient of an Ontario Graduate Scholarship in Science and Technology. We are extremely thankful to the anonymous reviewers, who have played an essential role in the development of this work. We are grateful to Marino Zerial (MPI-CBG Dresden, Germany) for the use of Rab5:CFP and Rab5:GST, Mike Ryan (La Trobe University, Australia) for Tom7-GFP and to Kazuhisa Nakayama (University of Tsukuba, Japan) for the DRP1K38A constructs used in this study. We thank members of the lab, Gordon Shore and Marta Miaczynska for critical comments on the manuscript. The authors have no competing interests for this work.

2.8 REFERENCES:

1. Santel, A., and M.T. Fuller. 2001. Control of mitochondrial morphology by a human mitofusin. *J. Cell Sci.* 114:867-874.
2. Rojo, M., F. Legros, D. Chateau, and A. Lombes. 2002. Membrane topology and mitochondrial targeting of mitofusins, ubiquitous mammalian homologs of the transmembrane GTPase Fzo. *J Cell Sci* 115:1663-1674.
3. Santel, A., S. Frank, B. Gaume, M. Herrler, R.J. Youle, and M.T. Fuller. 2003. Mitofusin-1 protein is a generally expressed mediator of mitochondrial fusion in mammalian cells. *J Cell Sci* 116:2763-2774.
4. Legros, F., A. Lombes, P. Frachon, and M. Rojo. 2002. Mitochondrial fusion in human cells is efficient, requires the inner membrane potential, and is mediated by mitofusins. *Mol Biol Cell* 13:4343-4354.
5. Eura, Y., N. Ishihara, S. Yokota, and K. Mihara. 2003. Two mitofusin proteins, mammalian homologues of FZO, with distinct functions are both required for mitochondrial fusion. *J Biochem (Tokyo)* 134:333-344.
6. Chen, H., S.A. Detmer, A.J. Ewald, E.E. Griffin, S.E. Fraser, and D.C. Chan. 2003. Mitofusins Mfn1 and Mfn2 coordinately regulate mitochondrial fusion and are essential for embryonic development. *J Cell Biol* 160:189-200.
7. Koshiba, T., S.A. Detmer, J.T. Kaiser, H. Chen, J.M. McCaffery, and D.C. Chan. 2004. Structural basis of mitochondrial tethering by mitofusin complexes. *Science* 305:858-862.
8. Fritz, S., D. Rapaport, E. Klanner, W. Neupert, and B. Westermann. 2001. Connection of the mitochondrial outer and inner membranes by Fzo1 is critical for organellar fusion. *J. Cell Biol.* 152:683-692.
9. Ishihara, N., Y. Eura, and K. Mihara. 2004. Mitofusin 1 and 2 play distinct roles in mitochondrial fusion reactions via GTPase activity. *J Cell Sci* 117:6535-6546. Epub 2004 Nov 6530.
10. Cipolat, S., O. Martins de Brito, B. Dal Zilio, and L. Scorrano. 2004. OPA1 requires mitofusin 1 to promote mitochondrial fusion. *Proc Natl Acad Sci U S A* 101:15927-15932. Epub 12004 Oct 15927.
11. Sesaki, H., and R.E. Jensen. 2001. UGO1 encodes an outer membrane protein required for mitochondrial fusion. *J Cell Biol* 152:1123-1134.
12. Wong, E.D., J.A. Wagner, S.V. Scott, V. Okreglak, T.J. Holewinski, A. Cassidy-Stone, and J. Nunnari. 2003. The intramitochondrial dynamin-related GTPase,

- Mgm1p, is a component of a protein complex that mediates mitochondrial fusion. *J Cell Biol* 160:303-311.
13. Sesaki, H., and R.E. Jensen. 2004. Ugo1p links the Fzo1p and Mgm1p GTPases for mitochondrial fusion. *J Biol Chem* 14:14.
 14. Sesaki, H., S.M. Southard, A.E. Hobbs, and R.E. Jensen. 2003. Cells lacking Pcp1p/Ugo2p, a rhomboid-like protease required for Mgm1p processing, lose mtDNA and mitochondrial structure in a Dnm1p-dependent manner, but remain competent for mitochondrial fusion. *Biochem Biophys Res Commun* 308:276-283.
 15. McQuibban, G.A., S. Saurya, and M. Freeman. 2003. Mitochondrial membrane remodelling regulated by a conserved rhomboid protease. *Nature* 423:537-541.
 16. Herlan, M., F. Vogel, C. Bornhovd, W. Neupert, and A.S. Reichert. 2003. Processing of Mgm1 by the rhomboid-type protease Pcp1 is required for maintenance of mitochondrial morphology and of mitochondrial DNA. *J Biol Chem* 278:27781-27788.
 17. Fritz, S., N. Weinbach, and B. Westermann. 2003. Mdm30 is an F-box protein required for maintenance of fusion-competent mitochondria in yeast. *Mol Biol Cell* 14:2303-2313.
 18. Dimmer, K.S., S. Fritz, F. Fuchs, M. Messerschmitt, N. Weinbach, W. Neupert, and B. Westermann. 2002. Genetic Basis of Mitochondrial Function and Morphology in *Saccharomyces cerevisiae*. *Mol Biol Cell* 13:847-853.
 19. Kijima, K., C. Numakura, H. Izumino, K. Umetsu, A. Nezu, T. Shiiki, M. Ogawa, Y. Ishizaki, T. Kitamura, Y. Shozawa, and K. Hayasaka. 2005. Mitochondrial GTPase mitofusin 2 mutation in Charcot-Marie-Tooth neuropathy type 2A. *Hum Genet* 116:23-27. Epub 2004 Nov 2011.
 20. Zuchner, S., I.V. Mersiyanova, M. Muglia, N. Bissar-Tadmouri, J. Rochelle, E.L. Dadali, M. Zappia, E. Nelis, A. Patitucci, J. Senderek, Y. Parman, O. Evgrafov, P.D. Jonghe, Y. Takahashi, S. Tsuji, M.A. Pericak-Vance, A. Quattrone, E. Battologlu, A.V. Polyakov, V. Timmerman, J.M. Schroder, and J.M. Vance. 2004. Mutations in the mitochondrial GTPase mitofusin 2 cause Charcot-Marie-Tooth neuropathy type 2A. *Nat Genet* 36:449-451.
 21. Chen, K.H., X. Guo, D. Ma, Y. Guo, Q. Li, D. Yang, P. Li, X. Qiu, S. Wen, R.P. Xiao, and J. Tang. 2004. Dysregulation of HSG triggers vascular proliferative disorders. *Nat Cell Biol* 6:872-883. Epub 2004 Aug 2022.
 22. Yoon, Y., E.W. Krueger, B.J. Oswald, and M.A. McNiven. 2003. The mitochondrial protein hFis1 regulates mitochondrial fission in mammalian cells through an interaction with the dynamin-like protein DLP1. *Mol Cell Biol* 23:5409-5420.

23. James, D.I., P.A. Parone, Y. Mattenberger, and J.C. Martinou. 2003. hFis1, a novel component of the mammalian mitochondrial fission machinery. *J Biol Chem* 278:36373-36379.
24. Stojanovski, D., O.S. Koutsopoulos, K. Okamoto, and M.T. Ryan. 2004. Levels of human Fis1 at the mitochondrial outer membrane regulate mitochondrial morphology. *J Cell Sci* 117:1201-1210.
25. Lee, Y.J., S.Y. Jeong, M. Karbowski, C.L. Smith, and R.J. Youle. 2004. Roles of the mammalian mitochondrial fission and fusion mediators Fis1, Drp1, and Opa1 in apoptosis. *Mol Biol Cell* 15:5001-5011. Epub 2004 Sep 5008.
26. Breckenridge, D.G., M. Stojanovic, R.C. Marcellus, and G.C. Shore. 2003. Caspase cleavage product of BAP31 induces mitochondrial fission through endoplasmic reticulum calcium signals, enhancing cytochrome c release to the cytosol. *J Cell Biol* 160:1115-1127.
27. Olichon, A., L. Baricault, N. Gas, E. Guillou, A. Valette, P. Belenguer, and G. Lenaers. 2003. Loss of OPA1 perturbs the mitochondrial inner membrane structure and integrity, leading to cytochrome c release and apoptosis. *J Biol Chem* 278:7743-7746.
28. Sugioka, R., S. Shimizu, and Y. Tsujimoto. 2004. Fzo1, a protein involved in mitochondrial fusion, inhibits apoptosis. *J Biol Chem* 279:52726-52734. Epub 52004 Sep 52730.
29. Barbacid, M. 1987. Ras Genes. *Ann. Rev. Biochem.* 56:779-827.
30. Franken, S.M., A.J. Scheidig, U. Krengel, H. Rensland, A. Lautwein, M. Geyer, K. Scheffzek, R.S. Goody, H.R. Kalbitzer, E.F. Pai, and et al. 1993. Three-dimensional structures and properties of a transforming and a nontransforming glycine-12 mutant of p21H-ras. *Biochemistry* 32:8411-8420.
31. Futatsugi, N., and M. Tsuda. 2001. Molecular dynamics simulations of Gly-12-->Val mutant of p21(ras): dynamic inhibition mechanism. *Biophys J* 81:3483-3488.
32. Vetter, I.R., and A. Wittinghofer. 2001. The guanine nucleotide-binding switch in three dimensions. *Science* 294:1299-1304.
33. Bucci, C., R.G. Parton, I.H. Mather, H. Stunnenberg, K. Simons, B. Hoflack, and M. Zerial. 1992. The small GTPase rab5 functions as a regulatory factor in the early endocytic pathway. *Cell* 70:715-728.
34. Scheidig, A.J., S.M. Franken, J.E. Corrie, G.P. Reid, A. Wittinghofer, E.F. Pai, and R.S. Goody. 1995. X-ray crystal structure analysis of the catalytic domain of the oncogene product p21H-ras complexed with caged GTP and mant dGppNHp. *J Mol Biol* 253:132-150.

35. Richter, M.F., M. Schwemmle, C. Herrmann, A. Wittinghofer, and P. Staeheli. 1995. Interferon-induced MxA protein. GTP binding and GTP hydrolysis properties. *J Biol Chem* 270:13512-13517.
36. Rybin, V., O. Ullrich, M. Rubino, K. Alexandrov, I. Simon, M.C. Seabra, R. Goody, and M. Zerial. 1996. GTPase activity of rab5 acts as a timer for endocytic membrane fusion. *Nature* 383:266-269.
37. Simon, I., M. Zerial, and R.S. Goody. 1996. Kinetics of interaction of Rab5 and Rab7 with nucleotides and magnesium ions. *J Biol Chem* 271:20470-20478.
38. Karbowski, M., Y.J. Lee, B. Gaume, S.Y. Jeong, S. Frank, A. Nechushtan, A. Santel, M. Fuller, C.L. Smith, and R.J. Youle. 2002. Spatial and temporal association of Bax with mitochondrial fission sites, Drp1, and Mfn2 during apoptosis. *J Cell Biol* 159:931-938.
39. Desagher, S., A. Osen-Sand, A. Nichols, R. Eskes, S. Montessuit, S. Lauper, K. Maundrell, B. Antonsson, and J.C. Martinou. 1999. Bid-induced conformational change of Bax is responsible for mitochondrial cytochrome c release during apoptosis. *J Cell Biol* 144:891-901.
40. Wei, M.C., W.X. Zong, E.H. Cheng, T. Lindsten, V. Panoutsakopoulou, A.J. Ross, K.A. Roth, G.R. MacGregor, C.B. Thompson, and S.J. Korsmeyer. 2001. Proapoptotic BAX and BAK: a requisite gateway to mitochondrial dysfunction and death. *Science* 292:727-730.
41. Pavlov, E.V., M. Priault, D. Pietkiewicz, E.H. Cheng, B. Antonsson, S. Manon, S.J. Korsmeyer, C.A. Mannella, and K.W. Kinnally. 2001. A novel, high conductance channel of mitochondria linked to apoptosis in mammalian cells and Bax expression in yeast. *J Cell Biol* 155:725-731. Epub 2001 Nov 2026.
42. Yoon, Y., K.R. Pitts, and M.A. McNiven. 2001. Mammalian dynamin-like protein dlp1 tubulates membranes. *Mol. Biol. Cell* 12:2894-2905.
43. Smirnova, E., D.-L. Shurland, S.N. Ryazantsev, and A.M. van der Blik. 1998. A human dynamin-related protein controls the distribution of mitochondria. *J. Cell Biol.* 143:351-358.
44. Smirnova, E., L. Griparic, D.L. Shurland, and A.M. van Der Blik. 2001. Dynamin-related protein drp1 is required for mitochondrial division in mammalian cells. *Mol Biol Cell* 12:2245-2256.
45. Frank, S., B. Gaume, E.S. Bergmann-Leitner, W.W. Leitner, E.G. Robert, F. Catez, C.L. Smith, and R.J. Youle. 2001. The role of dynamin-related protein 1, a mediator of mitochondrial fission, in apoptosis. *Dev Cell* 1:515-525.

46. Collins, T.J., M.J. Berridge, P. Lipp, and M.D. Bootman. 2002. Mitochondria are morphologically and functionally heterogeneous within cells. *Embo J* 21:1616-1627.
47. De Giorgi, F., L. Lartigue, and F. Ichas. 2000. Electrical coupling and plasticity of the mitochondrial network. *Cell Calcium* 28:365-370.
48. Huser, J., and L.A. Blatter. 1999. Fluctuations in mitochondrial membrane potential caused by repetitive gating of the permeability transition pore. *Biochem J* 343:311-317.
49. Bach, D., S. Pich, F.X. Soriano, N. Vega, B. Baumgartner, J. Oriola, J.R. Dugaard, J. Lloberas, M. Camps, J.R. Zierath, R. Rabasa-Lhoret, H. Wallberg-Henriksson, M. Laville, M. Palacin, H. Vidal, F. Rivera, M. Brand, and A. Zorzano. 2003. Mitofusin-2 determines mitochondrial network architecture and mitochondrial metabolism. A novel regulatory mechanism altered in obesity. *J Biol Chem* 278:17190-17197.
50. Karbowski, M., D. Arnoult, H. Chen, D.C. Chan, C.L. Smith, and R.J. Youle. 2004. Quantitation of mitochondrial dynamics by photolabeling of individual organelles shows that mitochondrial fusion is blocked during the Bax activation phase of apoptosis. *J Cell Biol* 164:493-499. Epub 2004 Feb 2009.
51. Karbowski, M., and R.J. Youle. 2003. Dynamics of mitochondrial morphology in healthy cells and during apoptosis. *Cell Death Differ* 10:870-880.
52. Bossy-Wetzell, E., M.J. Barsoum, A. Godzik, R. Schwarzenbacher, and S.A. Lipton. 2003. Mitochondrial fission in apoptosis, neurodegeneration and aging. *Curr Opin Cell Biol* 15:706-716.
53. Harder, Z., R. Zunino, and H. McBride. 2004. Sumo1 conjugates mitochondrial substrates and participates in mitochondrial fission. *Curr. Biol.* 14:340-345.
54. Christoforidis, S., and M. Zerial. 2001. Purification of EEA1 from bovine brain cytosol using Rab5 affinity chromatography and activity assays. *Methods Enzymol* 329:120-132.

3.0 ~ MANUSCRIPT #2

**Cargo-selected transport from the mitochondria to peroxisomes
is mediated by vesicular carriers.**

3.1 CHAPTER INTRODUCTION

This research is presented as a manuscript recently published in press in the journal *Current Biology*, entitled “Cargo-selected transport from the mitochondria to peroxisomes is mediated by vesicular carriers” Margaret Neuspiel#, Astrid C. Schauss#, Emelie Braschi, Rodolfo Zunino, Peter Rippstein, Richard A. Rachubinski, Miguel A. Andrade-Navarro and Heidi M. McBride.

It provides new, important, and extremely interesting insights into vesicular trafficking and inter-organelle communication. Convincing data are presented which support a novel cellular phenomenon: the generation of mitochondrial derived vesicles and the delivery of these structures to peroxisomes. This work originated from the discovery of a novel protein of the mitochondrial outer membrane which is involved in mitochondrial fission.

In attempts to identify a SUMO E3 ligase, a bioinformatics screen was used to identify candidate mitochondrial anchored SUMO or ubiquitin E3 ligases (Figure 3.1). Mammalian unidentified open reading frames were analyzed for those that contained a RING finger domain. Proteins were then sub-screened for those with predicted mitochondrial targeting sequences using MitoPred and TargetP (<http://bioinformatics.albany.edu/~mitopred/>) (<http://www.cbs.dtu.dk/services/TargetP/>) algorithms to search for potential mitochondrial targeting sequences. Finally the remaining sequences were then sub-screened for the presence of at least one transmembrane domain. This approach resulted in the identification of 828 distinct RING finger proteins, 110 of which contain transmembrane domains, and 10 of which are predicted to be mitochondrial.

Figure 3.1

Bioinformatics screen

A) Bioinformatics screen to identify candidate mitochondrial anchored ubiquitin or SUMO E3 ligases. Sequences were selected which contained a conserved RING finger domain common to these enzymes (according to the SMART domain search), and at least one potential transmembrane domain (using TMHMM). B) One of these sequences was an unidentified open reading frame (ORF) FLJ12875 which we named MAPL (mitochondrial anchored protein ligase). The translated protein contains 352 amino acids with a C-terminal RING domain, and two predicted transmembrane helices. Predicted transmembrane domains illustrated in blue, and the RING finger domain in red.

A. Bioinformatics approach

Total Ring fingers: 828
Those containing TMD: 110
Those positive in Mitoprot (cutoff 0.1): 79
Those positive in TargetP (cutoff 0.3): 56
Overlapping positive hits, redundancy removed: 14

B. Sequence

Mitochondrial Anchored Protein Ligase, MAPL *Human protein: Q969V5 - Hypothetical protein FLJ12875*

1 MESGGRPSL CQFILLGTTSV VTAA LYSVYR QKARVSQELK GAKKVHLGED LKSILSEAPG
TRANSMEMBRANE DOMAIN
61 KCV PYAVIEG AVRSV KETLN SQFVENCKGV IQRLTLQEHK MVWNRTHLW NDCSKIIHQ
121 TNTVPFDLVP HEDGVDV AVR V LKPLDSV DL GLETV YEKFH PSIQSFTDVI GHYISGERPK
181 GIQETEMLK V GATLTGV GE LV LDNNSVRL QPPKQGMQY Y LSSQDFDSSL QRQESSVRLW
241 KVLALVFGFA TCATLFFILR KQYLQRQERL RLKQMEEFQ EHEAQLLSRA KPEDRESLKS
TRANSMEMBRANE DOMAIN
301 ACVVCLSSFK SCVFLECGHV CSCTECYRAL PEPKKCPICR QAITRVIPLY NS
RING DOMAIN



Figure 3.1

Bioinformatics screen

This screen was performed by Dr. McBride with the assistance of Miguel A. Andrade-Navarro a bioinformatics specialist of the OHRI. The first protein identified from this list was the hypothetical protein FLJ12875, accession number Q969V5. We have since named this protein MAPL (Mitochondrial Anchored Protein Ligase) The translated protein contains 352 amino acids with two predicted transmembrane helices, a c-terminal RING domain and an uncharacterized highly conserved domain in the middle region between the two transmembranes (Figure 3.1) The second half of my research was spent characterizing this novel protein and investigating its effect on mitochondrial dynamics, more specifically its role in fission and activity on Drp1. The findings presented summarize the characterization of this protein. Subsequent research performed by Emelie Braschi, has uncovered that this protein is a SUMO E3 ligase but this finding will not be discussed within the context of this manuscript.

This project was initially solely the subject of my doctoral research, however as the data unfolded, it was apparent that this was a much greater discovery than what one student could manage. Current members as well as other new recruits to the laboratory of Dr. McBride commenced research on different aspects of this project. I am a co- first author of this manuscript which is shared with Astrid Schauss a Postdoctoral fellow in the laboratory. She made the discovery that the mitochondrial derived vesicles containing MAPL target to the peroxisome and was responsible for all peroxisome experiments in this manuscript.

This work required the generation of many tools such as rabbit polyclonal antibodies, recombinant proteins, and a variety of MAPL DNA constructs. All tools utilized within this work were generated by me unless otherwise indicated. Emelie Braschi was responsible for the microscopy images in Figure 3.3 A,B and Figure 3.4 A,B,C. Rudolfo Zunino, was

responsible for technical assistance with the protease protection experiment and the siRNA experiments. Peter Rippstein, was responsible for the preparation of all samples for electron microscopy, and finally Richard A. Rachubinski was responsible for peroxisome biology insight.

3.2 ABSTRACT

Peroxisomes and mitochondria share a number of common biochemical processes, including the β -oxidation of fatty acids and the scavenging of peroxides. Here, we identify a new outer membrane mitochondrial anchored protein ligase (MAPL) containing a RING finger domain. Overexpression of MAPL leads to mitochondrial fragmentation, indicating a regulatory function controlling mitochondrial morphology. However, confocal and electron microscopy studies of MAPL-YFP led to the observation that MAPL is also incorporated within unique, DRP1-independent, 70-100 nm diameter mitochondrial derived vesicles (MDV). Importantly, MDVs selectively incorporate their cargo, where for example, vesicles containing MAPL exclude another outer membrane marker TOM20, and vesicles containing TOM20 exclude MAPL. We demonstrate that MAPL-containing vesicles fuse with a subset of peroxisomes, marking the first evidence for a direct relationship between these two functionally related organelles. In contrast, a distinct vesicle population labelled with TOM20 do not fuse with peroxisomes, indicating that the incorporation of specific cargo is a primary determinant of their fate. These data are the first to identify MAPL, describe and characterize MDVs and define a new intracellular transport route between mitochondria and peroxisomes.

3.3 RESULTS

3.3.1 Identification of a Novel Mitochondrial RING Finger-containing Protein

We were interested in identifying candidate mitochondrial proteins that participate in the regulation of mitochondrial morphology. It has been shown that mitochondrial morphology can be regulated both by ubiquitination and SUMOylation [1-6]. We therefore performed a bioinformatics screen to identify candidate mitochondrial anchored ubiquitin or SUMO E3 ligases. One of these sequences was a mitochondrial targeted, ubiquitously expressed, unidentified open reading frame FLJ12875, that we named MAPL for mitochondrial anchored protein ligase (Figure 3.2) The translated protein contains 352 amino acids with both the N-terminus and the C-terminal RING domain exposed to the cytosol, and two predicted transmembrane helices (Figure 3.2 A, B). Transient transfection of MAPL-YFP in HeLa or COS7 cells resulted in a fragmented mitochondrial phenotype (Figures 3.3 A and 3.3 E). This was in contrast to the tubular morphology of the TOM20-labelled mitochondria in neighbouring, untransfected control cells (Figure 3.3 A, top middle). The increase in mitochondrial fragmentation was dependent upon the RING finger domain of MAPL, since transfection of MAPL1-296-YFP lacking the RING finger domain did not induce this phenotype (Figure 3.3 A, bottom). To determine whether this phenotype required the mitochondrial fission GTPase DRP1, we cotransfected cells with the dominant interfering mutant, DRP1(K38E)-CFP [7-9]. As expected, the fragmentation induced by MAPL expression was blocked in the presence of the DRP1 mutant, and the resulting mitochondria were highly fused (Figure 3.3 B). These data indicate that MAPL participates in the regulation of mitochondrial fragmentation. However, in cells expressing both dominant negative DRP1 and either wild type MAPL or MAPL(1-296), a pool of very small MAPL- or TOM20-positive fragments remained within the otherwise highly interconnected

Figure 3.2

Characterization of MAPL, a novel mitochondrial outer membrane protein

(A) Representation of the domain organization of MAPL is shown with the RING finger motif at the C-terminus and two predicted transmembrane domains (blue). (B) MAPL is ubiquitously expressed. A northern blot indicates increased MAPL RNA transcript in heart and placenta. (C) Confocal Immunofluorescence images of Cos7 cells fixed and stained with anti-MAPL and anti-cytochrome c antibodies. (D) Both termini of MAPL are exposed to the cytosol. N-terminal CFP- and C-terminal YFP-tagged forms of MAPL were transfected into COS7 cells, and mitochondria were isolated and incubated with trypsin in the presence or absence of Triton X-100, as indicated. Both tags of MAPL were degraded like the outer membrane marker protein TOM20, while the intermembrane space protein cytochrome c was protease-resistant. (E) As in (D), except that endogenous MAPL was examined within isolated COS7 mitochondria using two antibodies, the first raised against the C-terminal RING finger domain and the second raised against the internal region between the transmembrane domains. Like TOM20, the C-terminal epitope is lost upon treatment with trypsin (top most panel); however the internal epitope reveals a shift to a lower molecular weight upon trypsin treatment, consistent with a loss of ~15 kDa (second panel from top). The solid arrows show the full-length MAPL protein and the open arrowhead reveals the trypsin-resistant fragment of MAPL. The asterisk indicates a non-specific band.

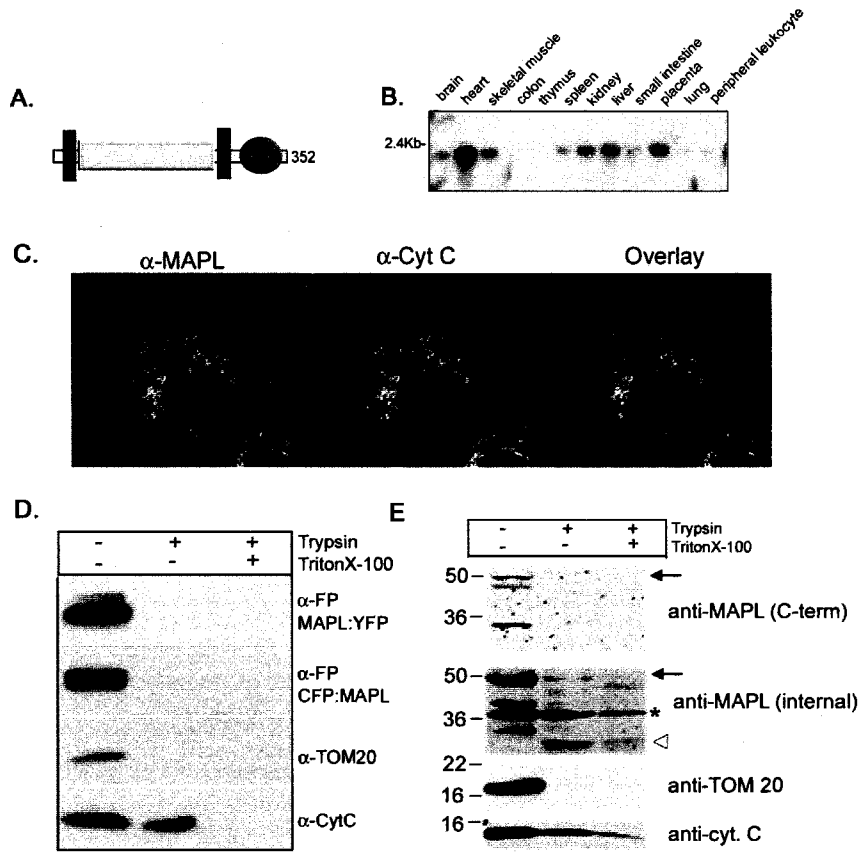


Figure 3.2

Characterization of MAPL, a novel mitochondrial outer membrane protein

mitochondrial reticulum (Figure 3.3 B circles). In order to examine the mitochondrial ultrastructure, we transfected cells with MAPL-YFP and prepared sections for electron microscopy (EM). EM analysis revealed the presence of highly distinct structures, 70-100 nm in diameter, emanating from the sides of the mitochondria expressing MAPL-YFP (Figure 3.4 C, arrows). These profiles contained either one or both mitochondrial membranes and showed an increase in electron density around the surface. Preembedded immunogold labeling of MAPL-YFP revealed small, ~100-nm structures resembling intracellular transport vesicles that were not attached to the larger mitochondria (Figure 3.3D, i). They often contained inner mitochondrial membrane: however, cristae were rarely observed and, instead the outer and inner membranes appeared as two concentric circles (Figure 3.3D, i). Standard immunogold labelling of fixed sections also revealed multiple enrichments of MAPL-YFP along mitochondria (arrows in Figure 1D, ii, iii, iv, arrows). To follow the formation of the small MAPL-containing fragments in real-time, we employed time-lapse confocal microscopy. In addition to the expected general fragmentation of the mitochondria in cells expressing MAPL-CFP we also observed a few unique fission events consistent with the EM analysis. In the time series presented in Figure 3.3E (Movie 3.1), we first observed a lateral enrichment of MAPL-CFP along the tubular mitochondria (Figure 3.3E, arrow). This enriched region of the mitochondria was then seen to pinch off from the side of the organelle, liberating a highly spherical mitochondrial fragment. This event was qualitatively distinct from previously documented mitochondrial fission, which instead involves a constriction along the tubule mediated by DRP1, leading to a smooth separation of the two halves of the mitochondrion (Movie 3.2). Taken together, the EM and confocal

Video 3.1 Confocal video analysis of MAPL-CFP-positive vesicle formation in COS7 cells.

Seventy images were captured every second with the 434 nm laser line on an Olympus FV1000 confocal microscope and are played here at 10 frames per second. Note a vesicle that emerges from the side of a mitochondrial tubule

Video 3.2. Confocal video analysis of mitochondrial fission.

HeLa cells were labeled with MitoFluorRed 633 and imaged with the 647-nm laser line every second on an Olympus FV1000 microscope. Here, 100 frames are played at 10 frames per second. Note that the tubular mitochondrion is severed across the whole organelle. This process is known to require DRP1-mediated whole organelle constriction, which is distinct from the budding event observed in Supplemental video 1

Figure 3.3

MAPL induces mitochondrial fragmentation and marks unique mitochondrial structures

(A) Mitochondria in HeLa cells were transfected with either MAPL-YFP (top panels) or MAPL(1-296)YFP (lower panels), and fixed cells were stained with anti-TOM20 and imaged by confocal microscopy. Boxed regions were enlarged. Scale bars, 20 μm . (B) As in (A), except that cells were co-transfected with DRP1(K38E)-CFP, which is shown in the insets (grey). Some small fragmented structures are circled. (C) COS7 cells transfected with MAPL-YFP were fixed and prepared for electron microscopy. Arrows highlight vesicular profiles. Scale bars, 100 nm. (D) (i) COS7 cells transfected with MAPL-YFP were fixed on coverslips, permeabilized with saponin and labeled with anti-YFP antibodies followed by goat anti-rabbit gold secondary antibodies. (ii), (iii), and (iv) Standard immunogold labelling with anti-FP antibodies on thin sections. Scale bars, 100 nm. Arrows highlight enrichments of MAPL. (E) Confocal time-lapse imaging of MAPL-YFP transfected into COS7 cells shows the formation of a mitochondrial vesicle. Arrows highlight the enrichment of MAPL-YFP along the side of a mitochondrial tubule that eventually separates into an individual vesicle. Note the mixture of the rod-like and spherical mitochondrial fragments. Scale bar. 5 μm .

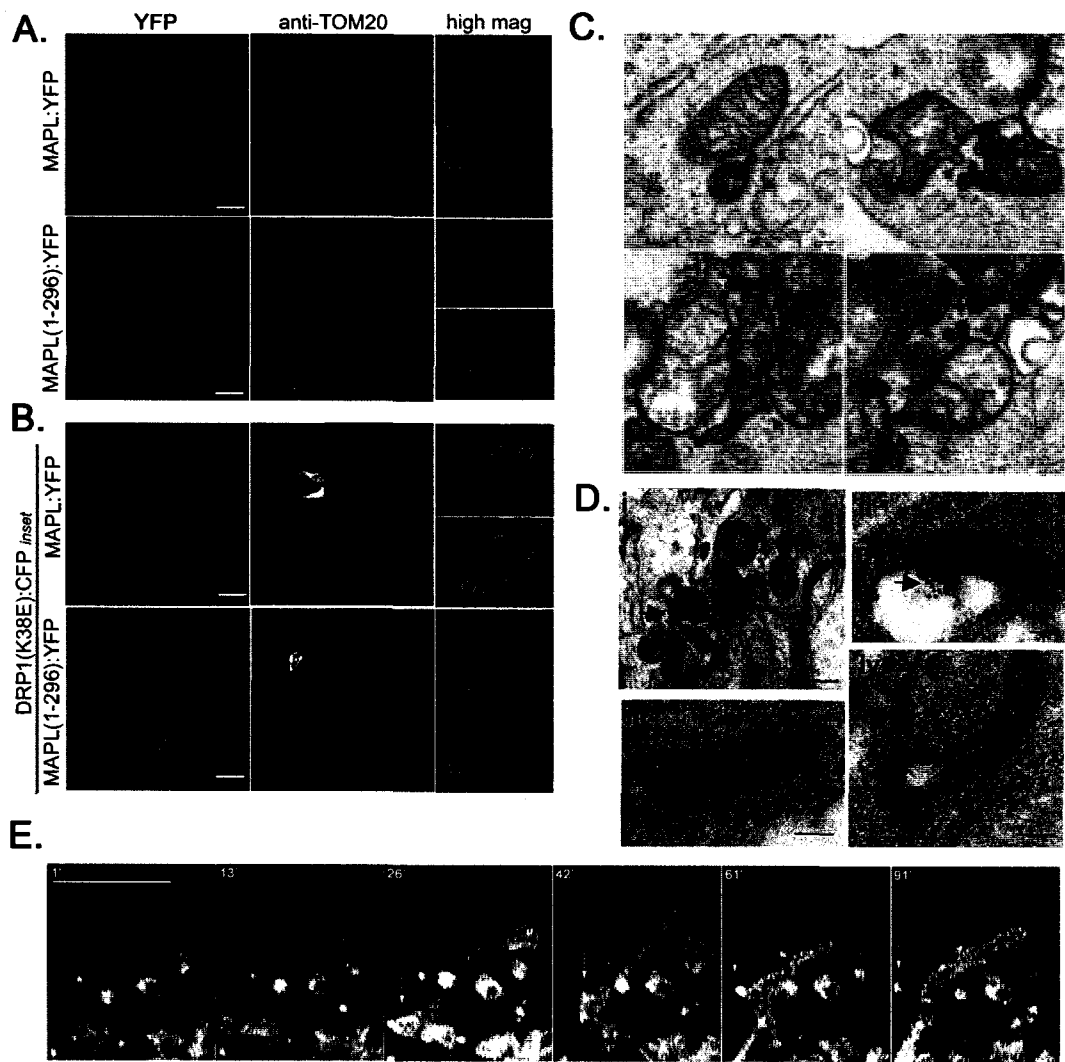


Figure 3.3

MAPL induces mitochondrial fragmentation and marks unique mitochondrial structures

analysis of MAPL-CFP indicates that MAPL is incorporated within small mitochondrial fragments that form in a distinct, DRP1-independent manner.

3.3.2 MDV's Exhibit DRP1-independent Cargo Selection

EM and video examination suggested that there may be an enrichment or selection of specific mitochondrial cargo within these structures. To test this directly, we co-transfected MAPL-YFP with a mitochondrial matrix marker, pOCT-CFP and performed either live-cell experiments with the potentiometric dye MitoFluorRed633, or fixed cells and stained them with antibodies against the outer membrane import receptor TOM20 (Figures 3.4 A and 3.4 B). Surprisingly, we observed multiple combinations of cargo incorporated within very small mitochondrial fragmented structures. Representative images reflecting the diversity of cargo within these structures are shown in Figure 3.5. For example, in the bottom panel of Figure 3.4 A, structures are seen containing only MAPL-YFP or $\Delta\Psi$ are seen (circles), but one structure is seen containing both OCT-CFP and $\Delta\Psi$ but lacking MAPL-YFP (arrows). In fixed cells stained with anti-TOM20 antibodies, we observe a similar mixture of vesicular profiles (Figure 3.4 B, circles). These images also reveal small mitochondrial profiles containing all three markers, which is expected from the generation of DRP1-dependent fragments (Figure 3.4 B, bottom panels, arrows). Co-expression of MAPL-YFP with DRP1(K38E)-CFP resulted in a highly interconnected mitochondrial reticulum (Figures 3.3B and 3.4 C, left panels). However, careful examination of the remaining fragments revealed that they also contained either MAPL-YFP or TOM20 (Figure 3.4 C top panels, circles), or $\Delta\Psi$ (Figure 3.4 C bottom panels, circles) with few, if any fragments labelled for both markers. Although microscopy may not eliminate the possibility of small amounts of each cargo present, the data show that the vesicles selectively exclude, and are significantly

Figure 3.4

Evidence of cargo selection within mitochondrial vesicles

HeLa cells were cotransfected with MAPL-YFP and pOCT-CFP, loaded with MitoFluorRed633 and imaged live (A) or fixed and stained with anti-TOM20 antibodies (B). In (C), HeLa cells were cotransfected with DRP1(K38E)-CFP (magenta) and MAPL-YFP and either loaded with MitoFluorRed633 (bottom panels) or fixed and stained with anti-TOM20 antibodies (top panels). Circles indicate mitochondrial structures that carry a single label and arrows indicate vesicles carrying more than one label. Scale bars, 2 μ m. (D) Non-targeting siRNA or MAPL siRNA were transfected into HeLa cells that were fixed and stained with anti-MAPL antibodies (top panels) or anti-TOM20 antibodies. The quantification of the number of TOM20 positive structures in 150 cells from 3 independent experiments are shown in the vertical box plot

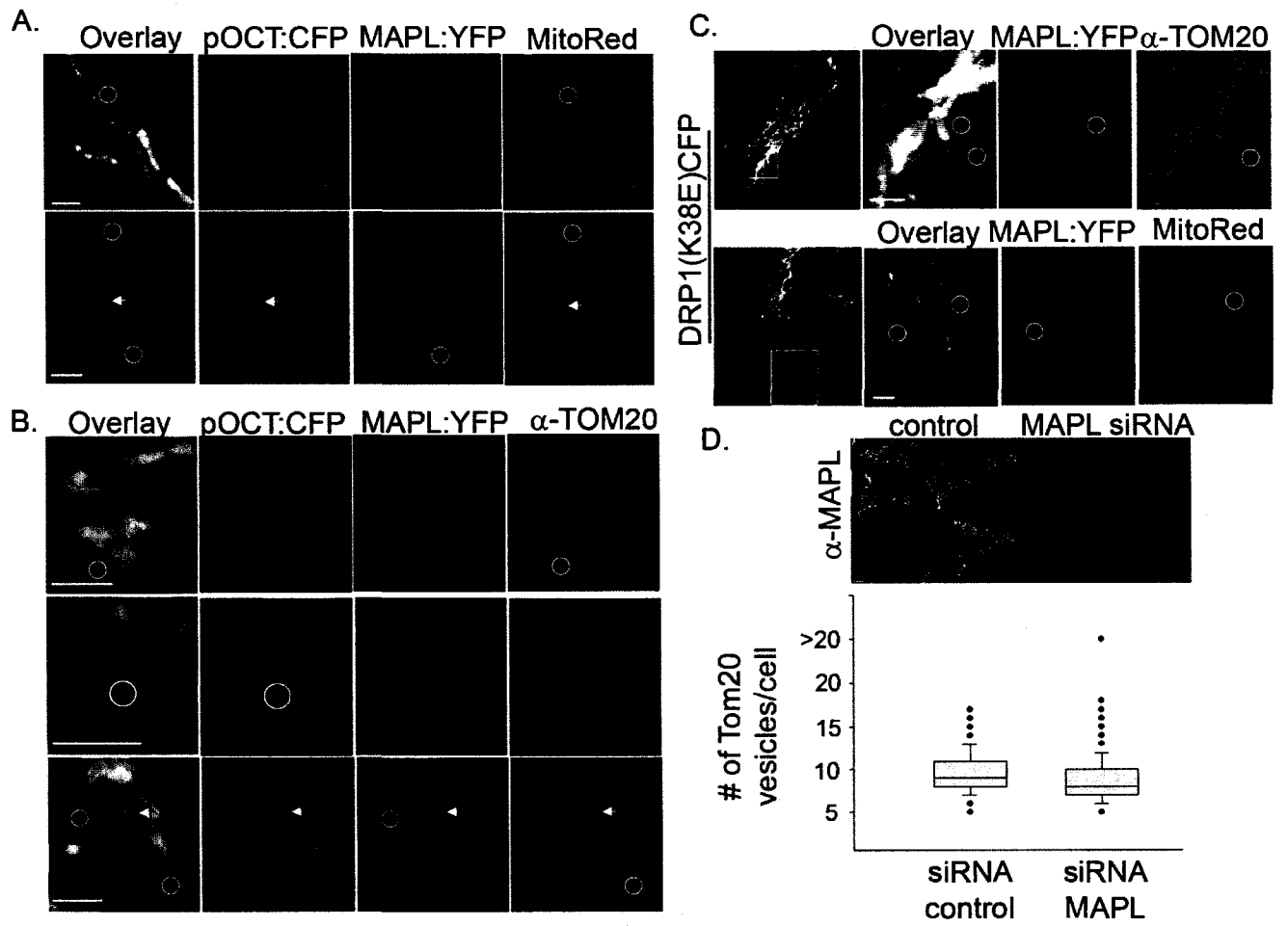


Figure 3.4

Evidence of cargo selection within mitochondrial vesicles

enriched for, specific cargo. This indicates that mitochondria have the capacity to segregate specific cargo even within a single membrane. Therefore, we suggest that in addition to their DRP1-independence and uniform size of 70-100 nm, another criterion to define a MDV is evidence of cargo selectivity.

Although MAPL expression stimulates mitochondrial fragmentation and is itself incorporated within these small vesicles, it was unclear whether MAPL was a regulator of vesicle formation. To test this, we quantified the number of small TOM20-positive structures in cells expressing endogenous or silenced MAPL (Figure 3.4 D). Analysis showed that the overall mitochondrial morphology was not dramatically altered Figure 3.6, and that the number of TOM20-labelled mitochondrial vesicular structures was similar in cells lacking MAPL (Figure 3.4D). This indicates that although MAPL can be incorporated within vesicles and stimulates DRP1-dependent mitochondrial fragmentation (Figures 3.3 and 3.4 A, 3.4 B, and 3.4 C), it is not a core component of the machinery required for MDV formation.

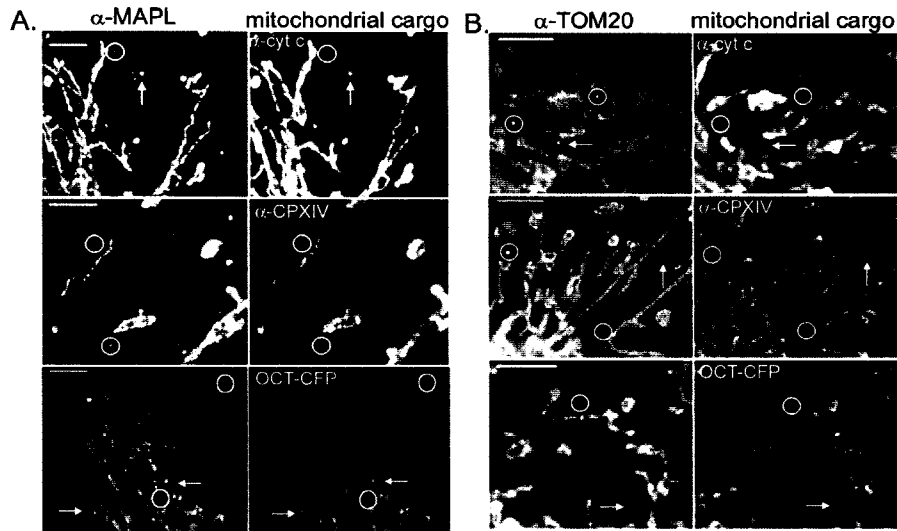
3.3.3 Quantification of Cargo Selectivity and DRP1-independent Vesicles

We next quantified both the extent of MDV cargo selectivity (Figures 3.5 A , 3.5 B and 3.5 C) and the total number of vesicles within cells (Figure 3.5 D) using endogenous markers. Immunofluorescence of endogenous MAPL revealed a number of distinct, very small punctate, vesicular structures in addition to a mitochondrial location (Figure 3.5 A, left panels). This antibody staining was specific since the silencing of MAPL through siRNA abolished this signal (Figure 3.4D, top panels). To further investigate the cargo selection observed above (Figure 3.4A and 3.4B) using endogenous markers, we co-stained the untransfected cells with either anti-MAPL or anti-TOM20 antibodies together with one of

Figure 3.5

Quantification of cargo selectivity and DRP1-independent vesicle formation

(A) COS7 cells were fixed and stained with anti-MAPL polyclonal antibodies and anti-cytochrome c (top panels), anti-subunit 1 of complex IV (middle panels) or with a matrix OCT-CFP marker (bottom panels). Circles illustrate vesicles positive for only MAPL, and arrows point to vesicles containing both cargoes. Scale bars, 1 μm . (B) As in (A) except the outer membrane marker examined is anti-TOM20. (C) A table quantifying the percentage colocalization of each marker pair. Data are taken from 50 vesicles from each of 3 independent experiments. (D) COS7 or HeLa cells untransfected or transfected with DRP1(K38E)-CFP were fixed and stained for anti-TOM20. The number of MAPL-positive vesicles within HeLa cells expressing DRP1(K39E)-CFP and MAPL-YFP are quantified in the last lane. The total number of vesicles was counted per cell from 150 cells from 3 independent experiments and plotted in the vertical box plot shown. To confirm that the DRP1(K38E)-CFP was functionally blocking DRP1 activity, only cells expressing the CFP tagged protein and that also contained highly fused, interconnected mitochondria were included.



C.

	MAPL	TOM20
cytochrome c	33 +/- 9.0	38.0 +/- 11.1
sub1 ComplexIV	50 +/- 8.0	37.3 +/- 7.5
OCT-CFP	48 +/- 11.3	42 +/- 7.2

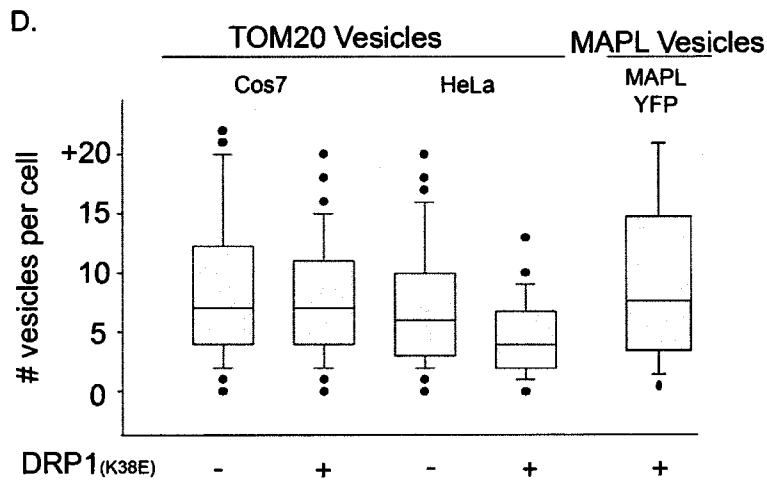


Figure 3.5

Quantification of cargo selectivity and DRP1-independent vesicle formation

Figure 3.6

Mitochondrial and peroxisomal morphology in MAPL silenced cells

(A) HeLa cells silenced with control siRNA or MAPL-targeted siRNA were fixed and stained with anti-cytochrome c antibodies or transfected with CFP-SKL. Peroxisomes appear to be of normal shape in the MAPL-silenced cells. Scale bars, 10 μ m. (B) Silencing of MAPL within total HeLa cell extracts was confirmed by western blotting of total extracts with anti-MAPL antibodies. anti-Hsp60 was used as a loading control.

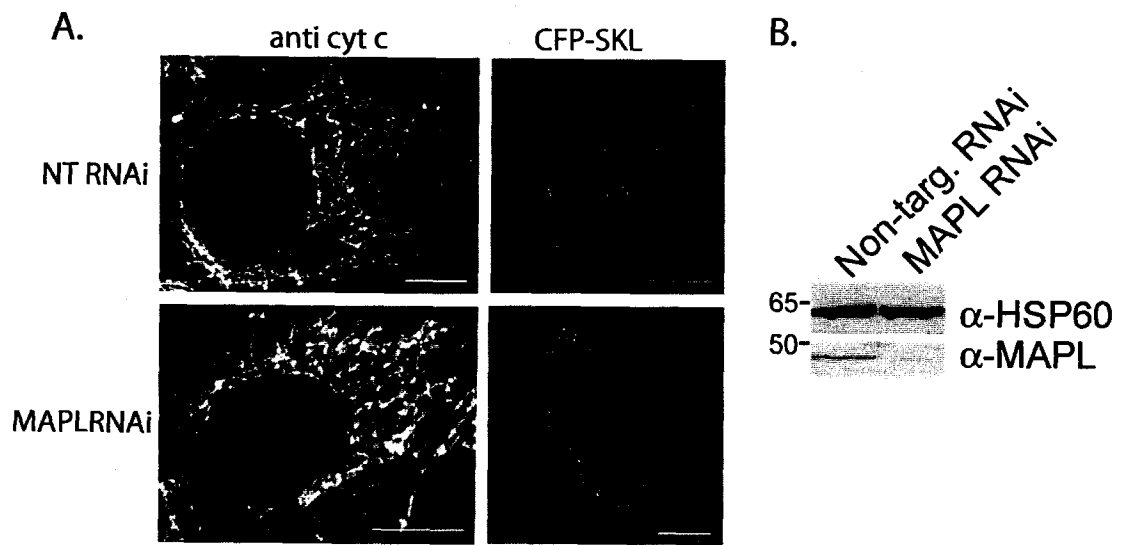


Figure 3.6

Mitochondrial and peroxisomal morphology in MAPL silenced cells

the following markers: cytochrome c of the intermembrane space (Figures 3.5 A and 3.5 B, top panels), subunit 1 of complex IV of the inner mitochondrial membrane (Figures 3.5 A and 3.5 B, middle panels), and a matrix targeted CFP (Figures 3.5 A and 3.5 B, bottom panels). Quantification revealed that only 33-50% of vesicles containing either TOM20 or MAPL also contained a second mitochondrial marker.

We next quantified the number of vesicles in cells expressing the dominant interfering mutant of DRP1, DRP1(K38E)-CFP in COS7 and HeLa cells. Quantification showed that cells expressing DRP1(K38E)-CFP and showing completely interconnected mitochondria exhibited nearly the same number of vesicles as controls (Figure 3.5 D). The slight reduction observed within HeLa cells upon inhibition of DRP1 likely reflects the inclusion of some DRP1-dependent fragments with vesicles during the counting in control cells. Quantification of the number of MAPL-YFP positive vesicles in DRP1(K38E)-CFP expressing cells indicated that they are present in numbers similar to TOM20-labeled vesicles (Figure 3.5 D). Together, the data confirm that both TOM20 and MAPL positive MDVs are formed by a mechanism distinct from DRP1-mediated mitochondrial fission.

3.3.4 MAPL-containing MDVs are targeted to peroxisomes

We tested a number of cellular markers in order to determine the fate of MDVs. Surprisingly, we found that the MAPL-positive vesicles were targeted to peroxisomes, whereas TOM20 containing vesicles did not share this fate (Figure 3.7 A). We quantified the colocalization of MAPL-YFP positive, TOM20 negative vesicles with peroxisomes and found that a mean of ~65% MAPL-containing vesicles colocalize with CFP-SKL labelled peroxisomes (Figure 3.7 B). The targeting of MAPL vesicles to the peroxisome was independent of the RING finger motif since a mean of ~91% of MAPL-positive vesicles

Figure 3.7

MAPL vesicles target the peroxisomes

(A) HeLa cells were co-transfected with CFP-SKL and MAPL-YFP, and after 16 hours, were fixed and stained with polyclonal anti-TOM20 antibodies. A representative confocal image shows the colocalization of MAPL-YFP-positive vesicles (green) with peroxisomes (red). The magenta TOM20 signal is excluded from the peroxisomal structures. Red arrowheads depict peroxisomes that do not contain MAPL, green arrowheads designate MAPL-positive vesicles that do not contain CFP-SKL or TOM20, and magenta arrowheads reveal TOM20 positive vesicles that do not colocalize with either MAPL or CFP-SKL. Circles reveal vesicles that are labeled for both CFP-SKL and MAPL-YFP, but exclude TOM20. (B) HeLa cells co-transfected with MAPL-YFP or MAPL1-296-YFP and CFP-SKL were fixed and immunostained for TOM20 (anti-Alexa647). The percentage of colocalization of MAPL-positive or TOM20-positive vesicles with CFP-SKL ($n = 42$ for each data set) is shown in the vertical box plot. (C) As in A, except that HeLa cells were transfected with YFP-Fis1 (green), CFP-SKL (red) and stained for Tom20 (magenta). Scale bar is 5 μ m. (D) Confocal time lapse series showing MAPL-YFP-labeled vesicles (in green) and CFP-SKL-labelled peroxisomes. The series shown was extracted from a 2 minute video and occurs over a 30 second period. Arrows point to two independent structures that are shown to fuse in the last three panels. Scale bar, 1 μ m.

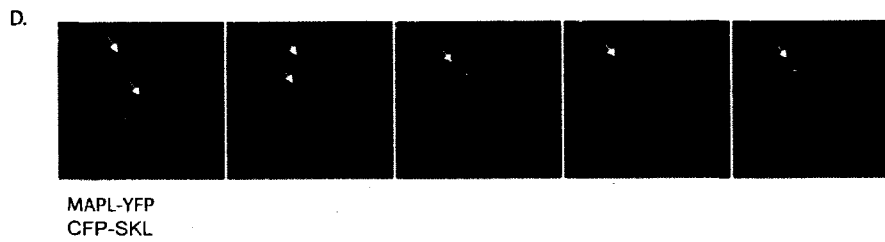
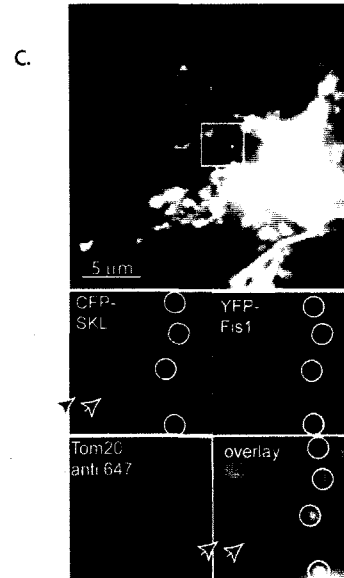
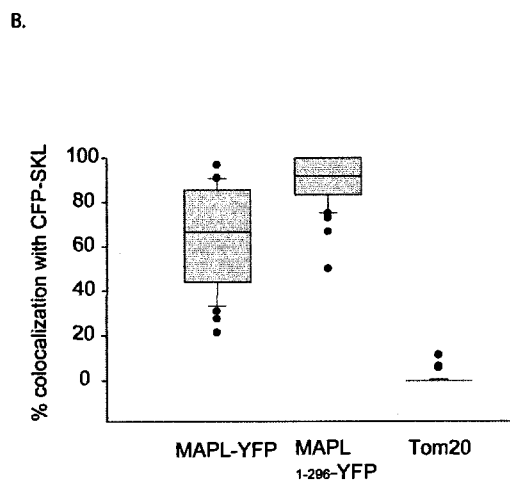
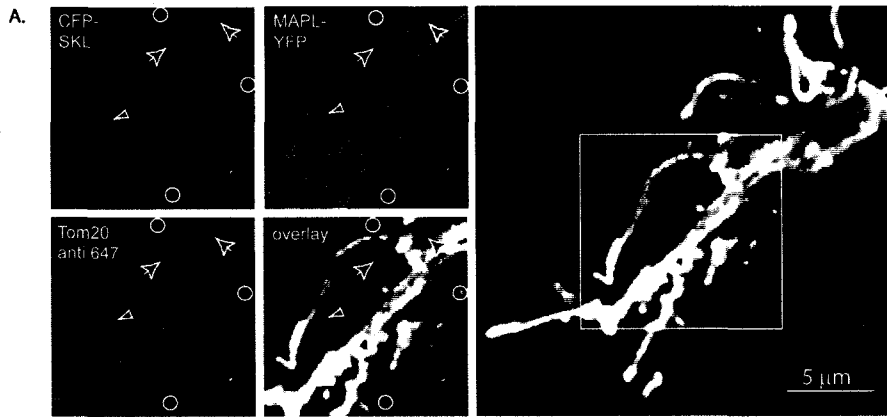


Figure 3.7

MAPL vesicles target the peroxisomes

colocalized with peroxisomes in cells expressing MAPL1-296-YFP lacking the motif (Figure 3.7 B). Importantly, vesicles positive for TOM20 and negative for MAPL did not colocalize with peroxisomes, further demonstrating the specificity for the cargo incorporation and the transport event (Figure 3.7 B). As shown earlier, the total number of DRP1-independent MAPL vesicles within a given cell are relatively low, between 5 and 15 vesicles per cell. This is far below the number of peroxisomes per cell, which ranges between 50 and a few hundred, indicating that most peroxisomes do not contain MAPL. Unlike CFP-SKL, it is evident that MAPL is not imported into peroxisomes, since it would also be found equally in all peroxisomes. Another outer membrane protein Fis1 has been dually localized to the peroxisomes. As previously shown [10], YFP-Fis1 is found in the vast majority of peroxisomes (Figure 3.7 C), which is distinct from the highly restricted localization of MAPL-YFP in only a few peroxisomes. This is more consistent with an import mechanism of targeting for YFP-Fis1. However, we did note the presence of some peroxisomes that were devoid of YFP-Fis1 (Figure 3.7 C, arrows), which further suggests the presence of distinct sub-populations of peroxisomes. Given that peroxisomes grow and divide [11], we also considered that very low levels of MAPL within the entire peroxisomal population may have been missed by our confocal analysis. Indeed, using higher sensitivities of both excitation and detection, we could observe low amounts of MAPL within many additional peroxisomes, although this still represented a sub-population of peroxisomes (Figure 3.8). Therefore, we consider that the initial delivery of the bright, MAPL-containing vesicles to peroxisomes would target a bulk of protein to a subset of these organelles. Following this, the MAPL protein may then become diluted throughout the peroxisomal population over time. To further confirm the direct transport of MDVs to

Video 3.3. Confocal video analysis of a MAPL-YFP-positive vesicle fusing with a CFP-SKL-containing peroxisome.

HeLa cells were transfected with MAPL-YFP (green) and CFP-SKL (red) and imaged on an Olympus FV1000 microscope using the 434 nm and 515 nm laser lines, respectively, every 30 sec. 42 frames are shown played at 4.3 frames per second.

Figure 3.8

Saturated exposures reveal low levels of MAPL within a larger sub-population of peroxisomes

Confocal imaging at higher laser intensity revealed more MAPL-YFP-positive vesicles (green), the majority of which colocalized with the peroxisome marker CFP-SKL (red), negative for Tom20 staining (magenta). Scale bar 2 um

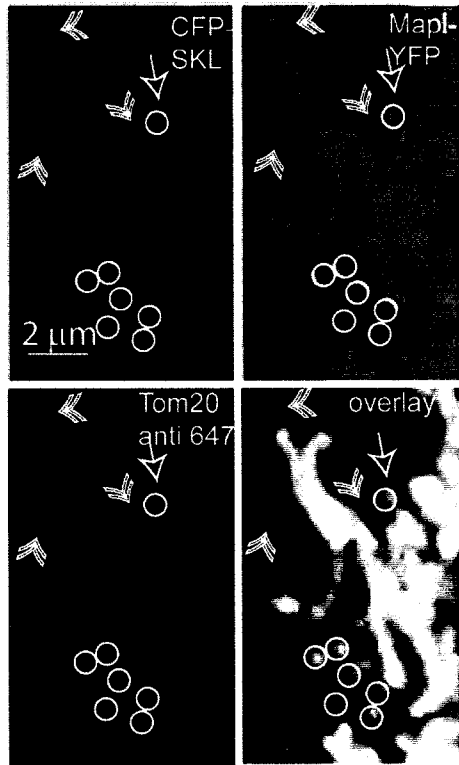


Figure 3.8

Saturated exposures reveal low levels of MAPL within a larger sub-population of peroxisomes

peroxisomes, we performed time-lapse imaging and observed a MAPL positive MDV fusing directly with a peroxisome labeled with CFP-SKL (Figure 3.7 D, Movie 3.3). Together, these data indicate that MDVs specifically containing MAPL are targeted to, and fuse with a sub-population of peroxisomes.

3.4 DISCUSSION

We have identified a novel mitochondrial outer membrane protein MAPL that participates in the regulation of DRP1-mediated mitochondrial fission in a RING-finger dependent manner. In addition, our study is the first to report the novel observation that MAPL is sorted into previously uncharacterized mitochondrial derived vesicles. We have defined MDVs using four independent criteria: 1) they are formed in a DRP1-independent manner, 2) they are highly uniform 70-100 nm structures, 3) they form from the lateral segregation of mitochondrial membrane in a manner distinct from previously characterized whole organelle constriction and 4) they incorporate selected mitochondrial cargo. Importantly, our data reveal that MAPL-containing vesicles are targeted to fuse with a subset of peroxisomes. In contrast TOM20-containing vesicles do not share this fate, providing further evidence that the incorporated cargo is an important determinant of vesicle fate. Peroxisomes share common metabolic functions with the mitochondria, as well as their fission machinery, DRP1 and Fis1 [10, 12-16]. However, the expression or silencing of MAPL did not visibly alter peroxisomal morphology (Figure 3.6), indicating a more subtle role, if any, in peroxisome fission. Many examples of metabolite shuttling between the mitochondria and peroxisomes, including ammonium, carnitine, and the flux of metabolites involved in the TCA cycle have been reported [17, 18]. In addition, the mitochondrial specific lipid cardiolipin has been found in significant levels within peroxisomes [19, 20].

Our work represents the first report of vesicular transport and communication between the mitochondria and peroxisomes. Future work will determine the precise function of MAPL within peroxisomes and the nature of the peroxisomal population that fuses with MDVs. For now, we have identified an unexpected intracellular transport route that provides a direct link between two organelles that are known to operate in a highly coordinated manner. Since many MAPL-YFP containing MDVs appear to have two membranes, it will be important to investigate the mechanism of fusion with the single-membrane bound peroxisomes, and the potential fate of the inner membrane-derived lipids once inside the peroxisomes. In addition, the observation that there are multiple MDVs containing specific subsets of cargo represents an important new aspect of mitochondrial dynamics. The function and fates of MDVs carrying TOM20 and other specific cargo is the focus of ongoing studies.

3.5 MATERIALS AND METHODS

Antibodies and Reagents

Antibodies were purchased from the following providers: anti-Cytochrome c, BD Bioscience Pharmingen; anti-Hsp60, Sigma; anti-complexIV, Mitoscience; anti-FP, BD Biosciences; anti-FLAG, Sigma. Anti-TOM20 rabbit serum was a generous gift from Dr. Gordon Shore (McGill University, Canada). Secondary goat anti-mouse or goat anti-rabbit conjugated (515 or 647) antibodies (Molecular Probes) were used for immunohistochemistry. For the generation of MAPL polyclonal antibodies directed against the IMS domain (MAPL29- 237-GST), bacterial expressed recombinant protein was sent to

21st Century Biochemicals (Marlboro, MA) for serum production. Antibodies raised against the C-terminal RING domain were prepared by injecting bacterially expressed recombinant GST-MAPL(257-352) following standard procedures.

DNA Constructs

MAPL (hypothetical human protein FLJ12875, accession number Q969V5) cDNA fused to an N-terminus CFP tag and a C-terminal YFP tag was a kind gift of Dr. Jeremy Simpson (EMBL, Germany). MAPL1-296-YFP was made using cDNA corresponding to amino acids 1-296 of MAPL amplified by PCR and engineered with BamHI and EcoRI sites for insertion into the vector pEYFP-N1 vector (Clontech). MAPL257-352-GST and MAPL29-237-GST constructs were made using cDNA corresponding to the desired regions amplified by PCR engineered with BamHI and EcoRI sites for insertion into the pGEX-2TK vector (Pharmacia) for bacterial expression and antibody production. CFP-SKL (Peroxi-CFP) was obtained from Clontech. YFP-Fis1 was obtained from Richard Youle (NIH, Bethesda MD) [21]. DRP1(K38E)-CFP and the matrix marker DNA construct containing the first 32 amino acids of ornithine carbamyl transferase fused to CFP (pOCT-CFP) or YFP (pOCT-YFP) have been described [4].

Cell Culture, Transfection and Immunofluorescence

HeLa and COS7 cells were maintained in Dulbecco's Modified Eagle Medium (Gibco Invitrogen) supplemented with 10% fetal bovine serum, penicillin and streptomycin. For immunofluorescence, cells previously seeded onto coverslips were washed three times with PBS and fixed in 3.7% paraformaldehyde/PBS for 15 min at 37°C. Cells were then

quenched with 50 mM ammonium chloride in PBS for 30 min at room temperature, permeabilized with 0.1% Triton X-100/PBS for 10 min and blocked with 5% bovine serum albumin/ 5% fetal bovine serum in PBS for 2 hours at room temperature. Cells were then incubated with primary antibody for 2 hours and washed with blocking solution. Cells were then incubated in goat anti-mouse or goat anti-rabbit conjugated (515 or 647 nm) secondary antibodies (Molecular Probes). Extensive washing with PBS was performed between each step.

Microscopy

Live or fixed cells transfected with fluorescent constructs were imaged on Olympus IX70 microscope with a 100X U Plan Apochromat, NA 1.35 – 0.50 objective, excited at 514 nm (YFP), or 434 nm (CFP), with the Polychrome IV monochromator (TillPhotonics, Grafelfing, Germany). The emitted light was filtered through a Till double CFP/YFP pass filter. Images acquired were saved as .tif images and overlaid in Adobe Photoshop for image assembly. Confocal images and movies were obtained with a 100X NA1.4 objective on an Olympus IX81 inverted microscope with appropriate lasers (440 nm diode laser for CFP, 515 nm argon laser for YFP, and the 633nm helium-neon laser for Alexa 647nm), using Olympus FV1000 confocal scanning microscope. 50 vesicles labelled with either anti-MAPL or anti-TOM20 were counted and scored for the presence of the second mitochondrial marker 1) anti-cytochrome c, 2) subunit 1 of complex IV, or 3) matrix marker oct-cfp. The average of three independent experiments was calculated and cargo selection was expressed as a percentage of total MAPL or TOM20-positive vesicles. To determine the number of vesicles per cell, COS7 or HeLa cells either untransfected or expressing DRP1(K38E) were fixed and immunostained for TOM20. A total of 150 cells were counted

and the number of TOM20 vesicles was scored for each cell. Data was plotted as a vertical box plot (Sigma Plot). To determine the fate of the vesicles, HeLa cells were co-transfected with either MAPL-YFP or MAPL1-296-YFP and CFP-SKL, fixed and immunostained for TOM20 (anti-Alexa647). In three independent experiments a total number of 42 cells for each combination were imaged and the amount of MAPL-YFP or TOM20 containing vesicles was counted. The percentage of MAPL-YFP, MAPL1-296-YFP or TOM20 positive vesicles containing CFP-SKL was determined and plotted as a vertical box plot (Sigma Plot). Images shown in Figure 5 were smoothed using a Gaussian filter at 0.5 pixels using Adobe Photoshop. For the MAPL RNAi vesicle quantification, HeLa cells were fixed and processed as described above.

Subcellular Fractionation and Trypsin Digestion experiments

COS7 cells alone, or expressing the indicated constructs for 16 hours, were collected by trypsinization, centrifugation and broken on ice ball bearing cell breaker in Mitochondrial Isolation Buffer (MIB): 220 mM mannitol, 68mM sucrose, 80 mM KCL, 0.5 mM EGTA, 2mM magnesium acetate, 20 mM Hepes pH7.4, protease inhibitor cocktail (Roche Diagnostics). Lysates were centrifuged at 800 x g for 10 min at 4C in a microfuge to pellet unbroken cells and nuclei. The supernatant was then centrifuged at 9,500 x g for 20 min at 4°C, to yield a mitochondrial enriched pellet and a light membrane fraction. The supernatant was removed and the mitochondrial pellet was washed three times in mitochondrial isolation buffer. For mitochondrial digestion experiments, 50 micrograms of mitochondria were incubated with either 10 mg/ml trypsin alone or trypsin and 1% Triton X-100 for 20 min on ice. Sample buffer was added to stop the reaction and the

mitochondria were boiled for 10 min. Samples were then separated on a 4-20% polyacrylamide gel. The proteins were transferred to nitrocellulose membranes and western blots were performed following standard protocols.

Fusion Protein for Antibody Generation

MAPL GST fusion proteins were produced in E. coli BL21 strain. Briefly, the production of fusion proteins was induced with 0.5 mM IPTG in log phase for 2 h. Bacteria were recovered by centrifugation, resuspended in 20 mM Hepes, pH 7.4, 200 mM NaCl, 2 mM MgCl₂, 5 mM BME, protease inhibitor cocktail, and lysed in a French press at 1500 psi. The lysate was supplemented with 1% Triton X-100, incubated for 30 min at 4°C and centrifuged at 35000 rpm for 30 min at 4°C using a Ti55.2 rotor (Beckman). The resulting supernatant was incubated for 2 h at 4°C with glutathione-Sepharose beads (Amersham Biosciences). Beads were then washed in the above buffer supplemented with 0.1% Triton X-100 and the fusion proteins were eluted from the beads following a standard protocol. Fusion proteins were then used for antibody generation (MAPL29-237-GST and MAPL257-352-GST).

Electron Microscopy

COS7 cells were transfected with the appropriate cDNA in 10-cm dishes using Lipofectamine 2000 for 16 h. Cells expressing MAPL-YFP were first examined using the Olympus IX70 microscope (as described above) to ensure that transfection was at least 70% prior to trypsin treatment, and washing of the cells in PBS. The washed cells were then fixed in 1.6% glutaraldehyde in 0.1 M sodium cacodylate buffer and pelleted prior to postfixation

in osmium tetroxide and uranyl acetate en bloc staining. Samples were then processed and embedded in Spurr epoxy resin, thin sectioned, and the grids counterstained with lead citrate. For immunoelectron microscopy, a preembedding silver enhancement immunogold method was used. Briefly, COS7 cells were grown on collagen-coated plastic cover slips and transfected with MAPL-YFP as indicated above. Cells were fixed in 4% paraformaldehyde and 0.1% glutaraldehyde in PBS. The cells were then washed in PBS three times and permeabilized in PBS containing 0.25% saponin and 5% BSA for 30 min, then blocked for 30 min in PBS containing 0.005% saponin, 10% BSA, and 10% FBS. The cells were then immunolabeled with mouse monoclonal anti-FP in the blocking solution overnight. Then, the cells were washed six times in PBS containing 0.005% saponin for 10 min and incubated with goat anti-mouse IgG that was conjugated to colloidal gold (1.4 nm diameter) for 2 h. Cells were washed six times with PBS for 10 min. and fixed with 1% glutaraldehyde in PBS for 10 min. After washing, the gold labeling was intensified by using a silver enhancement kit (SPI supplies, West Chester, PA) for 7.5 min. at 20°C in the dark. After washing with distilled water, cells were post fixed in 0.5% OsO₄ for 90 min. at 4°C, washed with distilled water, incubated with 50% ethanol for 10 min, and stained with 2% uranyl acetate in 70% ethanol for 2 h. The cells were further dehydrated with a graded series of ethanol and embedded in Spurr epoxy resin. Ultra thin sections were counter stained with uranyl acetate and lead citrate. Digital images were taken using a JEOL 1230 TEM at 60 kV adapted with a 2,000 by 2,000 pixel bottom mount CCD digital camera (Hamamatsu, Japan) and AMT software. For postembedding immuno-electronmicroscopy, cells were fixed in freshly made 4% paraformaldehyde - 0.05% glutaraldehyde in 0.1M Na cacodylate buffer, pH 7.2, for 2hrs at 4C. The cells were then briefly washed in 0.1M Na cacodylate buffer and

subsequently processed and embedded in LR White resin (Marivac, PQ, Canada) as previously described [22]. Ultrathin sections were collected on formvar coated nickel grids and immunolabelled with polyclonal anti-FP antibody (Clonotech, Palo Alto, CA) and 15 nm gold labelled goat anti-rabbit IgG secondary antibody (EY Laboratories, San Mateo, CA). The grids were then lightly counterstained with uranyl acetate and Reynold's lead citrate. Digital images were obtained with a Jeol 1230 TEM at 60KV adapted with a 2K x 2k bottom mount CCD digital camera (Hamamatsu, Japan and AMT software).

Northern Blot

To detect MAPL message, a Human 12-Lane MTN Premade Northern blot containing approximately 1ug of polyA+ RNA per lane from twelve different human tissues was used (BD Biosciences Clonotech). The MAPL full length cDNA was 32P labelled using standard random primers for DNA labelling (Invitrogen), then hybridization was performed according to manufacture's protocol using ExpressHyb Hybridization Solution. After washing, the membrane was exposed to X-ray film at -70°C using an intensifying screen.

RNAi

The siGENOME SMARTpool reagent directed against MAPL and the siCONTROL non-targeting or GAPDH siRNA were obtained from Dharmacon (Lafayette, CO). Transfection of the cells was performed using Dharmacon siGENOME SMARTpool transfection reagent according to manufactures protocols. Briefly, HeLa cells were seeded in 10 cm dishes, at ~80% confluency and were transfected with siRNA using Dharmafect 3 (Dharmacon, Lafayette, CO). The cells were exposed to the transfection mixture for 16 h, at which time

the transfection medium was replaced with Dulbecco's modified Eagle's medium supplemented with 10% fetal bovine serum. Twenty-four hours and forty-eight hours after removal of the transfection media, the cells were collected and analyzed for protein expression. Coverslips included in the dishes were fixed and stained with either anti-MAPL or TOM-20 to evaluate vesicle formation and knock-down efficiency. The remaining cells in the 10 cm dishes were separated by SDS-PAGE, transferred to nitrocellulose membranes and blotted for α -MAPL, as well as for loading and purification controls (α -HSP60). Cells were also transfected with CFP-SKL to examine the peroxisomal morphology upon silencing of MAPL.

3.6 ACKNOWLEDGEMENTS

This work was supported by the Heart and Stroke Foundation of Ontario, and a CIHR New Investigator Award to H.M.M. M.N and E.B. were supported by an Ontario Heart and Stroke Doctoral and Ontario Graduate Scholarship in Science and Technology, respectively. A.C.S was supported by a CIHR Post-doctoral fellowship. M.A.A. is a Canada Research Chair in Bioinformatics. We would like to thank Alex Stewart (University of Ottawa Heart Institute, ON) for technical help, Gordon Shore (McGill University, PQ) for anti-TOM20 antibodies, Richard Youle (NIH, MD) for YFP-Fis1 cDNA, and Jeremy Simpson (EMBL, Heidelberg) for sharing plasmids. We thank members of the Group, Luca Pellegrini (Laval University, PQ), Robert Sreaton (ARC, University of Ottawa) and Gordon Shore for stimulating discussions and insightful comments on the manuscript.

3.7 REFERENCES:

1. Yonashiro, R., Ishido, S., Kyo, S., Fukuda, T., Goto, E., Matsuki, Y., Ohmura-Hoshino, M., Sada, K., Hotta, H., Yamamura, H., Inatome, R., and Yanagi, S. (2006). A novel mitochondrial ubiquitin ligase plays a critical role in mitochondrial dynamics. *EMBO J* 25, 3618-3626.
2. Nakamura, N., Kimura, Y., Tokuda, M., Honda, S., and Hirose, S. (2006). MARCH-V is a novel mitofusin 2- and Drp1-binding protein able to change mitochondrial morphology. *EMBO Rep* 7, 1019-1022.
3. Karbowski, M., Neutzner, A., and Youle, R.J. (2007). The mitochondrial E3 ubiquitin ligase MARCH5 is required for Drp1 dependent mitochondrial division. *J Cell Biol* 178, 71-84.
4. Harder, Z., Zunino, R., and McBride, H. (2004). Sumo1 conjugates mitochondrial substrates and participates in mitochondrial fission. *Curr. Biol.* 14, 340-345.
5. Wasiak, S., Zunino, R., and McBride, H.M. (2007). Bax/Bak promote sumoylation of DRP1 and its stable association with mitochondria during apoptotic cell death. *J Cell Biol* 177, 439-450.
6. Zunino, R., Schauss, A., Rippstein, P., Andrade-Navarro, M., and McBride, H.M. (2007). The SUMO protease SENP5 is required to maintain mitochondrial morphology and function. *J Cell Sci* 120, 1178-1188.
7. Smirnova, E., Griparic, L., Shurland, D.L., and van Der Bliek, A.M. (2001). Dynamin-related protein drp1 is required for mitochondrial division in mammalian cells. *Mol Biol Cell* 12, 2245-2256.
8. Yoon, Y., Pitts, K.R., and McNiven, M.A. (2001). Mammalian dynamin-like protein dlp1 tubulates membranes. *Mol. Biol. Cell* 12, 2894-2905.
9. Hoppins, S., Lackner, L., and Nunnari, J. (2007). The machines that divide and fuse mitochondria. *Annu Rev Biochem* 76, 751-780.
10. Koch, A., Yoon, Y., Bonekamp, N.A., McNiven, M.A., and Schrader, M. (2005). A role for Fis1 in both mitochondrial and peroxisomal fission in mammalian cells. *Mol Biol Cell* 16, 5077-5086.
11. Fagarasanu, A., Fagarasanu, M., and Rachubinski, R.A. (2007). Maintaining peroxisome populations: a story of division and inheritance. *Annu Rev Cell Dev Biol* 23, 321-344.

12. Koch, A., Thiemann, M., Grabenbauer, M., Yoon, Y., McNiven, M.A., and Schrader, M. (2003). Dynamin-like protein 1 is involved in peroxisomal fission. *J Biol Chem* 278, 8597-8605.
13. Koch, A., Schneider, G., Luers, G.H., and Schrader, M. (2004). Peroxisome elongation and constriction but not fission can occur independently of dynamin-like protein 1. *J Cell Sci* 117, 3995-4006.
14. Tanaka, A., Kobayashi, S., and Fujiki, Y. (2006). Peroxisome division is impaired in a CHO cell mutant with an inactivating point-mutation in dynamin-like protein 1 gene. *Exp Cell Res* 312, 1671-1684.
15. Kobayashi, S., Tanaka, A., and Fujiki, Y. (2007). Fis1, DLP1, and Pex11p coordinately regulate peroxisome morphogenesis. *Exp Cell Res* 313, 1675-1686.
16. Schrader, M. (2006). Shared components of mitochondrial and peroxisomal division. *Biochim Biophys Acta* 1763, 531-541.
17. Linka, M., and Weber, A.P. (2005). Shuffling ammonia between mitochondria and plastids during photorespiration. *Trends Plant Sci* 10, 461-465.
18. Scott, I., Sparkes, I.A., and Logan, D.C. (2007). The missing link: inter-organellar connections in mitochondria and peroxisomes? *Trends Plant Sci* 12, 380-381.
19. Wriessnegger, T., Gubitz, G., Leitner, E., Ingolic, E., Cregg, J., de la Cruz, B.J., and Daum, G. (2007). Lipid composition of peroxisomes from the yeast *Pichia pastoris* grown on different carbon sources. *Biochim Biophys Acta* 1771, 455-461.
20. Leber, R., Zinser, E., Zellnig, G., Paltauf, F., and Daum, G. (1994). Characterization of lipid particles of the yeast, *Saccharomyces cerevisiae*. *Yeast* 10, 1421-1428.
21. Lee, Y.J., Jeong, S.Y., Karbowski, M., Smith, C.L., and Youle, R.J. (2004). Roles of the mammalian mitochondrial fission and fusion mediators Fis1, Drp1, and Opal in apoptosis. *Mol Biol Cell* 15, 5001-5011.
22. Neuspiel, M., Zunino, R., Gangaraju, S., Rippstein, P., and McBride, H.M. (2005). Activated Mfn2 signals mitochondrial fusion, interferes with Bax activation and reduces susceptibility to radical induced depolarization. *J Biol Chem* 280, 25060-25070.

4.0 DISCUSSION

4.1 MITOFUSIN 2 AND MITOCHONDRIAL FUSION

In this research, I have shown for the first time that Mfn2 exhibits properties of a signaling GTPase capable of regulating not only mitochondrial fusion, but that its nucleotide state also plays a critical role in regulating the mitochondrial response to apoptotic and free radical-induced damage(1). Through the creation of mutants, the functional role of GTPase activity and of the intermembrane space domain within Mfn2 was dissected. The results are consistent with the recently published work showing that Mfn2 has a higher affinity to nucleotide and dramatically slower rates of hydrolysis relative to Mfn1 (1, 2). Most importantly, it was characterized that the nucleotide binding and hydrolysis properties of a mutant form of Mfn2, Mfn2RasG12V, has slower hydrolysis and increased nucleotide exchange when compared directly with the wild type protein (1). This mutant allowed us to examine the functional consequences of a GTP hydrolysis-deficient, dominant active form of Mfn2 on intracellular signaling for fusion and on apoptosis. It was concluded that the GTP bound form of Mfn2 triggers a dramatic stimulation of mitochondrial fusion and ultra structural analysis of the fused mitochondrial clusters revealed a striking proliferation of interconnected membranes. These findings support the our initial hypothesis that Mfn2 does not function as a mitochondrial Snare (1).

It was further determined that the conserved tryptophan residue within the intermembrane space region of Mfn2 is not essential to form a fusion pore but is required to activate fusion within the context of the wild type GTPase domain (1). The finding that the double mutant Mfn2RVWP-CFP, is capable of fusion and stimulates it to the same relative extent as Mfn2RasG12V-CFP, suggest that it is the nucleotide state of Mfn2 that is important

for fusion rather than the residue conservation of the intermembrane space loop, and/or interacting intermembrane space proteins. The inability of the mitochondria to fuse in cells expressing Mfn2W631PCFP suggests that this loop is not essential for fusion pore formation, however it is required for protein activation and nucleotide exchange of GDP for GTP (1). It is therefore proposed, that this residue, relays intra-mitochondrial fusion signals, to stimulate changes in the nucleotide state of the GTPase domain (Figure 4.1). These data indicate that the signal for mitochondria to fuse, can be initiated from a protein that resides in the inner membrane or intermembrane space, arguing that fusion is triggered from the inside out. We cannot however exclude the possibility of cytosolic factors such as GDP exchange factors whose function involves the activation of the GTPase domain from the cytoplasmic face.

4.1.1 SIGNALLING

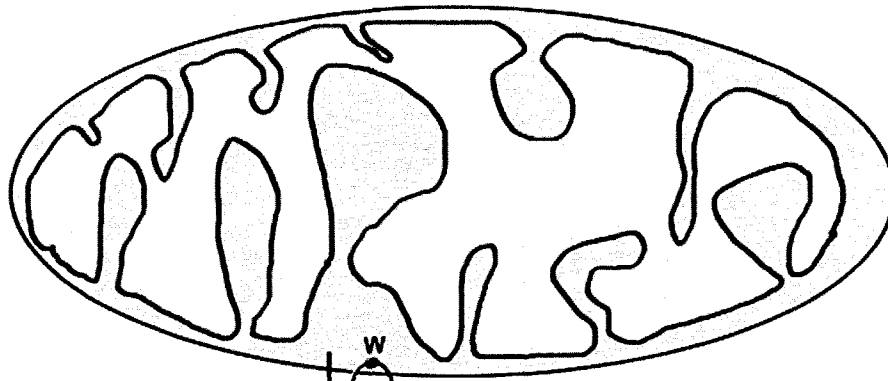
These mitofusin proteins are distantly related to the dynamin family of GTPases, however although Mfn1 has been shown to exhibit low nucleotide binding affinity and very fast rates of hydrolysis, we clearly demonstrated that Mfn2 is very distinct, and instead functions as a signaling GTPase more reminiscent of the Rab family of GTPases (3-4)

Clearly there are a number of molecular events that contribute to the dramatic increase in fusion observed in cells expressing the Mfn2RasG12V, including the involvement of cytosolic effectors that relay the signal between organelles, increased mitochondrial motility events, the activation of kinesins, recruitment of tethering factors, as well as the activation of the core fusion machinery. These signaling events likely include the cooperation and/or activation of Mfn1, which has been shown to function directly with Opa1 in driving mitochondrial tethering and fusion (5). Mfn2 may as well play a dual role,

Figure 4.1

Mfn2 and internal signaling

Summary cartoon, illustrating the role of the conserved intermembrane space tryptophan residue for fusion. Fusion signals are initiated from within the mitochondria, and this W residue is required to relay the signal to activate the GTPase domain. However, the conservation of this residue is not required for the formation of the fusion pore. The activation of the GTPase domain, is downstream of this residue, in that it can overcome the W631P inhibition.



1. IMS tryptophan is required to signal fusion.
2. Activated GTPase can overcome W631P inhibition.

Therefore:

- W is upstream of activated GTPase
- W is not required for fusion pore formation.
- Strongly suggests Mfn2 is a signalling GTPase.

Figure 4.1

Mfn2 and internal signaling

both as a direct constituent of the tethering/fusion machinery (minimally through the coiled coil domains) and through *in trans* interactions with Mfn1.

Evidence supporting a primary role for Mfn2 as a signaling GTPase has come from previous studies demonstrating that mouse embryonic fibroblast cells lacking Mfn2 show a loss of long range motility events, consistent with a role for Mfn2 in regulating mitochondrial movement (6). Our data are also consistent with the recently identified role for Mfn2 as a regulator of the Ras signaling pathway (7). Given that Ras signaling occurs at the plasma membrane, the ability of Mfn2 to invoke a signaling cascade would provide a mechanism for it to act upstream of events at a separate intracellular location. The continuous overexpression of Mfn2 leads to a cell cycle arrest at the G1/S transition induced by PDGF stimulation (7). This arrest was demonstrated to be through the activation of Ras and ERK was inhibited upon expression of Mfn2 through mechanisms that were not determined. In this study similar results were obtained using a soluble form of Mfn2 that was not targeted to the mitochondria. This is consistent with our finding that Mfn2 possesses signaling capabilities since it can act on the mitochondria without being localized on the outer membrane. It is now considered that the machinery governing mitochondrial morphology may be regulated in part by cell cycle specific kinases (8). Furthermore, that the morphology, may reflect the metabolic state of the mitochondria which could function as a novel cell cycle check point (8).

In collaboration with Ruth Slack and Arezu Jahani-Asl, of the neuroscience institute of the University of Ottawa, we also characterized the fusion activity, and the anti-apoptotic effects of Mfn2 and Mfn2RasG12V in cerebellar granular neurons (Appendix 1) (9). Interestingly, in primary cells, the stimulated fusion observed upon expression the hydrolysis deficient mutant Mfn2RasG12V in Cos-7 cells did not occur. Both wild type Mfn2 and

Mfn2RasG12V function equally to promote fusion and lengthening of mitochondria in neurons(9). This ability to fuse mitochondria does not depend on the nucleotide state of the protein, in that Mfn2 was able to stimulate fusion to the same extent as the activated mutant. The expression of Mfn2 or Mfn2RasG12V caused a dramatic increase in the mitochondrial lengths to greater than 30 μm (9). This neuronal response of dramatic mitochondrial lengthening is unlike that previously found in Cos-7 cells where the expression of Mfn2 resulted in mitochondrial fusion within a non-motile perinuclear cluster. This finding suggests that the mitochondria in neurons are highly sensitive to the levels of Mfn2 and not to the nucleotide state. It further suggests that perhaps Mfn2 levels are maintained very low and or that the activity is tightly regulated and maintained in the GDP bound state. Consistent with this hypothesis is the observation that mitochondria in cerebellar granular neurons are relatively quite fragmented, a phenotype indicative of minimal steady state fusion activity(9).

The Mfn2 data supporting a role of this protein as a signaling GTPase as well as additional data highlighted above have provided the framework by which the holistic view of the fusion machinery being integrated within cellular signaling cascades was formed. It can be envisioned that the fusion machinery regulate mitochondrial behavior and dynamics through the use of common switches and check points like cellular kinase's, GTPases and other signaling proteins (8). A number of approaches to identify new components and to investigate the mechanisms by which mitochondrial fusion is linked to the global changes that occur under different cellular conditions are currently being explored in Dr. McBride's laboratory. For example, research in the laboratory has discovered that the regulation of PARL activity is due its phosphorylation by an unknown kinase and proteolytic cleavage, further highlighting the fact that mitochondrial fusion is an event regulated at least in part by

the action of kinases, GTPases and phosphatases (10). The laboratory is currently developing experimental tools such as an *in vitro* mitochondrial fusion assay to define the mechanisms by which the Mfn2 and other mitochondrial fusion proteins are integrated into different cell signaling cascades. Furthermore, screens to identify signaling cascades implicated in the control of mitochondrial fusion have been developed with the assistance of Dr. Robert Scream of the Apoptosis Research Center at the University of Ottawa. Two approaches are currently being used. First, to examine the signaling pathways affected by Mfn2 activation, an approach using a panel of phospho-specific antibodies is used to search for Mfn2 dependent changes in signaling kinase's upon transient overexpression of the activated Mfn2RasG12V protein in HeLa cells. Secondly, a functional kinase screen has been developed, using siRNA of a broad panel of kinase's in cells expressing the dominant negative Drp1 mutant for fission, DrpK38E. The rationale behind this approach, is that the mitochondria, in the absence of functional Drp1, characteristically adopt a fused interconnected phenotype. Mitochondria, which cannot form this interconnected network, as a result of specific kinase siRNA, will allow for the identification of signaling cascades which impinge upon mitochondrial morphology and the ability to fuse membranes. These approaches should aid in the dissection of the relationship between morphology and cell cycle transitions, as well as to uncover the mechanisms of steady state fusion.

4.1.2 APOPTOSIS

The decision of life or death of a cell is largely regulated by the Bcl-2 family of both anti- and pro- apoptotic proteins (11). These are known to respond to various apoptotic signals and interact with opposing members of this family to regulate the initiation of the

proteolytic apoptotic caspase cascade. The finding that activated Mfn2 stimulates fusion, significantly represses Bax activation, cytochrome *c* release, and free radical-induced permeability transition, reveal for the first time a role for Mfn2 as a regulator of mitochondrial fusion and as a nucleotide-dependent modulator of the apoptotic response (1).

Stimulation of programmed cell death by STS treatment in cells expressing Mfn2-CFP resulted in a reduction of efficient recruitment and activation of Bax to the mitochondria and of cytochrome *c* release (1). Of those cells which were sensitive to STS, Bax recruitment to the mitochondria was found to colocalize with Mfn2-CFP puncta (1). In contrast, the fusion-incompetent Mfn2W631PCFP did not provide protection against external apoptotic stimuli, Bax activation or cytochrome *c* release. As with Mfn2-CFP, activated Bax often colocalized with Mfn2W631P-CFP-containing puncta. Increased inhibition was observed in cells expressing Mfn2RasG12V-CFP and Mfn2RVWP-CFP which both repressed Bax activation and cytochrome *c* release (1).

The loss of PARL or Opa1 also leads to sensitivity to cell death, suggesting that these proteins have general protective functions (10). It is now clear that during apoptosis, the fission machinery is used by the cell to promote cell death and cytochrome *c* release(12-13), and the fusion machinery through signaling and/or maintaining a fused reticulum exerts an anti-apoptotic force (1, 9, 14). Together this demonstrates that mitochondrial dynamics and the regulatory machinery that governs these processes are highly integrated with the cellular signal cascades that drive or inhibit cell death.

Consistent with this Mfn2 mediated protection, the dissection of Mfn2 function during apoptosis in primary neurons also supported this nucleotide dependent function of Mfn2 (9). More specifically, the nucleotide dependent protection that Mfn2 exerts on the neurons is sufficient for both Bax and Bax independent forms of cell death, including

excitotoxicity in primary neurons. Neurons exposed to DNA damage or oxidative stress exhibit extensive mitochondrial fission, which is an early event preceding neuronal loss. The extent of mitochondrial fragmentation and remodeling is variable and depends on the mode and the severity of the death stimuli. The down regulation of mitofusin 2 significantly induces cell death in the absence of any cell death stimuli (9). This finding in neurons is consistent with the cytochrome *c* release observed upon transient overexpression of the fusion incompetent mutant lacking the GTPase domain Mfn2(460–757) in Cos-7 cells (1). Consistently, expression of mitofusin2 by adenovirus in these neurons prevented cell death following DNA damage, oxidative stress and K⁺ deprivation induced apoptosis similarly to the overexpression of Mfn2 in tissue culture cells(9). Interestingly, the sensitivity of the neurons to apoptotic stimuli, varied greatly dependent on the nucleotide state of Mfn2; the activated Mfn2RasG12V mutant significantly protects neurons against cell death and release of pro-apoptotic factor cytochrome *c* compared to the wildtype Mfn2 (9). These findings further highlight the nucleotide dependence and signaling role for Mfn2 in the regulation of apoptosis that extends beyond its role in mitochondrial fusion.

4.1.2.1 MFN2 AND APOPTOTIC PORE FORMATION

Cells transfected with the dominant negative truncation mutant Mfn2(460–757)-CFP lacking the GTPase domain were highly sensitive to STS treatment. Interestingly, the amount of cytochrome *c* release in this condition (80%) did not mirror the amount of Bax activation (40%) (1). Interestingly, the mitochondria in cells expressing this mutant had cytochrome *c* release in the absence of any apoptotic trigger and in the absence of Bax activation. This result suggests that somehow the presence of the GTPase domain of Mfn2 is required to maintain the permeability pore in a closed state. This result is not due to the lack

of fusion in these mitochondria since our other fusion incompetent mutant Mfn2W631P did not have pore opening and cytochrome c release in the absence of a death stimulus (1). Instead, it indicates additional functions of the GTPase domain of Mfn2 in maintaining mitochondrial both membrane integrity and the permeability pore in a closed state. Mitochondrial permeability pores during steady state and apoptosis have confounded researches for many years and the regulation and precise protein composition is still undetermined. It is believed that PTP opening leads to matrix swelling and rupture of both inner and outer mitochondrial membranes, resulting in a non-specific release of soluble intermembrane proteins into the cytosol (15). Many believe that this sort of cytochrome c release is not specific and not important for apoptosis. Others also believe that PTP opening is a consequence of apoptosis, and this channel is thought to principally play a role in necrosis, not apoptosis (15). Activation of the mitochondrial apoptotic channel (MAC) on the other hand is tightly regulated by Bcl-2 family proteins, only forms post apoptotic trigger and the multi-domain pro-apoptotic protein Bax and Bak are putative components of this channel.

This finding is highly suggestive of a direct function of Mfn2 in regulating this pore, however the mechanistic role of Mfn2 remains to be elucidated.

4.1.2.2 MFN2 AND BAX/BAK

Consistent with a role of Mfn2 in maintaining the apoptotic pore in a closed state, Mfn2 has recently been found to interact with Bak at the mitochondrial membrane and this interaction prevents mitochondrial fragmentation, pore opening and the apoptotic cascade. Both Bax and Bak are pro-apoptotic Bcl-2 family proteins and as members of this family are critical regulators of mitochondrial injury during apoptosis (16). Bax is cytosolic, whereas

Bak circumscribes the outer mitochondrial membrane. Recently, it was found that Bak interacts with both Mfn2 and Mfn1(17). Using a loss- of function and gain-of-function approaches, Bak, but not Bax, was demonstrated to have a critical role in mitochondrial fragmentation during apoptosis. Under steady state conditions Bak interacts with Mfn2 through its BH3 domain, however upon apoptotic trigger, Bak dissociates form Mfn2 and binds Mfn1. Interestingly, a mutation within the BH3 domain of Bak, prevents its dissociation from Mfn2 and inhibits death. Mitochondrial fragmentation was only observed when Bak dissociated from Mfn2 and bound Mfn1 (17). The complex of Bak-Mfn2, observable by FRET, was fusion competent and anti-apoptotic, conversely the complex of Bak-Mfn1 had no mitochondrial fusion activity and the apoptotic program was allowed to proceed (17). These intriguing finding suggests that Mfn2 is the critical regulator of apoptosis and needs to be dissociated from Bak to facilitate apoptotic pore opening. It also supports the growing theme that Mfn1 is the critical fusion GTPase, whereas Mfn2 has a more regulatory function (1). Consistently, apoptotic fragmentation is attenuated in primary neurons isolated from the brain cortex of Bak-deficient mice further implicating this protein in the regulation of mitochondrial dynamics in the neuron (17).

It is interesting to speculate as to what function the nucleotide state of Mfn2 would play on the interaction between Bak and Mfn2? One could envision that in the GTP bound fusion active state of Mfn2, it would be associated with Bak to promote fusion. Furthermore, it could be speculated that this interaction would be highly dynamic and depend on cell type, metabolic demand and intracellular signaling cascades. In our study, the relationship of Bak and Mfn2 was not examined, however taken together these findings demonstrate that Mfn2, Bak and Bax need to co-localize and interact on mitochondrial membranes to evoke full pore

opening, to inhibit mitochondrial fusion and to allow for the apoptotic program to proceed (Figure 4.2).

Other groups have since provided supporting evidence along this line. Firstly, Mfn2 is colocalized in puncta with Bax and Drp1 at sites of future fission events and affects mitochondrial recruitment of Bax or Drp1 during cell death, indicating a spatial relationship between fusion and fission during cell death (18). Secondly, it was shown that cytosolic Bax plays a specific role in the steady state activity of Mfn2 as a regulator of mitochondrial fusion (19). In this study, mitochondria within the Bax/Bak double knock-out (DKO) cells demonstrated a reduced rate of mitochondrial fusion. The punctate distribution we observed of Mfn2 is lost, in Bax/Bak DKO cells and the protein circumscribes the outer membrane (1, 19) The introduction of Bax into the DKO cells resulted in a stable shift of Mfn2 within the outer mitochondrial membrane into foci, which rescued the rates of fusion. These findings in addition to the Bak-Mfn2 relationship discussed above are intriguing; however more studies are clearly needed to resolve the functions of both Bax and Bak in regulating the localization and function of Mfn2. Consistent with our study, the GTP bound form of Mfn2 did not respond to Bax/Bak expression and retained its even distribution along the outer membrane regardless of Bax/Bak expression levels (19). This resistance of Mfn2^{RasG12V} to assemble into Bax dependent foci may interfere with the efficient assembly of pro-apoptotic complexes required for the progression of cell death.

Taken together, a model is proposed whereby the activated GTP bound form of Mfn2 is not able to dissociate from Bak. It is upon Mfn2-Bak dissociation that fusion is inhibited and permeability pores are opened. This would at least partially explain the increased protection of the activated mutant to multiple Bax dependent apoptotic stimuli that we have observed in both tissue culture Cos-7 cells and in primary neurons. It is also interesting to

Figure 4.2

Mfn2 signaling and apoptosis

Summary cartoon, illustrating the role of the nucleotide state of Mfn2 in signaling and apoptosis. In the GDP bound state, fusion is inhibited, PTP pores can open, Bax related pores can form and cytochrome c can be released. In the GTP bound state, fusion is activated, PTP pores are closed, Bax activation is inhibited and cytochrome c cannot be released.

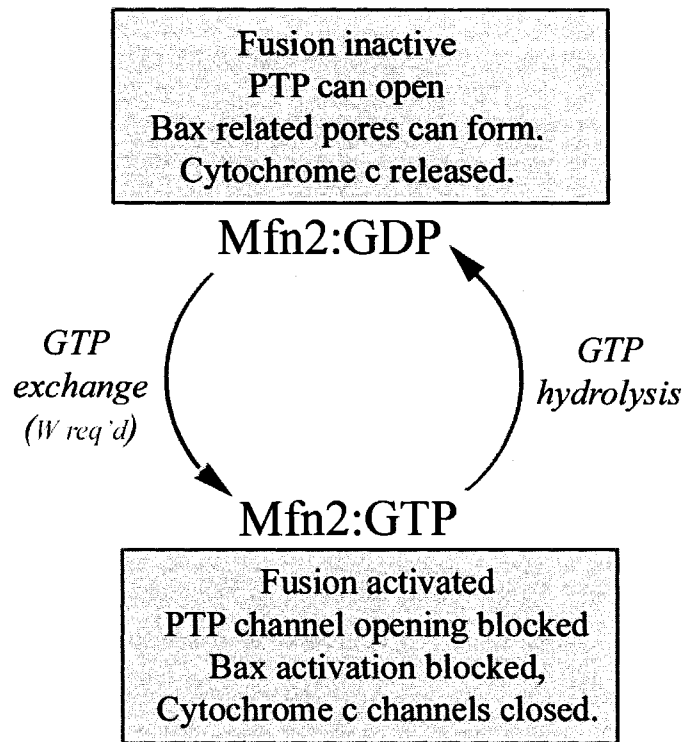


Figure 4.2

Mfn2 signaling and apoptosis

note that Bak was not found to interact with Drp1 or Fis1 in steady state or under apoptotic conditions, further supporting a role of Mfn2 in mediating Bax recruitment to the mitochondrial and in the regulated inhibition of fusion for death (17). Consistently, expression of Drp1K38A does not inhibit Bax translocation to membranes in Cos-7 cells, however both fragmentation and apoptosis are delayed (19). These findings suggest that Drp1 is not required for Bax activation; however in the absence of Drp1, the mitochondria can not undergo fission. Furthermore, in healthy HeLa and Cos-7 cells Bax does not colocalize with Drp1 puncta on mitochondrial membranes, however post STS treatment Bax translocates from the cytoplasm to co-localize with Drp1 in puncta. These data together with the findings that Mfn2 co-localizes with Bax during apoptosis(1), that the anti-apoptotic effects of Mfn2 depend on its nucleotide state(1) and the new finding that Mfn2 interacts with Bak on the mitochondria during steady state, lead to the hypothesis that Mfn2 acts as an upstream regulator of apoptosis and marks the future sites of apoptotic Drp1 and Bax recruitment to the membranes for fission.

To further confound the relationship between these proteins, the Bax/Bak dependent SUMOylation of Drp1 during apoptosis must also be considered. The laboratory has recently shown that Drp1 undergoes a transition from a rapidly recycling protein on and off the mitochondrial membranes, to a stable association (20). Bax and Bak are required for this transition to occur and this transition is concurrent with the SUMOylation of Drp1. The mechanisms of Drp1 recruitment and assembly, on mitochondrial membranes in steady state and during apoptosis has yet to be fully characterized. Furthermore, the role of Drp1 SUMOylation during the Mfn2-Bak mediated morphology transition during apoptosis, the relationship between the SUMO E3 ligase and Mfn2-Bak/Bax interactions together represent a highly novel and intriguing research focus. Investigations into these relationships should

expose some unknown mitochondrial proteins involved in the apoptotic transition. As an obvious first step, the relationship between the Mfn2-Bak pro fusion complex vs. the Mfn1-Bak pro-fission complexes and Drp1 activity, during apoptosis needs to be investigated to fully understand the regulation of mitochondrial dynamics during apoptosis.

4.2 Mitochondrial Derived Vesicles

It has been long considered that the impetus for mitochondrial motility fission and fusion events has been to ensure the equal segregation of mitochondrial content; mitochondrial proteins, lipids, metabolites and mtDNA within the network. Equal sharing between mitochondria would provide a mechanism by which high levels of mutant mtDNA, or toxic levels of ROS could not accumulate and would be diluted throughout the network. Mitochondrial fusion is thought to provide a mechanism through which these toxic elements would be diluted and buffered by the total reticulum. It is also believed that when the levels of ROS, damaged proteins and or mutated mtDNA overwhelm the mitochondria resulting in irreversible damage, the mitochondria would be selectively removed. In an effort to protect the functional output of the mitochondria, it is currently believed, that the fission and fusion proteins function to ensure the equal distribution of damaging agents. Furthermore it is also hypothesized, that these compromised mitochondria are selectively removed (presumably through mitophagy). A major confounding problem with these theories is that we do not yet understand the mechanisms and or stimuli (cellular and metabolic) which initiate the motility factors, fusion pore formation and or fission complex assembly to facilitate these processes. Currently, it is hypothesized that the mitochondria undergo fusion events as a protective measure to ensure cell survival and to inhibit apoptosis. However, under conditions of high ROS, or following peroxide treatment, mitochondrial fragmentation and swelling occur, as

opposed to the movement of two organelles towards each other for the diluting fusion events. This example above, the discovery of MAPL, a novel mitochondrial protein implicated in fission, as well as the identification of two distinct mitochondrial derived vesicle populations highlight both the infancy and the complexity of the mitochondrial dynamics field. Furthermore it demonstrates that although the current theories on dynamics seem well founded, the discovery of mitochondrial derived vesicles, illustrates that they may still be immature.

This current study identifies for the first time a novel mitochondrial outer membrane protein MAPL, which upon overexpression stimulates mitochondrial fragmentation, indicating a regulatory function controlling mitochondrial morphology. It identifies for the first time unique, DRP1-independent, 70-100 nm mitochondrial derived vesicles (MDV) which selectively incorporate their cargo (21). It furthermore demonstrates that MAPL containing vesicles fuse with a subset of peroxisomes, marking the first evidence for a direct relationship between these two functionally related organelles (21).

4.2.1 MAPL EVOLUTION

MAPL was the first protein investigated from the initial bioinformatics screen and examination of the sequence of this ORF indicated that it is a founding member of a novel protein family. This domain is conserved in uncharacterized proteins from archeabacteria to humans. It contains two predicted transmembrane domains that are separated by ~210 residues of unknown function. This conservation of this middle domain across the phyla defines a new protein family. It is subsequently named BAM (Beside a Membrane Domain). (Figure 4.3). The RING finger motif appears to have evolved in higher organisms, including plants, and is located at the C-terminus of the protein. A specific rabbit polyclonal antibody

Figure 4.3

MAPL phylogenetic tree

A) The phylogenetic MAPL tree. Sequence features of representative sequences containing the new beside a membrane domain (BAM) in sequences from bacteria to plants and mammals are shown. The RING finger domain is found only in higher organisms. Each sequence is identified by the organism: Homo sapiens gi:13375705; Arabidopsis thaliana (plant) gi:22655310; Chloroflexus aurantiacus (Bacteria, Chloroflexi) gi:76258461; Dehalococcoides ethenogenes (Bacteria, Chloroflexi) gi:57225528; Natronomonas pharaonis (Archaeobacteria) gi:76558351. The cartoon indicates predicted transmembrane alpha helices according to the SMART web server (dark blue box), the BAM domain (light blue box with position range), RING domain (purple circle), lemA domain (green box), and the length of the sequence. The sequences have been arranged in a simplified phylogenetic tree for illustrative purposes.

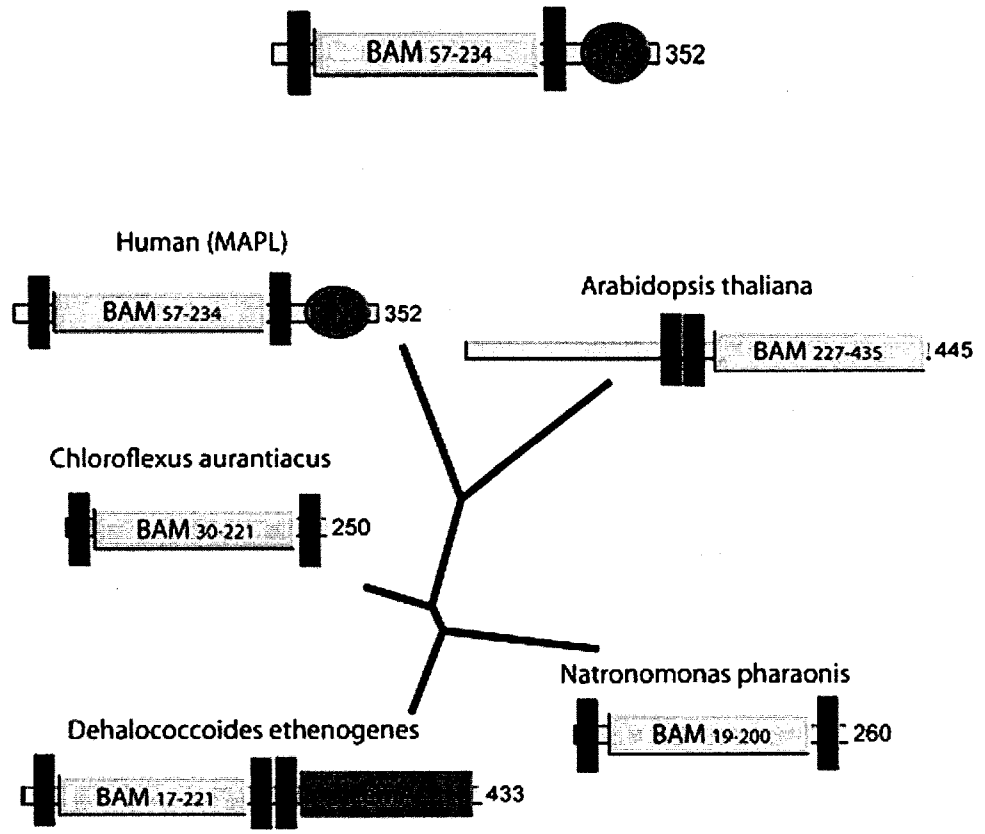


Figure 4.3 *MAPL* phylogenetic tree

raised against MAPL was used for immunodecoration of COS7 cells which demonstrated that as predicted the protein colocalized with the mitochondrial marker cytochrome c. The protease protection experiments demonstrated that this novel BAM domain is localized within the intermembrane space and the RING domain exposed to the cytosol. Sequence features of representative sequences containing the new beside a membrane domain (BAM) in sequences from bacteria to plants and mammals are shown (Figure 4.4). Interestingly, this protein and the BAM domain are not conserved in yeast. The preparation of a bioinformatics manuscript detailing the identification and characterization of this domain is currently being planned in the laboratory.

The function of this domain is currently being investigated in the laboratory, and due to its localization, we envision that it interacts with proteins in the intermembrane space or inner membrane. It could function in mitochondrial fission, perhaps coordinating inner and outer membrane fission, or perhaps it functions in the recognition of MAPL as cargo for peroxisomal transport. As future studies elucidate the role of MAPL in both Drp1 dependent fission and Drp1 independent MDV formation, the function of the BAM domain and interacting partners will hopefully become apparent.

4.2.2 FUNCTION OF THE RING DOMAIN

Although MAPL was previously uncharacterized, the predictions of FLJ12785 suggested that it was likely a ubiquitin E3 ligase due to the presence of the RING finger domain. Sequence of a RING finger alone, cannot easily distinguish the difference between a Ubiquitin E3 Ligase, a SUMO1 E3 ligase or a FYVE finger PI(3)P binding domain. As an initial component of my research project, I generated a series of constructs representing the carboxyl-terminus of the protein including the RING domain, just the RING

Figure 4.4

Identification of a previously uncharacterized domain, Beside A Membrane(BAM domain)

Sequence analysis of the N-terminal region of MAPL before a predicted transmembrane (TM) helix and the RING domain suggested the presence of a domain of approximately 200 amino acids conserved in a number of protein families (upper alignment). To investigate the possible function and phylogenetic distribution of this domain, the protein sequence database for homologous sequences was inspected. First, eukaryotic homologous sequences to the corresponding MAPL fragment using iterative searches with PSI-BLAST were obtained. Next other sequences with the domain in N-terminal position, followed by a predicted TM helix, often with a RING domain at the C-termini were found. Prokaryotic sequences are illustrated with the domain in N-terminal position followed by a TM helix but lacking the RING domain. The persistent presence of two or more TM helices in proteins containing the domain suggest that it has a membrane related function. We named this domain BAM for beside a membrane.

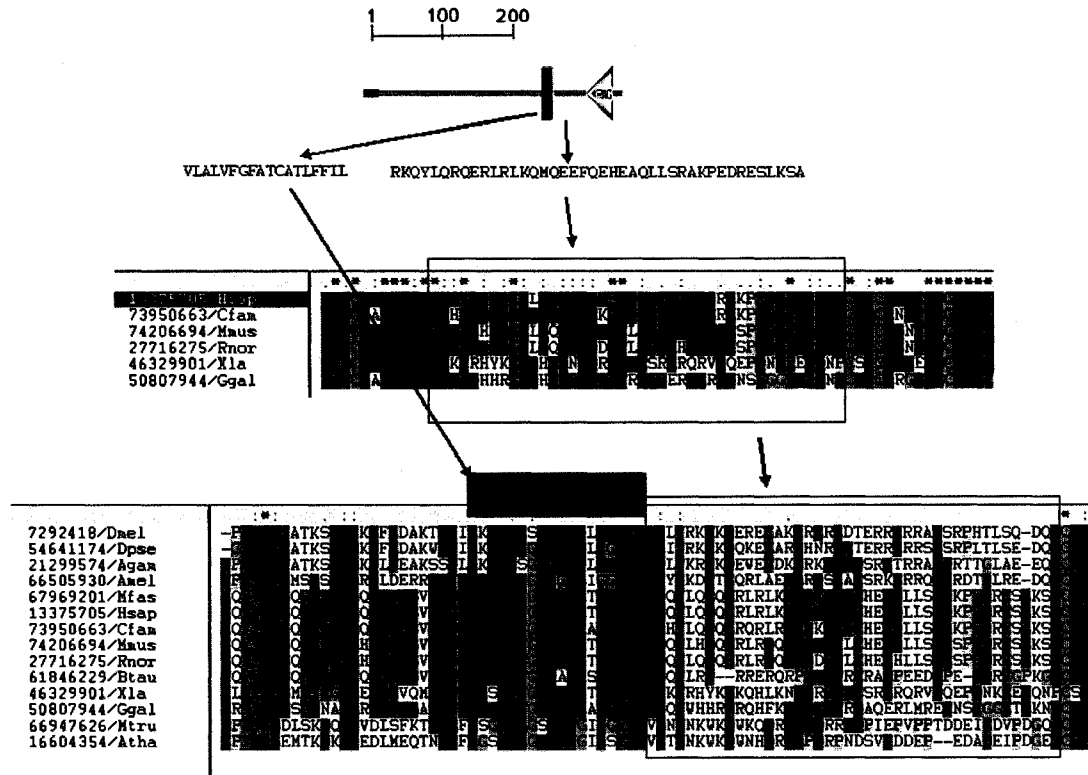


Figure 4.4

Identification of a previously uncharacterized domain, Beside A Membrane(BAM domain)

finger alone, and a RING finger point mutation, were generated as well as rabbit polyclonal antibodies to determine the function of the RING finger domain. It was initially, hypothesized that MAPL, functioned as a SUMO E3 ligase for Drp1 based on the rationale of the bioinformatics screen. Preliminary experiments did not indicate that this was correct; therefore I next investigated the possibility that MAPL was a ubiquitin E3 ligase.

The recent discovery of the MARCH-5 E3 ubiquitin ligase, which ubiquitinates Drp1, Fis1 and Mfn2 suggests the involvement of the proteosomal pathway in the selective turnover of these proteins. Consistent with this is the proteosomal dependent turnover of Fzo1 in alpha arrested yeast cells. Fis1 and Mfn2, both integral outer membrane proteins must be excised from the membrane in order to be degraded by the ubiquitin-proteosomal pathway. Given that many mitochondrial proteins function within large protein complexes of 20-40 proteins, and that many of these are integral membrane proteins, it is unclear how these complexes may be disassembled and membrane proteins/channels extracted from the bilayer.

Ubiquitin E3 ligases, possess the ability to auto-ubiquitinate *in vitro*, in the presence of recombinant E1, E2 enzymes, ATP, and ubiquitin. The hypothesis that the RING domain functions as a ubiquitin E3 ligase was initially tested using this *in vitro* auto-ubiquitination assay. These experiments are only described briefly, since they did not yield any positive results. Additionally, they were not pursued, since the discovery of MDV's became the focus of my research project. These experiments were performed using a panel of recombinant E2 enzymes, since E2 enzymes are known to have different affinities for E3 enzymes. The investigations into this potential function of the RING domain did not yield any positive results and it was concluded that MAPL did not function as a mitochondrial outer membrane ubiquitin E3 ligase.

Furthermore, during the later stages of my degree just prior to my maternity leave, I trained Emelie Braschi, a new master's student in the lab. She took over many aspects of my project, and together we revisited and revised both the ubiquitination assay and the SUMOylation assays.

Her research has yielded some very interesting results which will not be discussed in detail within the context of this thesis. Briefly, the *in vitro* SUMOylation assay, using the recombinant RING domain, purified mitochondria, recombinant Drp1 or a SUMO consensus peptide, clearly indicate that MAPL is a SUMO E3 ligase, SUMOylates a number of mitochondrial targets and specifically SUMOylates Drp1. This finding is consistent with the topology of MAPL, in that its RING domain is exposed to the cytosol. We therefore envision that the majority of SUMOylated mitochondrial targets reside on the outer membrane as either integral membrane proteins or as cytosolic membrane associated proteins. This finding also is suggestive of a role of MAPL in the progression of apoptosis, since Drp1 undergoes an apoptotic transition on the mitochondrial membrane from rapid recycling to stable association which is SUMO dependent and Bax/Bak dependent. Furthermore, it is suggestive of a possible direct relationship between MAPL and Bax/Bak.

4.2.3 MAPL AND MITOCHONDRIAL FISSION

Mitochondrial fission is a complex process with many unknown regulatory and signaling proteins. The identification of a new mammalian protein for fission represents a significant advancement for the field. The finding that MAPL functions as a SUMO E3 ligase is indicative of more complex regulation compared to the mechanisms of fission in yeast, where MAPL is absent. Interestingly, the expression of the dominant negative Drp1 mutant DrpK38E rescues MAPL stimulated fission indicating that MAPL functions upstream

of Drp1 for fission (21). Furthermore, a functional RING domain is required for MAPL fission stimulation suggesting that its SUMOylation activity for Drp1 is required for fission. Surprisingly, the loss of MAPL through siRNA did not yield a fused phenotype, demonstrating that although it may stimulate fission, its ability to SUMOylate Drp1 is not essential for fission (21). The specific role of MAPL in fission and its relationship with Drp1 has not yet been uncovered and this work is ongoing in the laboratory.

Since MAPL is an outer membrane protein which induces mitochondrial fragmentation and is found on vesicles, it is logical to assume that MAPL co-localizes with Drp1 on these mitochondrial structures. Drp1 localizes to constriction sites as well as to discrete puncta on mitochondrial tubules, therefore it was logical to assume that Drp1 and MAPL co-localized. Immunofluorescence of endogenous MAPL and Drp1 and overexpression studies of MAPL-CFP and Drp1-YFP transfected Cos-7 and HeLa cells revealed that some of the MAPL puncta contained Drp1 protein and that some of the Drp1 puncta on mitochondrial surfaces contained MAPL protein. As expected, in both cases, the co-localization was not mutually exclusive (data not shown), with many Drp1 puncta residing in isolation on the mitochondria membrane.

One can speculate that the ability of MAPL to sequester into un-described mitochondrial microdomains for cargo selected budding, suggests, that it possesses the ability to laterally migrate within the membrane. This ability may be one of the critical factors for Drp1 recruitment and assembly into puncta on the outer membrane. During apoptosis, post fission the recycling ability of Drp1 puncta changes dramatically dependent upon SUMOylation, Bax and Bak (20). The relationship between MAPL and other known fission proteins such as Fis1, Endophilin B together with Drp1 have not been investigated in this series of initial research projects. Future studies by other laboratories will undoubtedly

expand on this initial characterization and hopefully uncover the mechanistic relationships between these proteins for fission.

4.3 MAPL AND TOM20 VESICLES

As a part of the initial characterization of MAPL, transient overexpression studies into Cos-7 and HeLa cells were routinely performed. It was documented early in these studies that MAPL stimulated fragmentation, however, we additionally observed the presence of very small MAPL positive structures which did not always contain other mitochondrial proteins. Electron microscopy imaging of mitochondria from cells expressing MAPL-YFP was instrumental in the identification of MDV's. It was not until the unusual appearance of the membranes and the accumulation of electron density into buds forming along the outer membrane was observed, that the notion of vesicle formation was entertained (21). What is presented in manuscript #2 represents some of what we have learned thus far about the ability of the mitochondria to form vesicles. This remarkable phenotype observed in MAPL expressing cells took considerable time to decipher, and was the focus of three years of my research. Currently, we have been able to conclude that there two distinct populations of MDV's, those carrying MAPL as selected cargo which traffic to the peroxisome and those carrying TOM20 as cargo of unknown function and destination. Many questions arise from this work; however a critical point to recognize from this study is the important difference between mitochondrial fission and mitochondrial budding. Whole organelle constriction for fission may not require extensive cargo selection since the entire organelle is effectively divided in two, whereas the formation of MDV's would require selective cargo sequestration into the bud. Furthermore, the interesting result that mitochondrial budding occurs in the presence of the dominant negative mutant of Drp1

indicates that although MAPL stimulated fission requires the action of Drp1, the budding event does not. Alternative protein machinery therefore must function at the mitochondria to facilitate specific cargo selection and these budding events. This is an ongoing project in the laboratory.

A series of experiments were initially designed and considerable time was spent trying to uncover what the fate of the mitochondrial derived vesicles would be. Three hypotheses were initially formed; that the vesicles would fuse back into the mitochondrial reticulum acting as protein, lipid and or mtDNA carriers between mitochondria, that the vesicles would target the proteosomal pathway for protein turnover, and that the vesicles would traffic towards the lysosomal pathway for proteins degradation (Figure 4.5). The last two fates were based on the hypothesis that MDVs represented a novel protein degradation pathway for the mitochondria. It was therefore surprising when it was uncovered that MAPL positive vesicles trafficked to and fused with a subset of peroxisomes (21). This finding was not expected, however this research has identified a highly exciting new avenue for mitochondrial and peroxisomal research.

4.3.1 MAPL DELIVERY TO THE PEROXISOME

The discovery and potential implications of MDVs in peroxisomal function, the integration of MDVs into the secretory pathway as well as the role of MDVs in the cooperative metabolic activities of both these organelles remain unknown but represent a significant breakthrough for the peroxisome and mitochondrial fields of cell biology. This study revealed that MDVs contain distinct cargo, which have distinct fates where, nearly 85% of MAPL positive vesicles colocalize with peroxisomal markers (21). This colocalization is highly significant since it provides evidence for selective cargo segregation

within mitochondrial membranes since MAPL positive MDVs which trafficked to the peroxisomes excluded $\Delta\Psi$, pOCT-CFP and Tom20. Furthermore, only 10-30% of all peroxisomes contained MAPL positive MDVs, demonstrating that MAPL is targeted to a small subset of peroxisomes (21).

Some mitochondrial proteins can be dually targeted to both peroxisomes and mitochondria through alternative splicing. Since MAPL, contains only one message, it is unlikely that MAPL is dually targeted to both peroxisome and mitochondria. Furthermore, direct fusion events between MAPL-YFP containing vesicles and a subset of peroxisomes have been observed providing evidence to support the claim that it is not dually imported. Since MAPL is not imported into both peroxisomes and mitochondria, this work concluded that there is selective transport of mitochondrial content via MDV, of which MAPL is a cargo protein to the peroxisome for fusion within the peroxisomal network. These data reveal for the first time a novel intracellular transport route between the mitochondria and the peroxisome.

Interestingly, MAPL appears to fuse only with a sub-population of peroxisomes resulting in about 10% of peroxisomes labeling for MAPL (21). This result raises some very interesting questions for both mitochondrial and peroxisome cell biologists. From a mitochondrial perspective, since very little is known about mitochondrial fusion, the discovery of MDV-peroxisomal fusion events is highly captivating and opens up a new cell biology field of research. Some specific questions; Do the mitofusin proteins need to be on the vesicles for fusion with the peroxisome? And if so, is a similar GTPase switch mechanism used for the fusion event? Furthermore, if Mfn1 and or Mfn2 are required on the MDV, what do they interact with on the peroxisomal surface for tethering? It is easy to

speculate that this process would be analogous to the Mfn1-Mfn1 *trans* mitochondrial pairing? However, if these proteins are not found on the MDV surfaces, then it must be considered that an additional set of fusion proteins exist either on the mitochondrial surface or on the peroxisome surface. It is also interesting to note that some vesicles, but not all, contained particular inner membrane cargo and matrix content or none at all. If double membrane MDV's traffic towards the peroxisome, then the fusion into the peroxisomal reticulum would be that much more complex. Additionally, since OPA1 cooperates with Mfn1 for fusion, one therefore must also consider a potential role of OPA1 in MDV-peroxisomal fusion.

In mammalian cells, peroxisome proliferation is regulated by the peroxisome proliferator-activated receptor α (PPAR α). This is a ligand-dependent nuclear transcription factor which regulates gene expression patterns of different genes associated with lipid metabolism and adipocyte differentiation (22). Peroxisomes have a unique complement of different enzymes and their primary functions are to participate in metabolic functions according to cellular needs. Within the matrix of peroxisomes, enzymes are linked to diverse biochemical pathways such as the beta-oxidation of fatty acids and the detoxification of the hydrogen peroxide (23). In mammalian cells the beta-oxidation of fatty acids is shared between the peroxisomes and mitochondria. Due to the importance of the shared functionality of the mitochondria and peroxisomes, several inherited diseases are caused by defects in both metabolic enzymes (24) and of peroxisomal biogenesis factors (25). Additionally, the production and removal of both hydrogen peroxide and other reactive oxygen species implicates both organelles in the aging process (26). Furthermore, both the peroxisomes and mitochondria share some protein content. The mitochondrial fission

proteins Dnm1p, as well as the Dnm1p-anchoring protein Fis1p both function at the peroxisome for organelle fission events (27-28). Peroxisomes have also recently been proposed to undergo retrograde transport from the peroxisome back to the ER in mammalian cells, (23, 29) and are now believed to be an partially independent part of the secretory pathway (23).

Within the peroxisome field, the discovery of MDV-peroxisome fusion is also highly intriguing. An interesting question to consider is that what is specific about this population of peroxisomes which marks them for MDV targeting and fusion? Furthermore, what is the function of this specific population of peroxisomes which receive the MDVs? Currently, in the laboratory, three possibilities have been suggested and are currently being investigated by Astrid Schauss, a Post Doctoral fellow in the Dr. McBride research group. Firstly; that these peroxisomes represent a population of premature peroxisomes, possibly recently formed from the ER. Perhaps these would require the specific delivery of mitochondrial proteins, Ca²⁺ and or lipids for maturation. Secondly, that they represent a population of dysfunctional peroxisomes destined to be degraded. Why these would need mitochondrial content for degradation remains unknown. Perhaps these peroxisomes once fused with MDVs, assist in the initiation of mitophagy and or the formation of the autophagic membranes? Or that they need some of the mitochondrial proteases for degradation (30). Finally, the third hypothesis suggested is that they represent a distinct population of peroxisomes with an unknown function.

It is also interesting to consider what other factors in the cell may trigger these specific cargo selections, budding, trafficking and fusion events. Perhaps MAPL positive MDVs form in response to apoptotic and or autophagy stimuli, metabolic demands, mitochondrial biogenesis signals, or cell cycle triggers? MDV-peroxisome trafficking needs

to be investigated during all of these alterations in steady state cell situations to further understand the nature and dynamic of this relationship. Since it is an emerging theme that the mitochondria are important regulators of cell cycle, it follows that perhaps MDVs-peroxisomal trafficking plays an unknown role in these checks. Consistently, both Drp1, Mfn2 have been implicated in cell cycle regulation in one way or another. Studies performed by both Rudolfo Zunino and Emelie Braschi, have identified a novel cell cycle check point which hinges on the SUMOylation activity at the mitochondria. This work is highly novel and identifies the role of the mitochondrial SUMO1 protease SenP5 and the SUMO E3 ligase MAPL in defining a novel mitochondrial cell cycle check point at G2/M (unpublished manuscript). Since MAPL is a cargo of the peroxisome destined vesicles, it will be important in the future to investigate the potential effect of both SUMOylation and cell cycle on MDV-peroxisome trafficking.

4.3.2 FATE OF TOM20 POSITIVE VESICLE POPULATION

An outstanding question in fields of mitochondrial biology and development, is how this highly oxidative organelle can survive throughout evolution given the high levels of damaging ROS, peroxides and nitric oxides that are integral to mitochondrial function? It has been well documented that mtDNA mutations lead to diverse disease, and that these mutations increase within tissues and individual people over a lifetime. Considering this, it is remarkable that the maternally inherited germline “stock” of mtDNA and mitochondria has remained relatively clear of mutations. Rescuing mitochondrial damage through the ability to degrade mitochondrial proteins in a specific and efficient fashion without whole organelle mitophagy represents a novel hypothesis. We envision that the discovery of the TOM20

positive mitochondrial derived vesicles which contain cargo selected proteins may facilitate the removal of damage proteins/mitochondria and preserve mitochondrial integrity (21).

Although the MAPL vesicles transport cargo to the peroxisome, the exclusion of the TOM20 positive vesicle population from the peroxisome indicates minimally a second intracellular transport route (21). In order to understand the physiology of both populations of vesicles, the cargo must first be identified. A number of approaches are currently being investigated to uncover the nature of the cargo. This work is being performed by Vincent Soubannier, a Post Doctoral fellow and Emelie Braschi, a master's student in the laboratory of Dr. McBride. A mitochondrial *in vitro* budding assay has been developed which is currently being used to determine; the protein cargo of the vesicles, the cytosolic factors required for vesicle formation and the physiologic stimuli for vesicle formation.

Three hypotheses are entertained for the fate of TOM20 MDV's. (Figure 4.5) That the vesicles would fuse back into the mitochondrial reticulum acting as protein, lipid and or mtDNA carriers between mitochondria. In this case, although we do not understand the purpose of this kind of mitochondrial protein/lipid/mtDNA segregation and targeting, it could be envisioned that this is a mechanism for mtDNA sharing or complementation. It could be a way of sharing lipid, re-shuffling components of the OXPHOS complexes or dispersing accumulated ROS. Perhaps the transport of smaller MDVs may be an advantage in certain cell types, for example in neurons, where there are longer distances to travel. Additionally, in order for the vesicles to re-fuse with the mitochondria, they would require fusion proteins on their surface such as Mfn2. Since we do not yet know the protein composition of the vesicles it is difficult to ascertain if Mfn2 or other fusion proteins are present. 2) That the vesicles would target the proteosomal pathway for protein turnover. Finally 3) that the vesicles would traffic towards the lysosomal pathway for proteins

Figure 4.5

Potential Tom20 vesicle fates

Cartoon illustrating potential TOM20 vesicle fates. Three hypothesis are entertained: 1) that the TOM20 vesicle's re-fuse back into the mitochondrial reticulum. 2) That the TOM20 vesicles target the proteasome for ubiquitin mediated proteosomal degradation. And 3) that the TOM20 vesicles target the lysosome for either selective protein turnover or for mitophagy.

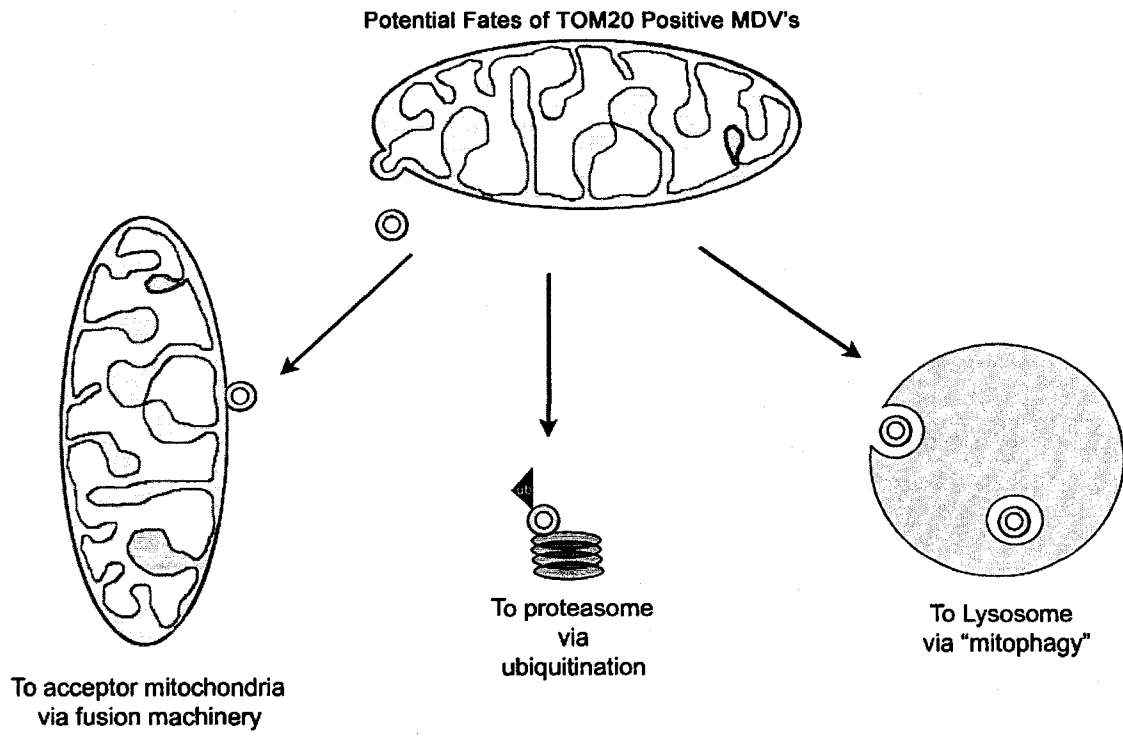


Figure 4.5

Potential Tom20 vesicle fates

degradation or selected mitophagy. The last two fates were based on the hypothesis that MDVs represented a novel protein degradation pathway for the mitochondria. Recent studies suggest that organelles do not become aged as an individual unit, begging the questions as to why an entire organelle would be degraded when only sub-compartments are damaged (31)? It is conceivable that damaged content within healthy mitochondria would be sorted into MDV's that would be competent for internalization into the lysosome/autophagosome. This cargo selection would prevent compromising and avoid the loss of healthy, intact organelles during stress and or starvation. This hypothesis was consistent with unexpected finding that Fzo1p turnover and degradation can occur in a non-proteosomal and non-vacuolar pathway in vegetatively growing yeast cells (32). Interestingly, new research performed by Vincent Soubannier, has revealed that the TOM20 vesicles, do in fact target the lysosome under conditions of sub-lethal dosage of ROS.

It has recently been proposed that Atg9, one of the only integral membrane proteins of the autophagy pathway is localized to the mitochondria. In this it is thought that, Atg9 through an unknown pathway forms the precursor autophagic membrane. The origin of the autophagic membranes has been an unsolved question in cell biology for many years. It has been proposed that this membrane originates from the endoplasmic reticulum. The discovery of MDV's may provide an unexpected clue to the origin of this membrane. Fusion of Atg9-containing double membrane MDVs may be one of the initial steps in the formation of the pre-autophagosome.

4.4 CONCLUSIONS:

The research performed throughout the course of this doctoral thesis has profound impacts on cell biology, impacting mitochondrial dynamics, programmed cell death,

intracellular signaling, and peroxisome biology. The discoveries can be summarized into four major contributions; 1) *that Mfn2 is a signaling GTPase for mitochondrial fusion rather than a mechanoenzyme*, 2) *that activated Mfn2 protects against both cytosolic and mitochondrial apoptosis as well as inhibits Bax activation*, 3) *that MAPL is a novel morphology protein of the outer mitochondrial membrane*, and finally 4) *that the mitochondria bud two distinct cargo selected vesicles, one of which traffics to the peroxisome*. Each of these contributions at the time of initial discovery was highly novel and represented a significant advancement in the field of mitochondrial dynamics.

The research performed on Mfn2, the signaling activity of its GTPase domain and its role in inhibiting Bax activation, provided insightful tools to formulate novel hypothesis regarding mitochondrial function many of which have resulted in new advancements to the field. These themes have been accepted amongst peers and are currently being pursued by many other mitochondrial and apoptosis research groups.

The discovery of MDVs represents a groundbreaking advancement to cell biology. It was not previously thought that the mitochondria participate in intracellular vesicle trafficking events, and as such this discovery was not predicted or anticipated. Due to the novelty of this work, it may take years before it is well endorsed amongst peers and the mechanisms and functions of different vesicle populations truly understood. The results however are compelling and to quote directly from the manuscript reviews “These findings represent some of the most exciting of recent advances in the field of mitochondrial dynamics” Additionally; “This manuscript is of great novelty and broad general interest for biologists interested in mitochondrial and peroxisomal biogenesis, as well as for scientist with an interest in inter-organellar communication. I think that it will fall in the top papers

regarding mitochondrial biogenesis, morphology and intercommunication with other organelles and for sure it will prompt new research in the field”

The research discoveries herein, will hopefully lead towards fundamentally new perspectives on the function of the mitochondria. Through this work and the future work of others, the relationship between the phenomenon of mitochondrial fusion, fission and budding, and what these dynamics mean to the function and survival of the cell, will hopefully be elucidated.

4.5 REFERENCES

1. Neuspiel, M., R. Zunino, S. Gangaraju, P. Rippstein, and H.M. McBride. 2005. Activated Mfn2 signals mitochondrial fusion, interferes with Bax activation and reduces susceptibility to radical induced depolarization. *J Biol Chem* 280:25060-25070.
2. Ishihara, N., Y. Eura, and K. Mihara. 2004. Mitofusin 1 and 2 play distinct roles in mitochondrial fusion reactions via GTPase activity. *J Cell Sci* 117:6535-6546. Epub 2004 Nov 6530.
3. Rybin, V., O. Ullrich, M. Rubino, K. Alexandrov, I. Simon, M.C. Seabra, R. Goody, and M. Zerial. 1996. GTPase activity of rab5 acts as a timer for endocytic membrane fusion. *Nature* 383:266-269.
4. Simon, I., M. Zerial, and R.S. Goody. 1996. Kinetics of interaction of Rab5 and Rab7 with nucleotides and magnesium ions. *J Biol Chem* 271:20470-20478.
5. Cipolat, S., O. Martins de Brito, B. Dal Zilio, and L. Scorrano. 2004. OPA1 requires mitofusin 1 to promote mitochondrial fusion. *Proc Natl Acad Sci U S A* 101:15927-15932. Epub 12004 Oct 15927.
6. Chen, H., S.A. Detmer, A.J. Ewald, E.E. Griffin, S.E. Fraser, and D.C. Chan. 2003. Mitofusins Mfn1 and Mfn2 coordinately regulate mitochondrial fusion and are essential for embryonic development. *J Cell Biol* 160:189-200.
7. Chen, K.H., X. Guo, D. Ma, Y. Guo, Q. Li, D. Yang, P. Li, X. Qiu, S. Wen, R.P. Xiao, and J. Tang. 2004. Dysregulation of HSG triggers vascular proliferative disorders. *Nat Cell Biol* 6:872-883. Epub 2004 Aug 2022.
8. McBride, H.M., M. Neuspiel, and S. Wasiak. 2006. Mitochondria: more than just a powerhouse. *Curr Biol* 16:R551-560.
9. Jahani-Asl, A., E.C. Cheung, M. Neuspiel, J.G. MacLaurin, A. Fortin, D.S. Park, H.M. McBride, and R.S. Slack. 2007. Mitofusin 2 protects cerebellar granule neurons against injury-induced cell death. *J Biol Chem* 282:23788-23798.
10. Jeyaraju, D.V., L. Xu, M.C. Letellier, S. Bandaru, R. Zunino, E.A. Berg, H.M. McBride, and L. Pellegrini. 2006. Phosphorylation and cleavage of presenilin-associated rhomboid-like protein (PARL) promotes changes in mitochondrial morphology. *Proc Natl Acad Sci U S A* 103:18562-18567.
11. Wei, M.C., W.X. Zong, E.H. Cheng, T. Lindsten, V. Panoutsakopoulou, A.J. Ross, K.A. Roth, G.R. MacGregor, C.B. Thompson, and S.J. Korsmeyer. 2001. Proapoptotic BAX and BAK: a requisite gateway to mitochondrial dysfunction and death. *Science* 292:727-730.

12. Breckenridge, D.G., M. Stojanovic, R.C. Marcellus, and G.C. Shore. 2003. Caspase cleavage product of BAP31 induces mitochondrial fission through endoplasmic reticulum calcium signals, enhancing cytochrome c release to the cytosol. *J Cell Biol* 160:1115-1127.
13. Frank, S., B. Gaume, E.S. Bergmann-Leitner, W.W. Leitner, E.G. Robert, F. Catez, C.L. Smith, and R.J. Youle. 2001. The role of dynamin-related protein 1, a mediator of mitochondrial fission, in apoptosis. *Dev Cell* 1:515-525.
14. Sugioka, R., S. Shimizu, and Y. Tsujimoto. 2004. Fzo1, a protein involved in mitochondrial fusion, inhibits apoptosis. *J Biol Chem* 279:52726-52734.
15. Kinnally, K.W., and B. Antonsson. 2007. A tale of two mitochondrial channels, MAC and PTP, in apoptosis. *Apoptosis* 12:857-868.
16. Cory, S., D.C. Huang, and J.M. Adams. 2003. The Bcl-2 family: roles in cell survival and oncogenesis. *Oncogene* 22:8590-8607.
17. Brooks, C., Q. Wei, L. Feng, G. Dong, Y. Tao, L. Mei, Z.J. Xie, and Z. Dong. 2007. Bak regulates mitochondrial morphology and pathology during apoptosis by interacting with mitofusins. *Proc Natl Acad Sci U S A* 104:11649-11654.
18. Karbowski, M., Y.J. Lee, B. Gaume, S.Y. Jeong, S. Frank, A. Nechushtan, A. Santel, M. Fuller, C.L. Smith, and R.J. Youle. 2002. Spatial and temporal association of Bax with mitochondrial fission sites, Drp1, and Mfn2 during apoptosis. *J Cell Biol* 159:931-938.
19. Karbowski, M., K.L. Norris, M.M. Cleland, S.Y. Jeong, and R.J. Youle. 2006. Role of Bax and Bak in mitochondrial morphogenesis. *Nature* 443:658-662.
20. Wasiak, S., R. Zunino, and H.M. McBride. 2007. Bax/Bak promote sumoylation of DRP1 and its stable association with mitochondria during apoptotic cell death. *J Cell Biol* 177:439-450.
21. Neuspiel, M., A.C. Schauss, E. Braschi, R. Zunino, P. Rippstein, R.A. Rachubinski, M.A. Andrade-Navarro, and H.M. McBride. 2008. Cargo-selected transport from the mitochondria to peroxisomes is mediated by vesicular carriers. *Curr Biol* 18:102-108.
22. Kliewer, S.A., K. Umesono, D.J. Noonan, R.A. Heyman, and R.M. Evans. 1992. Convergence of 9-cis retinoic acid and peroxisome proliferator signalling pathways through heterodimer formation of their receptors. *Nature* 358:771-774.
23. Platta, H.W., and R. Erdmann. 2007. Peroxisomal dynamics. *Trends Cell Biol* 17:474-484.
24. Wanders, R.J., and H.R. Waterham. 2006. Peroxisomal disorders: the single peroxisomal enzyme deficiencies. *Biochim Biophys Acta* 1763:1707-1720.

25. Steinberg, S.J., G. Dodt, G.V. Raymond, N.E. Braverman, A.B. Moser, and H.W. Moser. 2006. Peroxisome biogenesis disorders. *Biochim Biophys Acta* 1763:1733-1748.
26. Terlecky, S.R., J.I. Koepke, and P.A. Walton. 2006. Peroxisomes and aging. *Biochim Biophys Acta* 1763:1749-1754.
27. Koch, A., Y. Yoon, N.A. Bonekamp, M.A. McNiven, and M. Schrader. 2005. A role for Fis1 in both mitochondrial and peroxisomal fission in mammalian cells. *Mol Biol Cell* 16:5077-5086.
28. Kuravi, K., S. Nagotu, A.M. Krikken, K. Sjollema, M. Deckers, R. Erdmann, M. Veenhuis, and I.J. van der Klei. 2006. Dynamin-related proteins Vps1p and Dnm1p control peroxisome abundance in *Saccharomyces cerevisiae*. *J Cell Sci* 119:3994-4001.
29. Lay, D., K. Gorgas, and W.W. Just. 2006. Peroxisome biogenesis: where Arf and coatamer might be involved. *Biochim Biophys Acta* 1763:1678-1687.
30. Haynes, C.M., K. Petrova, C. Benedetti, Y. Yang, and D. Ron. 2007. ClpP mediates activation of a mitochondrial unfolded protein response in *C. elegans*. *Dev Cell* 13:467-480.
31. Mijaljica, D., M. Prescott, and R.J. Devenish. 2007. Different fates of mitochondria: alternative ways for degradation? *Autophagy* 3:4-9.
32. Escobar-Henriques, M., B. Westermann, and T. Langer. 2006. Regulation of mitochondrial fusion by the F-box protein Mdm30 involves proteasome-independent turnover of Fzo1. *J Cell Biol* 173:645-650.

Margaret Neuspiel

EDUCATION:

University of Ottawa, Ottawa, ON

Doctorate of Philosophy

(in progress 2003-2008)

Faculty of Medicine, Department of Biochemistry, Microbiology and Immunology,

University of Ottawa Heart Institute

Thesis: Mechanisms and Meaning of Mitochondrial dynamics. Dr. Heidi McBride

McGill University Montreal, PQ

Bachelor of Science

1998-2002

Faculty of Medicine, Department of Biochemistry

Major in Biochemistry; Minor in Biotechnology.

EXPERIENCE

University of Ottawa

Ottawa, ON

Vice President Finance, BMIGSA

2004 to 2006

- Founding member of BMIGSA, (Biochemistry, Microbiology and Immunology Graduate Students Association).
- Strategically planned, developed and implemented BMIGSA, planned student recruiting events, website development and prepared reports of business transactions and kept expense accounts.

University of Ottawa

Ottawa, ON

Faculty of Medicine Advisory Board

2005 to 2006

Committee Member

- Faculty of Medicine graduate student representative.
- Was instrumental in facilitating increased graduate student representation within the faculty of medicine. Communicated the needs of the graduate students during monthly meetings to the faculty and provided feedback to departmental subcommittees.

Carleton University

Ottawa, ON

Women's Waterpolo Varsity Coach

2002 to 2005

- Assistant Head Coach.
- Mentor to high school and university female athletes.

Sport Canada

National Team Athlete

1996 to 2002

- Member of Women's National Waterpolo Team.

- Completed public relations and media training seminars and participated in numerous provincial and national television and radio interviews.
- Canadian Athlete representative, host and delegate for the 1st (WADA) World Anti-Doping Association international meeting.
- Silver medalist Women's Waterpolo Jr. World Championships, Messina Italy 1999

Athletes World

Montreal, PQ

Sales Representative

2000 to 2001

- Commissioned based bilingual sales representative for Montreal's downtown flagship superstore.
- Promoted and increased sales of new active wear clothing division "Out there" for Athletes world.

Government of Canada,

Hull, PQ

Senior Clerk, Department of Indian and Northern Affairs

2000

- Assisted in the planning and representation of Indian and Northern Affairs at the NEXIS aboriginal trade show.
- Increased awareness of government procurement services at NEXIS.

AWARDS:

- Doctoral Research Award, Heart and Stroke Foundation of Ontario, 2006-2008.
- Doctorate Research Award, Ontario Graduate Scholarship, 2006-2007
- National Award of Excellence Tuition Scholarship, University of Ottawa, 2006-2008.
- FGPS Doctoral Tuition award, University of Ottawa, 2006-2007.
- Doctorate Poster award, first prize, University of Ottawa faculty of Medicine, Biochemistry poster competition, 2006.
- Member of Women's Waterpolo Olympic Team Program, 1998-2002.
- Member of National Women's Waterpolo Team, Sport Canada, 1996-2002.

PUBLICATIONS:

5) *Mitochondria to peroxisome transport is mediated by vesicular carriers*

Margaret Neuspiel, Astrid Schauss, Emelie Braschi, Rodolfo Zunino, Peter Rippstein, Miguel A. Andrade-Navarro and Heidi M. McBride..

4) *Mitofusin 2 Protects Cerebellar Granule Neurons against Injury-induced Cell Death.*

Jahani-Asl A, Cheung EC, **Margaret Neuspiel**, MacLaurin JG, Fortin A, Park DS, McBride HM, Slack RS. Journal of Biological Chemistry. 2007 Aug 17;282(33):23788-98.

3) *Dissociating the dual roles of apoptosis-inducing factor in maintaining mitochondrial structure and apoptosis*

Cheung EC, Joza N, Steenaart NA, McClellan KA, **Margaret Neuspiel**, McNamara S, MacLaurin JG, Rippstein P, Park DS, Shore GC, McBride HM, Penninger JM, Slack RS. EMBO J. 2006 Sep 6;25(17):4061-73.

2) *Mitochondria: more than just a powerhouse*

McBride H, Margaret Neuspiel, Wasiak S.

Current Biology, 2006 Jul 25;16(14):R551-60.

1) *Activated mitofusin 2 signals mitochondrial fusion, interferes with Bax activation, and reduces susceptibility to radical induced depolarization*

Margaret Neuspiel, Zunino R, Gangaraju S, Rippstein P, McBride H. Journal of Biological Chemistry. 2005 Jul 1;280(26):25060-70.

Oral presentations:

***Poster presentation unless otherwise noted**

Identification of a novel mitochondrial SUMO1 E3 ligase that stimulates the formation of mitochondrial derived vesicles

Margaret Neuspiel. Cell Biology and Signaling Seminar Series, University of Ottawa, November 2006. **(Oral Presentation)**

Mitochondria form buds and vesicles in a process dependant upon a novel RING finger containing protein MAPL and target to the Endoplasmic Reticulum for transport

Margaret Neuspiel, Peter Ripstein and Heidi M. McBride Ottawa Hospital Lipoproteins Research Group seminar series, December, 2006. **(Oral Presentation)**

Mitochondria form buds and vesicles in a process dependant upon a novel RING finger containing protein MARI-1 and target to the Endoplasmic Reticulum for transport

Margaret Neuspiel, Peter Ripstein and Heidi M. McBride Gordon Research Conference, Tilton New Hampshire July2-7, 2006

Mitochondria form buds and vesicles in a process dependant upon a novel RING finger containing protein MARI-1 and DRP1

Margaret Neuspiel, Sylwia Wasiak, Peter Ripstein and Heidi M. McBride University of Ottawa Faculty of Medicine Biochemistry and Microbiology Immunology poster competition. **1st prize, Doctoral Award winning poster**

Mitochondria form buds and vesicles in a process dependant upon a novel RING finger containing protein MARI-1 and DRP1

Margaret Neuspiel, Sylwia Wasiak, Peter Ripstein and Heidi M. McBride Canadian Lipoproteins Conference, Montebello QC, September 29-October 2nd, 2005

Activated Mfn2 has signaling capabilities, represses Bax activation and protects against permeability transition

Neuspiel, M., Zunino, R., Gangaraju, S., Rippstein, P. and McBride H.M Heart Institute Annual Research Symposium, May 2005. **(Oral Presentation)**

Identification of a novel mitochondrial anchored ring finger protein that localizes to sites of membrane remodeling”

Margaret Neuspiel and H. M. McBride Ottawa Hospital Lipoproteins Research Group seminar series, February 2005. (**Oral Presentation**)

Mfn2 is a signaling GTPase for Mitochondrial fusion

Neuspiel, M., Zunino, R., Gangaraju, S., Rippstein, P. and McBride H.M University of Ottawa Biochemistry student seminar series, February 2005. (**Oral Presentation**)

Activated Mfn2 has signaling capabilities, represses Bax activation and protects against permeability transition

Neuspiel, M., Zunino, R., Gangaraju, S., Rippstein, P. and McBride H.M University of Ottawa Biochemistry student seminar series, 2005. (**Oral Presentation**)

Identification of a novel mitochondrial anchored ring finger protein that localizes to sites of membrane remodeling

M. Neuspiel, H. McBride American Society of Cell Biology 44th Annual Meeting Washington, DC, December 4-8, 2004.

Mfn2 is a signaling GTPase for Mitochondrial fusion

Neuspiel, M., Zunino, R., Gangaraju, S., Rippstein, P. and McBride H.M. Ottawa Hospital Lipoproteins Research Group seminar series, February 2004. (**Oral Presentation**)

Appendix 1

Mitofusin 2 Protects Cerebellar Granule Neurons against Injury Induced Cell Death

Mitofusin 2 Protects Cerebellar Granule Neurons against Injury-induced Cell Death^{*[S]}

Received for publication, May 9, 2007. Published, JBC Papers in Press, May 30, 2007, DOI 10.1074/jbc.M703812200

Arezu Jahani-Asl[†], Eric C. C. Cheung[‡], Margaret Neuspiel[§], Jason G. MacLaurin[†], Andre Fortin[†], David S. Park[‡], Heidi M. McBride^{§1}, and Ruth S. Slack^{‡2}

From the [†]Department of Cellular and Molecular Medicine, University of Ottawa, Neurosciences Program, Ottawa Health Research Institute, Ottawa, Ontario K1H 8M5, Canada and the [§]University of Ottawa Heart Institute, University of Ottawa, Ontario K1Y 4W7, Canada

Of the GTPases involved in the regulation of the fusion machinery, mitofusin 2 (Mfn2) plays an important role in the nervous system as point mutations of this isoform are associated with Charcot Marie Tooth neuropathy. Here, we investigate whether Mfn2 plays a role in the regulation of neuronal injury. We first examine mitochondrial dynamics following different modes of injury in cerebellar granule neurons. We demonstrate that neurons exposed to DNA damage or oxidative stress exhibit extensive mitochondrial fission, an early event preceding neuronal loss. The extent of mitochondrial fragmentation and remodeling is variable and depends on the mode and the severity of the death stimuli. Interestingly, whereas mitofusin 2 loss of function significantly induces cell death in the absence of any cell death stimuli, expression of mitofusin 2 prevents cell death following DNA damage, oxidative stress, and K⁺ deprivation induced apoptosis. More importantly, whereas wild-type Mfn2 and the hydrolysis-deficient mutant of Mfn2 (Mfn2_{RasG12V}) function equally to promote fusion and lengthening of mitochondria, the activated Mfn2_{RasG12V} mutant shows a significant increase in the protection of neurons against cell death and release of proapoptotic factor cytochrome *c*. These findings highlight a signaling role for Mfn2 in the regulation of apoptosis that extends beyond its role in mitochondrial fusion.

It has been recently demonstrated that the apoptotic program includes the regulated induction of mitochondrial fragmentation (1, 2). In addition, it has been shown that the rate of mitochondrial fusion is reduced early in the apoptotic program (3, 4), which together with the activation of the fission machinery leads to a morphological shift of the mitochondria to the fragmented state. The regulatory mechanisms and functional

importance of these events during death remain unclear. For example, it is not clear whether the inhibition of mitochondrial fusion is an essential step in apoptosis or if fragmentation is promoted mainly because of the increase in fission. In addition, it has been shown that the loss of either Drp1 or hFis1 delayed, but did not block cell death, questioning the importance of the mitochondria morphological shift in the apoptotic cascade (5, 6). In this context, there is an emerging emphasis on the examination of mitochondrial fusion in the context of cell death.

Mitochondrial fusion is regulated by at least three essential GTPases, the outer membrane-anchored proteins mitofusin 1 (Mfn1),³ and mitofusin 2 (Mfn2) along with the intermembrane space GTPase, Opa1 (7, 8). Although the functions of Mfn2 overlap with Mfn1 in the process of mitochondrial fusion (9), there are clear distinctions between these two GTPases. Perhaps most informative of their distinct function is their biochemical difference in nucleotide binding and hydrolysis properties, where Mfn1 has a faster GTPase hydrolysis rate and higher affinity for nucleotide relative to Mfn2 (10, 11). In addition, Mfn1, but not Mfn2, has been shown to genetically interact with Opa1 (12), a member of the dynamin family of mechanoenzymes. This relationship with Opa1 would suggest that Mfn1 plays a central role with Opa1 in the fusion process. In an *in vitro* mitochondrial docking assay, expression of Mfn1 significantly enhanced the tethering reaction, whereas Mfn2 resulted in tethering with low efficiency, suggesting a secondary role for Mfn2 in docking (10). Recently, compelling evidence has emerged supporting additional roles for Mfn2 that goes beyond the regulation of the mitochondrial fusion. First, Mfn2 is colocalized in punctate with Bax and Drp1 at sites of future fission (13). This suggests that Mfn2 activity may affect mitochondrial recruitment of Bax or Drp1 during cell death. Second, Mfn2, but not Mfn1, can interact directly with Ced9 or Bclxl in HEK293 cells, suggesting a mechanism for cross-talk with anti-apoptotic Bcl family proteins (3). Third, Mfn2, not Mfn1, has been shown to modulate metabolism through function of complex I, IV, and V (14, 15). Fourth, it was also shown that cytosolic Bax plays a specific role in the steady state activity of Mfn2 as a regulator of mitochondrial fusion (16). Most importantly, Mfn2 seems to be critical for the function of the nervous system

^{*} This work was supported by grants from the Canadian Institutes of Health Research (CIHR) and Heart and Stroke Foundation of Canada (HSFC) (to R. S. S.). A. J.-A., E. C. C. C., and A. F. are supported by CIHR studentships. The costs of publication of this article were defrayed in part by the payment of page charges. This article must therefore be hereby marked "advertisement" in accordance with 18 U.S.C. Section 1734 solely to indicate this fact.

^[S] The on-line version of this article (available at <http://www.jbc.org>) contains supplemental Fig. S1 and Movies 1–5.

¹ To whom correspondence may be addressed: University of Ottawa Heart Inst., University of Ottawa, 40 Ruskin St., Rm. H445A, Ottawa K1Y 4W7, Canada. E-mail: hmcbride@ottawaheart.ca.

² To whom correspondence may be addressed: Ottawa Health Research Inst., University of Ottawa, 451 Smyth Rd., Rm. 2452, Ottawa, Ontario K1H 8M5, Canada. E-mail: rslack@uottawa.ca.

³ The abbreviations used are: Mfn, mitofusin; CGN, cerebellar granule neurons; MOI, multiplicity of infection; ROS, reactive oxygen species; PBS, phosphate-buffered saline; MTT, 3-(4,5-dimethylthiazol-2-yl)-2,5-diphenyltetrazolium bromide; GFP, green fluorescent protein; OCT, ornithine carbamyl transferase; YFP, yellow fluorescent protein; DIV, days *in vitro*.

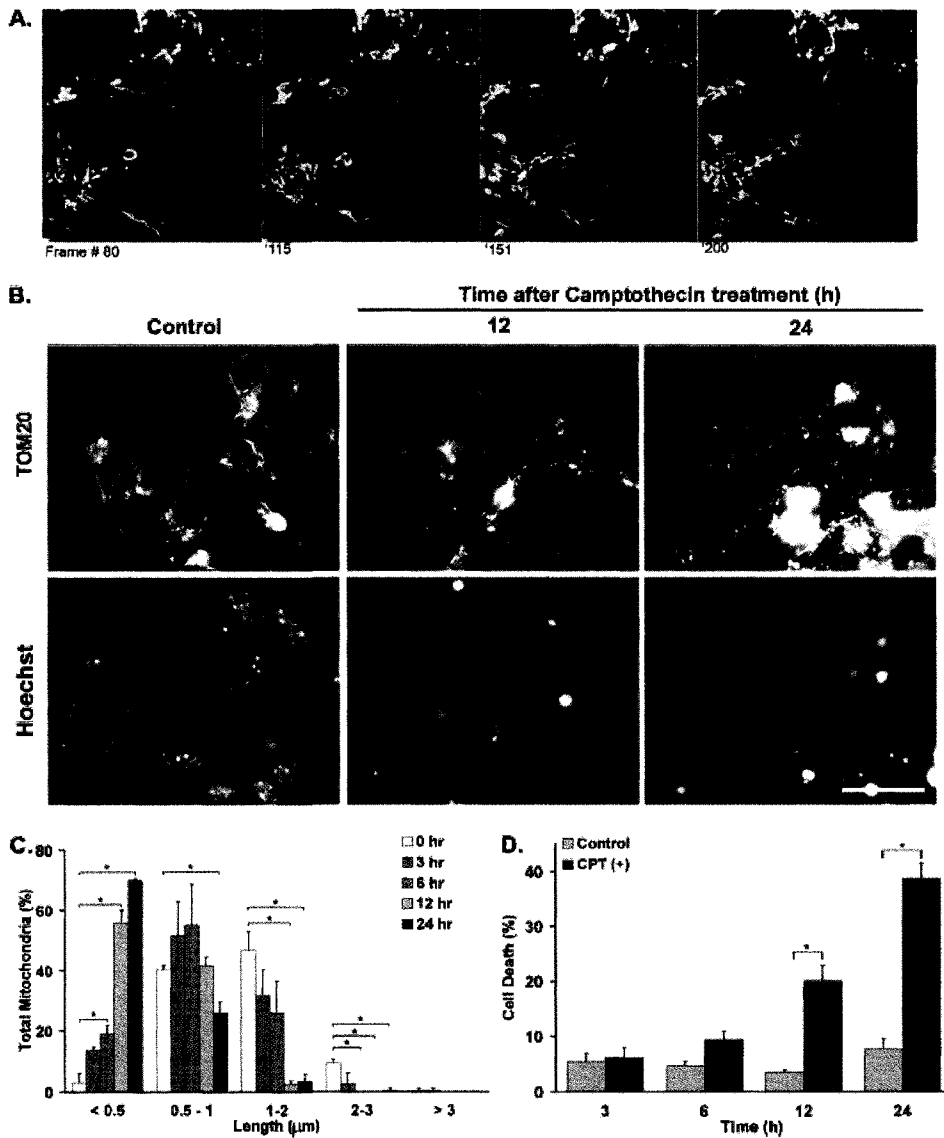


FIGURE 1. Mitochondrial fragmentation following DNA damage-induced cell death. *A*, CGNs expressing YFP-tagged OCT-YFP were treated with $10\ \mu\text{M}$ camptothecin. Individual mitochondria were tracked by exciting the YFP with the 515-nm line of a multiple line Ar laser. 200 frames (15 s per frame) were taken using confocal microscopy. (This figure represents still images for supplemental movie 1.) The boxed area indicates fragmentation of a swollen mitochondrion. *B*, CGNs were treated with $10\ \mu\text{M}$ camptothecin at 2 DIV. Neurons were fixed and stained with antibody directed against Tom20 and nuclei stained with Hoechst at indicated time points following treatment. The panel shows representative images of mitochondria stained for Tom20 at 0, 12, and 24 h. Hoechst images for nuclei corresponding to each field are presented. *C*, mitochondrial length was assessed at indicated time points following camptothecin treatment, and measurements were binned according to length. The length is classified based on the frequency at different lengths (less than $0.5\ \mu\text{m}$, $0.5\text{--}1$, $1\text{--}2$, and greater than $3\ \mu\text{m}$). *D*, cell death was assessed at the indicated times by nuclear morphology revealed by Hoechst staining. Bar, $30\ \mu\text{m}$. *, $p < 0.05$.

as point mutations in this molecule have been associated with Charcot Marie Tooth neuropathy type 2A (17). Understanding the role of mitofusin 2 in response to acute neuronal injury is therefore crucial for development of novel therapeutic strategies. Because of the importance of Mfn2 in fusion as well as its importance in the nervous system, we therefore asked whether Mfn2 is involved in the regulation of acute injury using primary cerebellar granule neurons. To examine the role of this GTPase in apoptosis signaling, we have constructed adenoviral vectors carrying both wild type and a hydrolysis-deficient mutant of Mfn2, Mfn2_{RasG12V} (18), and Mfn2_{RasG12V} lentivirus for long

term transduction of these neurons. We asked: (a) whether Mfn2 could protect neurons against different mechanisms of injury and (b) whether this protection is by promoting mitochondrial fusion and shifting the morphological equilibrium or through an additional role for Mfn2 that is distinct from the stimulation of mitochondrial fusion.

The results of our studies demonstrate that mitochondrial fragmentation in response to neuronal injury is dramatic and occurs as an early event. Furthermore, we show that Mfn2 signals mitochondrial fusion in neurons and protects against neuronal death. Our results indicate that the increased activation of mitochondrial fusion by expression of Mfn2 or Mfn2_{RasG12V} cause an equally dramatic increase in the mitochondrial lengths to greater than $30\ \mu\text{m}$ extending throughout the processes. Interestingly, while both wild type Mfn2 and Mfn2_{RasG12V} result in the equal lengthening of mitochondria, the Mfn2_{RasG12V} is most protective against neuronal cell death and release of pro-apoptotic factors. These findings emphasize a signaling role for Mfn2 that goes beyond its role in the regulation of mitochondrial fusion.

EXPERIMENTAL PROCEDURES

Primary Neuronal Cultures and Adenoviral Construction—Cerebellar granule neurons (CGNs) were cultured from CD1 mice at postnatal day 7 or 8 as described previously (19). Recombinant adenoviral vectors carrying ornithine carbonyl transferase (OCT), human mitofusin 2 (Mfn2), or its active mutant,

Mfn2_{RasG12V}, expression cassettes were prepared using AdEasy system, as described previously (20). Mfn2 antisense adenovirus was a kind gift from Dr. Antonio Zorzano (14). Cells were infected at the time of plating with different multiplicity of infection (MOI) ranging from 25 to 150. 50 MOI was chosen based on the high efficiency and low toxicity. To measure the toxicity and efficiency of infection, Live/Dead assay (Molecular Probes, Eugene, OR) was performed 2 days postinfection. Three random fields were chosen for each group, and the images of cells in these fields were taken with a fluorescence microscope using the appropriate filters. Phase contrast micro-

Role of Mitofusin 2 in Neuronal Injury

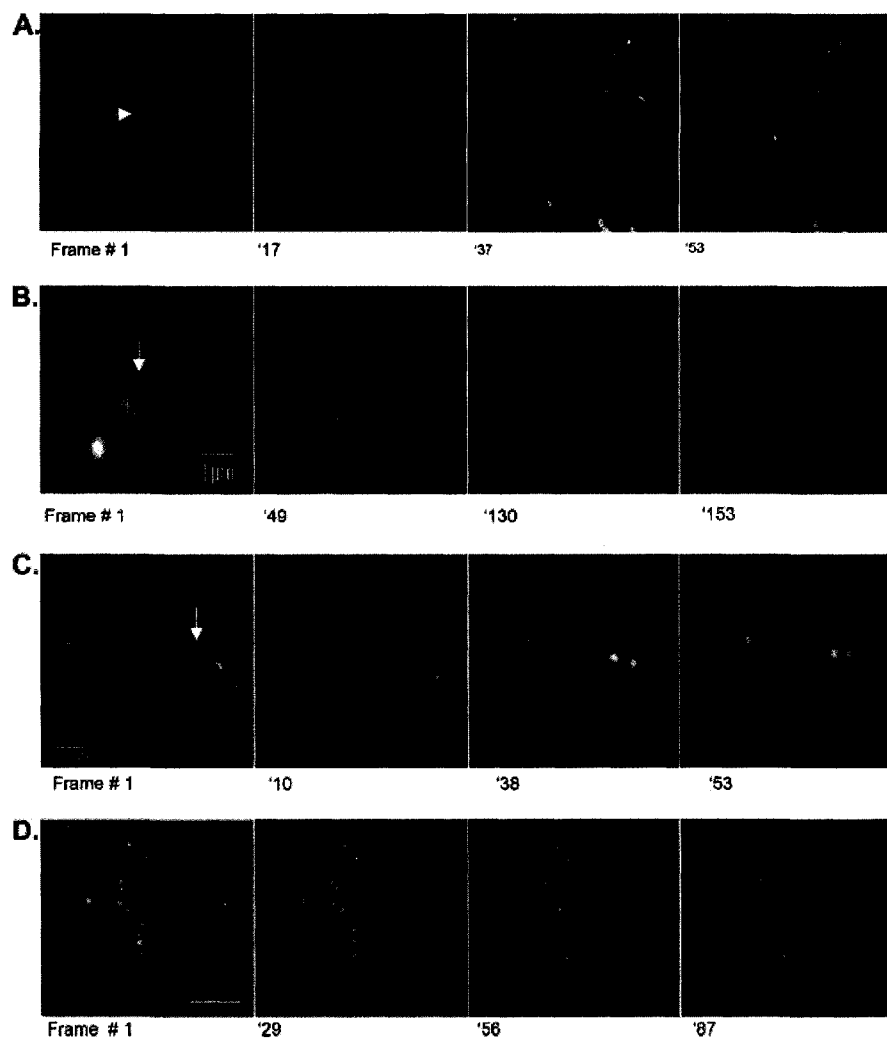


FIGURE 2. Mitochondrial dynamics following oxidative stress. CGNs expressing OCT-YFP were treated with $100\ \mu\text{M}$ H_2O_2 for 5 min after which the media was switched to conditioned media (panels A, B, and D). Neurons were treated with $100\ \mu\text{M}$ H_2O_2 for 20 min without switching to conditioned media (panel C). Individual mitochondria were tracked by exciting the YFP at 515 nm. A, 200 frames (15 s per frame) were taken at 1 h following treatment. Confocal images represent still figures for supplemental movie 2. B, 200 frames (15 s per frame) were taken following treatment (supplemental movie 3). C, 60 frames were taken following 20 min of treatment with $100\ \mu\text{M}$ of H_2O_2 . Confocal images represent still figures for supplemental movie 4. D, 100 frames were taken following treatment. Representative images are still figures corresponding to supplemental movie 5. $n > 10$.

graphs of the same fields were taken with light microscopy, and the number of cells infected was compared with the total number of cells in the field. To measure toxicity the number of infected dead cells was compared with the total number of infected cells in the field.

Cell Viability Assays—Cell death was measured by condensed nuclear morphology revealed by Hoechst staining. MTT or Live/Dead assay (supplemental Fig. S1) was used to confirm the results of Hoechst staining, as described previously (21). In each replicate, three to five different fields were randomly chosen per treatment group. Representative samples were photographed using a Zeiss Axiovert 100 (Oberkochen, Germany) fluorescence microscope equipped with a QiCam Digital camera (QImaging Corporation, Burnaby, Canada) and Northern Eclipse software (Empix Imaging Inc. Mississauga, ON, Canada). The total number of cells in each field was counted. Cell death was expressed as a percentage of total cells.

DNA Damage, K^+ Deprivation, and Reactive Oxygen Species (ROS)-induced Cell Death—To model *in vitro* DNA damage-induced cell death, CGNs were treated with $10\ \mu\text{M}$ camptothecin (Sigma-Aldrich) following 2 days *in vitro* (2 DIV). Hydrogen peroxide (H_2O_2) was used to model ROS-induced cell death. CGNs were treated with H_2O_2 following 2 DIV for 5 min after which the medium was replaced with conditioned medium taken from the parallel cultures with no treatment. Because of unstable nature of H_2O_2 , the concentration used in each replicate was optimized prior to each treatment and $75\text{--}100\ \mu\text{M}$ was used to induce $50\text{--}70\%$ cell death following 24 h of treatment. To model K^+ deprivation-induced cell death, neurons were transduced at the time of plating with purified lentiviruses 1.5 MOI and after 7 days *in vitro* the media containing $25\ \text{mM}$ K^+ was changed to a low potassium media of $5\ \text{mM}$.

Cytochrome c Release—Neurons were fixed and stained with cytochrome c and/or Tom20 and Hoechst following treatment with hydrogen peroxide or camptothecin. For each replicate, a total of 100 neurons were counted from 3–5 different fields. In each case, a Z stack of the field was taken for analysis using a Zeiss 510 meta confocal microscope. A diffuse cytochrome c staining or complete lack of staining was identified as release.

Time Lapse Microscopy—CGNs were seeded on 4-well plates (Nalgen Nunc International, Rochester, NY) with attached glass coverslips coated with poly D-lysine (VWR International), and infected with the YFP-tagged ornithine carbamyl transferase (OCT-YFP), a mitochondrial matrix protein, at the time of seeding. Following each treatment, neurons were imaged to track individual mitochondria in real time. The coverslips were mounted in a temperature-controlled chamber ($37\ ^\circ\text{C}$) in regular growth media supplemented with $20\ \text{mM}$ HEPES (pH 7.4), and visualized with an Olympus $\times 100$ oil immersion objective, numerical aperture 1.4, on an Olympus IX80 Laser scanning confocal microscope operated by FV1000 software v1.4a. The YFP was excited with 515-nm line of a multiple line Ar laser, the Mitofluor Red was excited with the 543-nm line of He/Ne green laser, and the Alexa 647 was excited with the 633-nm line of He/Ne red laser. All images shown demonstrate cells that are representative of

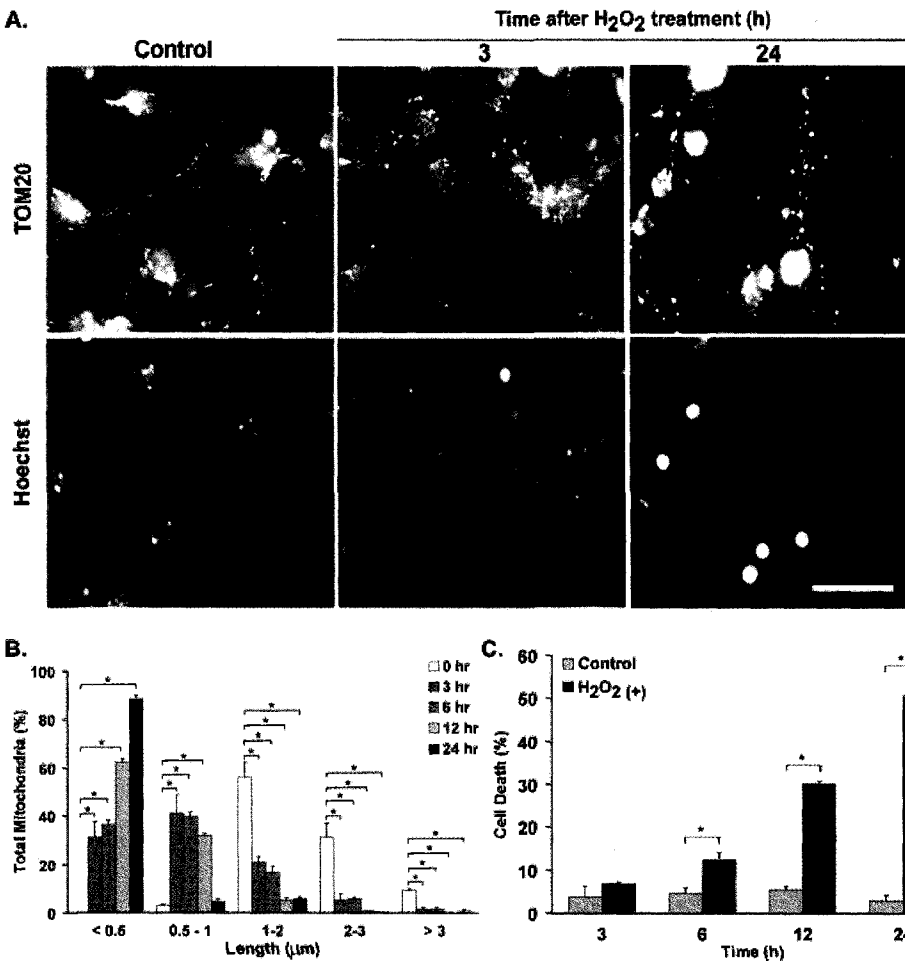


FIGURE 3. Mitochondrial fragmentation following oxidative stress. CGNs were treated with $100\ \mu\text{M}$ H_2O_2 at 2 DIV. Neurons were stained as described in the legend to Fig. 1. A, panel shows representative images of mitochondria at each time point stained for Tom20 and Hoechst. B, mitochondrial length was assessed at the indicated time points following H_2O_2 treatment and measurements were binned according to length. The length is classified based on the frequency at different lengths (less than 0.5 , 0.5 – 1 , 1 – 2 , and greater than $3\ \mu\text{m}$). C, cell death was assessed at the indicated times by nuclear morphology revealed by Hoechst stain. $n = 3$, $*$, $p < 0.05$; bar, $30\ \mu\text{m}$.

moderate infection efficiencies and that have been obtained from at least three independent experiments.

Immunofluorescence—At each time point, neurons were fixed for 30 min with ice-cold 4% paraformaldehyde in $1\times$ phosphate-buffered saline ($1\times$ PBS) and then rinsed twice with $1\times$ PBS. Cells were permeabilized with $300\ \mu\text{l}$ of ice-cold 0.4% Triton-X in $1\times$ PBS for 10 min. Cells were stained with the primary antibodies in 10% normal goat serum-0.4% Triton X/PBS for 1 h. The cells were washed 3×5 min with ice-cold $1\times$ PBS. Cells were incubated with the secondary antibodies to either TOM 20 (1:250, a kind gift from Dr. Gordon Shore) (22) or cytochrome *c* (1:250; BD Biosciences, Franklin Lake, NJ) in 10% normal goat serum-0.4% Triton X/PBS for 1 h. The cells were washed for 5 min and stained with Hoechst for 5 min. Following Hoechst staining, neurons were washed with $1\times$ PBS for 3×5 min and mounted. Representative samples were photographed using a Zeiss Axiovert 100 (Oberkochen, Germany) fluorescence microscope equipped with a QiCam Digital camera (QImaging Corporation) and Northern Eclipse software (Empix Imaging Inc.).

Mitochondrial Length Measurement—Whole cell images were acquired by exciting at 549 nm with the CY3 filter (Chroma Technology Corp., Rockingham, VT). Mitochondrial length was measured by tracing the mitochondria using Northern Eclipse software. Mitochondrial length varied remarkably even in control neurons. For comparison purposes mitochondria were classified into different categories with a length ranging from less than $0.5\ \mu\text{m}$, 0.5 – $1\ \mu\text{m}$, 1 – $2\ \mu\text{m}$, 2 – $3\ \mu\text{m}$, and greater than $3\ \mu\text{m}$.

Quantification and Statistical Analysis—For cell death studies, a minimum of 500 cells per field (three fields per replicate) was scored for each treatment at the indicated time points. For mitochondrial length measurements, a minimum of 500 mitochondria for each treatment (per replicate) was scored. The data represent the mean and S.D. from three independent experiments ($n = 3$), where n stands for each independent experiment. p values were obtained using two-way analysis of variance and Tukey post-hoc tests or Student's t test. A p value < 0.05 was considered significant and was indicated on the graphs by an asterisk.

RESULTS

Mitochondrial Fragmentation Occurs Following DNA Damage-induced Neuronal Death

It has been suggested that mitochondria remodel following acute neuronal injury (23). We therefore asked whether mitochondria undergo fragmentation or remodeling following DNA damage-induced neuronal death. The DNA damage model induced by topoisomerase inhibitor, camptothecin, occurs physiologically following stroke or trauma and is believed to contribute to the extensive neuronal loss after acute injury (24). To model *in vitro* DNA damage-induced cell death, primary cerebellar granule neurons (CGNs) were treated with $10\ \mu\text{M}$ camptothecin. This concentration of camptothecin was shown to induce a slow cell death resulting in about 40% neuronal loss by 24 h (Fig. 1D). To track individual mitochondria in real time, we created adenovirus vectors containing the 32 amino acid targeting signal of ornithine carbamyl transferase fused to YFP (OCT-YFP) (25), and infected the CGN cultures at the time of seeding. Mitochondrial dynamics were documented within the first 16 h using fluorescence time lapse microscopy. We quantified the percentage and timing of mitochondrial fragmentation following treatment with camptothecin. CGN cultures were fixed and stained with anti-

Role of Mitofusin 2 in Neuronal Injury

TOM20, a mitochondrial protein import receptor (22) and Hoechst to identify cell nuclei at different time points following treatment (Fig. 1B). Mitochondria in neurons exhibited variable length. The data were therefore binned into different length categories from less than 0.5 to greater than 3 μm . Quantification of mitochondrial lengths showed that immediately following exposure to camptothecin, 96% of mitochondria had a length of greater than 0.5 μm , as in the control neurons (Fig. 1C). Of these 41 \pm 1% ranged within 0.5–1 μm ; 47 \pm 4% had a length of between 1 and 2 μm , and 9.3 \pm 0.9% had a length of 2–3 μm . At 6 h following treatment with camptothecin, 20 \pm 2.5% of the mitochondria were fragmented with a length of less than 0.5 μm . Following 12 h of treatment, however, there was a dramatic change in morphology where 56 \pm 3% of mitochondria exhibited a length of less than 0.5 μm . The fragmentation was maximal by 24 h where 70.2 \pm 0.4% of mitochondria exhibited a length of less than 0.5 μm . Only 3.4 \pm 1.7% of mitochondria had a length of 2–3 μm at 24 h. These results demonstrate that mitochondrial fragmentation is initiated 3–6 h following exposure of neurons to camptothecin and there is a remarkable difference in the mitochondria pool by 12 h.

To confirm whether this change in morphology was because of mitochondrial membrane scission rather than organelle swelling, we performed a video analysis of mitochondria within cells treated with camptothecin. In many videos, mitochondria were observed to clearly divide into much smaller fragments upon 6 h of treatment with camptothecin. Therefore, although we did observe some mitochondrial swelling (Fig. 1A, *box*), we also observed mitochondrial fission (Fig. 1A and supplemental movie 1).

To ask whether mitochondrial fragmentation correlates with the cell death, the rate of cell death was evaluated by counting the percentage of cells exhibiting pyknotic nuclei. Pyknotic nuclei indicative of apoptosis were observed following 12 h of treatment (Fig. 1D). Cell death increased to 20 \pm 3% at 12 h and was maximal at 24 h (39 \pm 2.6%) within the given time frame. Based on these results, we conclude that mitochondrial fragmentation is initiated 6–9 h prior to the degradation of the nucleus following DNA damage-induced cell death.

Mitochondrial Fragmentation Is an Early Event Following Oxidative Stress—In many types of acute neuronal injury such as stroke, a primary cause of death is the exposure to ROS, which initiates a complex signaling cascade (26). We next asked whether mitochondrial fragmentation also occurs following oxidative stress. CGN cultures were infected with OCT-YFP at the time of seeding and treated with H₂O₂ for 5 min after which the medium was replaced by conditioned media. Time lapse microscopy studies revealed that mitochondria undergo fragmentation within 1 h following treatment (Fig. 2A and supplemental movie 2). Mitochondria were also documented to transition from rod-like to spherical following fragmentation. This kind of mitochondrial remodeling following fission was indeed a common event in this mode of cell death (Fig. 2B and supplemental movie 3). Interestingly exposure of neurons to hydrogen peroxide for longer than 5 min resulted directly in mitochondrial remodeling within first 20 min (Fig. 2C and supplemental movie 4). This concentration was toxic to cells as 100% of neurons were dead following first 2 h of treatment. Interestingly,

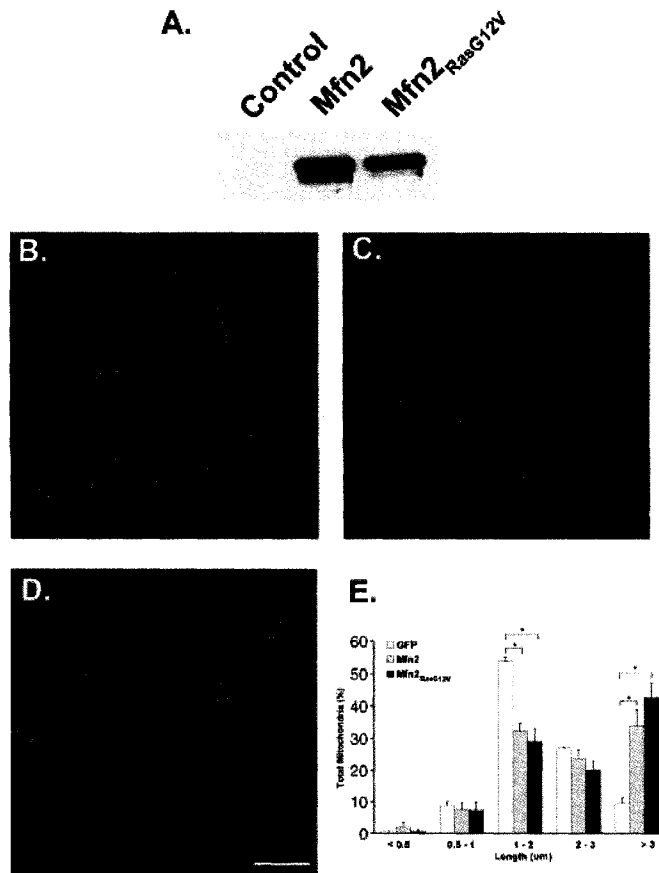


FIGURE 4. Mfn2 expression induces mitochondria fusion in CGNs. CGNs were infected at the time of plating with recombinant adenoviral vectors containing an expression cassette for Mfn2 or Mfn2_{RasG12V} at 50 MOI. Whole cell lysates were analyzed in parallel with the control (no virus) by Western blot using an antibody against FP (A). CGNs were infected at the time of plating with recombinant adenoviral vectors containing an expression cassette for Mfn2 (C) or Mfn2_{RasG12V} (D) or GFP control (B) at 50 MOI. E, neurons expressing the indicated constructs were fixed and stained with TOM 20 to assess changes in mitochondrial morphology following increased expression of Mfn2 and Mfn2_{RasG12V}. Mitochondrial length of the indicated group is classified based on the frequency at different lengths (less than 0.5, 0.5–1, 1–2 and greater than 3 μm). $n = 3$; *, $p < 0.05$; mag bar, 20 μm ; cyan, nuclei; green, mitochondria.

unlike treatment with camptothecin where the fragmented mitochondria remained highly motile, the motility of fragmented mitochondria was substantially attenuated upon treatment with hydrogen peroxide (Fig. 2D and supplemental movies 1 and 5). To quantify the timing and percentage fragmentation of mitochondria and its correlation to cell death, mitochondrial and nuclear morphology were evaluated (Fig. 3A). Immediately following exposure to ROS, greater than 94% of mitochondria had a length of greater than 0.5 μm (Fig. 3B). Neurons treated with hydrogen peroxide exhibited signs of mitochondrial fragmentation as early as 3 h where 31 \pm 6% of mitochondria had a length of less than 0.5 μm . Mitochondrial fragmentation continued to increase to 62.3 \pm 1.4% and 88.5 \pm 1.2% at 12 and 24 h, respectively. To ask whether the onset of mitochondrial fragmentation correlates with cell death, apoptosis was examined by Hoechst to detect pyknotic nuclei (Fig. 3C). The results of cell death studies were confirmed using colorimetric MTT survival assay (data not shown). At 12 h following treatment, 30 \pm 2.5% of neurons exhibited pyknotic nuclei

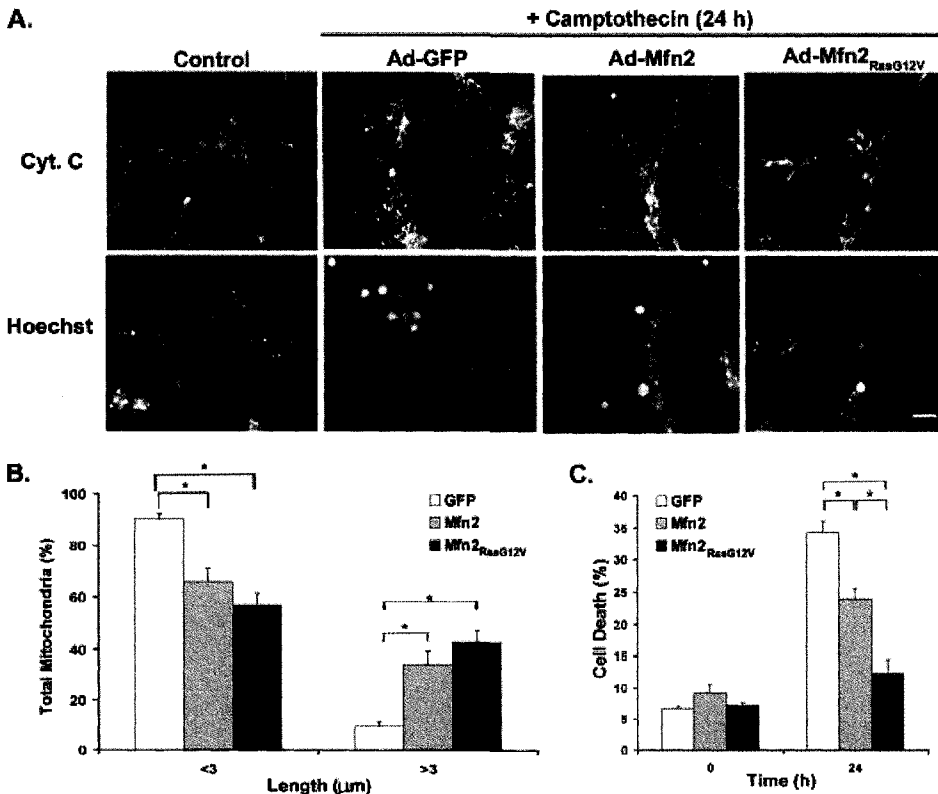


FIGURE 5. Increased activity of Mfn2 maintains the mitochondrial structure and protects cells against DNA damage. CGNs were infected at the time of plating with Ad-Mfn2, Mfn2_{RasG12V}, or GFP control at 50 MOI and were treated with camptothecin (10 μ M). At indicated time points, cells were fixed, and mitochondria were stained with an antibody against cytochrome c. Nuclei were stained with Hoechst. *A*, panel contains representative fields of mitochondrial structure and nuclear morphology 24 h following treatment with camptothecin. *B*, mitochondrial length as determined at 24 h. The length is classified as described previously. *C*, cell death was assessed at 24 h following treatment by nuclear morphology revealed by Hoechst stain. $n = 3$; *, $p < 0.05$; bar, 20 μ m.

whereas cell death was maximal by 24 h when 50 \pm 2% of neurons exhibited pyknotic nuclei. These results show that mitochondrial fragmentation was detected 3 h after treatment and 9 h before the apoptotic nuclei were considerably detected. These findings suggest that mitochondrial fragmentation may serve as an early apoptotic signaling event in this mode of injury.

Together, our results demonstrate that mitochondrial fragmentation is an early common event following acute injury in CGNs. We therefore asked whether preventing the fragmentation of the mitochondria by activation of the mitochondrial fusion machinery could prevent cell death induced by DNA damage and oxidative stress.

Increased Activation of Mfn2 Blocks Mitochondrial Fragmentation and Protects Neurons against Acute Injury—To examine whether activating mitochondrial fusion could protect neurons against cell death, we created adenovirus vectors containing the CFP-tagged wild-type Mfn2 and the hydrolysis-deficient, constitutively active mutant Mfn2_{RasG12V} (18). Primary neurons were infected 48 h prior to exposure to oxidative stress or DNA damage. We first examined whether these proteins could affect the mitochondrial morphology in untreated neurons. Cells were infected in parallel with adenovirus vectors carrying Mfn2, Mfn2_{RasG12V}, or GFP control, and the mitochondrial morphology was evaluated 48-h later (Fig. 4). To confirm pro-

tein expression a Western blot analysis was performed with neurons infected with Mfn2 or Mfn2_{RasG12V} (Fig. 4A). In unchallenged neurons (Fig. 4, *B* and *E*) the majority of mitochondria had an average length between 1 and 2 μ m (53.8 \pm 1.3%); however, increased expression of Mfn2:CFP (Fig. 4C) or Mfn2_{RasG12V}:CFP (Fig. 4D) resulted in a significant increase in the length of the mitochondria. The majority of mitochondria were greater than 3 μ m as a result of increased levels of Mfn2 (33.97 \pm 5%) and Mfn2_{RasG12V}:CFP (42.9 \pm 4.2%) expression (Fig. 4E). These results demonstrate that enhanced activation of Mfn2 results in increased mitochondrial length.

We next asked whether activation of Mfn2 could prevent mitochondrial fragmentation and ultimately protect neurons against death induced by neuronal injury. To test whether activation of Mfn2 could protect neurons against DNA damage, parallel cultures were exposed to 10 μ M camptothecin. The mitochondrial morphology and apoptosis were evaluated following 24 h (Fig. 5A). Mitochondrial fragmentation was dramatically inhibited

with both Mfn2:CFP or Mfn2_{RasG12V}:CFP expression (Fig. 5A). Following 24 h of treatment, GFP-infected neurons showed only 9.6 \pm 1.1% of mitochondria measuring greater than 3 μ m, whereas the expression of Mfn2:CFP and Mfn2_{RasG12V}:CFP resulted in 33.4 \pm 3.2% and 42.17 \pm 7% of mitochondria being greater than 3 μ m. Interestingly, the group of mitochondria measuring greater than 3 μ m had a widely varied length distribution, with some single mitochondria spanning long projections and measuring greater than 30 μ m. These results reveal that expression of Mfn2 or constitutive activation by expression of Mfn2_{RasG12V} could equally prevent the breakdown of the mitochondria typically seen following DNA damage. Most importantly, increasing the levels of Mfn2 resulted in increased protection against cell death induced by DNA damage (Fig. 5C). Following 24 h of treatment, 34 \pm 1.6% of neurons exhibited pyknotic nuclei in the GFP control, and this was reduced to 23.9 \pm 1.6% in the Mfn2 cultures. Increased activation of Mfn2 through delivery of Mfn2_{RasG12V}:CFP was significantly more protective than the wild type counterpart as it reduced cell death to 12.3 \pm 2.1% (Fig. 5C). These results demonstrate that whereas Mfn2 and Mfn2_{RasG12V} result in equal fusion of mitochondria, the GTP bound form of Mfn2_{RasG12V} shows a 2-fold increase in protection of these neurons against DNA damage.

Role of Mitofusin 2 in Neuronal Injury

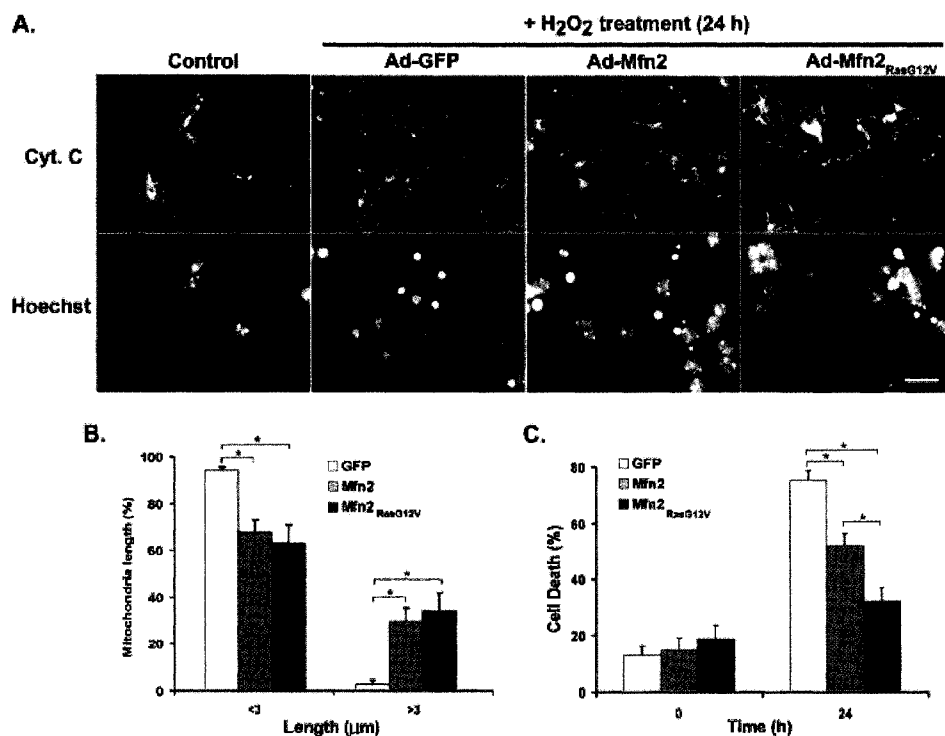


FIGURE 6. Increased activity of Mfn2 maintains mitochondrial structure and protects cells against ROS-mediated injury. CGNs were infected as described in the legend to Fig. 5, and the neurons were treated with H_2O_2 ($75 \mu\text{M}$). At indicated time points, cells were fixed and stained with Hoechst for nuclei and cytochrome *c* antibody for mitochondria. *A*, panel shows representative fields for the structure of mitochondria and corresponding Hoechst at 24 h. *B*, mitochondrial length as determined at 24 h. *C*, cell death was assessed at 24 h following treatment by nuclear morphology revealed by Hoechst stain. $n = 3$; *, $p < 0.05$; bar, $20 \mu\text{m}$.

We then examined whether activation of Mfn2 could protect neurons against injury induced by ROS. Neuronal cultures were infected in parallel with adenovirus-expressing GFP control, Mfn2:CFP, and Mfn2_{RasG12V}:CFP. After 48 h, cells were exposed to H_2O_2 , and mitochondrial morphology and cell death were evaluated as described above. Increased expression of Mfn2:CFP or enhanced activation of Mfn2 by delivery of Mfn2_{RasG12V}:CFP protected neurons against the ROS-induced fragmentation, and resulted in significantly increased mitochondrial lengths (Fig. 6*A*). At 24 h following treatment with hydrogen peroxide, only $3.09 \pm 1.81\%$ of mitochondria had a length of greater than $3 \mu\text{m}$ in cells expressing the GFP control (Fig. 6*B*). This number increased to $30.65 \pm 5.7\%$ and $35.05 \pm 7.9\%$ in the parallel cultures expressing Mfn2:CFP and Mfn2_{RasG12V}:CFP, respectively (Fig. 6*B*). More importantly, whereas expression of wild type Mfn2 resulted in an increased survival with an intermediate $47.8 \pm 3.2\%$ of cells remaining alive, Mfn2_{RasG12V} led to a dramatic 2–3-fold increase in survival, with $68 \pm 4.77\%$ of cells expressing Mfn2_{RasG12V}:CFP remaining viable relative to only $24.59 \pm 1.62\%$ in GFP-expressing controls (Fig. 6*C*).

These data demonstrate that increased levels of Mfn2 prevents the breakdown of the mitochondria in response to injury and maintains the mitochondrial integrity in neurons. Most importantly, stabilization of the GTP-bound form of Mfn2 provides additional protection against death induced by ROS and DNA damage. These results highlight a novel therapeutic target to maintain neuronal survival after acute injury.

*Mfn2 Protects Neurons against Injury by Attenuating Cytochrome *c* Release*—Cytochrome *c* protein, a critical component of the electron transport chain, is normally localized to the mitochondria intermembrane space where it is sequestered within the cristae. Permeabilization of the outer mitochondria membrane results in partial release of the accessible cytochrome *c* into the cytosol; however the release of the majority of mitochondrial cytochrome *c* pool demands structural remodeling of mitochondria cristae (27, 28). We therefore asked whether mitofusin 2 regulates release of cytochrome *c* following different cell death stimuli. 24 h following treatment of the neurons with camptothecin, the neurons were fixed and stained with an antibody against cytochrome *c*, Tom 20, and/or Hoechst. $61.85 \pm 1.31\%$ of neurons had their cytochrome *c* released from the mitochondria in the LacZ control group. The cytochrome *c* release was decreased to $43.29 \pm 4.6\%$ in the wild type mitofusin group and to $22.32 \pm 1.77\%$ in

the Mfn2_{RasG12V} group (Fig. 7*E*). Similarly, following treatment with hydrogen peroxide, Mfn2 and Mfn2_{RasG12V} attenuated release of cytochrome *c* to $47.8 \pm 2.21\%$ and $26.42 \pm 0.98\%$, respectively when compared with control at $84.6 \pm 12.7\%$ (Fig. 7*F*). Our data not only indicate that activation of mitofusin 2 results in attenuation of the cytochrome *c* release following both DNA damage and ROS, but it further supports the distinction in protective response between wild type mitofusin 2 and the activated Mfn2_{RasG12V} mutant. These findings also have identified Mfn2:GTP as an inhibitor of cell death upstream of cytochrome *c* release, which positions the function of Mfn2 within the apoptotic cascade in primary neuronal models of cell death.

Transduction of Neurons by a Mfn2_{RasG12V} Lentivirus Protects Neurons against Potassium Deprivation-induced Apoptosis—Cell excitability is a critical determinant of neuronal survival during brain development (29). K^+ channels set both the resting membrane potential and the duration of the action potential. Opening of these channels can influence neuronal death or neuronal survival (30). Low K^+ exposure of granule neurons initiates a complex set of proapoptotic, metabolic, and signal transduction mechanisms that include up-regulation of c-Jun target genes and inhibition of glycolysis (31). Also, it has been recently demonstrated that upon K^+ deprivation, CGN exhibit an immediate reduction in mitochondrial respiration, a decrease in ATP turnover which correlates with decreased calcium concentration (32) and depletion of NF κ B (33). Because cerebellar granule neurons yield a classic

Role of Mitofusin 2 in Neuronal Injury

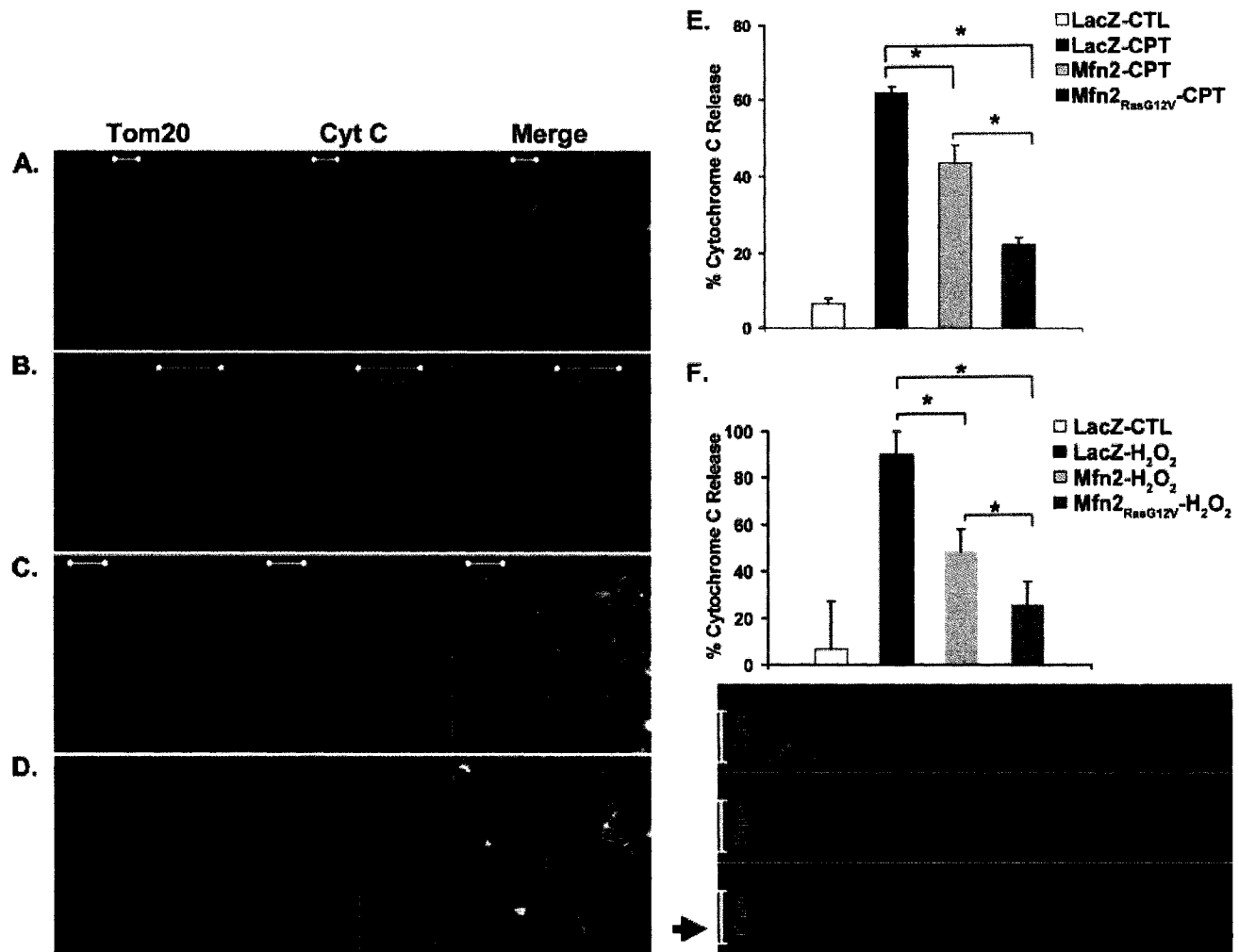


FIGURE 7. Mfn2 attenuates cytochrome c release following DNA damage and ROS-mediated injury. CGNs were infected as described and treated with either H₂O₂ (75 μ M) or camptothecin (10 μ M). The cells were fixed and stained with cytochrome c and Tom 20 following 24 h of treatment with camptothecin or hydrogen peroxide. Z stack sections of different fields were taken for each replicate. *A*, colocalization of Tom 20 and cytochrome c in the control neurons. *B*, representative field demonstrating release of cytochrome c from mitochondria following treatment with camptothecin and *C*, following treatment with hydrogen peroxide. *D*, cytochrome c and Tom 20 colocalization in the neurons infected with Mfn2_{RasG12V} following treatment with hydrogen peroxide. *E*, percentage of cytochrome c release following camptothecin treatment in CTL, Mfn2, and Mfn2_{RasG12V} group. *F*, quantification of cytochrome c release following treatment with hydrogen peroxide in CTL, Mfn2, and Mfn2_{RasG12V} group. $n = 3$; $p < 0.05$.

model for depolarization-induced apoptosis, we asked whether mitofusin 2 protects against this mode of cell death. We constructed a lentivirus for the Mfn2_{RasG12V} to transduce CGN. The media containing 25 mM K⁺ was changed to the media of 5 mM K⁺ following 7 DIV and following 24 h in the low potassium media, the percentage of cell death was evaluated using the "Live/dead" assay. The percentage cell death declined from 74.06% in the control group to 49.1% in the Mfn2_{RasG12V} group. Following correction for the basal cell death (15% in CTL to 22% in Mfn2_{RasG12V} group) Mfn2_{RasG12V} counts for a greater than 50% protection against K⁺ deprivation-mediated apoptosis (Fig. 8).

Mfn2 Loss of Function Induces Cell Death in Cerebellar Granule Neurons—To further support the antiapoptotic role of mitofusin 2 in primary neuronal culture, we induced Mfn repression by antisense adenoviral expression, previously described (14) (Fig. 9). Following 48 h of infection of CGN (MOI 50), neuronal survival was assessed by live/dead assay. Our results show that Mfn2-knocked-down neurons exhibit a

significant 33 \pm 3.0%, cell death, when compared with LacZ-CTL at 9 \pm 0.9% in the primary neurons even in the absence of any cell death stimuli.

DISCUSSION

The results of our studies support a number of conclusions: first we show that mitochondrial fragmentation occurs as an early event in response to injury in cerebellar granule neurons. The extent of mitochondrial fragmentation, however, is variable and depends on the mode of neuronal injury and the severity of the death stimuli. Second, expression of Mfn2 prevents mitochondrial fragmentation in response to oxidative stress and DNA damage-induced neuronal death. Third, we show that in addition to stimulating the fusion machinery, Mfn2 protects neurons against different modes of neuronal injury including DNA damage, oxidative stress, and K⁺ deprivation-induced apoptosis. Most importantly, we demonstrate that while the wild type Mfn2 and the constitutively activated mutant Mfn2_{RasG12V} function equally to promote fusion and

Role of Mitofusin 2 in Neuronal Injury

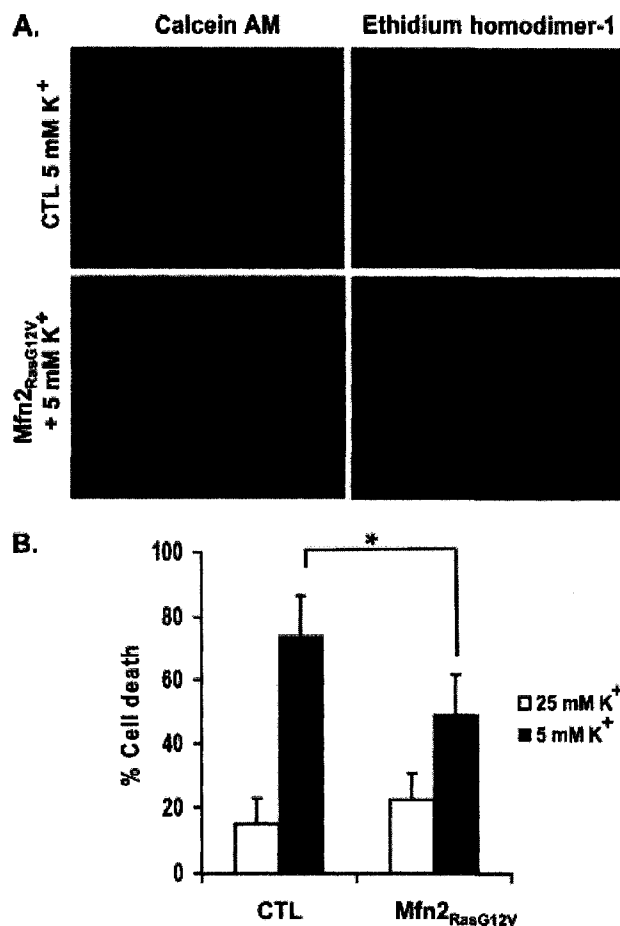


FIGURE 8. Transduction of neurons by Mfn2_{RasG12V} protects against K⁺ deprivation-mediated cell death. CGNs were transduced with Mfn2_{RasG12V} concentrated lentivirus at the time of seeding (1.5 MOI). Following 7 days *in vitro* the media with 25 mM K⁺ was completely switched to the media containing 5 mM K⁺. At 24 h, the rate of cell death was assessed with the live/dead assay. *A*, CTL at 5 mM K⁺ (top panel) and Mfn2_{RasG12V} at 5 mM K⁺ (lower panel); *B*, assessment of cell death by live/dead assay following 24 h of K deprivation. *n* = 3; *, *p* < 0.05.

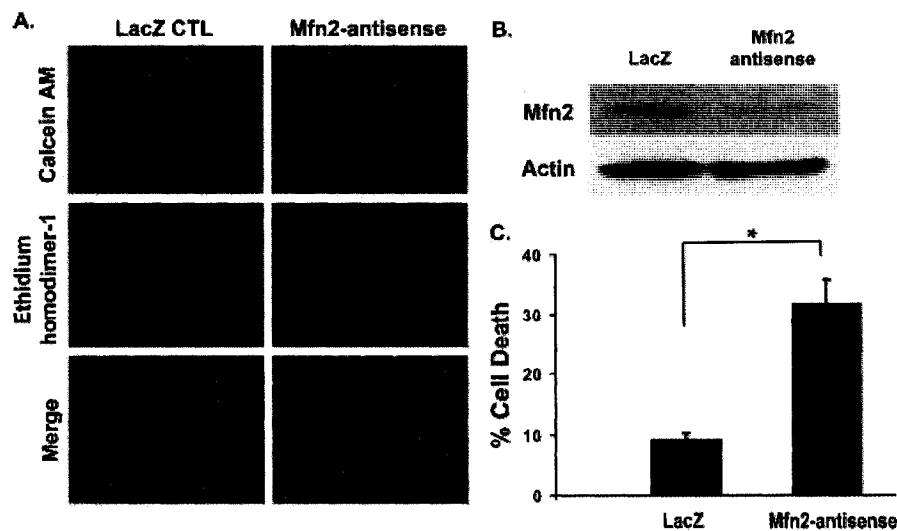


FIGURE 9. Mfn2 loss of function induces cell death in the absence of any cell death stimuli. CGN were infected with an Mfn2-antisense adenovirus at the time of plating at 50 MOI. Following 48 h, neuronal survival was evaluated by live/dead assay. *A*, live/dead assay to show representative fields of Mfn2-antisense and LacZ CTL group at 48 h. *B*, Western blot demonstrating repression of Mfn2. *C*, a significant 33% increase in cell death is evident following Mfn2 loss of function compared with CTL (*, *p* < 0.05, *n* = 3).

lengthening of mitochondria, neuronal protection against acute injury is much more effective in the GTPase hydrolysis-deficient Mfn2 mutant *versus* the wild type Mfn2. Furthermore, mitofusin 2 exerts its protective effect at an early stage upstream of cytochrome *c* release. Finally, down-regulation of mitofusin 2 induces cell death in the absence of any apoptotic stimuli. Taken together, these findings implicate an anti-apoptotic role for Mfn2 during death models representative of acute neuronal injury and neuronal development.

Mfn2 has been proposed to function along with its homologue Mfn1 as a direct tethering/fusion component (8, 10). Our results indicate that the increased activation of mitochondrial fusion by expression of Mfn2 or Mfn2_{RasG12V} could cause a dramatic increase in the mitochondrial lengths to greater than 30 μ m. This neuronal response exhibiting a dramatic lengthening of the mitochondria is unlike that previously found in other cell types where the ectopic expression of Mfn2 resulted in mitochondrial fusion within a non-motile perinuclear cluster (18). Neurons may therefore be unique in their ability to respond to these factors and may express a distinct repertoire of proteins that regulate mitochondrial fusion relative to other cell types.

A key question is whether the longer tubular mitochondria are more supportive of survival than the short fragmented mitochondria or alternatively; do molecules involved in the fusion machinery interact with cell death signaling? Previous studies have demonstrated that inducing fusion by overexpression of Mfn1 or a dominant negative mutant of Drp1 protects against nitric oxide-mediated cell death (34). Unlike Mfn1, which interacts with Opal1 to induce fusion, Mfn2 has been associated with apoptotic signaling proteins (16, 18). Interestingly, we show here that expression of both the wild type Mfn2 and the constitutively active mutant, Mfn2_{RasG12V}, had similar effects on mitochondrial lengthening; however, the hydrolysis-deficient mutant exhibited a more profound protection against cell death. These distinct biological responses suggest that the

protection from death may not be due only to the increased fusion because both the wild type and mutant Mfn2 result in similar increases in mitochondrial length. Instead, the data suggest that the nucleotide state of Mfn2 may regulate other interactions on the mitochondrial membrane that are critical for the cell death. Our data supporting an additional role for Mfn2 beyond the activation of fusion is consistent with recent findings that demonstrate interactions with the Bcl family proteins. First Mfn2 is colocalized in punctate with Bax and Drp1 at sites of future fission and affects mitochondrial recruitment of Bax or Drp1 during cell death, indicating a spatial relationship between fusion and fission during cell death (13). Second, it was

shown that cytosolic Bax plays a specific role in the steady state activity of Mfn2 as a regulator of mitochondrial fusion (16). In that study, the mitochondria within the Bax/Bak double knock-out (DKO) cells demonstrated a reduced rate of mitochondrial fusion. Mfn2 is normally found in a punctate pattern (18); however, in Bax/Bak DKO cells, the protein circumscribed the outer membrane (16). The introduction of Bax into the DKO cells resulted in a stable shift of Mfn2 within the outer mitochondrial membrane into foci, which rescued the rates of fusion. Interestingly, the GTP-bound form of Mfn2 did not respond to Bax/Bak expression and retained its highly mobile, even distribution along the outer membrane regardless of Bax/Bak expression levels (16). Given that this mutant was not affected by Bax/Bak expression, it is possible that Mfn2^{RasG12V} is also resistant to Bax/Bak-induced changes on the membrane during apoptotic stimuli. This resistance of Mfn2^{RasG12V} to assemble into Bax-dependent foci may interfere with the efficient assembly of proapoptotic complexes required for the progression of cell death. This would at least partially explain the increased protectivity of the activated mutant to multiple Bax-dependent apoptotic stimuli that we have observed in primary neurons. Finally, Mfn2 can interact directly with Ced9 or BclXI in HEK293 cells further suggesting a mechanism for protective cross-talk with antiapoptotic Bcl family proteins (3). Because Mfn2 protein levels have not yet been shown to be reduced during apoptosis, the nucleotide state of Mfn2 could be required to mediate cross talk with the apoptotic machinery. We envision a model whereby the GTP-bound form of Mfn2 may interact with the Bcl-2 family of proteins, remaining circumscribed along the outer membrane, functioning in a protective manner and protect against cell death. In contrast, the GDP-bound form would be susceptible to modulation by Bax to allow foci formation and assembly of the death machinery on the outer membrane. Future studies will be required to determine how this activity is regulated in the context of the apoptosis signaling cascade.

Finally, there is growing evidence to support the idea that the machineries that govern mitochondrial fusion are linked to the metabolic processes within the organelle. For example, Mfn2 has been shown to modulate metabolism through function of complex I, IV, and V (14, 15). Consistent with this idea, down-regulation of fusion proteins (Mfn1 and Mfn2) led to fragmented mitochondria with reduced oxygen consumption and electrochemical potential (35). This suggests that mitochondrial fusion is likely to be a central player in relating mitochondrial dynamics to mitochondrial metabolism, and could also be a mechanism for modulating cell death during neuronal injury.

In conclusion, we show that mitochondria undergo extensive fragmentation in acute neuronal injury and that activating the mitochondrial fusion machinery can protect neurons against injury induced cell death. These results demonstrate the importance of mitochondrial dynamics in acute injuries such as trauma and stroke. Demonstrating that the control of the nucleotide state of Mfn2 can dramatically affect the outcome of cell death suggests that Mfn2 may serve as an accessible therapeutic target for the treatment of these human diseases. Future work to investigate the factors that control the nucleotide state of Mfn2 and to delineate the interaction with the apoptotic machinery should further elucidate these mechanisms.

Role of Mitofusin 2 in Neuronal Injury

Acknowledgments—We thank Dr. Antonio Zorzano (University of Barcelona) for his generous gift of Mfn2-antisense adenoviruses. We also thank Dr. Edward Bampton (Leicester University) and Dr. Jackie Vanderluit for the critical review of this manuscript. The viral vector facility is supported by a grant from the Canadian Stroke Network (to R. S. S. and D. S. P.).

REFERENCES

- Frank, S., Gaume, B., Bergmann-Leitner, E. S., Leitner, W. W., Robert, E. G., Catez, F., Smith, C. L., and Youle, R. J. (2001) *Dev. Cell* **1**, 515–525
- Lee, Y. J., Jeong, S. Y., Karbowski, M., Smith, C. L., and Youle, R. J. (2004) *Mol. Biol. Cell* **15**, 5001–5011
- Delivani, P., Adrain, C., Taylor, R. C., Duriez, P. J., and Martin, S. J. (2006) *Mol. Cell* **21**, 761–773
- Karbowski, M., Arnoult, D., Chen, H., Chan, D. C., Smith, C. L., and Youle, R. J. (2004) *J. Cell Biol.* **164**, 493–499
- Estaquier, J., and Arnoult, D. (2007) *Cell Death Differ.* **14**, 1086–1094
- Parone, P. A., James, D. I., Da Cruz, S., Mattenberger, Y., Donze, O., Barja, F., and Martinou, J. C. (2006) *Mol. Cell Biol.* **26**, 7397–7408
- Shaw, J. M., and Nunnari, J. (2002) *Trends Cell Biol.* **12**, 178–184
- Chen, H., Detmer, S. A., Ewald, A. J., Griffin, E. E., Fraser, S. E., and Chan, D. C. (2003) *J. Cell Biol.* **160**, 189–200
- Detmer, S. A., and Chan, D. C. (2007) *J. Cell Biol.* **176**, 405–414
- Ishihara, N., Eura, Y., and Mihara, K. (2004) *J. Cell Sci.* **117**, 6535–6546
- Eura, Y., Ishihara, N., Yokota, S., and Mihara, K. (2003) *J. Biochem. (Tokyo)* **134**, 333–344
- Cipolat, S., Martins de Brito, O., Dal Zilio, B., and Scorrano, L. (2004) *Proc. Natl. Acad. Sci. U. S. A.* **101**, 15927–15932
- Karbowski, M., Lee, Y. J., Gaume, B., Jeong, S. Y., Frank, S., Nechushtan, A., Santel, A., Fuller, M., Smith, C. L., and Youle, R. J. (2002) *J. Cell Biol.* **159**, 931–938
- Bach, D., Pich, S., Soriano, F. X., Vega, N., Baumgartner, B., Oriola, J., Dugaard, J. R., Lloberas, J., Camps, M., Zierath, J. R., Rabasa-Lhoret, R., Wallberg-Henriksson, H., Laville, M., Palacin, M., Vidal, H., Rivera, F., Brand, M., and Zorzano, A. (2003) *J. Biol. Chem.* **278**, 17190–17197
- Pich, S., Bach, D., Briones, P., Liesa, M., Camps, M., Testar, X., Palacin, M., and Zorzano, A. (2005) *Hum. Mol. Genet.* **14**, 1405–1415
- Karbowski, M., Norris, K. L., Cleland, M. M., Jeong, S. Y., and Youle, R. J. (2006) *Nature* **443**, 658–662
- Zuchner, S., Mersyanova, I. V., Muglia, M., Bissar-Tadmouri, N., Rochelle, J., Dadali, E. L., Zappia, M., Nelis, E., Patitucci, A., Senderek, J., Parman, Y., Evgrafov, O., Jonghe, P. D., Takahashi, Y., Tsuji, S., Pericak-Vance, M. A., Quattrone, A., Battologlu, E., Polyakov, A. V., Timmerman, V., Schroder, J. M., and Vance, J. M. (2004) *Nat. Genet.* **36**, 449–451
- Neuspiel, M., Zunino, R., Gangaraju, S., Rippstein, P., and McBride, H. M. (2005) *J. Biol. Chem.* **280**, 25060–25070
- Fortin, A., Cregan, S. P., MacLaurin, J. G., Kushwaha, N., Hickman, E. S., Thompson, C. S., Hakim, A., Albert, P. R., Cecconi, F., Helin, K., Park, D. S., and Slack, R. S. (2001) *J. Cell Biol.* **155**, 207–216
- He, T. C., Zhou, S., da Costa, L. T., Yu, J., Kinzler, K. W., and Vogelstein, B. (1998) *Proc. Natl. Acad. Sci. U. S. A.* **95**, 2509–2514
- Cregan, S. P., Fortin, A., MacLaurin, J. G., Callaghan, S. M., Cecconi, F., Yu, S. W., Dawson, T. M., Dawson, V. L., Park, D. S., Kroemer, G., and Slack, R. S. (2002) *J. Cell Biol.* **158**, 507–517
- Goping, I. S., Millar, D. G., and Shore, G. C. (1995) *FEBS Lett.* **373**, 45–50
- Rintoul, G. L., Filiano, A. J., Brocard, J. B., Kress, G. J., and Reynolds, I. J. (2003) *J. Neurosci.* **23**, 7881–7888
- McGahan, L., Hakim, A. M., and Robertson, G. S. (1998) *Brain Res. Mol. Brain Res.* **56**, 133–145
- Harder, Z., Zunino, R., and McBride, H. (2004) *Curr. Biol.* **14**, 340–345
- Cole, K., and Perez-Polo, J. R. (2004) *Int. J. Dev. Neurosci.* **22**, 485–496
- Scorrano, L., and Korsmeyer, S. J. (2003) *Biochem. Biophys. Res. Commun.* **304**, 437–444
- Germain, M., Mathai, J. P., McBride, H. M., and Shore, G. C. (2005) *EMBO J.* **24**, 1546–1556
- Yuan, F., Wang, T., Luo, L., Sun, Y., Zhang, L., and Qu, B. (2000) *Chin.*

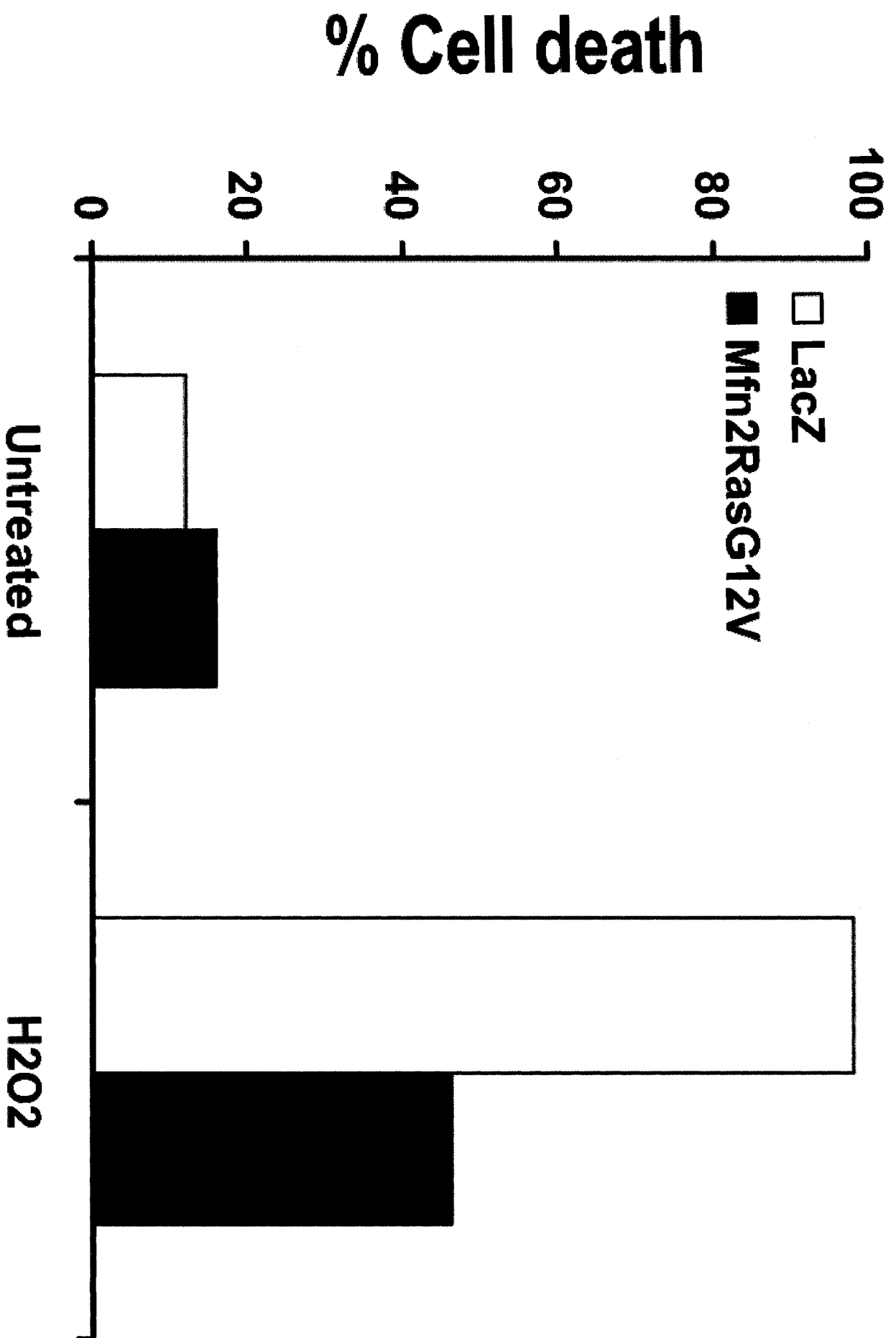
Role of Mitofusin 2 in Neuronal Injury

Med. J. (Engl.) **113**, 728–732

30. Yuan, Q., Xie, Y., So, K. F., and Wu, W. (2003) *Dev. Neurosci.* **25**, 72–78
31. Harris, C., Maroney, A. C., and Johnson, E. M., Jr. (2002) *J. Neurochem.* **83**, 992–1001
32. Jakobsons, M. B., and Nicholls, D. G. (2006) *Cell Death Differ.* **13**, 1595–1610
33. Piccioli, P., Porcile, C., Stanzione, S., Bisaglia, M., Bajetto, A., Bonavia, R., Florio, T., and Schettini, G. (2001) *J. Neurosci. Res.* **66**, 1064–1073
34. Barsoum, M. J., Yuan, H., Gerencser, A. A., Liot, G., Kushnareva, Y., Graber, S., Kovacs, I., Lee, W. D., Waggoner, J., Cui, J., White, A. D., Bossy, B., Martinou, J. C., Youle, R. J., Lipton, S. A., Ellisman, M. H., Perkins, G. A., and Bossy-Wetzell, E. (2006) *EMBO J.* **25**, 3900–3911
35. Chen, H., Chomyn, A., and Chan, D. C. (2005) *J. Biol. Chem.* **280**, 26185–26192



Supplemental figure 1. Confirmation of Hoechst data by Live Dead Assay. Neurons were infected with Mfn2_{RasG12V} or Lac Z adenoviruses and treated with H₂O₂ as described previously. Cell survival was evaluated with Live/Dead assay. (n = 2)



Supplemental Figure 1

Appendix 2

Mitochondria: more than just a powerhouse

Mitochondria: More Than Just a Powerhouse

Review

Heidi M. McBride,¹ Margaret Neuspiel,² and Sylwia Wasiaak²

Pioneering biochemical studies have long forged the concept that the mitochondria are the 'energy powerhouse of the cell'. These studies, combined with the unique evolutionary origin of the mitochondria, led the way to decades of research focusing on the organelle as an essential, yet independent, functional component of the cell. Recently, however, our conceptual view of this isolated organelle has been profoundly altered with the discovery that mitochondrial function within an integrated reticulum that is continually remodeled by both fusion and fission events. The identification of a number of proteins that regulate these activities is beginning to provide mechanistic details of mitochondrial membrane remodeling. However, the broader question remains regarding the underlying purpose of mitochondrial dynamics and the translation of these morphological transitions into altered functional output. One hypothesis has been that mitochondrial respiration and metabolism may be spatially and temporally regulated by the architecture and positioning of the organelle. Recent evidence supports and expands this idea by demonstrating that mitochondria are an integral part of multiple cell signaling cascades. Interestingly, proteins such as GTPases, kinases and phosphatases are involved in bi-directional communication between the mitochondrial reticulum and the rest of the cell. These proteins link mitochondrial function and dynamics to the regulation of metabolism, cell-cycle control, development, antiviral responses and cell death. In this review we will highlight the emerging evidence that provides molecular definition to mitochondria as a central platform in the execution of diverse cellular events.

Introduction

The biochemistry of mitochondria has been the subject of intense investigation over the past 50 years. Within these organelles, sugars and long chain fatty acids are broken down, ADP is recycled back into ATP, steroids and lipids are synthesized, ancient DNA is replicated, transcribed and proteins are translated, along with numerous other reactions that are essential for human life. From a structural perspective, the mitochondrion is unusual since it contains two membranes that separate four distinct compartments, the outer membrane, intermembrane space, inner

membrane and the matrix. The inner membrane is highly folded into cristae, which house the megadalton complexes of the electron transport chain and ATP synthase that control the basic rates of cellular metabolism. For the most part, the biochemistry of this organelle has been investigated in cell-free, isolated systems, leading us to imagine the mitochondrion as a lonely participant in the cell working tirelessly to provide the energy required for life. In the past 10 years, this view has changed as newer approaches have allowed the examination of dynamic mitochondrial function and behavior in response to cellular signals within intact cells. We now understand that mitochondria form a functional reticulum whose steady-state morphology is regulated by dynamic fission, fusion and motility events. Multiple proteins are involved in the remodeling of mitochondrial membranes [1]. Mitochondrial fusion is mediated through the action of at least three GTPases. Mitofusin 1 (Mfn1) and Mitofusin 2 (Mfn2) are integrated within the mitochondrial outer membrane, with their GTPase and coiled-coil domains exposed to the cytosol [2]. Mfn1 and Mfn2 exist as homotypic and heterotypic complexes that can form between adjacent organelles [3,4]. Mechanistically, it has been suggested that the carboxy-terminal coiled coils tether two organelles undergoing fusion, with the GTPase domains probably regulating the fusion reaction (Figure 1) [5–7]. Another dynamin-like GTPase, Opa1, resides in the intermembrane space, where it is associated with the inner membrane [8–10]. Opa1 exists as multiple splice and cleavage variants and its function in mitochondrial fusion has been linked genetically to that of Mfn1 (Figure 1) [11,12]. Mitochondrial fission relies on yet another GTPase from the dynamin family, DRP1 [13–15]. By analogy with dynamins, it has been suggested that DRP1 oligomerizes into ring-like structures around the fission sites, to constrict the organelle in a GTP-dependent manner. In fact, DRP1 forms puncta on the mitochondrial membrane, some of which mark future fission sites. The mechanism of recruitment of DRP1 into active fission complexes remains unclear, however. Also, other proteins have been demonstrated to function in tandem with the GTPases described above, and thus have been directly or indirectly linked to fission and fusion [1]. These proteins are listed in Table S1 (see Supplemental data published with this article online) and some of their roles in mitochondrial membrane remodeling as well as their wider impact on cellular events will be discussed below.

The identification and characterization of the protein machinery that controls mitochondrial membrane dynamics constitutes an important step towards a better understanding of mitochondrial behavior. Mitochondria are an integrated component of the cell and their actions are undoubtedly linked to cellular activities. The current focus of research within this field is to identify precise molecular links between mitochondrial

¹ University of Ottawa Heart Institute, 40 Ruskin St., Ottawa, Canada K1Y 4W7.

Email: HMcbride@ottawaheart.ca

² These authors contributed equally.

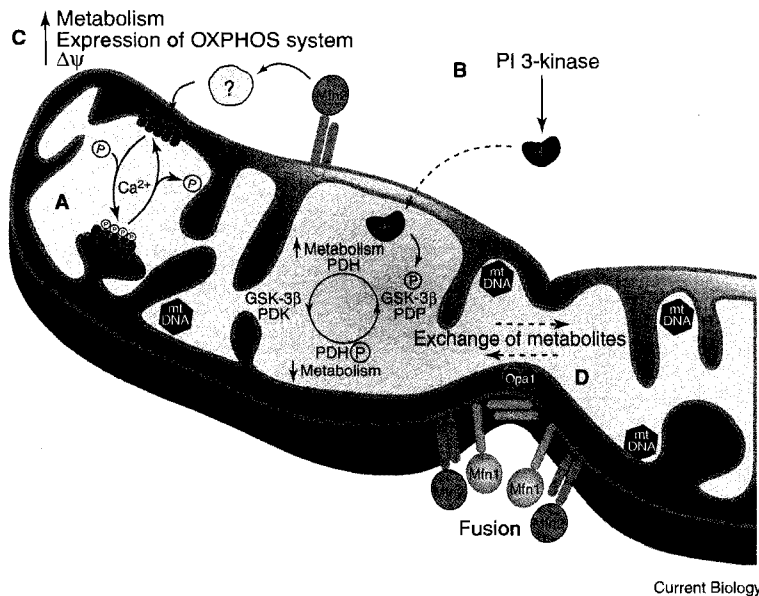


Figure 1. Regulation of mitochondrial metabolism through morphological changes and signaling. (A) Phosphorylation and dephosphorylation of metabolic enzymes, including subunits of the respiratory complexes I-V are modulated by calcium-mediated signaling. (B) In the mitochondrial matrix, phosphorylation and dephosphorylation of pyruvate dehydrogenase (PDH) are regulated through concerted actions of PDH kinases (PDK) and phosphatases (PDP). The activity of PDH is also modulated by a cytosolic signaling cascade that converges onto GSK-3 β , leading to PDH dephosphorylation and activation, ultimately promoting metabolic activity. (C) The fusion GTPase Mfn2 regulates metabolism, electrochemical potential and expression of the respiratory complexes through unknown signaling partners. (D) Membrane fusion facilitates the propagation of metabolites, such as calcium, reactive oxygen species and mitochondrial DNA (mtDNA), within the mitochondrial reticulum. The GTPases Mfn1, Mfn2 and Opa1 coordinate the reaction of mitochondrial membrane fusion. Mfn proteins are required on both sides of the membrane, with Mfn1 mediating membrane tethering. Solid lines indicate protein interactions and reaction pathways, dotted lines represent protein and metabolite translocation events. See text for details and references.

function and the machinery that governs morphology. In addition, recent evidence suggests that bi-directional signaling exists between mitochondria and other cellular components. The implication of the GTPase switch, both regulatory and mechanical, in the governance of mitochondrial dynamics has recently been shown to couple mitochondrial function to cellular demand. This integration allows mitochondrial function, localization and biogenesis to be responsive to changes in cell metabolism, development, death and division. These new insights into mitochondrial biology reveal a more central function for this organelle than previously appreciated and constitute the focus of this review.

Regulation of Metabolism

Recent evidence demonstrates that the machinery that governs mitochondrial dynamics also participates in the temporal regulation of metabolism (Figure 1). These findings may not be surprising since the assembly of the mitochondrial cristae and apparent condensation of the matrix space observed by electron microscopy has been long considered to reflect the metabolic state of mitochondria [16,17]. In more recent years, tomographic reconstructions of isolated mitochondria revealed a detailed variety of cristae morphologies, from simple tubular structures to large, flat lamella and vacuolated intercrystal spaces [18,19]. The dynamic shift in morphology coincides with a number of physiological events, such as transitions between different respiratory states and cristae remodeling during apoptosis [18,20,21]. Consistent with this, the loss or mutation of some inner membrane proteins affects cristae morphology and results in reduced

respiration. For example, lack of non-essential subunits within the ATP synthase in yeast leads to the loss of cristae with the inner membrane forming ring structures within the mitochondria [22–24]. Similarly, deletion of the intermembrane space GTPase Opa1 causes vesiculation of the inner membrane, and loss of the inner-membrane-anchored Mitofillin leads to concentric sheets of inner membrane ring structures. In all these cases, aberrations in cristae morphology are accompanied by alterations in metabolism [9,25–27]. Furthermore, cells lacking Opa1 or Mitofillin are highly susceptible to apoptotic death, indicating the importance of maintaining inner membrane morphology [9,27]. The details of how these proteins contribute to the inner membrane architecture are unknown, but these findings illustrate the fact that cristae do not form spontaneously and are created by active, regulated processes. A number of other proteins required for the maintenance of inner membrane morphology have been identified from genetic screens in yeast [28–30], and are listed in Table S1.

Recent evidence suggests that mitochondrial fission and fusion also regulate mitochondrial metabolism. The downregulation of Opa1 or both Mitofusin GTPases by RNA interference leads to fragmented mitochondria with greatly reduced oxygen consumption and electrochemical potential [26]. Although all three GTPases are known components of the mitochondrial fusion machinery [31], they are not directly linked to the metabolic machineries. Therefore it is unclear why the loss of these fusion proteins interferes with respiration. This effect is specific to the loss of the fusion proteins rather than the morphological transition alone since mitochondrial fragmentation induced upon

the stimulation of fission did not interfere with metabolism [26]. The metabolic dysfunction that characterizes fusion-incompetent mitochondria may be secondary to a requirement for exchange of specific cargo, for example mitochondrial DNA (mtDNA), calcium, and other metabolites (Figure 1). Complementation of mtDNA has been demonstrated to be one important aspect of mitochondrial fusion, since the nucleoids carrying the mtDNA are shared within the dynamic reticulum [32–35]. If a block in fusion results in small mitochondria that either completely lack mtDNA or become enriched with mutant mtDNA, these mitochondria would ultimately lose their functional electron transport chain, leading to compromised oxygen consumption. Interestingly, cells lacking Mfn1 and Mfn2 were maintained only in supplemented media containing high pyruvate and uridine, conditions that are also required to maintain *rho*⁰ cells lacking mtDNA [26]. In addition to the sharing of cargo, the fusion machinery may be required either directly or indirectly for the maintenance of inner membrane cristae dynamics, which, as mentioned above, regulate mitochondrial metabolism.

Consistent with the evidence that the loss of the fusion machinery leads to reduced metabolism, it has been recently demonstrated that overexpression of Mfn2 in cultured cells leads to an upregulation of the respiratory complexes, mitochondrial oxidation and glucose utilization by cells [36,37]. Interestingly, the expression of a fusion-deficient form of Mfn2 also increases the respiratory capacity with accompanying condensation of the cristae, suggesting that Mfn2 may have a role in metabolic regulation that is distinct from its role in fusion [37]. In addition, Mfn2 mRNA and protein expression within skeletal muscle is reduced in the Zucker rat model of obesity [36,37] and in human subjects with obesity and diabetes [38], highlighting the pathological implications of aberrant mitochondrial dynamics. Changes in Mfn2 expression are accompanied by altered mitochondrial network *in vivo* and reduced metabolism *in vitro* [37].

Experiments investigating the mitochondrial fission machinery are also consistent with the emerging functional link between the morphology and metabolic output of mitochondria. Cells exposed to high levels of glucose contain highly fragmented mitochondria [39,40] that are hyperpolarized and generate a transient increase in reactive oxygen species (ROS) production as a result of the increased respiration. Interestingly, the fragmentation event requires glucose entry into the cell, but precedes pyruvate uptake by mitochondria, placing it as an early event [40]. Importantly, the observed transition in mitochondrial morphology and increased ROS production return to baseline within 60 minutes, indicating that the process is reversible. In cells overexpressing Mfn2 or a dominant-interfering mutant of the mitochondrial DRP1, the mitochondria remain tubular and do not show any increased respiration, hyperpolarization or ROS production [40]. These data indicate that mitochondrial fragmentation is required for the hyperglycemia-induced increase in respiration. Interestingly, chronic hyperglycemia, as in the diabetic condition, results in downregulation of Mfn2 in muscle cells, which is consistent with a more stable

transition of the mitochondria to the fragmented state [36,38]. Taken together, this accumulating evidence supports the idea that the machineries that govern mitochondrial fusion and fission are intimately coupled to the metabolic processes within the organelle.

Mitochondrial Kinases and Phosphatases in Metabolic Regulation

Given that there are no direct links between the fusion/fission machineries and the metabolic complexes, the obvious question that arises is how are these morphological transitions translated into altered metabolic output? One possibility is that the morphology machinery might be integrated into pathways that regulate post-translational modifications of the metabolic complexes. Experiments published almost 40 years ago demonstrated that phosphorylation of the matrix-localized pyruvate dehydrogenase (PDH) complex inhibits the conversion of pyruvate to acetyl Co-A, the first step in the citric acid cycle [41]. PDH kinases 1–4 were later identified and their expression is now known to be tightly controlled through transcriptional regulation [42]. For example, they are upregulated during starvation when they efficiently phosphorylate PDH, resulting in the inactivation of the enzyme when the substrate levels are low [43]. Interestingly, a mechanism for a rapid regulation of PDH has been uncovered that may complement the activity of the PDH kinases. Insulin stimulation activates protein kinase B/Akt in a phosphatidylinositol (PI) 3-kinase-dependent manner [44]. Akt controls a number of metabolic and survival pathways and was recently found to translocate into the mitochondrial matrix in response to insulin stimulation [45]. A known target of activated Akt is glycogen synthase kinase 3 β (GSK-3 β) [46], which, although mainly cytosolic, has also been found within mitochondria [47]. The non-phosphorylated form of GSK-3 β is an active kinase that, among other substrates, targets PDH, leading to reduced metabolic activity [48]. Phosphorylation of GSK-3 β by Akt inhibits its kinase activity, which allows PDH to be dephosphorylated and therefore activated, leading to an increase in metabolism. Although these data require further substantiation, it represents a mechanism for the dynamic regulation of metabolic components by extracellular stimuli.

Very recently the mitochondrial phosphoproteome was shown to be much more extensive than previously anticipated and, remarkably, there was a dynamic change in the phosphorylation state of numerous proteins in response to calcium signaling [49]. The mitochondrial response to calcium flux has long been considered a central aspect of its morphology and function, both as a calcium buffer and in the propagation of intracellular calcium waves during muscle contraction and synaptic vesicle release [50–53]. The proteins phosphorylated in response to calcium include many components of the electron transport chain and the citric acid cycle [49], indicating that multiple mitochondrial kinases and phosphatases regulate mitochondrial function in a dynamic manner (Table S1). The recent identification of a novel phosphatase, termed PTPMT1, as a permanent resident of the mitochondrial matrix compartment provides insights into

this exciting new area of research [54]. The loss of PTPMT1 by RNA interference leads to an almost two-fold increase in ATP production and increases the kinetics of insulin release both at steady state and upon glucose stimulation [54]. Although substrates of this phosphatase within the matrix have not yet been identified, components of the electron transport chain and ATP synthase are obvious candidates. Many cytosolic kinases have been found to associate specifically with the mitochondrial surface under different conditions [55]. These kinases include members of the Src family, whose mitochondrial localization has also been shown to affect oxidative metabolism and cell signaling [56–58]. Two new mitochondrial kinases have also been recently identified, the intermembrane space PTEN-induced kinase 1 (PINK1) [59,60], and the peripherally associated leucine rich repeat kinase 2 (LRRK2) [61,62]. The substrates and function of PINK1 and LRRK2 are currently unknown; however, both proteins are affected in Parkinson's disease, highlighting the importance of mitochondrial phosphorylation in human pathophysiology. In addition, PINK1 was recently found to interact genetically with a third Parkinson's disease gene, Parkin [63,64], which encodes a cytosolic ubiquitin E3 ligase that has been found in the mitochondrial matrix of dividing cells [65]. Future experiments will confirm whether the machinery that regulates mitochondrial morphology is functionally linked to metabolic regulation through post-translational modifications such as phosphorylation.

Mitochondria and the Cell Cycle

It is understood that functional mitochondria are required for all cell processes due to common energetic requirements. Recent data expand on this requirement, however, and place the emphasis on this organelle as a relevant signaling platform for cell-cycle progression. For example, two important studies have recently defined the molecular basis for the previously observed cell-cycle arrest under conditions of low energy. AMPK is a heterotrimeric kinase that is activated in high AMP conditions, making it a sensor of the AMP:ATP ratio [66]. Upon activation of AMPK, a phosphorylation cascade is initiated that alters both consumption and production of ATP. Recently, activated AMPK was shown to phosphorylate Ser15 of p53 [67], a modification that is known to protect the protein from degradation and promote cell-cycle arrest during DNA damage and aberrant growth factor signaling [68]. Upon deletion of p53, nutrient deprivation results in continued cellular proliferation, with an eventual loss in cell viability, confirming the essential requirement for p53 in nutrient-dependent cell-cycle arrest [67]. This discovery has led to a more precise mechanistic understanding of how low glucose and ATP leads to cell-cycle arrest and promotes cell survival [67]. In a series of experiments expanding on this theme in *Drosophila*, it was demonstrated that defects in the cytochrome oxidase subunit Va (CoVa) induced a cell-cycle arrest in the developing eye [69]. Surprisingly, the reduction in ATP production observed in the CoVa mutant was not sufficient to arrest cell growth or interfere with the differentiation program, since cells within the eye showed many hallmark features of

differentiated neurons, rod and cone cells. Consistent with the work of Jones *et al.* [67], the block in cell division was due to the activation of AMPK and subsequent phosphorylation of p53, leading to the loss of cyclin E and cell-cycle arrest at the G1 to S phase transition. Interestingly, the *Drosophila* study proved that the secondary loss of either AMPK or p53 along with CoVa rescued progression from G1 to S phase, despite lower ATP production [69]. Together, these data define a novel low-energy cell-cycle checkpoint that monitors the metabolic activity of the mitochondria before committing to another round of cell division.

In addition to the metabolic control of cell-cycle transition, efforts have been made to identify cell-cycle-dependent mechanisms that regulate mitochondrial inheritance during mitosis. In the yeast *Candida albicans*, it has been observed that the mitochondria fragment upon entrance into M phase [70]. Genetic screens were then developed to identify factors required for these morphological transitions in *Saccharomyces cerevisiae*. These screens examined mitochondrial morphology and positioning, and were the first to uncover many genes responsible for mitochondrial fission and fusion, as well as those implicated in the targeted migration of mitochondria into the bud [28,31,71–75]. However, even with this new list of essential proteins, it remains unclear how the machinery that mediates movement and division is modulated during the cell cycle. In addition to changes during mitosis, yeast mitochondria form a highly fused reticulum that is tightly associated with the nucleus during meiosis [76]. In the late tetrad state, just prior to sporulation, the mitochondria are again highly fragmented, a process that is required for the formation of viable spores [77]. In addition, one of the yeast proteins required for mitochondrial fusion, Fuzzy Onion (Fzo1p) is actively degraded by a proteasome-dependent process during mating, in response to G-protein-coupled receptor signaling initiated by the yeast α -mating factor [78]. Together, these data show that the machinery that governs mitochondrial morphology is intimately linked with the signaling cascades that initiate cell-cycle and mating transitions. In the mammalian system, overexpression of Mfn2, in addition to stimulating mitochondrial fusion, induces a cell-cycle arrest at the G1 to S transition [79]. An examination of the upstream signals affected by the expression of Mfn2 reveals that, upon addition of epidermal growth factor, the Ras GTPase is not activated and the ERK phosphorylation cascade is not engaged. The inhibition of proliferation and lack of ERK activation occurs even following expression of a form of Mfn2 that is not targeted to the mitochondria, arguing for a specific signaling role of Mfn2 in cell-cycle arrest [79]. These data suggest that Mfn2 is able to interfere with very early signaling events following receptor–ligand binding. It is unclear why this GTPase would have any effect on signaling proteins like Ras, but it is interesting to note that Ras and some of the downstream signaling effectors in this pathway, including ERK1/2, have been localized to the mitochondria (Table S1). Further studies are required to provide more conclusive insights into these mechanisms.

Mitochondria and Signaling

Unexpected Guests: K-Ras, p53 and NF- κ B Signaling on the Mitochondria

Perhaps the best known example of the integration of mitochondria within an established signaling pathway is their central function within the apoptotic cascade. Morphologically, it has been determined that mitochondrial fragmentation and cristae remodeling are essential steps for cytochrome c release and cell death [80,81]. The field of apoptosis has been witness to a growing list of proteins that translocate to the mitochondria in a highly synchronized fashion, in addition to those that are systematically released from mitochondria in the dramatic cascade of events required to neatly package a dead cell. Interestingly, one of the key signal transduction GTPases, K-Ras, is a new addition to the list of proteins that translocate to the mitochondria and induce cell death [82]. K-Ras is primarily localized to the plasma membrane; however, upon phosphorylation by protein kinase C, a conformational change results in its extraction from the plasma membrane and rapid recruitment to the mitochondria [82]. Once positioned there, K-Ras interacts with Bcl-XL to promote activation-induced apoptosis of T cells [82]. The pro-death effects of mitochondrial-associated K-Ras are not completely understood, although its interactions with anti-apoptotic proteins like Bcl-XL and Bcl-2 may result in their sequestration and inactivation. Interestingly, this is not the first report of the recruitment of Ras family proteins to the mitochondria [83] and is consistent with the growing list of signaling adaptors and enzymes that can be found in mitochondrial fractions either biochemically or by fluorescence microscopy (Table S1). Given that K-Ras is known to partition selectively into lipid-based microdomains [84,85], it is possible that it could bring associated proteins, like Bcl-XL, into a novel type of mitochondrial platform that would change their functional activity. It is also conceivable that there are mitochondrial K-Ras exchange factors, GTPase activating proteins and effectors that may control the nucleotide state and function of Ras during its mitochondrial residence. In addition to K-Ras, the nuclear transcription factor p53 was found to translocate to the mitochondria during cell death and to interact directly with the anti-apoptotic proteins Bcl-2 and Bcl-XL [86]. Unlike K-Ras, mitochondrial p53 has also been shown to participate in the cytosolic activation of Bax, oligomerization of Bax and Bak and subsequent cytochrome c release [87]. The dynamic translocation of K-Ras and p53 to the mitochondria highlight the dual functionality of signaling proteins and their role in mitochondrial biology.

In the field of immunology, four independent groups recently identified a new mammalian protein called MAVS (mitochondrial anti-viral signaling protein). MAVS is an integral outer membrane protein that plays a central role in the signal transduction cascades that lead to the NF- κ B stress response and type 1 interferon response [88–91]. MAVS functions as an adaptor between the viral-dsRNA-binding protein RIG-1 [92] and the effectors TRAF2 and TRAF6, which are required for the activation of NF- κ B [88]. The NF- κ B and interferon responses are critical for the cellular

production of cytokines that alert the body to a viral infection. Interestingly, upon binding to TRAF2 and TRAF6, MAVS enters into a detergent resistant microdomain on the mitochondria, which regulates the efficacy of the downstream signaling cascades [88]. In an interesting twist, a protease encoded by the hepatitis C virus was shown to cleave MAVS, releasing it from the mitochondrial membrane and interfering with the host cell viral response [91]. Unexpectedly, these data place the mitochondria in the center of a signal transduction cascade that seemingly has no particular requirement for increased ATP consumption.

Mitochondria as a Signaling Platform

One explanation for the utilization of the mitochondrial surface in the propagation of signaling cascades is the possibility that the mitochondrion provides a unique membrane environment for the assembly of dynamic complexes (Figure 2). The lateral movement of MAVS into a detergent-resistant microdomain is consistent with this notion. Given that the lipid composition of the mitochondria is distinct from those found on the plasma membrane, the nature of the microdomain must be unique. High levels of cardiolipin in the inner membrane, for example, clearly distinguish this bilayer from all others. The lipid ceramide has been shown to form microdomains that can lead to channel formation during apoptosis [93,94], and the ganglioside GD3, which is derived from ceramide, has also been shown to translocate to mitochondrial microdomains during cell death [95,96]. Interestingly, GD3 has been shown to interfere with the activation of NF- κ B through unknown mechanisms [97]. It is possible that GD3 insertion in the mitochondrial outer membrane interferes with the translocation of MAVS into a functional raft, thereby inhibiting the NF- κ B survival response.

Functional microdomains may also form on the mitochondria through the lateral recruitment and amplification of phosphatidylinositol phosphates (PIPs), activated Rab GTPases, and/or protein scaffolds. Although the identity of specific species of PIPs on the mitochondria has not been clearly demonstrated, mitochondria do contain enzymes that modulate the formation of PIPs. There are at least two mitochondrial PI (5) phosphatases — synaptojanin 2A [98] and Inpp5B [99] — and interference with synaptojanin 2A recruitment has been shown to affect mitochondrial morphology [98]. Rab GTPases are known to recruit a variety of effectors, including PI kinases, phosphatases, and regulators of motility, docking and fusion [100–102]. The recruitment of these effectors contributes to the formation of functional microdomains on almost all types of intracellular membrane. Two Rab GTPases have been linked to mitochondrial function. In mammals, Rab32 is recruited to the outer membrane, where it binds protein kinase A in order to modulate mitochondrial morphology through as yet unknown mechanisms [103]. The yeast Rab GTPase Ypt11p binds to the myosin V actin motor Myo2p, and both Ypt11p and Myo2p are required to tether mitochondria within the growing bud during cell division [104]. Although our understanding of the role of Rab GTPases in mitochondrial function remains limited, it is likely that they contribute to the formation of functional surface microdomains and mitochondrial activity (Figure 2).

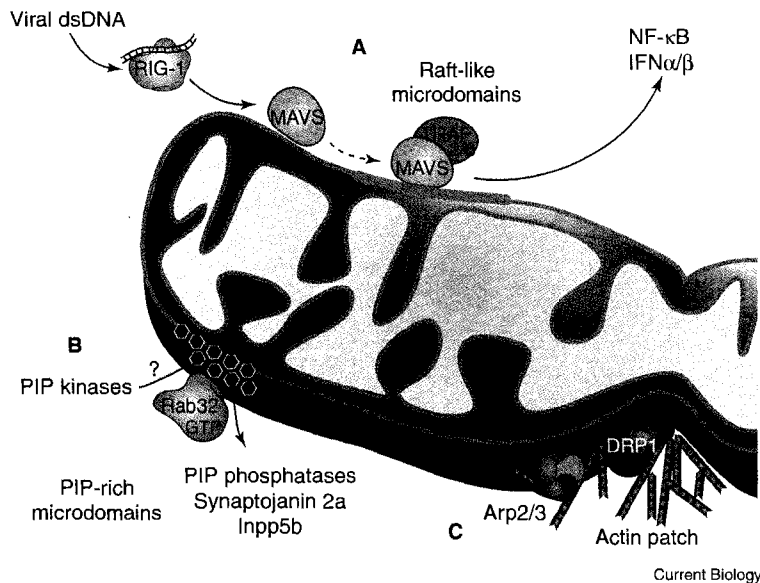


Figure 2. Assembly of lipid and protein microdomains on mitochondrial membranes. (A) Once activated by binding to viral dsRNA, the RIG-1 adaptor protein promotes incorporation of MAVS into detergent-resistant domains on mitochondrial membranes. From these raft-like domains, MAVS, together with TRAF2 and TRAF6, coordinates signals leading to NF- κ B and IFN α/β activation. (B) PI phosphatases synaptojanin 2a and Inpp5b and unknown PIP kinases potentially determine the composition of PIPs on mitochondrial membranes. The recruitment of these enzymes may be mediated through the action of regulatory enzymes like Rab32. The resulting enrichment in specific phosphorylated lipid species would act as a binding platform for dynamic protein complex assembly. (C) Oligomeric proteins like DRP1 localize to punctate foci on the mitochondrial surface. In yeast actin remodeling on mitochondrial membranes is performed by the Arp2/3 complex, and in the mammalian system actin promotes stable DRP1 association with mitochondrial membranes during stimu-

lated fission. The hypothetical participation of underlying PIP domains in the assembly of DRP1 and actin polymerization is indicated by an arrow. Solid lines indicate protein interactions and reaction pathways, dotted lines represent protein and metabolite translocation events. See text for details and references.

Actin polymerization on the surface of intracellular membranes is also known to provide a stable platform for the assembly of protein complexes [105]. In yeast, the actin-nucleating complex Arp2/3 is recruited to punctate spots on the mitochondrial surface where it mediates anterograde mitochondrial motility along actin cables [106–108]. In mammals, the increased stabilization of DRP1 on mitochondria upon stimulation of fission is also regulated in part by actin polymerization [109]. Together, this indicates that actin patches, in combination with both lipid raft and PIP-rich domains, may modulate the assembly of diverse functional complexes on the mitochondrial surface.

Mitochondria and Development

The mitochondrial network displays remarkable plasticity during development of certain tissues. For example, electron microscopy studies have revealed a transition from elliptical and rod-like mitochondria in embryonic rat myocardiocytes and skeletal muscle cells to an interconnected reticulum in the cardiac muscle and diaphragm of adult animals [110–113]. This morphological transition possibly reflects timed induction of mitochondrial fusion. Supporting this idea, expression levels of Mfn2 increase during differentiation of myoblasts [36] and spermatocytes [114], correlating with the extensive mitochondrial remodeling observed in these cells.

The loss of either Mfn1 or Mfn2 is embryonic lethal, highlighting the importance of mitochondrial dynamics during development [3]. Interestingly, the Mfn2 null embryos appear relatively normal, but are resorbed by embryonic day 11.5 due to unsuccessful placental implantation. Conversely, Mfn1 null embryos, although developmentally delayed and resorbed by embryonic day 12.5, display normal implantation, suggesting that the placental malfunction observed in Mfn2 null mice

is not directly related to a lack of mitochondrial fusion [3]. This is consistent with the emerging evidence that, in addition to its requirement for mitochondrial fusion, Mfn2 has additional roles both in protection from cell death [7,115,116] and in the regulation of metabolism [26,36,38]. In contrast, the data so far indicate that Mfn1 functions primarily as a core essential component of the fusion machinery. It has been shown that the heptad repeats of Mfn1 tether mitochondria together [4,5] and that Mfn1, but not Mfn2, participates with Opa1 in the fusion process [11]. In addition, the nucleotide-binding properties of Mfn1 and Mfn2 appear to be quite distinct, suggesting unique functional properties [5]. Mfn1 binds to nucleotide with low affinity and shows high rates of hydrolysis for GTP, consistent with its evolutionary relationship to the dynamin family of GTPases [5]. Although Mfn1 and Mfn2 have 60% sequence identity, Mfn2 binds nucleotides with high affinity and exhibits slow intrinsic hydrolysis rates reminiscent of the Rab family of regulatory GTPases [5,7]. Collectively, these findings strongly indicate that Mfn1 and Mfn2 are functionally distinct GTPases that are both essential for mitochondrial fusion and embryonic development.

Mitochondrial Responses in Neuronal Function

The genetic and cell biology systems used by neurobiologists have provided important new insights into the functional requirement and spatial positioning of mitochondria in polarized neurons both during development and within the adult. For example, recent experiments showed that local administration of nerve growth factor (NGF) to an axon of a primary neuron in culture increases mitochondrial movement into the stimulated region and triggers the arrest of anterograde-directed mitochondria. This arrest results in the accumulation of mitochondria within the vicinity

of the activated NGF receptor TrkA and is dependent upon activation of PI 3-kinase and actin polymerization [117]. These data imply that a signal transduction cascade downstream from TrkA results in the modulation of mitochondrial motility in active growth cones of developing neurons [117]. Interestingly, the actin-remodelling GTPase RhoA and its formin effector mDia1 play a role in the regulated arrest of mitochondrial motility in mammalian cells and in a *Drosophila* neuronal cell line [118], providing molecular cues responsible for actin-mediated modifications of mitochondrial movement.

Mitochondria are highly responsive to synaptic stimulation. In hippocampal neurons, dendritic mitochondria rapidly fragment and cluster in the proximity of dendritic spines in response to neuronal activity [119]. Activity also decreases mitochondrial motility, arguing for the existence of specific signals regulating mitochondrial behavior. Interestingly, overexpression of DRP1 results in an increased number of mitochondria within the dendrite, as well as an increased density of dendritic spines and synapses [119]. Conversely, expression of a dominant-negative DRP1 mutant results in fused mitochondria that remain primarily within the soma, resulting in very few mitochondria migrating into the dendrite [119]. Depletion of dendritic mitochondria upon expression of the mutant DRP1 has an adverse effect on spine development, suggesting that mitochondrial function is required and limiting for the formation and maintenance of synapses.

In the adult neuron, mitochondria are enriched at the synapse, which is commonly explained by the important functional role of mitochondria in buffering calcium fluxes during synaptic transmission and providing energy for synaptic vesicle release and recycling. However, experiments designed to remove mitochondria selectively from the synapse suggest that many of these assumptions are overly simplistic. Mutations in DRP1 in *Drosophila* are semilethal, with the survivors suffering neurodegeneration and lack of coordination (termed the *Fratsby* mutant) [120]. The mitochondria within mutant neurons are clustered and fused within the soma, with few migrating into synapses. Interestingly, although the resting cytosolic calcium within these synapses is increased, neurotransmitter release remains normal upon calcium stimulation. In addition, synaptic vesicle endocytosis proceeds normally, indicating that, even in mitochondria-depleted terminals, there is sufficient energy to drive this process. Intriguingly, prolonged stimulation reveals defective migration of the reserve pool of synaptic vesicles to the membrane [120]. This phenotype is due to a specific requirement for mitochondrial ATP in the activation of myosin motors required to mobilize the reserve pool of vesicles to the plasma membrane. Since the role of mitochondria in calcium buffering and local energy production has been well established, it is quite surprising that these neurons are so functional in the absence of mitochondria.

Mutations in *Drosophila* Miro1, an integral outer membrane protein with two Rho-like GTPase domains and calcium-binding EF hand motifs result in a loss of anterograde mitochondrial delivery into the axon [121]. Flies lacking dMiro1 die at the larval stage due to numerous defects, and the mitochondrial distribution in

muscles and neurons is limited to the cell body. Similar to the DRP1 mutants, both basal and fast calcium-stimulated neurotransmission are relatively normal, with functional defects observed mainly upon chronic stimulation. At the neuromuscular junction, the presynaptic boutons in the dMiro mutants are more abundant, smaller, structurally deformed and positioned close together. The increase in synaptic boutons in the absence of mitochondria is unexpected and also in contrast with the observed decrease in dendritic spines observed in mitochondria-depleted neurons expressing mutant DRP1 [119]. In general, the seemingly complex involvement of mitochondria in developmental processes suggests that the positioning of the mitochondria may be selectively required for the propagation of developmental signaling cascades. Future experiments will certainly shed more light on these exciting new aspects of mitochondrial function.

Conclusions and Perspectives

This review has focused on the idea that the mitochondria are intimately embedded in the signaling cascades and programs that operate within the cell. Evidence is emerging that these links include functions that extend beyond the primary role of mitochondria as ATP generators. We have supplied examples to illustrate mechanisms by which the mitochondria can receive cellular signals and propagate a targeted response. These examples include intuitive responses, such as altering the position of mitochondria within the cell in order to provide a local ATP supply, but also more surprising responses, such as the control of cell cycle and the dynamic modulation of respiratory capacity. In many cases, we have suggested that the interface between the cellular signal and mitochondrial response hinges upon the activity of a new cast of proteins that modulates mitochondrial morphology and movement. Some of these proteins appear to be unique mitochondrial proteins and enzymes, and others derive from the more familiar families of proteins, such as GTPases, lipid-modifying enzymes, kinases and phosphatases (Table S1).

By delving into the complex interconnected nature of mitochondria and cellular physiology, we will contribute to the development of intelligent treatment strategies for diseases characterized by mitochondrial dysfunction. Many of these diseases result from mutations in proteins that modulate mitochondrial behavior. Mutations in Mfn2 result in the disease Charcot-Marie Tooth Type 2A, characterized by a loss of peripheral motor neurons [122], and mutations in Opa1 (and recently also Mfn2) are responsible for autosomal dominant optic atrophy, causing progressive blindness [8,123]. Similarly, understanding the links to cell cycle and apoptosis will provide new concepts in the treatment of cancer, and the emerging understanding of the kinases and phosphatases involved in Parkinson's disease will shed new light on neurodegenerative conditions. In addition to the monogenic mitochondrial diseases, a better understanding of dynamic metabolic regulation will help to control diabetes, obesity, and complex mitochondrial myopathies. The fundamental insights to be gained through the investigation of dynamic mitochondrial function and the integration

of this organelle in cell signaling pathways will have far-reaching implications in many areas of biology.

Supplemental data

A supplemental table listing the proteins that modulate mitochondrial morphology and signaling is available at <http://www.current-biology.com/cgi/content/full/16/14/R551/DC1/>.

Acknowledgments

H.M.M. is supported by a CIHR New Investigator Award and CIHR operating grants. S.W. is supported by a CIHR Fellowship Award, and M.N. is supported by OGS Award. We would like to apologize for the omission of many important contributions to the study of mitochondrial dynamics due to space constraints. We are grateful to Gordon Shore, Luca Pellegrini and members of our group for insightful comments on the manuscript.

References

- Chan, D.C. (2006). Mitochondrial fusion and fission in mammals. *Annu. Rev. Cell Dev. Biol.*, May 11 [Epub ahead of print].
- Chen, H., and Chan, D.C. (2005). Emerging functions of mammalian mitochondrial fusion and fission. *Hum. Mol. Genet.* **14**, R283–R289.
- Chen, H., Detmer, S.A., Ewald, A.J., Griffin, E.E., Fraser, S.E., and Chan, D.C. (2003). Mitofusins Mfn1 and Mfn2 coordinately regulate mitochondrial fusion and are essential for embryonic development. *J. Cell Biol.* **160**, 189–200.
- Koshiba, T., Detmer, S.A., Kaiser, J.T., Chen, H., McCaffery, J.M., and Chan, D.C. (2004). Structural basis of mitochondrial tethering by mitofusin complexes. *Science* **305**, 858–862.
- Ishihara, N., Eura, Y., and Mihara, K. (2004). Mitofusin 1 and 2 play distinct roles in mitochondrial fusion reactions via GTPase activity. *J. Cell Sci.* **117**, 6535–6546.
- Griffin, E.E., and Chan, D.C. (2006). Domain interactions within Fzo1 oligomers are essential for mitochondrial fusion. *J. Biol. Chem.* **281**, 16599–16606.
- Neuspiel, M., Zunino, R., Gangaraju, S., Rippstein, P., and McBride, H.M. (2005). Activated Mfn2 signals mitochondrial fusion, interferes with Bax activation and reduces susceptibility to radical induced depolarization. *J. Biol. Chem.* **280**, 25060–25070.
- Alexander, C., Votruba, M., Pesch, U.E., Thiselton, D.L., Mayer, S., Moore, A., Rodriguez, M., Kellner, U., Leo-Kottler, B., Auburger, G., et al. (2000). OPA1, encoding a dynamin-related GTPase, is mutated in autosomal dominant optic atrophy linked to chromosome 3q28. *Nat. Genet.* **26**, 211–215.
- Olichon, A., Baricault, L., Gas, N., Guillou, E., Valette, A., Belenguer, P., and Lenaers, G. (2003). Loss of OPA1 perturbs the mitochondrial inner membrane structure and integrity, leading to cytochrome c release and apoptosis. *J. Biol. Chem.* **278**, 7743–7746.
- Satoh, M., Hamamoto, T., Seo, N., Kagawa, Y., and Endo, H. (2003). Differential sublocalization of the dynamin-related protein OPA1 isoforms in mitochondria. *Biochem. Biophys. Res. Commun.* **300**, 482–493.
- Cipolat, S., Martins de Brito, O., Dal Zilio, B., and Scorrano, L. (2004). OPA1 requires mitofusin 1 to promote mitochondrial fusion. *Proc. Natl. Acad. Sci. USA* **101**, 15927–15932.
- Delettre, C., Griffoin, J.M., Kaplan, J., Dollfus, H., Lorenz, B., Faivre, L., Lenaers, G., Belenguer, P., and Hamel, C.P. (2001). Mutation spectrum and splicing variants in the OPA1 gene. *Hum. Genet.* **109**, 584–591.
- Pitts, K.R., Yoon, Y., Krueger, E.W., and McNiven, M.A. (1999). The dynamin-like protein DLP1 is essential for normal distribution and morphology of the endoplasmic reticulum and mitochondria in mammalian cells. *Mol. Biol. Cell* **10**, 4403–4417.
- Yoon, Y., Pitts, K.R., and McNiven, M.A. (2001). Mammalian dynamin-like protein dlp1 tubulates membranes. *Mol. Biol. Cell* **12**, 2894–2905.
- Smirnova, E., Griparic, L., Shurland, D.L., and van der Bliek, A.M. (2001). Dynamin-related protein drp1 is required for mitochondrial division in mammalian cells. *Mol. Biol. Cell* **12**, 2245–2256.
- Hackenbrock, C.R. (1966). Ultrastructural bases for metabolically linked mechanical activity in mitochondria. I. Reversible ultrastructural changes with change in metabolic steady state in isolated liver mitochondria. *J. Cell Biol.* **30**, 269–297.
- Scalettar, B.A., Abney, J.R., and Hackenbrock, C.R. (1991). Dynamics, structure, and function are coupled in the mitochondrial matrix. *Proc. Natl. Acad. Sci. USA* **88**, 8057–8061.
- Mannella, C.A., Marko, M., Penczek, P., Barnard, D., and Frank, J. (1994). The internal compartmentation of rat-liver mitochondria: tomographic study using the high-voltage transmission electron microscope. *Microsc. Res. Tech.* **27**, 278–283.
- Mannella, C.A., Pfeiffer, D.R., Bradshaw, P.C., Moraru, I., Slepchenko, B., Loew, L.M., Hsieh, C.E., Buttle, K., and Marko, M. (2001). Topology of the mitochondrial inner membrane: dynamics and bioenergetic implications. *IUBMB Life* **52**, 93–100.
- Scorrano, L., Ashiya, M., Buttle, K., Weiler, S., Oakes, S.A., Mannella, C.A., and Korsmeyer, S.J. (2002). A distinct pathway remodels mitochondrial cristae and mobilizes cytochrome c during apoptosis. *Dev. Cell* **2**, 55–67.
- Germain, M., Mathai, J.P., McBride, H.M., and Shore, G.C. (2005). Endoplasmic reticulum BIK initiates DRP1-regulated remodelling of mitochondrial cristae during apoptosis. *EMBO. J.* **24**, 1546–1556.
- Arselin, G., Vaillier, J., Salin, B., Schaeffer, J., Giraud, M.F., Dautant, A., Brethes, D., and Velours, J. (2004). The modulation in subunits e and g amounts of yeast ATP synthase modifies mitochondrial cristae morphology. *J. Biol. Chem.* **279**, 40392–40399.
- Paumard, P., Vaillier, J., Couly, B., Schaeffer, J., Soubannier, V., Mueller, D.M., Brethes, D., di Rago, J.P., and Velours, J. (2002). The ATP synthase is involved in generating mitochondrial cristae morphology. *EMBO. J.* **21**, 221–230.
- Bornhøvd, C., Vogel, F., Neupert, W., and Reichert, A.S. (2006). Mitochondrial membrane potential is dependent on the oligomeric state of F1F0-ATP synthase supracomplexes. *J. Biol. Chem.* **281**, 13990–13998.
- Griparic, L., van der Wel, N.N., Orozco, I.J., Peters, P.J., and van der Bliek, A.M. (2004). Loss of the intermembrane space protein Mgm1/OPA1 induces swelling and localized constrictions along the lengths of mitochondria. *J. Biol. Chem.* **279**, 18792–18798.
- Chen, H., Chomyn, A., and Chan, D.C. (2005). Disruption of fusion results in mitochondrial heterogeneity and dysfunction. *J. Biol. Chem.* **280**, 26185–26192.
- John, G.B., Shang, Y., Li, L., Renken, C., Mannella, C.A., Selker, J.M., Rangell, L., Bennett, M.J., and Zha, J. (2005). The mitochondrial inner membrane protein mitofilin controls cristae morphology. *Mol. Biol. Cell* **16**, 1543–1554.
- Dimmer, K.S., Fritz, S., Fuchs, F., Messerschmitt, M., Weinbach, N., Neupert, W., and Westermann, B. (2002). Genetic basis of mitochondrial function and morphology in *Saccharomyces cerevisiae*. *Mol. Biol. Cell* **13**, 847–853.
- Messerschmitt, M., Jakobs, S., Vogel, F., Fritz, S., Dimmer, K.S., Neupert, W., and Westermann, B. (2003). The inner membrane protein Mdm33 controls mitochondrial morphology in yeast. *J. Cell Biol.* **160**, 553–564.
- Dimmer, K.S., Jakobs, S., Vogel, F., Altmann, K., and Westermann, B. (2005). Mdm31 and Mdm32 are inner membrane proteins required for maintenance of mitochondrial shape and stability of mitochondrial DNA nucleoids in yeast. *J. Cell Biol.* **168**, 103–115.
- Okamoto, K., and Shaw, J.M. (2005). Mitochondrial morphology and dynamics in yeast and multicellular eukaryotes. *Annu. Rev. Genet.* **39**, 503–536.
- Nunnari, J., Marshall, W.F., Straight, A., Murray, A., Sedat, J.W., and Walter, P. (1997). Mitochondrial transmission during mating in *Saccharomyces cerevisiae* is determined by mitochondrial fusion and fission and the intramitochondrial segregation of mitochondrial DNA. *Mol. Biol. Cell* **8**, 1233–1242.
- Nakada, K., Inoue, K., Ono, T., Isobe, K., Ogura, A., Goto, Y.I., Nonaka, I., and Hayashi, J.I. (2001). Inter-mitochondrial complementation: Mitochondria-specific system preventing mice from expression of disease phenotypes by mutant mtDNA. *Nat. Med.* **7**, 934–940.
- Garrido, N., Griparic, L., Jokitalo, E., Wartiovaara, J., van der Bliek, A.M., and Spelbrink, J.N. (2003). Composition and dynamics of human mitochondrial nucleoids. *Mol. Biol. Cell* **14**, 1583–1596.
- Legros, F., Malka, F., Frachon, P., Lombes, A., and Rojo, M. (2004). Organization and dynamics of human mitochondrial DNA. *J. Cell Sci.* **117**, 2653–2662.
- Bach, D., Pich, S., Soriano, F.X., Vega, N., Baumgartner, B., Oriola, J., Daugaard, J.R., Lloberas, J., Camps, M., Zierath, J.R., et al. (2003). Mitofusin-2 determines mitochondrial network architecture and mitochondrial metabolism. A novel regulatory mechanism altered in obesity. *J. Biol. Chem.* **278**, 17190–17197.
- Pich, S., Bach, D., Briones, P., Liesa, M., Camps, M., Testar, X., Palacin, M., and Zorzano, A. (2005). The Charcot-Marie-Tooth type 2A gene product, Mfn2, up-regulates fuel oxidation through expression of OXPHOS system. *Hum. Mol. Genet.* **14**, 1405–1415.
- Bach, D., Naon, D., Pich, S., Soriano, F.X., Vega, N., Rieusset, J., Laville, M., Guillet, C., Boirie, Y., Wallberg-Henriksson, H., et al. (2005). Expression of Mfn2, the Charcot-Marie-Tooth neuropathy type 2A gene, in human skeletal muscle: effects of type 2 diabetes, obesity, weight loss, and the regulatory role of tumor necrosis factor alpha and interleukin-6. *Diabetes* **54**, 2685–2693.

39. Paltauf-Doburzynska, J., Malli, R., and Graier, W.F. (2004). Hyperglycemic conditions affect shape and Ca²⁺ homeostasis of mitochondria in endothelial cells. *J. Cardiovasc. Pharmacol.* **44**, 423–436.
40. Yu, T., Robotham, J.L., and Yoon, Y. (2006). Increased production of reactive oxygen species in hyperglycemic conditions requires dynamic change of mitochondrial morphology. *Proc. Natl. Acad. Sci. USA* **103**, 2653–2658.
41. Linn, T.C., Pettit, F.H., and Reed, L.J. (1969). Alpha-keto acid dehydrogenase complexes. X. Regulation of the activity of the pyruvate dehydrogenase complex from beef kidney mitochondria by phosphorylation and dephosphorylation. *Proc. Natl. Acad. Sci. USA* **62**, 234–241.
42. Holness, M.J., and Sugden, M.C. (2003). Regulation of pyruvate dehydrogenase complex activity by reversible phosphorylation. *Biochem. Soc. Trans.* **31**, 1143–1151.
43. Wu, P., Sato, J., Zhao, Y., Jaskiewicz, J., Popov, K.M., and Harris, R.A. (1998). Starvation and diabetes increase the amount of pyruvate dehydrogenase kinase isoenzyme 4 in rat heart. *Biochem. J.* **329** (Pt 1), 197–201.
44. Taniguchi, C.M., Emanuelli, B., and Kahn, C.R. (2006). Critical nodes in signalling pathways: insights into insulin action. *Nat. Rev. Mol. Cell. Biol.* **7**, 85–96.
45. Bijur, G.N., and Jope, R.S. (2003). Rapid accumulation of Akt in mitochondria following phosphatidylinositol 3-kinase activation. *J. Neurochem.* **87**, 1427–1435.
46. Cross, D.A., Alessi, D.R., Cohen, P., and Andjelkovich, M., and Hemmings, B.A. (1995). Inhibition of glycogen synthase kinase-3 by insulin mediated by protein kinase B. *Nature* **378**, 785–789.
47. Bijur, G.N., and Jope, R.S. (2003). Glycogen synthase kinase-3 beta is highly activated in nuclei and mitochondria. *Neuroreport* **14**, 2415–2419.
48. Hoshi, M., Takashima, A., Noguchi, K., Murayama, M., Sato, M., Kondo, S., Saitoh, Y., Ishiguro, K., Hoshino, T., and Imahori, K. (1996). Regulation of mitochondrial pyruvate dehydrogenase activity by tau protein kinase I/glycogen synthase kinase 3beta in brain. *Proc. Natl. Acad. Sci. USA* **93**, 2719–2723.
49. Hopper, R.K., Carroll, S., Aponte, A.M., Johnson, D.T., French, S., Shen, R.F., Witzmann, F.A., Harris, R.A., and Balaban, R.S. (2006). Mitochondrial matrix phosphoproteome: Effect of extra mitochondrial calcium. *Biochemistry* **45**, 2524–2536.
50. Rutter, G.A., and Rizzuto, R. (2000). Regulation of mitochondrial metabolism by ER Ca²⁺ release: an intimate connection. *Trends Biochem. Sci.* **25**, 215–221.
51. Pacher, P., and Hajnoczky, G. (2001). Propagation of the apoptotic signal by mitochondrial waves. *EMBO J.* **20**, 4107–4121.
52. Yi, M., Weaver, D., and Hajnoczky, G. (2004). Control of mitochondrial motility and distribution by the calcium signal: a homeostatic circuit. *J. Cell. Biol.* **167**, 661–672.
53. Rizzuto, R. (2003). Calcium mobilization from mitochondria in synaptic transmitter release. *J. Cell. Biol.* **163**, 441–443.
54. Pagliarini, D.J., Wiley, S.E., Kimple, M.E., Dixon, J.R., Kelly, P., Worby, C.A., Casey, P.J., and Dixon, J.E. (2005). Involvement of a mitochondrial phosphatase in the regulation of ATP production and insulin secretion in pancreatic beta cells. *Mol. Cell* **19**, 197–207.
55. Pagliarini, D.J., and Dixon, J.E. (2006). Mitochondrial modulation: reversible phosphorylation takes center stage? *Trends Biochem. Sci.* **31**, 26–34.
56. Cardone, L., Carlucci, A., Affaitati, A., Livigni, A., DeCristofaro, T., Garbi, C., Varrone, S., Ullrich, A., Gottesman, M.E., Avvedimento, E.V., et al. (2004). Mitochondrial AKAP121 binds and targets protein tyrosine phosphatase D1, a novel positive regulator of src signaling. *Mol. Cell. Biol.* **24**, 4613–4626.
57. Itoh, S., Lemay, S., Osawa, M., Che, W., Duan, Y., Tompkins, A., Brookes, P.S., Sheu, S.S., and Abe, J. (2005). Mitochondrial Dok-4 recruits Src kinase and regulates NF-kappaB activation in endothelial cells. *J. Biol. Chem.* **280**, 26383–26396.
58. Livigni, A., Scorziello, A., Agnese, S., Adornetto, A., Carlucci, A., Garbi, C., Castaldo, I., Annunziato, L., Avvedimento, E.V., and Feliciello, A. (2006). Mitochondrial AKAP121 links cAMP and src signaling to oxidative metabolism. *Mol. Biol. Cell* **17**, 263–271.
59. Valente, E.M., Abou-Sleiman, P.M., Caputo, V., Muqit, M.M., Harvey, K., Gispert, S., Ali, Z., Del Turco, D., Bentivoglio, A.R., Healy, D.G., et al. (2004). Hereditary early-onset Parkinson's disease caused by mutations in PINK1. *Science* **304**, 1158–1160.
60. Silvestri, L., Caputo, V., Bellacchio, E., Atonio, L., Dallapiccola, B., Valente, E.M., and Casari, G. (2005). Mitochondrial import and enzymatic activity of PINK1 mutants associated to recessive parkinsonism. *Hum. Mol. Genet.* **14**, 3477–3492.
61. Shen, J. (2004). Protein kinases linked to the pathogenesis of Parkinson's disease. *Neuron* **44**, 575–577.
62. West, A.B., Moore, D.J., Biskup, S., Bugayenko, A., Smith, W.W., Ross, C.A., Dawson, V.L., and Dawson, T.M. (2005). Parkinson's disease-associated mutations in leucine-rich repeat kinase 2 augment kinase activity. *Proc. Natl. Acad. Sci. USA* **102**, 16842–16847.
63. Clark, I.E., Dodson, M.W., Jiang, C., Cao, J.H., Huh, J.R., Seol, J.H., Yoo, S.J., Hay, B.A., and Guo, M. (2006). Drosophila pink1 is required for mitochondrial function and interacts genetically with parkin. *Nature advance online publication* 3 May 2006, doi:10.1038/nature04779.
64. Park, J., Lee, S.B., Lee, S., Kim, Y., Song, S., Kim, S., Bae, E., Kim, J., Shong, M., Kim, J.M., et al. (2006). Mitochondrial dysfunction in Drosophila PINK1 mutants is complemented by parkin. *Nature advance online publication* 3 May 2006, doi:10.1038/nature04788.
65. Kuroda, Y., Mitsui, T., Kunishige, M., Shono, M., Akaike, M., Azuma, H., and Matsumoto, T. (2006). Parkin enhances mitochondrial biogenesis in proliferating cells. *Hum. Mol. Genet.* **15**, 883–895.
66. Hardie, D.G. (2005). New roles for the LKB1→AMPK pathway. *Curr. Opin. Cell Biol.* **17**, 167–173.
67. Jones, R.G., Plas, D.R., Kubek, S., Buzzai, M., Mu, J., Xu, Y., Birnbaum, M.J., and Thompson, C.B. (2005). AMP-activated protein kinase induces a p53-dependent metabolic checkpoint. *Mol. Cell* **18**, 283–293.
68. Harris, S.L., and Levine, A.J. (2005). The p53 pathway: positive and negative feedback loops. *Oncogene* **24**, 2899–2908.
69. Mandal, S., Guptan, P., Owusu-Ansah, E., and Banerjee, U. (2005). Mitochondrial regulation of cell cycle progression during development as revealed by the tenured mutation in Drosophila. *Dev. Cell* **9**, 843–854.
70. Tanaka, K., Kanbe, T., and Kuroiwa, T. (1985). Three-dimensional behaviour of mitochondria during cell division and germ tube formation in the dimorphic yeast *Candida albicans*. *J. Cell Sci.* **73**, 207–220.
71. McConnell, S.J., Stewart, L.C., Talin, A., and Yaffe, M.P. (1990). Temperature-sensitive yeast mutants defective in mitochondrial inheritance. *J. Cell Biol.* **111**, 967–976.
72. Yaffe, M.P. (1999). The machinery of mitochondrial inheritance and behavior. *Science* **283**, 1493–1497.
73. Sesaki, H., and Jensen, R.E. (1999). Division versus fusion: Dnm1p and Fzo1p antagonistically regulate mitochondrial shape. *J. Cell Biol.* **147**, 699–706.
74. Scott, S.V., Cassidy-Stone, A., Meeusen, S.L., and Nunnari, J. (2003). Staying in aerobic shape: how the structural integrity of mitochondria and mitochondrial DNA is maintained. *Curr. Opin. Cell Biol.* **15**, 482–488.
75. Boldogh, I.R., Fehrenbacher, K.L., Yang, H.C., and Pon, L.A. (2005). Mitochondrial movement and inheritance in budding yeast. *Gene* **354**, 28–36.
76. Miyakawa, I., Aoi, H., Sando, N., and Kuroiwa, T. (1984). Fluorescence microscopic studies of mitochondrial nucleoids during meiosis and sporulation in the yeast, *Saccharomyces cerevisiae*. *J. Cell Sci.* **66**, 21–38.
77. Gorsich, S.W., and Shaw, J.M. (2004). Importance of mitochondrial dynamics during meiosis and sporulation. *Mol. Biol. Cell* **15**, 4369–4381.
78. Neutzner, A., and Youle, R.J. (2005). Instability of the mitofusin Fzo1 regulates mitochondrial morphology during the mating response of the yeast *Saccharomyces cerevisiae*. *J. Biol. Chem.* **280**, 18598–18603.
79. Chen, K.H., Guo, X., Ma, D., Guo, Y., Li, Q., Yang, D., Li, P., Qiu, X., Wen, S., Xiao, R.P., et al. (2004). Dysregulation of HSG triggers vascular proliferative disorders. *Nat. Cell Biol.* **6**, 872–883. Epub. 2004, Aug 2002.
80. Bossy-Wetzel, E., Barsoum, M.J., Godzik, A., Schwarzenbacher, R., and Lipton, S.A. (2003). Mitochondrial fission in apoptosis, neurodegeneration and aging. *Curr. Opin. Cell Biol.* **15**, 706–716.
81. Youle, R.J., and Karbowski, M. (2005). Mitochondrial fission in apoptosis. *Nat. Rev. Mol. Cell Biol.* **6**, 657–663.
82. Bivona, T.G., Quatela, S.E., Bodemann, B.O., Ahearn, I.M., Soskis, M.J., Mor, A., Miura, J., Wiener, H.H., Wright, L., Saba, S.G., et al. (2006). PKC regulates a farnesyl-electrostatic switch on K-Ras that promotes its association with Bcl-XL on mitochondria and induces apoptosis. *Mol. Cell* **21**, 481–493.
83. Rebollo, A., Perez-Sala, D., and Martinez, A.C. (1999). Bcl-2 differentially targets K-, N-, and H-Ras to mitochondria in IL-2 supplemented or deprived cells: implications in prevention of apoptosis. *Oncogene* **18**, 4930–4939.
84. Plowman, S.J., Muncke, C., Parton, R.G., and Hancock, J.F. (2005). H-ras, K-ras, and inner plasma membrane raft proteins operate in nanoclusters with differential dependence on the actin cytoskeleton. *Proc. Natl. Acad. Sci. USA* **102**, 15500–15505.

85. Prior, I.A., Muncke, C., Parton, R.G., and Hancock, J.F. (2003). Direct visualization of Ras proteins in spatially distinct cell surface microdomains. *J. Cell Biol.* **160**, 165–170.
86. Mihara, M., Erster, S., Zaika, A., Petrenko, O., Chittenden, T., Pancoska, P., and Moll, U.M. (2003). p53 has a direct apoptogenic role at the mitochondria. *Mol. Cell* **11**, 577–590.
87. Moll, U.M., Wolff, S., Speidel, D., and Deppert, W. (2005). Transcription-independent pro-apoptotic functions of p53. *Curr. Opin. Cell Biol.* **17**, 631–636.
88. Seth, R.B., Sun, L., Ea, C.K., and Chen, Z.J. (2005). Identification and characterization of MAVS, a mitochondrial antiviral signaling protein that activates NF- κ B and IRF 3. *Cell* **122**, 669–682.
89. Xu, L.G., Wang, Y.Y., Han, K.J., Li, L.Y., Zhai, Z., and Shu, H.B. (2005). VISA is an adapter protein required for virus-triggered IFN- β signaling. *Mol. Cell* **19**, 727–740.
90. Kawai, T., Takahashi, K., Sato, S., Coban, C., Kumar, H., Kato, H., Ishii, K.J., Takeuchi, O., and Akira, S. (2005). IPS-1, an adaptor triggering RIG-I- and Mda5-mediated type I interferon induction. *Nat. Immunol.* **6**, 981–988.
91. Meylan, E., Curran, J., Hofmann, K., Moradpour, D., Binder, M., Bartenschlager, R., and Tschopp, J. (2005). Cardif is an adaptor protein in the RIG-I antiviral pathway and is targeted by hepatitis C virus. *Nature* **437**, 1167–1172.
92. Kawai, T., and Akira, S. (2006). Innate immune recognition of viral infection. *Nat. Immunol.* **7**, 131–137.
93. Siskind, L.J., Kolesnick, R.N., and Colombini, M. (2002). Ceramide channels increase the permeability of the mitochondrial outer membrane to small proteins. *J. Biol. Chem.* **277**, 26796–26803.
94. van Blitterswijk, W.J., van der Luit, A.H., Veldman, R.J., Verheij, M., and Borst, J. (2003). Ceramide: second messenger or modulator of membrane structure and dynamics? *Biochem. J.* **369**, 199–211.
95. Garcia-Ruiz, C., Colell, A., Morales, A., Calvo, M., Enrich, C., and Fernandez-Checa, J.C. (2002). Trafficking of ganglioside GD3 to mitochondria by tumor necrosis factor- α . *J. Biol. Chem.* **277**, 36443–36448.
96. Garcia-Ruiz, C., Colell, A., Mari, M., Morales, A., Calvo, M., Enrich, C., and Fernandez-Checa, J.C. (2003). Defective TNF- α -mediated hepatocellular apoptosis and liver damage in acidic sphingomyelinase knockout mice. *J. Clin. Invest.* **111**, 197–208.
97. Colell, A., Garcia-Ruiz, C., Roman, J., Ballesta, A., and Fernandez-Checa, J.C. (2001). Ganglioside GD3 enhances apoptosis by suppressing the nuclear factor- κ B-dependent survival pathway. *Faseb. J.* **15**, 1068–1070.
98. Nemoto, Y., and De Camilli, P. (1999). Recruitment of an alternatively spliced form of synaptotagmin 2 to mitochondria by the interaction with the PDZ domain of a mitochondrial outer membrane protein. *EMBO J.* **18**, 2991–3006.
99. Speed, C.J., Matzaris, M., Bird, P.I., and Mitchell, C.A. (1995). Tissue distribution and intracellular localisation of the 75-kDa inositol polyphosphate 5-phosphatase. *Eur. J. Biochem.* **234**, 216–224.
100. Zerial, M., and McBride, H. (2001). Rab proteins as membrane organizers. *Nat. Rev. Mol. Cell Biol.* **2**, 107–117.
101. Munro, S. (2002). Organelle identity and the targeting of peripheral membrane proteins. *Curr. Opin. Cell Biol.* **14**, 506–514.
102. Seabra, M.C., and Coudrier, E. (2004). Rab GTPases and myosin motors in organelle motility. *Traffic* **5**, 393–399.
103. Alto, N.M., Soderling, J., and Scott, J.D. (2002). Rab32 is an A-kinase anchoring protein and participates in mitochondrial dynamics. *J. Cell Biol.* **158**, 659–668.
104. Boldogh, I.R., Ramcharan, S.L., Yang, H.C., and Pon, L.A. (2004). A type V myosin (Myo2p) and a Rab-like G-protein (Ypt11p) are required for retention of newly inherited mitochondria in yeast cells during cell division. *Mol. Biol. Cell* **15**, 3994–4002.
105. Starnes, M. (2002). Regulating the actin cytoskeleton during vesicular transport. *Curr. Opin. Cell Biol.* **14**, 428–433.
106. Boldogh, I.R., Yang, H.C., Nowakowski, W.D., Karmon, S.L., Hays, L.G., Yates, J.R., III, and Pon, L.A. (2001). Arp2/3 complex and actin dynamics are required for actin-based mitochondrial motility in yeast. *Proc. Natl. Acad. Sci. USA* **98**, 3162–3167.
107. Fehrenbacher, K.L., Yang, H.C., Gay, A.C., Huckaba, T.M., and Pon, L.A. (2004). Live cell imaging of mitochondrial movement along actin cables in budding yeast. *Curr. Biol.* **14**, 1996–2004.
108. Fehrenbacher, K.L., Boldogh, I.R., and Pon, L.A. (2005). A role for Jsn1p in recruiting the Arp2/3 complex to mitochondria in budding yeast. *Mol. Biol. Cell* **16**, 5094–5102.
109. De Vos, K.J., Allan, V.J., Grierson, A.J., and Sheetz, M.P. (2005). Mitochondrial function and actin regulate dynamin-related protein 1-dependent mitochondrial fission. *Curr. Biol.* **15**, 678–683.
110. Bakeeva, L.E., Chentsov Yu, S., and Skulachev, V.P. (1978). Mitochondrial framework (reticulum mitochondriale) in rat diaphragm muscle. *Biochim. Biophys. Acta.* **501**, 349–369.
111. Bakeeva, L.E., Chentsov, Y.S., and Skulachev, V.P. (1981). Ontogenesis of mitochondrial reticulum in rat diaphragm muscle. *Eur. J. Cell Biol.* **25**, 175–181.
112. Bakeeva, L.E., Chentsov Yu, S., and Skulachev, V.P. (1983). Intermitochondrial contacts in myocardiocytes. *J. Mol. Cell Cardiol.* **15**, 413–420.
113. Bereiter-Hahn, J., and Voth, M. (1994). Dynamics of mitochondria in living cells: shape changes, dislocations, fusion, and fission of mitochondria. *Microsc. Res. Tech.* **27**, 198–219.
114. Honda, S., and Hirose, S. (2003). Stage-specific enhanced expression of mitochondrial fusion and fission factors during spermatogenesis in rat testis. *Biochem. Biophys. Res. Commun.* **311**, 424–432.
115. Sugioka, R., Shimizu, S., and Tsujimoto, Y. (2004). Fzo1, a protein involved in mitochondrial fusion, inhibits apoptosis. *J. Biol. Chem.* **279**, 52726–52734.
116. Delivani, P., Adrain, C., Taylor, R.C., Duriez, P.J., and Martin, S.J. (2006). Role for CED-9 and Egl-1 as regulators of mitochondrial fission and fusion dynamics. *Mol. Cell* **21**, 761–773.
117. Chada, S.R., and Hollenbeck, P.J. (2004). Nerve growth factor signaling regulates motility and docking of axonal mitochondria. *Curr. Biol.* **14**, 1272–1276.
118. Minin, A.A., Kulik, A.V., Gyoeva, F.K., Li, Y., Goshima, G., and Gelfand, V.I. (2006). Regulation of mitochondria distribution by RhoA and formins. *J. Cell Sci.* **119**, 659–670.
119. Li, Z., Okamoto, K., Hayashi, Y., and Sheng, M. (2004). The importance of dendritic mitochondria in the morphogenesis and plasticity of spines and synapses. *Cell* **119**, 873–887.
120. Verstreken, P., Ly, C.V., Venken, K.J., Koh, T.W., Zhou, Y., and Bellen, H.J. (2005). Synaptic mitochondria are critical for mobilization of reserve pool vesicles at *Drosophila* neuromuscular junctions. *Neuron* **47**, 365–378.
121. Guo, X., Macleod, G.T., Wellington, A., Hu, F., Panchumarthi, S., Schoenfield, M., Marin, L., Charlton, M.P., Atwood, H.L., and Zinsmaier, K.E. (2005). The GTPase dMiro is required for axonal transport of mitochondria to *Drosophila* synapses. *Neuron* **47**, 379–393.
122. Kijima, K., Numakura, C., Izumino, H., Umetsu, K., Nezu, A., Shiiki, T., Ogawa, M., Ishizaki, Y., Kitamura, T., Shozawa, Y., et al. (2005). Mitochondrial GTPase mitofusin 2 mutation in Charcot-Marie-Tooth neuropathy type 2A. *Hum. Genet.* **116**, 23–27.
123. Delettre, C., Lenaers, G., Griffoin, J.M., Gigarel, N., Lorenzo, C., Belleguer, P., Pelloquin, L., Grosgeorge, J., Turc-Carel, C., Perret, E., et al. (2000). Nuclear gene OPA1, encoding a mitochondrial dynamin-related protein, is mutated in dominant optic atrophy. *Nat. Genet.* **26**, 207–210.

Supplemental Table 1: Proteins Modulating Mitochondrial Morphology and Signaling.

Protein*	Location**	Known Function	Ref.
Proteins Implicated in Fusion			
Fzo1p / Mfm1 / Fzo	OMM	Dynamain family of GTPases, contains 2 heptad repeats required for tethering and fusion.	[1-6]
Mfm2 / HSG/dMfn	OMM	Dynamain family of GTPases, shown to also exhibit regulatory properties, 60% identical to Mfm1. Mutations found in CMT2A	[113-17]
Mgm1p / Opa1 / Opa1-like	IMS and IMM	Dynamain like GTPase, coiled coils. 8 splice variants in human, cleavage patterns upon import are complex. Opa1 mutations found in DOA. Required for fusion and cristae structure. Mgm1p binds Fzo1p in complex with Ugo1p. Fly mutant also shows mitochondrial dysfunction, similar to rhomboid-7 mutations.	[20-27, 164]
Rbd1p/pcp1p / Mdm37 / PARL / rhomboid-7	IMM	Rhomboid family of 7 transmembrane IMM serine protease. PARL is processed upon import. Rbd1p cleaves Mgm1p in yeast. Fly knock-out shows mitochondrial dysfunction and neurological defects.	[29-33, 164]
Usp1p / PRELI	IMS	Usp1p is involved in the sorting and cleavage of Mgm1p and maintaining mitochondrial shape. Human PRELI rescued the Usp1p null.	[162]
Ugo1p	OMM	Contains a carrier Motif, and is part of complex with Fzo1p and Mgm1p. Human orthologue unknown.	[26, 27, 36]
Mdm30p	Peripheral	F-Box motif. Involved in mitochondrial protein degradation.	[40, 41, 163]
Proteins Implicated in Fission			
Dnm1p / DRP1/Dlp1	Peripheral	GTPase, mechanoenzyme. Dnm1p is recruited through Mdv1p/Fis1p complex. Oligomerizes to form rings that constrict around the mitochondria. DRP1 required for fission and cristae remodeling during apoptotic stimuli.	[46-51]
Fis1p / hFis1	OMM	TPR repeats, implicated in the control of Drp1 recruitment and activation of fission complexes. Required for apoptosis.	[53-57]
Mdv1p	Peripheral	WD40 Repeats. adaptor linking Fis1p with Dnm1p and regulates Dnm1p self-assembly.	[54, 59-61]
Ca4	Peripheral	WD40 Repeats, component of the mitochondrial fission machinery and recruits Dnm1p to mitochondria	[63]
Endophilin B / Bif1	Peripheral	Contains BAR membrane binding domain, binds Bax. Loss of Endophilin leads to outer membrane tubules without apparent inner membrane.	[65-67]
SUMO1	Peripheral	Ubiquitin-like modifying enzyme that covalently and reversibly modifies DRP1, stimulates fission	[71]
GDAP1	OMM	Required for fission, function unknown. Contains GST domains. Mutations found in CMT4A	[73]
Mip18	IMM	Involved in fission of the mitochondrial IMM. Mip18 activity is regulated by phosphatidylinositol 3-kinase activity.	[75, 76]
Dap3	Matrix	Involved in mitochondrial fission post apoptosis. Contains a GTPase domain essential for fission.	[79-81]
Rab32	Peripheral	Regulatory GTPase, participates in both mitochondrial anchoring of PKA and mitochondrial dynamics.	[7]
Proteins required for Maintenance of IMM Architecture			
Mdm31	IMM	Maintenance of mitochondrial shape and stability of mitochondrial DNA nucleoids. Regulates mitochondrial cation homeostasis.	[87, 88]
Mdm32	IMM	Maintenance of mitochondrial shape and stability of mitochondrial DNA nucleoids. Regulates mitochondrial cation homeostasis.	[87, 88]
Mdm33	IMM	Loss of Mdm33 results in large, fused, hollow mitochondria.	[91]
Mdm2	OMM	Maintains mitochondrial shape and required for mtDNA segregation	[87, 94]
IBID	OMM	BH3 only pro-apoptotic protein that causes rapid remodeling of the IMM, including membrane inversion and formation of large cristae junctions. Binds cardiolipin.	[95, 96]
Subunits e or g of ATP synthase	IMM	Non-essential subunits are required to dimerize across the cristae, which appears to hold them together.	[97-99]
Mgm1p / Opa1	IMM/IMS	Dynamain-like protein, required for both fusion (above) and maintenance of cristae architecture.	[20, 22, 24, 101, 102]
Proteins Implicated in Motility			
Mdm10	OMM	Links to mtDNA nucleoids, required for movement, also involved in protein import and assembly	[106, 107]
Mdm12	OMM	Links to mtDNA nucleoids, required for movement.	[110]
Mmm1	Outer and IMM	Links to mtDNA containing nucleoids, required for movement	[106, 112]
Arp23 complex	Peripheral	Complex to initiate the polymerization of actin for mitochondrial motility	[115, 116]
Jsn1p	Peripheral	Pumilo repeats that bind RNA. Recruits Arp23.	[116, 117]
Myo2p	Peripheral	Myosin motor required for retention of mitos in the bud, binds Ypt11p and Mmr1p	[120, 121]
Ypt11p	Peripheral	Regulatory small Rab GTPase required for retention of mitos within the yeast bud.	[121, 123]
Mmr1p	Peripheral	Myo2p-dependent inheritance of mitochondria in the budding yeast	[120]
synaptojanin 2A	Peripheral	Inositol 5'-phosphatase which binds to OMM protein, OMP25. Maintenance of intracellular distribution of mitochondria.	[126, 127]
Mitofin	IMM	Critical organizer of mitochondrial cristae morphology	[130]
mDia1 / Diaphanous	Cytosolic	Formin family effector of RhoA involved in actin polymerization. Arrests mitochondrial motility.	[133]
Milton	Peripheral	Contains coiled coil domains, function in kinesin-mediated transport of mitochondria to nerve terminals. Interacts with Miro for KHC mediated anterograde transport.	[135-138]
OIP106 / Grif-1	Peripheral	Member of Milton family with long coiled coils. Associates with Kifs5a and Kifs5b	[137]
Gem1 / dMiro	OMM	Contains two EF hands, and two Rho-like GTPase domains, required for motility, function of domains unknown.	[140, 141]
Kif1b/kinesin-1	Peripheral	Primary kinesin to move mitochondria in the anterograde direction	[143, 144]
Kinesin Binding Protein	Peripheral	Regulates mitochondria localization by interaction with a kinesin-like protein Kif1b	[147]
Kif5c	Peripheral	Primary kinesin to move mitochondria in the anterograde direction	[137]
Kinesin 120	Peripheral	Links kinesin to mitochondria	[149]
syntabulin	Peripheral	Mediates anterograde transport of mitochondria along neuronal processes	[151, 152]
tau	Peripheral	Involved in intracellular transport, links to kinesin. GSK-3beta phosphorylation required for mitochondrial transport. Implications in Alzheimer's disease	[154, 155]
KLPG7A	Peripheral	Mitotic kinesin that may direct mitochondria to the spindle pole.	[158]
dynein APLIP1 / JIP-1	Peripheral	Microtubule motor for retrograde transport of mitochondria	[144, 160]
1	Peripheral	Kinesin binding adaptor protein, adaptor for JNK	[161]

Supplemental Table 1: Proteins Modulating Mitochondrial Morphology and Signaling (con't).

Protein	Location	Known Function	Ref.	Protein	Location	Known Function	Ref.
Protein Kinase A	Peripheral	Amplifies cAMP signaling at the mitochondria. Anchored by AKAPs. Recruitment to mitochondria is essential during oocyte maturation. Binds Rab32, phosphorylates BAD. PARK6 gene implicated in autosomal recessive early onset Parkinson Disease. PINK1 reduces the basal neuronal pro-apoptotic activity and protects neurons from staurosporine-induced apoptosis. In flies pink1 genetically interacts with parkin and the null has profound mitochondrial dysfunction.	[7-12]	PTP1D	Peripheral	Non-receptor tyrosine phosphatase recruited to mitochondria by AKAP121. Regulates src activation and EGF signaling.	[8, 12]
PINK1/pink1	IMS	Parkinson's disease gene PARK8 encodes a Leucine-rich repeat kinase 2 protein that contains a GTPase domain and WD40 motifs. Rapid translocation post insulin, or stress signal. Regulatory mechanism affecting mitochondrial glycogen synthase kinase-3beta and ATP beta subunit phosphorylation. Survival-mediated kinase.	[18, 19, 157, 158]	PTPMT1	Matrix	Dual-specific protein tyrosine phosphatase (DS-PTP) family. Regulates ATP production and insulin secretion.	[100]
LRRK2	Peripheral		[28]	SHP-2	IMS	Src homology 2 domain-containing tyrosine phosphatase 2.	[103]
AK1/PKB	Matrix		[34, 35]	PP1	Peripheral	Serine/threonine protein phosphatases targets MC-LR and BCL-2 during mitosis. Ceramide-activated protein phosphatase. Early regulator of Abeta-induced bim expression and cerebral endothelial cell apoptosis via the AK/FKHL1 signaling pathway.	[104, 105]
p53	Peripheral	Pro-apoptotic signal transducer which translocates to the mitochondria. Induces permeabilization of the outer mitochondrial membrane. Metabolic cell cycle checkpoint. Mitochondrial localized pool phosphorylates pyruvate dehydrogenase, leading to reduced enzymatic activity.	[37-39]	PP2A	Peripheral	Serine/threonine phosphatases acting on cAMP-dependent phosphoproteins.	[108, 109]
GSK3-β	Matrix	Translocates upon apoptotic stimuli and phosphorylates pyruvate dehydrogenase kinase and PLS3. PKCδ has been demonstrated to rapidly translocate to mitochondria within the first 5 min of reperfusion.	[42]	PP2Cγ	IMS/IMS	Pyruvate dehydrogenase phosphatase, important in dephosphorylating BMP-activated Smad1 but not TGF-beta-activated Smad2 or Smad3.	[111]
PKC-δ	Peripheral/Matrix	Found to cofractionate with mitochondria and may be involved in mitochondrial tyrosine phosphorylation. Same study also found Src, Fyn, and Csk to cofractionate with mitochondria. Lyn was shown to be within the inner membrane by immunogold labeling. Localizes to mitochondria in response to ROS. PKC-δ and the c-Ab1 kinase function are required for translocation.	[43-45]	Met / PDPs	Matrix and IMS	Other proteins implicated in signaling.	[113, 114]
RIP3	Peripheral	Induces apoptosis and NF-κappaB nuclear translocation. RIP-like Kinase	[52]	PDPs	IMS	PKA adaptor proteins which concentrate and immobilize RI (PKAI) isoforms at the cytoplasmic face of the mitochondria. Implicated in regulation of metabolism, signaling and morphology.	[7-11, 116, 119]
MEK	Matrix	Found to phosphorylate and activate ERK1/2 in the matrix. ERK phosphorylates BAD and functions as an anti-apoptotic.	[58]	S-AKAP84, AKAP121, D AKAP1, AKAP148	Peripheral	Sensitizes resting human T lymphocytes to Fas (CD95)-mediated cell death via mitochondrial hyperpolarization, budding, and fission	[122]
Raf-1	Peripheral	Mitochondrial localization regulated by p21-activated Kinase 1 (Pak1)-dependent phosphorylation. Protects cells from apoptosis, independently of its signals to MEK and ERK, by translocating to the mitochondria where it binds Bcl-2 and displaces BAD.	[62]	Gal-1	Peripheral	Translocates to the mitochondria of breast cancer. Inhibit mROS by rapidly up-regulating manganese superoxide dismutase activity effectively interfering survival of the tumor cells	[124]
ERK1/2	Matrix	Pivotal regulator of endothelial cell survival during angiogenesis	[64]	Estrogen Receptor	Peripheral	Interacts with the mitochondrial-associated Raf-1 pool. May regulate signaling between plasma membrane receptors and the mitochondria	[125]
JNK	Peripheral	Component of Raf/MEK signaling pathway. ERK1/2 translocation to mitochondria in brain during development. Phosphorylated ERK/MAP kinases localized to mitochondria and autophagosomes in Lewy body diseases.	[68-70]	Grib10	Peripheral	possesses phosphatase activity. Important for both mitochondrial function and early neuronal development. Cooperates with Tim23, to facilitate transfer of the translocating protein from the TOM complex to the TIM23 complex.	[128, 129]
SAPK3	Peripheral	Stress activated protein kinase 3 phosphorylates the mitochondrial protein Sab, an in vitro substrate of c-Jun N-terminal kinase (JNK). Binds to OMP25, which inhibits SAPK3 catalytic activity.	[74]	Tim50 / Tim50	IMS	K-Ras is phosphorylated by PKC then translocates to mitochondria. Associates with Bcl-XL on mitochondria and induces apoptosis	[131, 132]
CDK1	Peripheral	Subfamily of Cdc2-related Ser/Thr kinase specifically expressed in neurons. Interacts with Trap.	[77, 78]	K-Ras / N-Ras / H-Ras	Peripheral	MAPK phosphatase 1. Following NGF stimulation, MKP-1 protein mainly localizes on mitochondria, where it interacts with p38 MAPK.	[134]
PCTAIRE-2	Peripheral	Myotonic dystrophy protein kinase is a member of the Rho kinase family with a tail-anchored domain. Spliced variants target mitochondria. Human variant A causes altered mitochondrial distribution and dynamics possibly via cytoskeletal regulation.	[82]	MKP-1	Peripheral	Membrane-associated Dub (deubiquitinating enzymes)	[139]
DMPK	OMM	Phosphatidylinositol kinase-related kinase family localized at plasma membrane and regulates cell growth, however a mitochondrial pool is involved in the regulation of osmotic stress.	[83, 84]	Ubp16	OMM	Tudor repeat associator with PCTAIRE 2 Physiological partner of PCTAIRE 2 in terminally differentiated neurons. Localized to mitochondria.	[83, 84]
mTOR	Peripheral	Recruited through AKAP121 and PTPD1 complex as well as through the adaptor Dok-4. Involved in NF-κb and EGF signaling, and shown to participate with PKA in regulating the expression and activity of Complex 1 subunits.	[89]	Trap	Peripheral	2',3'-cyclic nucleotide-3'-phosphodiesterase localized specifically to mitochondria in non-myelinating cells. PKC-mediated phosphorylation of the targeting signal inhibits CNP2 translocation to mitochondria. Is imported in the prenylated form. Proposed function in RNA metabolism.	[142]
Src	Matrix/Peripheral	Regulate glucose oxidation through inhibitory phosphorylation of the pyruvate dehydrogenase complex (PDC). deltaPKC localizes to the mitochondria during reperfusion resulting in activation of PDK2 and phosphorylation-dependent inhibition of PDH.	[8, 12, 90]	CNP2	IMS	Regulates TGF-β superfamily signaling. Shown to protect cardiomyocytes from apoptosis	[145, 146]
PDK(1-4)	Matrix		[45, 92, 93]	Smaad5	ND	Transmembrane glycoprotein overexpressed in most human carcinomas is delivered to mitochondria by a mechanism involving activation of the ErbB receptor-γ-c-Src pathway and transport by the molecular chaperone HSP70/HSP90 complex.	[148]

*Black: *S. cerevisiae*. Red: *H. sapiens*. Blue: *D. melanogaster*

**OMM: integral outer mitochondrial membrane; IMM: integral inner mitochondrial membrane; IMS: intermembrane space; ND: sub-mitochondrial localization not determined.

Supplementary References

1. Hales, K.G., and Fuller, M.T. (1997). Developmentally regulated mitochondrial fusion mediated by a conserved, novel, predicted GTPase. *Cell* 90, 121-129.
2. Hermann, G.J., Thatcher, J.W., Mills, J.P., Hales, K.G., Fuller, M.T., Nunnari, J., and Shaw, J.M. (1998). Mitochondrial fusion in yeast requires the transmembrane GTPase Fzo1p. *J. Cell Biol.* 143, 359-373.
3. Rapaport, D., Brunner, M., Neupert, W., and Westerman, B. (1998). Fzo1p is a mitochondrial outer membrane protein essential for the biogenesis of functional mitochondria in *Saccharomyces cerevisiae*. *J. Biol. Chem.* 273, 20150-20155.
4. Legros, F., Lombes, A., Frachon, P., and Rojo, M. (2002). Mitochondrial fusion in human cells is efficient, requires the inner membrane potential, and is mediated by mitofusins. *Mol Biol Cell* 13, 4343-4354.
5. Santel, A., Frank, S., Gaume, B., Herrler, M., Youle, R.J., and Fuller, M.T. (2003). Mitofusin-1 protein is a generally expressed mediator of mitochondrial fusion in mammalian cells. *J Cell Sci* 116, 2763-2774.
6. Griffin, E.E., and Chan, D.C. (2006). Domain interactions within Fzo1 oligomers are essential for mitochondrial fusion. *J Biol Chem.* 281:16599-606
7. Alto, N.M., Soderling, J., and Scott, J.D. (2002). Rab32 is an A-kinase anchoring protein and participates in mitochondrial dynamics. *J Cell Biol* 158, 659-668.
8. Cardone, L., Carlucci, A., Affaitati, A., Livigni, A., DeCristofaro, T., Garbi, C., Varrone, S., Ullrich, A., Gottesman, M.E., Avvedimento, E.V., and Feliciello, A. (2004). Mitochondrial AKAP121 binds and targets protein tyrosine phosphatase D1, a novel positive regulator of src signaling. *Mol Cell Biol* 24, 4613-4626.
9. Harada, H., Becknell, B., Wilm, M., Mann, M., Huang, L.J., Taylor, S.S., Scott, J.D., and Korsmeyer, S.J. (1999). Phosphorylation and inactivation of BAD by mitochondria-anchored protein kinase A. *Mol Cell* 3, 413-422.
10. Huang, L.J., Wang, L., Ma, Y., Durick, K., Perkins, G., Deerinck, T.J., Ellisman, M.H., and Taylor, S.S. (1999). NH2-Terminal targeting motifs direct dual specificity A-kinase-anchoring protein 1 (D-AKAP1) to either mitochondria or endoplasmic reticulum. *J Cell Biol* 145, 951-959.
11. Newhall, K.J., Criniti, A.R., Cheah, C.S., Smith, K.C., Kafer, K.E., Burkart, A.D., and McKnight, G.S. (2006). Dynamic anchoring of PKA is essential during oocyte maturation. *Curr Biol* 16, 321-327.
12. Livigni, A., Scorziello, A., Agnese, S., Adornetto, A., Carlucci, A., Garbi, C., Castaldo, I., Annunziato, L., Avvedimento, E.V., and Feliciello, A. (2006). Mitochondrial AKAP121 links cAMP and src signaling to oxidative metabolism. *Mol Biol Cell* 17, 263-271.
13. Santel, A., and Fuller, M.T. (2001). Control of mitochondrial morphology by a human mitofusin. *J. Cell Sci.* 114, 867-874.
14. Hwa, J.J., Hiller, M.A., Fuller, M.T., and Santel, A. (2002). Differential expression of the *Drosophila* mitofusin genes *fuzzy onions* (*fzo*) and *dmfn*. *Mech Dev* 116, 213-216.
15. Rojo, M., Legros, F., Chateau, D., and Lombes, A. (2002). Membrane topology and mitochondrial targeting of mitofusins, ubiquitous mammalian homologs of the transmembrane GTPase Fzo. *J Cell Sci* 115, 1663-1674.

16. Chen, K.H., Guo, X., Ma, D., Guo, Y., Li, Q., Yang, D., Li, P., Qiu, X., Wen, S., Xiao, R.P., and Tang, J. (2004). Dysregulation of HSG triggers vascular proliferative disorders. *Nat Cell Biol* 6, 872-883. Epub 2004 Aug 22.
17. Zuchner, S., Mersiyanova, I.V., Muglia, M., Bissar-Tadmouri, N., Rochelle, J., Dadali, E.L., Zappia, M., Nelis, E., Patitucci, A., Senderek, J., Parman, Y., Evgrafov, O., Jonghe, P.D., Takahashi, Y., Tsuji, S., Pericak-Vance, M.A., Quattrone, A., Battaloglu, E., Polyakov, A.V., Timmerman, V., Schroder, J.M., and Vance, J.M. (2004). Mutations in the mitochondrial GTPase mitofusin 2 cause Charcot-Marie-Tooth neuropathy type 2A. *Nat Genet* 36, 449-451.
18. Unoki, M., and Nakamura, Y. (2001). Growth-suppressive effects of BPOZ and EGR2, two genes involved in the PTEN signaling pathway. *Oncogene* 20, 4457-4465.
19. Beilina, A., Van Der Brug, M., Ahmad, R., Kesavapany, S., Miller, D.W., Petsko, G.A., and Cookson, M.R. (2005). Mutations in PTEN-induced putative kinase 1 associated with recessive parkinsonism have differential effects on protein stability. *Proc Natl Acad Sci U S A* 102, 5703-5708.
20. Alexander, C., Votruba, M., Pesch, U.E., Thiselton, D.L., Mayer, S., Moore, A., Rodriguez, M., Kellner, U., Leo-Kottler, B., Auburger, G., Bhattacharya, S.S., and Wissinger, B. (2000). OPA1, encoding a dynamin-related GTPase, is mutated in autosomal dominant optic atrophy linked to chromosome 3q28. *Nat. Genet.* 26, 211-215.
21. Delettre, C., Lenaers, G., Griffoin, J.M., Gigarel, N., Lorenzo, C., Belenguer, P., Pelloquin, L., Grosgeorge, J., Turc-Carel, C., Perret, E., Astarie-Dequeker, C., Lasquelléc, L., Arnaud, B., Ducommun, B., Kaplan, J., and Hamel, C.P. (2000). Nuclear gene OPA1, encoding a mitochondrial dynamin-related protein, is mutated in dominant optic atrophy. *Nat. Genet.* 26, 207-210.
22. Olichon, A., Emorine, L.J., Descoins, E., Pelloquin, L., Bricchese, L., Gas, N., Guillou, E., Delettre, C., Valette, A., Hamel, C.P., Ducommun, B., Lenaers, G., and Belenguer, P. (2002). The human dynamin-related protein OPA1 is anchored to the mitochondrial inner membrane facing the inter-membrane space. *FEBS Lett* 523, 171-176.
23. Satoh, M., Hamamoto, T., Seo, N., Kagawa, Y., and Endo, H. (2003). Differential sublocalization of the dynamin-related protein OPA1 isoforms in mitochondria. *Biochem Biophys Res Commun* 300, 482-493.
24. Shepard, K.A., and Yaffe, M.P. (1999). The yeast dynamin-like protein, Mgm1p, functions on the mitochondrial outer membrane to mediate mitochondrial inheritance. *J. Cell Biol.* 144, 711-720.
25. Wong, E.D., Wagner, J.A., Gorsich, S.W., McCaffery, J.M., Shaw, J.M., and Nunnari, J. (2000). The dynamin-related GTPase, Mgm1p, is an intermembrane space protein required for maintenance of fusion competent mitochondria. *J. Cell Biol.* 151, 341-352.
26. Wong, E.D., Wagner, J.A., Scott, S.V., Okreglak, V., Holewinski, T.J., Cassidy-Stone, A., and Nunnari, J. (2003). The intramitochondrial dynamin-related GTPase, Mgm1p, is a component of a protein complex that mediates mitochondrial fusion. *J Cell Biol* 160, 303-311.
27. Sesaki, H., and Jensen, R.E. (2004). Ugo1p links the Fzo1p and Mgm1p GTPases for mitochondrial fusion. *J Biol Chem* 14, 14.
28. Li, C., and Beal, M.F. (2005). Leucine-rich repeat kinase 2: a new player with a familiar theme for Parkinson's disease pathogenesis. *Proc Natl Acad Sci U S A* 102, 16535-16536.
29. Herlan, M., Vogel, F., Bornhovd, C., Neupert, W., and Reichert, A.S. (2003). Processing of Mgm1 by the rhomboid-type protease Pcp1 is required for maintenance of mitochondrial morphology and of mitochondrial DNA. *J Biol Chem* 278, 27781-27788.

30. Koonin, E.V., Makarova, K.S., Rogozin, I.B., Davidovic, L., Letellier, M.C., and Pellegrini, L. (2003). The rhomboids: a nearly ubiquitous family of intramembrane serine proteases that probably evolved by multiple ancient horizontal gene transfers. *Genome Biol* 4, R19.
31. McQuibban, G.A., Saurya, S., and Freeman, M. (2003). Mitochondrial membrane remodelling regulated by a conserved rhomboid protease. *Nature* 423, 537-541.
32. Sesaki, H., Southard, S.M., Hobbs, A.E., and Jensen, R.E. (2003). Cells lacking Pcp1p/Ugo2p, a rhomboid-like protease required for Mgm1p processing, lose mtDNA and mitochondrial structure in a Dnm1p-dependent manner, but remain competent for mitochondrial fusion. *Biochem Biophys Res Commun* 308, 276-283.
33. Sik, A., Passer, B.J., Koonin, E.V., and Pellegrini, L. (2004). Self-regulated cleavage of the mitochondrial intramembrane-cleaving protease PARL yields Pbeta, a nuclear-targeted peptide. *J Biol Chem* 279, 15323-15329.
34. Bijur, G.N., and Jope, R.S. (2003). Rapid accumulation of Akt in mitochondria following phosphatidylinositol 3-kinase activation. *J Neurochem* 87, 1427-1435.
35. Plas, D.R., and Thompson, C.B. (2005). Akt-dependent transformation: there is more to growth than just surviving. *Oncogene* 24, 7435-7442.
36. Sesaki, H., and Jensen, R.E. (2001). UGO1 encodes an outer membrane protein required for mitochondrial fusion. *J Cell Biol* 152, 1123-1134.
37. Mihara, M., Erster, S., Zaika, A., Petrenko, O., Chittenden, T., Pancoska, P., and Moll, U.M. (2003). p53 has a direct apoptogenic role at the mitochondria. *Mol Cell* 11, 577-590.
38. Jones, R.G., Plas, D.R., Kubek, S., Buzzai, M., Mu, J., Xu, Y., Birnbaum, M.J., and Thompson, C.B. (2005). AMP-activated protein kinase induces a p53-dependent metabolic checkpoint. *Mol Cell* 18, 283-293.
39. Moll, U.M., Wolff, S., Speidel, D., and Deppert, W. (2005). Transcription-independent pro-apoptotic functions of p53. *Curr Opin Cell Biol* 17, 631-636.
40. Fritz, S., Weinbach, N., and Westermann, B. (2003). Mdm30 is an F-box protein required for maintenance of fusion-competent mitochondria in yeast. *Mol Biol Cell* 14, 2303-2313.
41. Neutzner, A., and Youle, R.J. (2005). Instability of the mitofusin Fzo1 regulates mitochondrial morphology during the mating response of the yeast *Saccharomyces cerevisiae*. *J Biol Chem* 280, 18598-18603.
42. Bijur, G.N., and Jope, R.S. (2003). Glycogen synthase kinase-3 beta is highly activated in nuclei and mitochondria. *Neuroreport* 14, 2415-2419.
43. Majumder, P.K., Mishra, N.C., Sun, X., Bharti, A., Kharbanda, S., Saxena, S., and Kufe, D. (2001). Targeting of protein kinase C delta to mitochondria in the oxidative stress response. *Cell Growth Differ* 12, 465-470.
44. Liu, J., Chen, J., Dai, Q., and Lee, R.M. (2003). Phospholipid scramblase 3 is the mitochondrial target of protein kinase C delta-induced apoptosis. *Cancer Res* 63, 1153-1156.
45. Churchill, E.N., Murriel, C.L., Chen, C.H., Mochly-Rosen, D., and Szweda, L.I. (2005). Reperfusion-induced translocation of deltaPKC to cardiac mitochondria prevents pyruvate dehydrogenase reactivation. *Circ Res* 97, 78-85.
46. Bleazard, W., McCaffery, J.M., King, E.J., Bale, S., Mozdy, A., Tieu, Q., Nunnari, J., and Shaw, J.M. (1999). The dynamin-related GTPase Dnm1 regulates mitochondrial fission in yeast. *Nature Cell Biol* 1, 298 - 304.
47. Otsuga, D., Keegan, B.R., Brisch, E., Thatcher, J.W., Hermann, G.J., Bleazard, W., and Shaw, J.M. (1998). The dynamin-related GTPase, Dnm1p, controls mitochondrial morphology in yeast. *J. Cell Biol.* 143, 333-349.

48. Smirnova, E., Shurland, D.-L., Ryazantsev, S.N., and van der Blik, A.M. (1998). A human dynamin-related protein controls the distribution of mitochondria. *J. Cell Biol.* *143*, 351-358.
49. Yoon, Y., Pitts, K.R., and McNiven, M.A. (2001). Mammalian dynamin-like protein dlp1 tubulates membranes. *Mol. Biol. Cell* *12*, 2894-2905.
50. Frank, S., Gaume, B., Bergmann-Leitner, E.S., Leitner, W.W., Robert, E.G., Catez, F., Smith, C.L., and Youle, R.J. (2001). The role of dynamin-related protein 1, a mediator of mitochondrial fission, in apoptosis. *Dev Cell* *1*, 515-525.
51. Germain, M., Mathai, J.P., McBride, H.M., and Shore, G.C. (2005). Endoplasmic reticulum BIK initiates DRP1-regulated remodelling of mitochondrial cristae during apoptosis. *EMBO J* *24*, 1546-1556.
52. Salvi, M., Brunati, A.M., Bordin, L., La Rocca, N., Clari, G., and Toninello, A. (2002). Characterization and location of Src-dependent tyrosine phosphorylation in rat brain mitochondria. *Biochim Biophys Acta* *1589*, 181-195.
53. Mozdy, A.D., McCaffery, J.M., and Shaw, J.M. (2000). Dnm1p GTPase-mediated mitochondrial fission is a multi-step process requiring the novel integral membrane component Fis1p. *J Cell Biol.* *151*, 367-380.
54. Tieu, Q., Okreglak, V., Naylor, K., and Nunnari, J. (2002). The WD repeat protein, Mdv1p, functions as a molecular adaptor by interacting with Dnm1p and Fis1p during mitochondrial fission. *J Cell Biol* *158*, 445-452.
55. James, D.I., Parone, P.A., Mattenberger, Y., and Martinou, J.C. (2003). hFis1, a novel component of the mammalian mitochondrial fission machinery. *J Biol Chem* *278*, 36373-36379.
56. Yoon, Y., Krueger, E.W., Oswald, B.J., and McNiven, M.A. (2003). The mitochondrial protein hFis1 regulates mitochondrial fission in mammalian cells through an interaction with the dynamin-like protein DLP1. *Mol Cell Biol* *23*, 5409-5420.
57. Yu, T., Fox, R.J., Burwell, L.S., and Yoon, Y. (2005). Regulation of mitochondrial fission and apoptosis by the mitochondrial outer membrane protein hFis1. *J Cell Sci* *118*, 4141-4151.
58. Kumar, S., Bharti, A., Mishra, N.C., Raina, D., Kharbanda, S., Saxena, S., and Kufe, D. (2001). Targeting of the c-Abl tyrosine kinase to mitochondria in the necrotic cell death response to oxidative stress. *J Biol Chem* *276*, 17281-17285.
59. Fekkes, P., Shepard, K.A., and Yaffe, M.P. (2000). Gag3p, an outer membrane protein required for fission of mitochondrial tubules. *J. Cell Biol.* *151*, 333-340.
60. Cerveny, K.L., McCaffery, J.M., and Jensen, R.E. (2001). Division of mitochondria requires a novel DMN1-interacting protein, Net2p. *Mol Biol Cell* *12*, 309-321.
61. Naylor, K., Ingerman, E., Okreglak, V., Marino, M., Hinshaw, J.E., and Nunnari, J. (2006). Mdv1 interacts with assembled dnm1 to promote mitochondrial division. *J Biol Chem* *281*, 2177-2183.
62. Kasof, G.M., Prosser, J.C., Liu, D., Lorenzi, M.V., and Gomes, B.C. (2000). The RIP-like kinase, RIP3, induces apoptosis and NF-kappaB nuclear translocation and localizes to mitochondria. *FEBS Lett* *473*, 285-291.
63. Griffin, E.E., Graumann, J., and Chan, D.C. (2005). The WD40 protein Caf4p is a component of the mitochondrial fission machinery and recruits Dnm1p to mitochondria. *J Cell Biol* *170*, 237-248.
64. Alonso, M., Melani, M., Converso, D., Jaitovich, A., Paz, C., Carreras, M.C., Medina, J.H., and Poderoso, J.J. (2004). Mitochondrial extracellular signal-regulated kinases 1/2 (ERK1/2) are modulated during brain development. *J Neurochem* *89*, 248-256.

65. Takahashi, Y., Karbowski, M., Yamaguchi, H., Kazi, A., Wu, J., Sebti, S.M., Youle, R.J., and Wang, H.G. (2005). Loss of Bif-1 suppresses Bax/Bak conformational change and mitochondrial apoptosis. *Mol Cell Biol* 25, 9369-9382.
66. Karbowski, M., Jeong, S.Y., and Youle, R.J. (2004). Endophilin B1 is required for the maintenance of mitochondrial morphology. *J Cell Biol* 166, 1027-1039.
67. Pierrat, B., Simonen, M., Cueto, M., Mestan, J., Ferrigno, P., and Heim, J. (2001). SH3GLB, a new endophilin-related protein family featuring an SH3 domain. *Genomics* 71, 222-234.
68. Jin, S., Zhuo, Y., Guo, W., and Field, J. (2005). p21-activated Kinase 1 (Pak1)-dependent phosphorylation of Raf-1 regulates its mitochondrial localization, phosphorylation of BAD, and Bcl-2 association. *J Biol Chem* 280, 24698-24705.
69. Wang, H.G., Rapp, U.R., and Reed, J.C. (1996). Bcl-2 targets the protein kinase Raf-1 to mitochondria. *Cell* 87, 629-638.
70. Alavi, A., Hood, J.D., Frausto, R., Stupack, D.G., and Cheresh, D.A. (2003). Role of Raf in vascular protection from distinct apoptotic stimuli. *Science* 301, 94-96.
71. Harder, Z., Zunino, R., and McBride, H. (2004). Sumo1 conjugates mitochondrial substrates and participates in mitochondrial fission. *Curr. Biol.* 14, 340-345.
72. Zhu, J.H., Guo, F., Shelburne, J., Watkins, S., and Chu, C.T. (2003). Localization of phosphorylated ERK/MAP kinases to mitochondria and autophagosomes in Lewy body diseases. *Brain Pathol* 13, 473-481.
73. Niemann, A., Ruegg, M., La Padula, V., Schenone, A., and Suter, U. (2005). Ganglioside-induced differentiation associated protein 1 is a regulator of the mitochondrial network: new implications for Charcot-Marie-Tooth disease. *J Cell Biol* 170, 1067-1078.
74. Bricchese, L., Cazettes, G., and Valette, A. (2004). JNK is associated with Bcl-2 and PP1 in mitochondria: paclitaxel induces its activation and its association with the phosphorylated form of Bcl-2. *Cell Cycle* 3, 1312-1319.
75. Tondera, D., Santel, A., Schwarzer, R., Dames, S., Giese, K., Klippel, A., and Kaufmann, J. (2004). Knockdown of MTP18, a novel phosphatidylinositol 3-kinase-dependent protein, affects mitochondrial morphology and induces apoptosis. *J Biol Chem* 279, 31544-31555.
76. Tondera, D., Czauderna, F., Paulick, K., Schwarzer, R., Kaufmann, J., and Santel, A. (2005). The mitochondrial protein MTP18 contributes to mitochondrial fission in mammalian cells. *J Cell Sci* 118, 3049-3059.
77. Court, N.W., Kuo, I., Quigley, O., and Bogoyevitch, M.A. (2004). Phosphorylation of the mitochondrial protein Sab by stress-activated protein kinase 3. *Biochem Biophys Res Commun* 319, 130-137.
78. Court, N.W., Ingley, E., Klinken, S.P., and Bogoyevitch, M.A. (2005). Outer membrane protein 25-a mitochondrial anchor and inhibitor of stress-activated protein kinase-3. *Biochim Biophys Acta* 1744, 68-75.
79. Kissil, J.L., Deiss, L.P., Bayewitch, M., Raveh, T., Khaspekov, G., and Kimchi, A. (1995). Isolation of DAP3, a novel mediator of interferon-gamma-induced cell death. *J Biol Chem* 270, 27932-27936.
80. Mukamel, Z., and Kimchi, A. (2004). Death-associated protein 3 localizes to the mitochondria and is involved in the process of mitochondrial fragmentation during cell death. *J Biol Chem* 279, 36732-36738.
81. Berger, T., Brigl, M., Herrmann, J.M., Vielhauer, V., Luckow, B., Schlondorff, D., and Kretzler, M. (2000). The apoptosis mediator mDAP-3 is a novel member of a conserved family of mitochondrial proteins. *J Cell Sci* 113 (Pt 20), 3603-3612.

82. Feng, Y., Ariza, M.E., Goulet, A.C., Shi, J., and Nelson, M.A. (2005). Death-signal-induced relocalization of cyclin-dependent kinase 11 to mitochondria. *Biochem J* 392, 65-73.
83. Hirose, T., Kawabuchi, M., Tamaru, T., Okumura, N., Nagai, K., and Okada, M. (2000). Identification of tudor repeat associator with PCTAIRE 2 (Trap). A novel protein that interacts with the N-terminal domain of PCTAIRE 2 in rat brain. *Eur J Biochem* 267, 2113-2121.
84. Hirose, T., Tamaru, T., Okumura, N., Nagai, K., and Okada, M. (1997). PCTAIRE 2, a Cdc2-related serine/threonine kinase, is predominantly expressed in terminally differentiated neurons. *Eur J Biochem* 249, 481-488.
85. Wansink, D.G., van Herpen, R.E., Coerwinkel-Driessen, M.M., Groenen, P.J., Hemmings, B.A., and Wieringa, B. (2003). Alternative splicing controls myotonic dystrophy protein kinase structure, enzymatic activity, and subcellular localization. *Mol Cell Biol* 23, 5489-5501.
86. van Herpen, R.E., Oude Ophuis, R.J., Wijers, M., Bennink, M.B., van de Loo, F.A., Fransen, J., Wieringa, B., and Wansink, D.G. (2005). Divergent mitochondrial and endoplasmic reticulum association of DMPK splice isoforms depends on unique sequence arrangements in tail anchors. *Mol Cell Biol* 25, 1402-1414.
87. Dimmer, K.S., Jakobs, S., Vogel, F., Altmann, K., and Westermann, B. (2005). Mdm31 and Mdm32 are inner membrane proteins required for maintenance of mitochondrial shape and stability of mitochondrial DNA nucleoids in yeast. *J Cell Biol* 168, 103-115.
88. Kucejova, B., Kucej, M., Petrezselyova, S., Abelovska, L., and Tomaska, L. (2005). A screen for nigericin-resistant yeast mutants revealed genes controlling mitochondrial volume and mitochondrial cation homeostasis. *Genetics* 171, 517-526.
89. Desai, B.N., Myers, B.R., and Schreiber, S.L. (2002). FKBP12-rapamycin-associated protein associates with mitochondria and senses osmotic stress via mitochondrial dysfunction. *Proc Natl Acad Sci U S A* 99, 4319-4324.
90. Itoh, S., Lemay, S., Osawa, M., Che, W., Duan, Y., Tompkins, A., Brookes, P.S., Sheu, S.S., and Abe, J. (2005). Mitochondrial Dok-4 recruits Src kinase and regulates NF-kappaB activation in endothelial cells. *J Biol Chem* 280, 26383-26396.
91. Messerschmitt, M., Jakobs, S., Vogel, F., Fritz, S., Dimmer, K.S., Neupert, W., and Westermann, B. (2003). The inner membrane protein Mdm33 controls mitochondrial morphology in yeast. *J Cell Biol* 160, 553-564.
92. Gudi, R., Bowker-Kinley, M.M., Kedishvili, N.Y., Zhao, Y., and Popov, K.M. (1995). Diversity of the pyruvate dehydrogenase kinase gene family in humans. *J Biol Chem* 270, 28989-28994.
93. Sugden, M.C., Lall, H.S., Harris, R.A., and Holness, M.J. (2000). Selective modification of the pyruvate dehydrogenase kinase isoform profile in skeletal muscle in hyperthyroidism: implications for the regulatory impact of glucose on fatty acid oxidation. *J Endocrinol* 167, 339-345.
94. Youngman, M.J., Hobbs, A.E., Burgess, S.M., Srinivasan, M., and Jensen, R.E. (2004). Mmm2p, a mitochondrial outer membrane protein required for yeast mitochondrial shape and maintenance of mtDNA nucleoids. *J Cell Biol* 164, 677-688.
95. Scorrano, L., Ashiya, M., Buttle, K., Weiler, S., Oakes, S.A., Mannella, C.A., and Korsmeyer, S.J. (2002). A Distinct Pathway Remodels Mitochondrial Cristae and Mobilizes Cytochrome c during Apoptosis. *Dev Cell* 2, 55-67.
96. Kim, T.H., Zhao, Y., Ding, W.X., Shin, J.N., He, X., Seo, Y.W., Chen, J., Rabinowich, H., Amoscato, A.A., and Yin, X.M. (2004). Bid-cardiolipin interaction at mitochondrial contact

- site contributes to mitochondrial cristae reorganization and cytochrome C release. *Mol Biol Cell* *15*, 3061-3072. Epub 2004 Apr 3023.
97. Paumard, P., Vaillier, J., Couлары, B., Schaeffer, J., Soubannier, V., Mueller, D.M., Brethes, D., di Rago, J.P., and Velours, J. (2002). The ATP synthase is involved in generating mitochondrial cristae morphology. *Embo J* *21*, 221-230.
 98. Arselin, G., Vaillier, J., Salin, B., Schaeffer, J., Giraud, M.F., Dautant, A., Brethes, D., and Velours, J. (2004). The modulation in subunits e and g amounts of yeast ATP synthase modifies mitochondrial cristae morphology. *J Biol Chem* *279*, 40392-40399.
 99. Bornhovd, C., Vogel, F., Neupert, W., and Reichert, A.S. (2006). Mitochondrial Membrane Potential Is Dependent on the Oligomeric State of F1F0-ATP Synthase Supracomplexes. *J Biol Chem* *281*, 13990-13998.
 100. Pagliarini, D.J., Wiley, S.E., Kimple, M.E., Dixon, J.R., Kelly, P., Worby, C.A., Casey, P.J., and Dixon, J.E. (2005). Involvement of a mitochondrial phosphatase in the regulation of ATP production and insulin secretion in pancreatic beta cells. *Mol Cell* *19*, 197-207.
 101. Guan, K., Farh, L., Marshall, T.K., and Deschenes, R.J. (1993). Normal mitochondrial structure and genome maintenance in yeast requires the dynamin-like product of the MGM1 gene. *Curr Genet* *24*, 141-148.
 102. Kjer, B., Eiberg, H., Kjer, P., and Rosenberg, T. (1996). Dominant optic atrophy mapped to chromosome 3q region. II. Clinical and epidemiological aspects. *Acta Ophthalmol Scand* *74*, 3-7.
 103. Salvi, M., Stringaro, A., Brunati, A.M., Agostinelli, E., Arancia, G., Clari, G., and Toninello, A. (2004). Tyrosine phosphatase activity in mitochondria: presence of Shp-2 phosphatase in mitochondria. *Cell Mol Life Sci* *61*, 2393-2404.
 104. Chen, T., Cui, J., Liang, Y., Xin, X., Owen Young, D., Chen, C., and Shen, P. (2006). Identification of human liver mitochondrial aldehyde dehydrogenase as a potential target for microcystin-LR. *Toxicology* *220*, 71-80.
 105. Brichese, L., and Valette, A. (2002). PP1 phosphatase is involved in Bcl-2 dephosphorylation after prolonged mitotic arrest induced by paclitaxel. *Biochem Biophys Res Commun* *294*, 504-508.
 106. Boldogh, I.R., Nowakowski, D.W., Yang, H.C., Chung, H., Karmon, S., Royes, P., and Pon, L.A. (2003). A protein complex containing Mdm10p, Mdm12p, and Mmm1p links mitochondrial membranes and DNA to the cytoskeleton-based segregation machinery. *Mol Biol Cell* *14*, 4618-4627.
 107. Meisinger, C., Rissler, M., Chacinska, A., Szklarz, L.K., Milenkovic, D., Kozjak, V., Schonfisch, B., Lohaus, C., Meyer, H.E., Yaffe, M.P., Guiard, B., Wiedemann, N., and Pfanner, N. (2004). The mitochondrial morphology protein Mdm10 functions in assembly of the preprotein translocase of the outer membrane. *Dev Cell* *7*, 61-71.
 108. Nagase, T., Murakami, T., Nozaki, H., Inoue, R., Nishito, Y., Tanabe, O., Usui, H., and Takeda, M. (1997). Tissue and subcellular distributions, and characterization of rat brain protein phosphatase 2A containing a 72-kDa delta/B" subunit. *J Biochem (Tokyo)* *122*, 178-187.
 109. Yin, K.J., Hsu, C.Y., Hu, X.Y., Chen, H., Chen, S.W., Xu, J., and Lee, J.M. (2006). Protein phosphatase 2A regulates bim expression via the Akt/FKHRL1 signaling pathway in amyloid-beta peptide-induced cerebrovascular endothelial cell death. *J Neurosci* *26*, 2290-2299.

110. Berger, K.H., Sogo, L.F., and Yaffe, M.P. (1997). Mdm12p, a component required for mitochondrial inheritance that is conserved between budding and fission yeast. *J Cell Biol* 136, 545-553.
111. Signorile, A., Sardanelli, A.M., Nuzzi, R., and Papa, S. (2002). Serine (threonine) phosphatase(s) acting on cAMP-dependent phosphoproteins in mammalian mitochondria. *FEBS Lett* 512, 91-94.
112. Kondo-Okamoto, N., Shaw, J.M., and Okamoto, K. (2003). Mmm1p spans both the outer and inner mitochondrial membranes and contains distinct domains for targeting and foci formation. *J Biol Chem* 278, 48997-49005.
113. Simonot, C., Lerme, F., Louisot, P., and Gateau-Roesch, O. (1997). Sub-mitochondrial localization of the catalytic subunit of pyruvate dehydrogenase phosphatase. *FEBS Lett* 401, 158-162.
114. Chen, H.B., Shen, J., Ip, Y.T., and Xu, L. (2006). Identification of phosphatases for Smad in the BMP/DPP pathway. *Genes Dev* 20, 648-653.
115. Boldogh, I.R., Yang, H.C., Nowakowski, W.D., Karmon, S.L., Hays, L.G., Yates, J.R., 3rd, and Pon, L.A. (2001). Arp2/3 complex and actin dynamics are required for actin-based mitochondrial motility in yeast. *Proc Natl Acad Sci U S A* 98, 3162-3167.
116. McKane, M., Wen, K.K., Boldogh, I.R., Ramcharan, S., Pon, L.A., and Rubenstein, P.A. (2005). A mammalian actin substitution in yeast actin (H372R) causes a suppressible mitochondria/vacuole phenotype. *J Biol Chem* 280, 36494-36501.
117. Fehrenbacher, K.L., Boldogh, I.R., and Pon, L.A. (2005). A role for Jsn1p in recruiting the Arp2/3 complex to mitochondria in budding yeast. *Mol Biol Cell* 16, 5094-5102.
118. Lin, R.Y., Moss, S.B., and Rubin, C.S. (1995). Characterization of S-AKAP84, a novel developmentally regulated A kinase anchor protein of male germ cells. *J Biol Chem* 270, 27804.
119. Chen, Q., Lin, R.Y., and Rubin, C.S. (1997). Organelle-specific targeting of protein kinase AII (PKAII). Molecular and in situ characterization of murine A kinase anchor proteins that recruit regulatory subunits of PKAII to the cytoplasmic surface of mitochondria. *J Biol Chem* 272, 15247-15257.
120. Itoh, T., Toh, E.A., and Matsui, Y. (2004). Mmr1p is a mitochondrial factor for Myo2p-dependent inheritance of mitochondria in the budding yeast. *Embo J* 23, 2520-2530.
121. Boldogh, I.R., Ramcharan, S.L., Yang, H.C., and Pon, L.A. (2004). A type V myosin (Myo2p) and a Rab-like G-protein (Ypt11p) are required for retention of newly inherited mitochondria in yeast cells during cell division. *Mol Biol Cell* 15, 3994-4002.
122. Matarrese, P., Tinari, A., Mormone, E., Bianco, G.A., Toscano, M.A., Ascione, B., Rabinovich, G.A., and Malorni, W. (2005). Galectin-1 sensitizes resting human T lymphocytes to Fas (CD95)-mediated cell death via mitochondrial hyperpolarization, budding, and fission. *J Biol Chem* 280, 6969-6985.
123. Itoh, T., Watabe, A., Toh, E.A., and Matsui, Y. (2002). Complex formation with Ypt11p, a rab-type small GTPase, is essential to facilitate the function of Myo2p, a class V myosin, in mitochondrial distribution in *Saccharomyces cerevisiae*. *Mol Cell Biol* 22, 7744-7757.
124. Pedram, A., Razandi, M., Wallace, D.C., and Levin, E.R. (2006). Functional Estrogen Receptors in the Mitochondria of Breast Cancer Cells. *Mol Biol Cell*. 17:2125-37
125. Nantel, A., Huber, M., and Thomas, D.Y. (1999). Localization of endogenous Grb10 to the mitochondria and its interaction with the mitochondrial-associated Raf-1 pool. *J Biol Chem* 274, 35719-35724.

126. Nemoto, Y., and De Camilli, P. (1999). Recruitment of an alternatively spliced form of synaptojanin 2 to mitochondria by the interaction with the PDZ domain of a mitochondrial outer membrane protein. *EMBO J.* *18*, 2991-3006.
127. Nemoto, Y., Wenk, M.R., Watanabe, M., Daniell, L., Murakami, T., Ringstad, N., Yamada, H., Takei, K., and De Camilli, P. (2001). Identification and characterization of a synaptojanin 2 splice isoform predominantly expressed in nerve terminals. *J Biol Chem* *276*, 41133-41142.
128. Guo, Y., Cheong, N., Zhang, Z., De Rose, R., Deng, Y., Farber, S.A., Fernandes-Alnemri, T., and Alnemri, E.S. (2004). Tim50, a component of the mitochondrial translocator, regulates mitochondrial integrity and cell death. *J Biol Chem* *279*, 24813-24825.
129. Yamamoto, H., Esaki, M., Kanamori, T., Tamura, Y., Nishikawa, S., and Endo, T. (2002). Tim50 is a subunit of the TIM23 complex that links protein translocation across the outer and inner mitochondrial membranes. *Cell* *111*, 519-528.
130. John, G.B., Shang, Y., Li, L., Renken, C., Mannella, C.A., Selker, J.M., Rangell, L., Bennett, M.J., and Zha, J. (2005). The mitochondrial inner membrane protein mitofilin controls cristae morphology. *Mol Biol Cell* *16*, 1543-1554.
131. Rebollo, A., Perez-Sala, D., and Martinez, A.C. (1999). Bcl-2 differentially targets K-, N-, and H-Ras to mitochondria in IL-2 supplemented or deprived cells: implications in prevention of apoptosis. *Oncogene* *18*, 4930-4939.
132. Bivona, T.G., Quatela, S.E., Bodemann, B.O., Ahearn, I.M., Soskis, M.J., Mor, A., Miura, J., Wiener, H.H., Wright, L., Saba, S.G., Yim, D., Fein, A., Perez de Castro, I., Li, C., Thompson, C.B., Cox, A.D., and Philips, M.R. (2006). PKC regulates a farnesyl-electrostatic switch on K-Ras that promotes its association with Bcl-XL on mitochondria and induces apoptosis. *Mol Cell* *21*, 481-493.
133. Minin, A.A., Kulik, A.V., Gyoeva, F.K., Li, Y., Goshima, G., and Gelfand, V.I. (2006). Regulation of mitochondria distribution by RhoA and formins. *J Cell Sci* *119*, 659-670.
134. Rosini, P., De Chiara, G., Bonini, P., Lucibello, M., Marocci, M.E., Garaci, E., Cozzolino, F., and Torcia, M. (2004). Nerve growth factor-dependent survival of CESS B cell line is mediated by increased expression and decreased degradation of MAPK phosphatase 1. *J Biol Chem* *279*, 14016-14023.
135. Gorska-Andrzejak, J., Stowers, R.S., Borycz, J., Kostyleva, R., Schwarz, T.L., and Meinertzhagen, I.A. (2003). Mitochondria are redistributed in *Drosophila* photoreceptors lacking milton, a kinesin-associated protein. *J Comp Neurol* *463*, 372-388.
136. Stowers, R.S., Megeath, L.J., Gorska-Andrzejak, J., Meinertzhagen, I.A., and Schwarz, T.L. (2002). Axonal transport of mitochondria to synapses depends on milton, a novel *Drosophila* protein. *Neuron* *36*, 1063-1077.
137. Brickley, K., Smith, M.J., Beck, M., and Stephenson, F.A. (2005). GRIF-1 and OIP106, members of a novel gene family of coiled-coil domain proteins: association in vivo and in vitro with kinesin. *J Biol Chem* *280*, 14723-14732.
138. Glater, E.E., Megeath, L.J., Stowers, R.S., and Schwarz, T.L. (2006). Axonal transport of mitochondria requires milton to recruit kinesin heavy chain and is light chain independent. *J Cell Biol* *173*, 545-557.
139. Kinner, A., and Kolling, R. (2003). The yeast deubiquitinating enzyme Ubp16 is anchored to the outer mitochondrial membrane. *FEBS Lett* *549*, 135-140.
140. Frederick, R.L., McCaffery, J.M., Cunningham, K.W., Okamoto, K., and Shaw, J.M. (2004). Yeast Miro GTPase, Gem1p, regulates mitochondrial morphology via a novel pathway. *J Cell Biol* *167*, 87-98.

141. Guo, X., Macleod, G.T., Wellington, A., Hu, F., Panchumarthi, S., Schoenfield, M., Marin, L., Charlton, M.P., Atwood, H.L., and Zinsmaier, K.E. (2005). The GTPase dMiro is required for axonal transport of mitochondria to *Drosophila* synapses. *Neuron* *47*, 379-393.
142. Lee, J., O'Neill R, C., Park, M.W., Gravel, M., and Braun, P.E. (2006). Mitochondrial localization of CNP2 is regulated by phosphorylation of the N-terminal targeting signal by PKC: Implications of a mitochondrial function for CNP2 in glial and non-glial cells. *Mol Cell Neurosci* *31*, 446-462.
143. Nangaku, M., Sato-Yoshitake, R., Okada, Y., Noda, Y., Takemura, R., Yamazaki, H., and Hirokawa, N. (1994). KIF1B, a novel microtubule plus end-directed monomeric motor protein for transport of mitochondria. *Cell*, 1209-1220.
144. Pilling, A.D., Horiuchi, D., Lively, C.M., and Saxton, W.M. (2006). Kinesin-1 and Dynein Are the Primary Motors for Fast Transport of Mitochondria in *Drosophila* Motor Axons. *Mol Biol Cell*. *17*:2057-68
145. Jullig, M., and Stott, N.S. (2003). Mitochondrial localization of Smad5 in a human chondrogenic cell line. *Biochem Biophys Res Commun* *307*, 108-113.
146. Sun, Y., Zhou, J., Liao, X., Lu, Y., Deng, C., Huang, P., Chen, Q., and Yang, X. (2005). Disruption of Smad5 gene induces mitochondria-dependent apoptosis in cardiomyocytes. *Exp Cell Res* *306*, 85-93.
147. Wozniak, M.J., Melzer, M., Dorner, C., Haring, H.U., and Lammers, R. (2005). The novel protein KBP regulates mitochondria localization by interaction with a kinesin-like protein. *BMC Cell Biol* *6*, 35.
148. Ren, J., Bharti, A., Raina, D., Chen, W., Ahmad, R., and Kufe, D. (2006). MUC1 oncoprotein is targeted to mitochondria by heregulin-induced activation of c-Src and the molecular chaperone HSP90. *Oncogene* *25*, 20-31.
149. Santama, N., Er, C.P., Ong, L.L., and Yu, H. (2004). Distribution and functions of kinectin isoforms. *J Cell Sci* *117*, 4537-4549.
150. Liu, J., Dai, Q., Chen, J., Durrant, D., Freeman, A., Liu, T., Grossman, D., and Lee, R.M. (2003). Phospholipid scramblase 3 controls mitochondrial structure, function, and apoptotic response. *Mol Cancer Res* *1*, 892-902.
151. Su, Q., Cai, Q., Gerwin, C., Smith, C.L., and Sheng, Z.H. (2004). Syntabulin is a microtubule-associated protein implicated in syntaxin transport in neurons. *Nat Cell Biol* *6*, 941-953.
152. Cai, Q., Gerwin, C., and Sheng, Z.H. (2005). Syntabulin-mediated anterograde transport of mitochondria along neuronal processes. *J Cell Biol* *170*, 959-969.
153. Inui, M., and Asashima, M. (2004). Identification and characterization of *Xenopus* OMP25. *Dev Growth Differ* *46*, 405-412.
154. Ebner, A., Godemann, R., Stamer, K., Illenberger, S., Trinczek, B., and Mandelkow, E. (1998). Overexpression of tau protein inhibits kinesin-dependent trafficking of vesicles, mitochondria, and endoplasmic reticulum: implications for Alzheimer's disease. *J. Cell Biol.* *143*, 777-794.
155. Tatebayashi, Y., Haque, N., Tung, Y.C., Iqbal, K., and Grundke-Iqbal, I. (2004). Role of tau phosphorylation by glycogen synthase kinase-3beta in the regulation of organelle transport. *J Cell Sci* *117*, 1653-1663.
156. Kuroda, Y., Mitsui, T., Kunishige, M., Shono, M., Akaike, M., Azuma, H., and Matsumoto, T. (2006). Parkin enhances mitochondrial biogenesis in proliferating cells. *Hum Mol Genet* *15*, 883-895.

157. Park, J., Lee, S.B., Lee, S., Kim, Y., Song, S., Kim, S., Bae, E., Kim, J., Shong, M., Kim, J.M., and Chung, J. (2006). Mitochondrial dysfunction in *Drosophila* PINK1 mutants is complemented by parkin. *Nature*. advance online publication 3 May 2006 | doi:10.1038/nature04788
158. Clark, I.E., Dodson, M.W., Jiang, C., Cao, J.H., Huh, J.R., Seol, J.H., Yoo, S.J., Hay, B.A., and Guo, M. (2006). *Drosophila* pink1 is required for mitochondrial function and interacts genetically with parkin. *Nature*. advance online publication 3 May 2006 | doi:10.1038/nature04779
159. Pereira, A.J., Dalby, B., Stewart, R.J., Doxsey, S.J., and Goldstein, L.S. (1997). Mitochondrial association of a plus end-directed microtubule motor expressed during mitosis in *Drosophila*. *J. Cell Biol.* *136*, 1081-1090.
160. Varadi, A., Johnson-Cadwell, L.I., Cirulli, V., Yoon, Y., Allan, V.J., and Rutter, G.A. (2004). Cytoplasmic dynein regulates the subcellular distribution of mitochondria by controlling the recruitment of the fission factor dynamin-related protein-1. *J Cell Sci* *117*, 4389-4400. Epub 2004 Aug 4310.
161. Horiuchi, D., Barkus, R.V., Pilling, A.D., Gassman, A., and Saxton, W.M. (2005). APLIP1, a kinesin binding JIP-1/JNK scaffold protein, influences the axonal transport of both vesicles and mitochondria in *Drosophila*. *Curr Biol* *15*, 2137-2141.
162. Sesaki, H., Dunn, C.D., Iijima, M., Shepard, K.A., Yaffe, M.P., Machamer, C.E., and Jensen, R.E. (2006). Ups1p, a conserved intermembrane space protein, regulates mitochondrial shape and alternative topogenesis of Mgm1p. *J Cell Biol* *173*, 651-658.
163. Escobar-Henriques, M., Westermann, B., and Langer, T. (2006). Regulation of mitochondrial fusion by the F-box protein Mdm30 involves proteasome-independent turnover of Fzo1. *J Cell Biol* *173*, 645-650.
164. McQuibban, G.A., Lee, J.R., Zheng, L., Juusola, M., and Freeman, M. (2006). Normal mitochondrial dynamics requires rhomboid-7 and affects *Drosophila* lifespan and neuronal function. *Curr Biol* *16*, 982-989.
165. Warr, M.R., Acoca, S., Liu, Z., Germain, M., Watson, M., Blanchette, M., Wing, S.S., and Shore, G.C. (2005). BH3-ligand regulates access of MCL-1 to its E3 ligase. *FEBS Lett* *579*, 5603-5608.
166. Zhong, Q., Gao, W., Du, F., and Wang, X. (2005). Mule/ARF-BP1, a BH3-only E3 ubiquitin ligase, catalyzes the polyubiquitination of Mcl-1 and regulates apoptosis. *Cell* *121*, 1085-1095.

Appendix 3

**Dissociating the dual roles of apoptosis-inducing factor in
maintaining mitochondrial structure and apoptosis**

Dissociating the dual roles of apoptosis-inducing factor in maintaining mitochondrial structure and apoptosis

Eric CC Cheung¹, Nicholas Joza²,
Nancy AE Steenaert³, Kelly A McClellan¹,
Margaret Neuspiel⁴, Stephen McNamara¹,
Jason G MacLaurin¹, Peter Rippstein⁴,
David S Park¹, Gordon C Shore⁵,
Heidi M McBride⁴, Josef M Penninger^{2,*}
and Ruth S Slack^{1,*}

¹Ottawa Health Research Institute, Department of Cellular and Molecular Medicine, University of Ottawa, Ottawa, Ontario, Canada, ²IMBA, Institute of Molecular Biotechnology of the Austrian Academy of Sciences, Vienna, Austria, ³Gemin X Biotechnologies Inc., Montreal, Quebec, Canada ⁴Ottawa Heart Institute, University of Ottawa, Ottawa, Ontario, Canada and ⁵Department of Biochemistry, McGill University, Montreal, Quebec, Canada

The mitochondrial protein apoptosis-inducing factor (AIF) translocates to the nucleus and induces apoptosis. Recent studies, however, have indicated the importance of AIF for survival in mitochondria. In the absence of a means to dissociate these two functions, the precise roles of AIF remain unclear. Here, we dissociate these dual roles using mitochondrially anchored AIF that cannot be released during apoptosis. Forebrain-specific AIF null (tel. *Aif*^Δ) mice have defective cortical development and reduced neuronal survival due to defects in mitochondrial respiration. Mitochondria in AIF deficient neurons are fragmented with aberrant cristae, indicating a novel role of AIF in controlling mitochondrial structure. While tel. *Aif*^Δ *Apaf1*^{-/-} neurons remain sensitive to DNA damage, mitochondrially anchored AIF expression in these cells significantly enhanced survival. AIF mutants that cannot translocate into nucleus failed to induce cell death. These results indicate that the proapoptotic role of AIF can be uncoupled from its physiological function. Cell death induced by AIF is through its proapoptotic activity once it is translocated to the nucleus, not due to the loss of AIF from the mitochondria.

The EMBO Journal (2006) 25, 4061–4073. doi:10.1038/sj.emboj.7601276; Published online 17 August 2006

Subject Categories: differentiation & death

Keywords: apoptosis; apoptosis-inducing factor (AIF); DNA damage; mitochondria; neuron

*Corresponding authors. JM Penninger, Institute of Molecular Biotechnology of the Austrian Academy of Sciences, Dr Bohr-gasse 3, 1030 Vienna, Austria. Tel.: +43 (1) 790 44; Fax: +43 (1) 790 44-110; E-mail: josef.penninger@imba.oeaw.ac.at or RS Slack, Ottawa Health Research Institute, Department of Cellular and Molecular Medicine, University of Ottawa, 451 Smyth Road, Room 2452, Ottawa, Ontario, Canada K1H8M5. Tel.: +1 613 562 5800 ext 8459; Fax: +1 613 562 5403; E-mail: rslack@uottawa.ca

Received: 12 January 2006; accepted: 19 July 2006; published online: 17 August 2006

Introduction

Mitochondria are the central relaying stations for apoptotic signals. After the induction of apoptosis, cytochrome *c* is released from the mitochondria that interacts with Apaf1 and procaspase 9, which in turn activates the caspase cascade (reviewed in Yuan *et al*, 2003; Danial and Korsmeyer, 2004). Apart from the caspase-dependent pathway, mitochondrial factors also initiate a caspase-independent apoptotic signaling cascade (reviewed in Cregan *et al*, 2004; Hong *et al*, 2004). This pathway is initiated by the release of the mitochondrial protein, apoptosis-inducing factor (AIF), which translocates to the nucleus and induces DNA fragmentation through interactions with factors including EndoG in *Caenorhabditis elegans*, CypA in mice, and others such as FEN-1 (Susin *et al*, 1999; Daugas *et al*, 2000; Wang *et al*, 2002; Parrish and Xue, 2003; Cande *et al*, 2004). The significance of these interactions, however, are not yet clear, as EndoG and CypA null animals have no apparent defect in apoptosis (Colgan *et al*, 2000; Irvine *et al*, 2005).

The role of AIF in neuronal cell death was first suggested from the observation that AIF translocates to nucleus after the induction of various types of acute neuronal injury *in vitro* and *in vivo* (Zhang *et al*, 2002; Cao *et al*, 2003; Plesnila *et al*, 2004; Wang *et al*, 2004). Mitochondrial release of AIF has been shown to depend on PARP activity (Yu *et al*, 2002; Wang *et al*, 2004). We have previously demonstrated that AIF translocation following neuronal injury is caspase independent (Cregan *et al*, 2002; Cheung *et al*, 2005). Using *Apaf1*^{-/-} neurons, we have shown that AIF is translocated to the nucleus on induction of apoptosis, and this can be inhibited by microinjecting AIF neutralizing antibodies (Cregan *et al*, 2002). Depending on the cell type and death stimulus, the release of AIF may also be caspase dependent, as studies using *C. elegans* with BH-3 only protein EGL-1 (Wang *et al*, 2002), HeLa cells with staurosporine (Arnoult *et al*, 2003), and rat cortical neurons (Lang-Rollin *et al*, 2003) have previously shown. We have used *Harlequin* (*Hq*) mice, which exhibit only 20% AIF expression (Klein *et al*, 2002), to directly investigate the role of AIF in various models of neuronal cell death. Using *Hq*/*Apaf1*^{-/-} double mutant mice we have shown that reduced levels of AIF, along with inactivation of caspase activity, can sustain neuronal survival after DNA damage and excitotoxic induced cell death. These results revealed that AIF is involved in both Bax dependent and Bax independent mechanisms of cell death (Cheung *et al*, 2005). In mammalian systems, therefore, AIF is a key death inducer that functions in multiple mechanisms of neuronal cell death; thus understanding its mechanism of action is crucial.

Apart from the apoptotic role of AIF, studies with AIF depleted cells have indicated that AIF also has a physiological role in the mitochondria. Studies using *Hq* mice, which exhibit cerebellar degeneration and increased sensitivity to

oxidative stress (Klein *et al*, 2002), suggesting that AIF acts as an oxidative radical scavenger in the mitochondria (Lipton and Bossy-Wetzel, 2002). A recent study, however, revealed that AIF depleted cells (*Aif*^{-/-} ES and *Hq* cells) have defective oxidative phosphorylation and reduced expression of Complex I and III in the electron transport chain of the mitochondria. AIF, however, was not found to be associated with either Complex I or III (Vahsen *et al*, 2004); therefore, the mechanism by which AIF stabilizes complex I remains unknown.

Since AIF has dual roles, dissociating its functions in each of these cellular events has been difficult. For example, it remains unknown whether cell death is triggered by the loss of AIF from mitochondria. This would argue that AIF's proapoptotic role is not essential to the induction of apoptosis. Here, we resolve this controversy by dissociating the physiological role and the apoptotic role of AIF. To this end, we have constructed a mitochondrial inner membrane anchored form of AIF (anchored AIF) that cannot be released from the mitochondria during apoptosis and thus maintains its physiological role. These constructs were then introduced in AIF deficient neurons from a telencephalon specific conditional mutant of AIF. Here, we show that: (a) AIF plays an important role in neuronal survival by maintaining mitochondrial structure; and (b) AIF has a major role in proapoptotic signaling following nuclear translocation. Expression of anchored AIF in cells with endogenous AIF can offer protection only during the initial stages of apoptosis by maintaining the pool of AIF in mitochondria. At longer time points, however, the cells still succumb to death even when AIF is present in the mitochondria. This demonstrates that reconstitution of mitochondrial AIF is not sufficient to rescue cell death and that AIF plays an active role in proapoptotic signaling in the nucleus. In conclusion, we dissociated the dual functions of AIF and directly demonstrate the importance of the proapoptotic role of AIF, apart from its novel role in maintaining mitochondrial structure.

Results

Generation of telencephalon conditional *Aif*^Δ mice

AIF null embryos die around embryonic day (E) 12, and muscle-specific loss of AIF leads to mitochondrial dysfunction, skeletal muscle atrophy and dilated cardiomyopathy (Joza *et al*, 2005). To study the function of AIF in neurons, we generated telencephalon-specific AIF mutant mice (tel. *Aif*^Δ) by crossing *Aif*^{flox/flox} mice with mice carrying Cre driven by the promoter Foxg1. Cre mediated excision of the floxed allele occurs in neuronal precursors of the telencephalon at E9 (Hebert and McConnell, 2000), resulting in deletion of the targeted gene in all cortical neurons. Deletion of the floxed AIF allele was assessed by PCR and Western blot analysis. In the absence of Cre, the floxed allele was present (Figure 1A, lanes 1 and 2). Cre expression resulted in deletion of AIF (Figure 1A, lane 4). Western blot analysis confirmed the absence of AIF only in the mutant telencephalon (Figure 1B).

AIF is required for neuronal survival during cortical development

We next examined the telencephalon of the conditional mutants to investigate the role of AIF in cortical development.

Tel. *Aif*^Δ conditional mutants die by E17 (data not shown). The tel. *Aif*^Δ mice exhibited reduced cortical thickness at E15.5 compared to control littermates (Figure 1C). This reduction of thickness occurs mostly at the cortical plate (CP) and intermediate zone (IZ), and to a lesser extent at the subventricular zone (SVZ) (Figure 1C). To address whether this reduction in size is due to increased apoptosis or reduced numbers of progenitor cells, active caspase 3 and phosphohistone H3 (PH3) staining were used to assess cell death and progenitor proliferation, respectively (Ferguson *et al*, 2002). Active caspase 3 staining revealed a marked increase in cell death in the tel. *Aif*^Δ in regions of postmitotic cells (Figure 1D), whereas PH3 staining indicated similar numbers of proliferating progenitor cells along the ventricles in both the conditional mutants and their control littermates (Figure 1E). These data indicate that AIF is essential for survival of maturing neurons during cortical development, but AIF expression is dispensable for the proliferation of neuronal progenitors.

To assess whether cell death due to AIF depletion was cell autonomous, primary neuronal cultures were examined. After 2 days of culture, primary neuronal cells from E14.5 tel. *Aif*^Δ cortices exhibited increased cell death relative to neuronal cells from wild-type controls (Figure 2A). Consistent with previous reports on *Aif*^{-/-} ES cells (Vahsen *et al*, 2004), we found that expression of respiratory chain complex I was abrogated in mutant neurons compared to control neurons (Figure 2E). Importantly, the reduced viability of tel. *Aif*^Δ neurons can be rescued when cells were cultured in media enriched with pyruvate, uridine, and additional glucose (PU media) to bypass defects in mitochondrial respiration (Figure 2A). These supplements were used previously to culture cells lacking cytochrome *c* (Li *et al*, 2000) or mtDNA (King and Attardi, 1989), which exhibit defective mitochondrial respiration. These results show that AIF is required for neuronal cell survival and normal mitochondrial respiration in neurons.

Construction of AIF anchored to the inner membrane of the mitochondria

During apoptosis, AIF is released from mitochondria and translocates to the nucleus, inducing chromatin condensation and degradation. Since AIF depletion causes early lethality in neurons, the dual roles of AIF in mediating apoptosis and cellular homeostasis are difficult to resolve. In order to dissect the potential role of AIF in apoptosis from its role in mitochondria, we reconstituted AIF deficient neurons with mitochondrially anchored AIF constructs such that AIF was permanently tethered to the inner mitochondrial membrane. To this end, we exchanged the mitochondrial localization sequence (MLS) of AIF with the MLS of two proteins (ν -lactate dehydrogenase (Rojo *et al*, 1998; Flick and Konieczny, 2002) for D-AIF, and a modified form of pOSA-14114 for N-AIF (Steenart and Shore, 1997)) that are anchored to the outer leaflet of the inner membrane of mitochondria (Supplementary Figure 1A). Quantification of GFP fluorescence and Western blot analysis of infected cells revealed similar expression of these constructs, comparable to endogenous level (Supplementary Figure 1B and C). Western analysis of digitonin gradient treatment on isolated mitochondria with anchored AIF mutant, as well as immunocytochemical analysis on digitonin treated neurons with

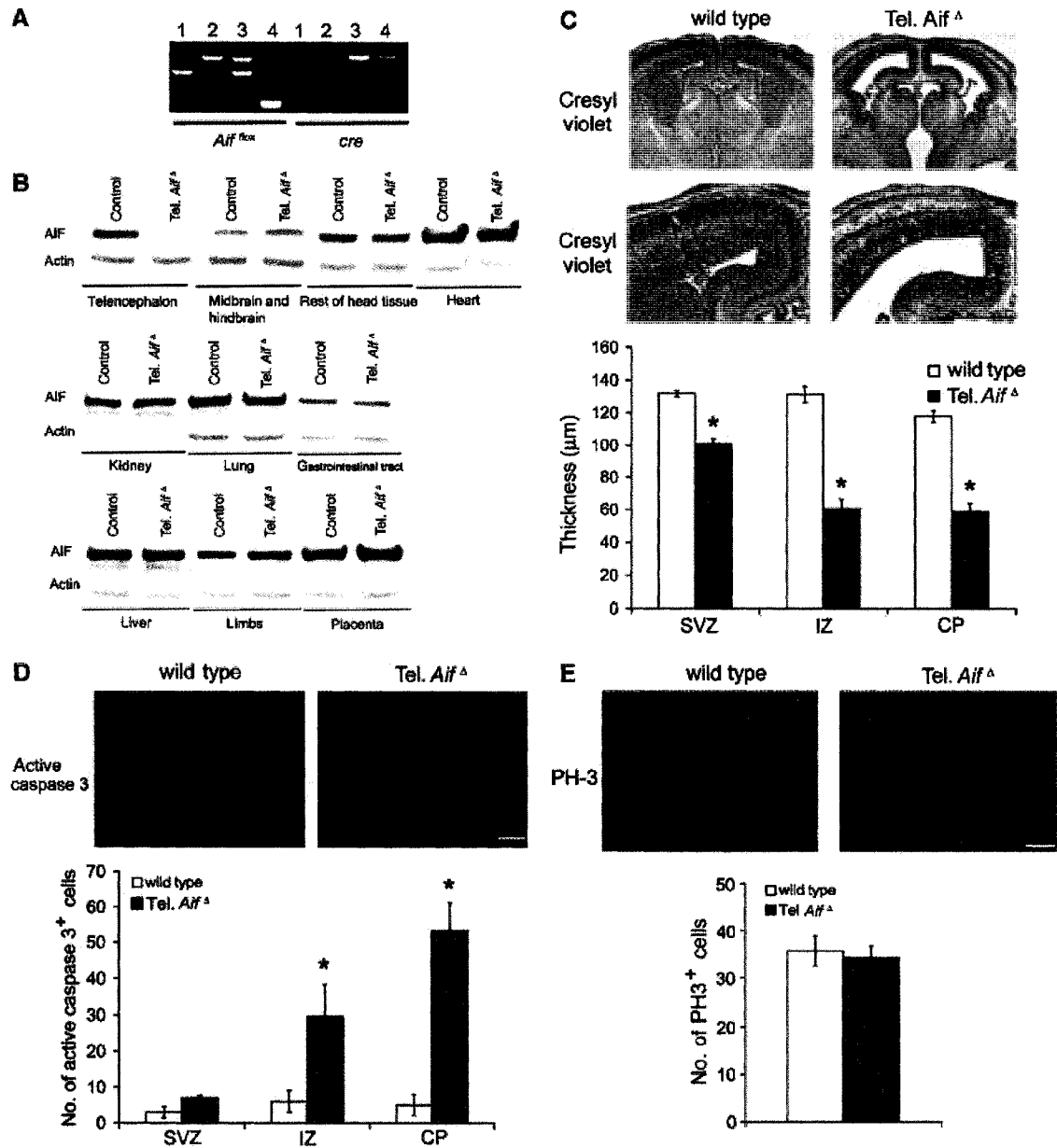


Figure 1 AIF is essential for neuronal survival during cortical development. (A) PCR analysis of E15.5 telencephalon tissue. Lane 1: *Aif*^{+/+}*cre*^{+/+}; lane 2: *Aif*^{lox/y}*cre*^{+/+}; lane 3: *Aif*^{lox/y}*cre*^{+/-}; lane 4: *Aif*^{lox/y}*cre*^{+/-} (tel. *Aif*^Δ). (B) Western blot analysis for AIF and control β-actin expression of various tissues from tel. *Aif*^Δ and wild-type littermates at E15.5. (C) Cresyl violet staining of control and tel. *Aif*^Δ mice coronal forebrain sections at E15.5. SVZ = subventricular zone, IZ = intermediate zone, CP = cortical plate. Bar = 250 μm. *n* = 3. (D) Active caspase 3 immunohistochemistry of control and tel. *Aif*^Δ coronal forebrain sections at E15.5. *n* = 3. (E) PH3 immunohistochemistry of control and tel. *Aif*^Δ coronal forebrain sections at E15.5. *n* = 3. **P* < 0.05 compared to wildtype.

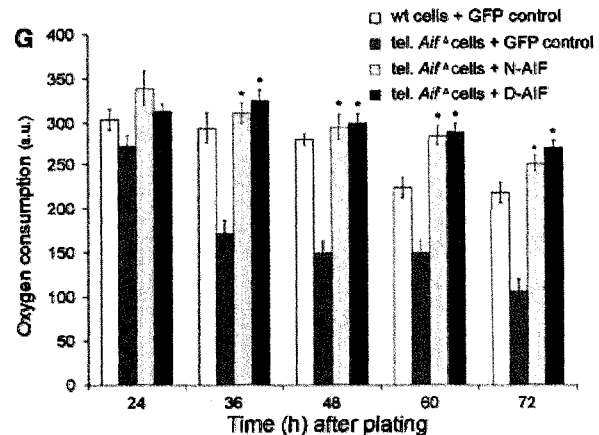
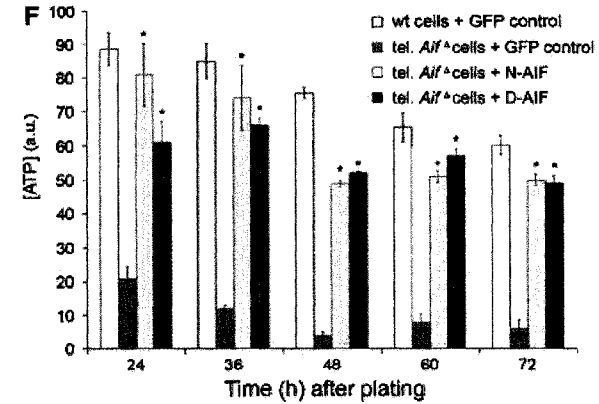
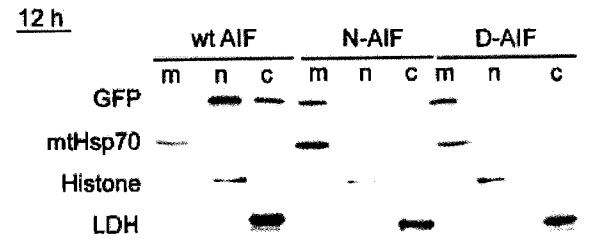
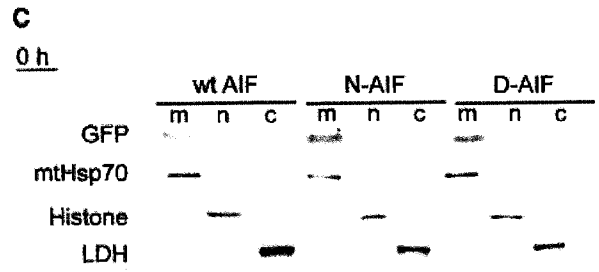
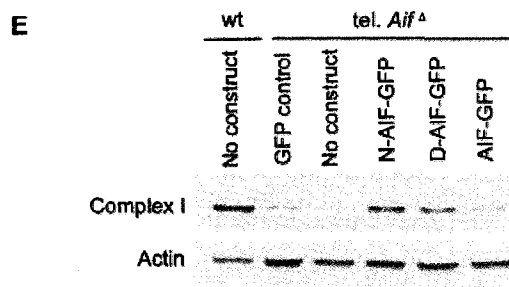
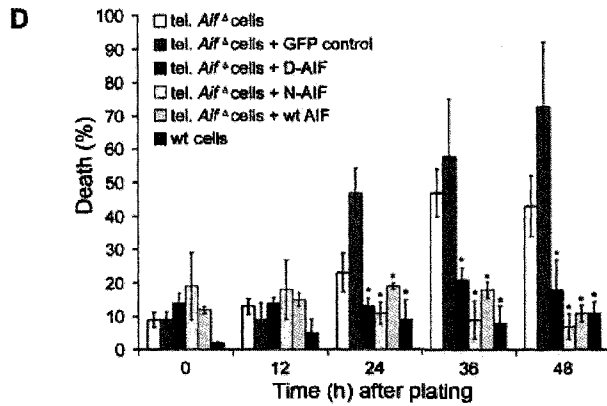
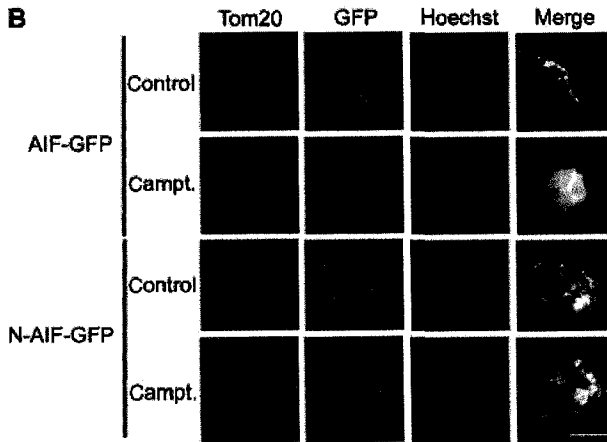
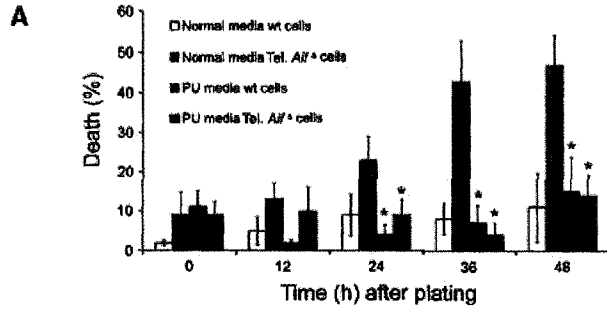
anchored AIF mutant, showed that the anchored AIF mutant is located in the intermembrane space, similar to wild-type AIF (Supplementary Figure 1D and E). These results indicate that the anchored AIF constructs maintained the normal orientation of AIF in the mitochondria. GFP fluorescence from these anchored AIF constructs showed that both D-AIF and N-AIF were localized in mitochondria. Importantly, in contrast to wild-type AIF, both D-AIF and N-AIF remained associated with mitochondria after an apoptotic insult at all time points, as shown by immunocytochemistry and subcellular fractionation followed by Western blot analysis (Figure 2B and C). Expression of respiratory chain complex I (Figure 2E) was restored in AIF deficient

neurons expressing mitochondrially anchored AIF, indicating that these constructs are functional. We next assessed survival of tel. *Aif*^Δ neurons expressing mitochondrially anchored AIF. After 2 days under normal nonenriched culture conditions, tel. *Aif*^Δ neurons with either one of the anchored AIF constructs maintained the same level of cell survival as wild-type neurons, which was not rescued by GFP control vector (Figure 2D). ATP production and oxygen consumption were also restored in AIF deficient neurons expressing the anchored AIF constructs compared to GFP control vector (Figure 2F and G). These experiments demonstrate that expression of mitochondrially anchored AIF rescues the cell death of tel. *Aif*^Δ neurons.

AIF is required for maintaining mitochondrial morphology and cristae structure

We next asked whether there was perturbation of mitochondrial morphology in tel. *Aif*^Δ neurons. The mitochondrial membrane potential sensitive dye TMRE was used to visualize mitochondria in cells cultured in enriched media. Wild-type neurons have elongated and tubular mitochondria that

often spread along neurites (Figure 3A). In contrast, tel. *Aif*^Δ neurons exhibited short and fragmented mitochondria that are often perinuclear (Figure 3A). Few mitochondria were observed in the neurites of tel. *Aif*^Δ neurons. Mitochondrial membrane potential of tel. *Aif*^Δ neurons was hyperpolarized relative to wild-type cells (Supplementary Figure 2A), which can be dissipated using FCCP, the mitochondrial potential



uncoupler (Supplementary Figure 2B). The hyperpolarized membrane potential as well as altered mitochondrial morphology were restored to normal by the expression of either anchored AIF or wild-type AIF in tel. *Aif*^Δ neurons (Figure 3A and Supplementary Figure 2). Interestingly, expression of anchored AIF in wild-type cells resulted in increased mitochondrial length compared to controls (Figure 3A and B), suggesting a role for AIF in maintaining mitochondrial morphology. Next, we asked if the mitochondrial ultrastruc-

ture is also disrupted in these cells. We used transmission electron microscopy to visualize mitochondria from neurons cultured in enriched PU media to eliminate secondary effects due to reduced survival in tel. *Aif*^Δ neurons. In wild-type cells, mitochondrial cristae are shaped as compact tubules in an orderly fashion (Figure 4A). Tel. *Aif*^Δ neurons, on the other hand, displayed aberrant cristae morphology. The cristae are dilated and do not orient in an orderly fashion (Figure 4A). The cross-sectional distance of tel. *Aif*^Δ mito-

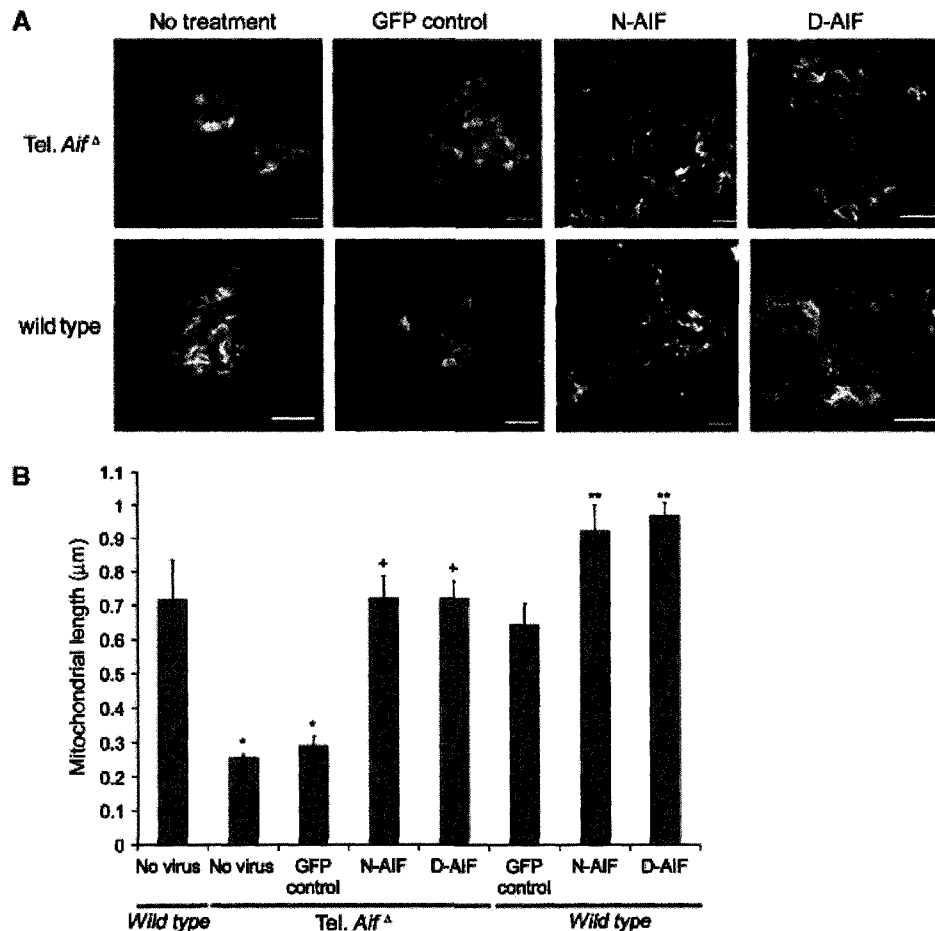


Figure 3 AIF controls mitochondrial structure. Cortical neurons from E15.5 tel. *Aif*^Δ and wild-type littermates were infected at time of plating with mitochondrially anchored N-AIF and D-AIF and a GFP control virus at 50 MOI in enriched PU media. (A, B) After 36 h, 50 nm TMRE was added to media and live cell images were taken. (A) Representative images of tel. *Aif*^Δ and wild-type mitochondria infected with the indicated constructs. Bars = 1 μm. (B) Average length of mitochondria of neurons. The cell types and treatments are as indicated (n = 4). *P < 0.05 compared to wild type with no virus; ⁺P < 0.05 compared to tel. *Aif*^Δ infected with the GFP control virus; ^{**}P < 0.05 compared to wild type with GFP control.

Figure 2 Mitochondrially anchored AIF rescues reduced survival of tel. *Aif*^Δ neurons. (A–C) Cortical neurons were isolated from E15.5 tel. *Aif*^Δ and wild-type littermates and cultured in normal media or enriched PU media containing 50 mg/l pyruvate, 110 mg/l uridine and 5 mM glucose. (A) Quantitative analysis of cell death of tel. *Aif*^Δ and wild-type neurons cultured in normal and PU media (n = 3). (B) Wild-type cortical neurons were infected with recombinant adenoviral vector containing GFP-tagged wild-type AIF (AIF-GFP) or GFP-tagged N-AIF (N-AIF-GFP) and were treated with or without camptothecin. After 36 h, cells were fixed and stained with Hoechst to visualize nuclei and an anti-Tom20 antibody (red) to detect mitochondria. Green GFP fluorescence indicates AIF localization. (C) Western analysis on subcellular fractionation of neurons infected with GFP-tagged wildtype AIF, N-AIF and D-AIF. Upper panel: no camptothecin, lower panel: 12 h after camptothecin treatment. m = mitochondrial fraction, n = nuclear fraction, and c = cytoplasmic fraction. (D) Quantitative analysis of spontaneous cell death of cortical neurons isolated from tel. *Aif*^Δ and wild-type littermates infected with control virus, wild-type AIF (wt AIF), or mitochondrially anchored AIF (N-AIF and D-AIF) at 50 MOI in normal media. Cell death was quantified by apoptotic nuclear morphology using Hoechst (n = 3). *P < 0.05 compared to tel. *Aif*^Δ in normal media. (E) Western analysis of complex I (39 kDa subunit) expression in tel. *Aif*^Δ neurons expressing either N-AIF and D-AIF compared to wild-type and control tel. *Aif*^Δ neurons. (F) ATP production of the tel. *Aif*^Δ neurons expressing either N-AIF, D-AIF, or GFP as control (n = 3). *P < 0.05 compared to tel. *Aif*^Δ neurons with GFP control. (G) Oxygen consumption of the tel. *Aif*^Δ neurons expressing either N-AIF, D-AIF, or GFP as control (n = 3). *P < 0.05 compared to tel. *Aif*^Δ neurons with GFP control.

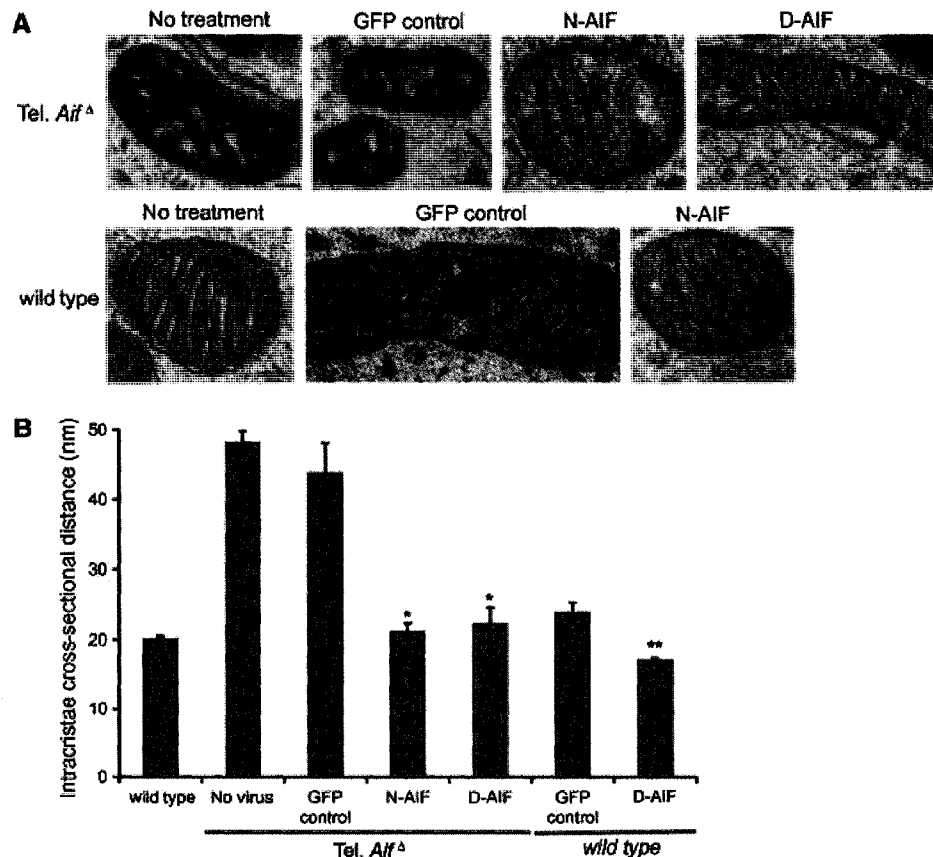


Figure 4 AIF depleted neurons have perturbed mitochondrial cristae structure. (A, B) Transmission electron microscopy of mitochondria. (A) Representative images of mitochondria of tel. *Aif*^Δ and wild-type mitochondria infected with the indicated constructs. Bars = 100 nm. (B) Quantification of the intracristal cross-sectional distances ($n=4$). * $P<0.05$ compared to tel. *Aif*^Δ infected with the GFP control virus; ** $P<0.05$ compared to wild-type neurons infected with the GFP control virus.

chondrial cristae is ~ 2.5 times wider than in control wild-type mitochondria (Figure 4B). Expression of anchored AIF in wild-type cells again reduced intracristal distances from 20 to 17 nm (Figure 4B), further supporting the notion that the defect seen in tel. *Aif*^Δ neurons does not result from secondary effects. A detailed analysis of intracristal cross-sectional distance is shown in Supplementary Figure 3A and B. These studies demonstrate a novel role for AIF in regulating mitochondrial structure and cristae morphology.

Mitochondrially anchored AIF revealed critical role of AIF during apoptosis

Defining the proapoptotic function of AIF has been confounded by recent findings demonstrating an essential physiological role for AIF in the mitochondria. Presently, it is unknown if mitochondrial release of AIF in itself induces apoptosis due to loss of AIF mitochondrial function, or whether AIF plays a proapoptotic role following nuclear translocation. First, we generated double tel. *Aif*^Δ *Apaf1*^{-/-} animals in which both caspase dependent and independent pathways have been inactivated. Double mutant embryos exhibit some increase in cortical thickness relative to tel. *Aif*^Δ animals (Figure 5A and B), possibly due to the increased survival of cells in *Apaf1*^{-/-} background. As reported previously (Cozzolino *et al*, 2004), *Apaf1*^{-/-} mice have increased numbers of progenitor cells compared to wild

type and tel. *Aif*^Δ mice (Figure 5A and D). Next, we asked if the double-mutant neurons exhibit protection against DNA damage induced cell death. After inducing cell death with camptothecin, the tel. *Aif*^Δ *Apaf1*^{-/-} double mutant neurons cultured in pyruvate supplemented media, exhibited increased survival relative to single mutants and wild-type control neurons (Figure 6A). AIF deficiency alone can offer transient but significant protection at 12 h (Figure 6A, $\sim 45\%$ for tel. *Aif*^Δ versus $\sim 55\%$ for wild type), and at later time points the percentage of cell death of tel. *Aif*^Δ cells becomes similar to wild-type cells due to the presence of caspases. This is in agreement with *Hq* neurons, which also showed a transient delay in chromatin condensation compared to wildtype during cell death (Cheung *et al*, 2005). Cytochrome *c* release in these mutants is not affected, suggesting that mitochondrial permeabilization is not affected by the deletion of *Apaf1* and AIF (Supplementary Figure 4). AIF release in *Apaf1* neurons is similar to wild-type cells (Supplementary Figure 5A and B), which is in agreement with our previous results showing AIF release in *Apaf1* neurons is similar to wild type after p53 and camptothecin induced cell death (Cregan *et al* 2002). Caspase activity was not detected in *Apaf1*^{-/-} and tel. *Aif*^Δ *Apaf1*^{-/-} compared to wild type and tel. *Aif*^Δ (Supplementary Figure 6A).

Using the anchored AIF mutants and tel. *Aif*^Δ *Apaf1*^{-/-} neurons, we asked whether AIF is indeed an apoptotic

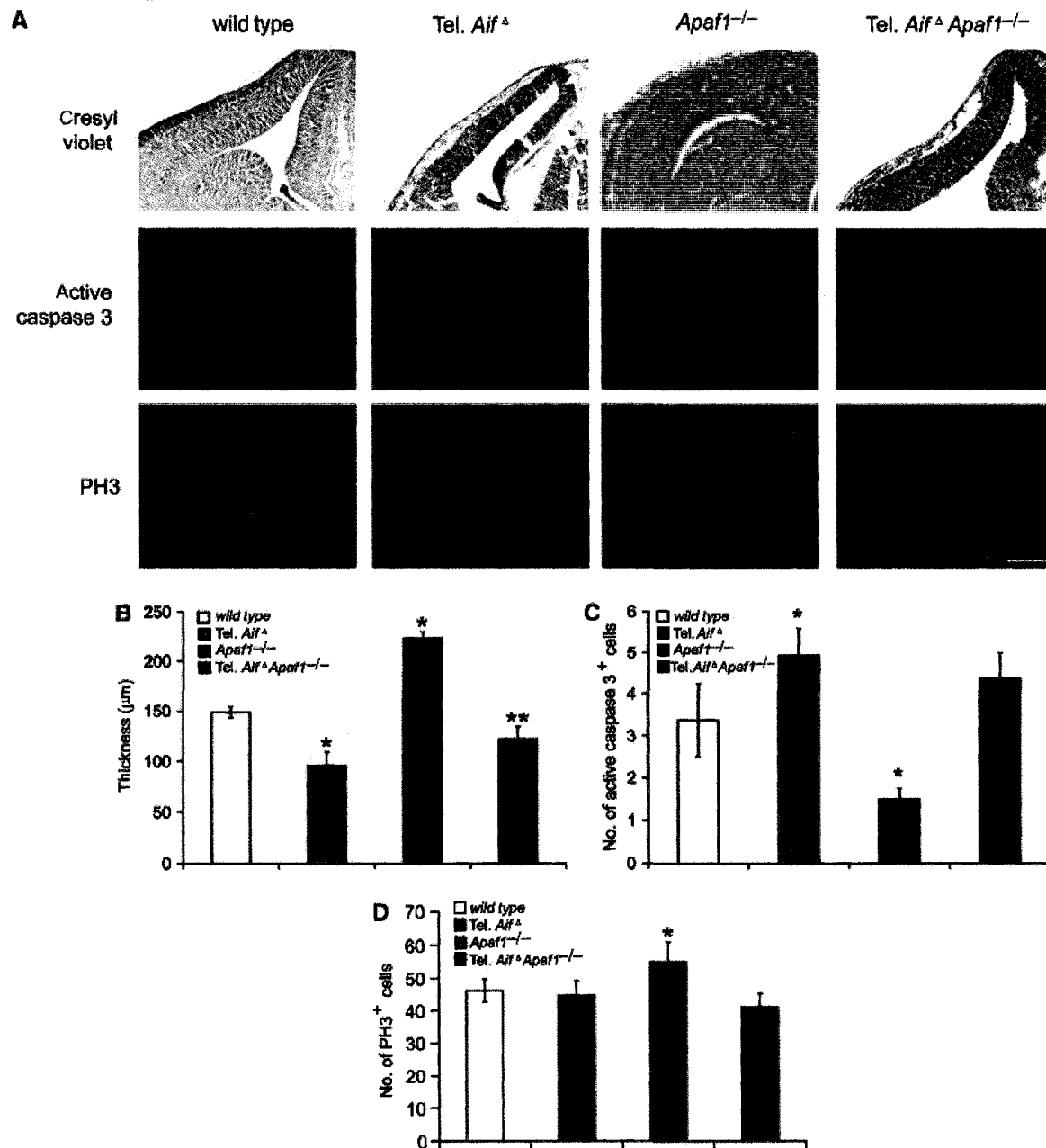


Figure 5 *Apaf1* deficiency can partially compensate neuronal loss due to AIF deficiency during development. (A) Cresyl violet staining, active caspase 3 staining, and PH3 staining of coronal telencephalon sections from control wild type, tel. *Aif* $^{\Delta}$, *Apaf1* $^{-/-}$, and tel. *Aif* $^{\Delta}$ *Apaf1* $^{-/-}$ double mutant mice (E14.5). Bar = 250 μm . (B–D) Quantitative analysis of (B) cortical thickness ($n = 3$), (C) active caspase 3 positive cells ($n = 3$) and (D) PH3 positive cells ($n = 3$); * $P < 0.05$ compared to wild type; ** $P < 0.05$ compared to tel. *Aif* $^{\Delta}$.

effector after induction of cell death. We first addressed if anchored AIF can provide further protection against cell death in tel. *Aif* $^{\Delta}$ *Apaf1* $^{-/-}$ neurons. Western analysis revealed that anchored AIF is not released during cell death but is retained in the mitochondria (Supplementary Figure 7), and similar to tel. *Aif* $^{\Delta}$ *Apaf1* $^{-/-}$ neurons, caspase was not activated (Supplementary Figure 6B). Strikingly, expression of either of the anchored AIF constructs in the double mutant neurons in enriched media could provide further protection against cell death for an extended time after insult (Figure 6B). Anchored mutants could also maintain oxygen consumption following camptothecin treatment (Figure 6C).

This indicates that by retaining AIF in the mitochondria during cell death, survival can be sustained first by inhibiting AIF's apoptotic role in the nucleus, and secondly by maintaining AIF's physiological function in the mitochondria. These data show that AIF is an important contributor to the execution of cell death following DNA damage.

We next asked whether the effects of AIF in the nucleus are crucial to its proapoptotic function. To address this, we generated an AIF construct harboring a nuclear exclusion signal (NES) (Fischer *et al*, 1995), which prevents AIF from translocating to the nucleus. After induction of apoptosis, tel. *Aif* $^{\Delta}$ *Apaf1* $^{-/-}$ double mutant neurons reconstituted with

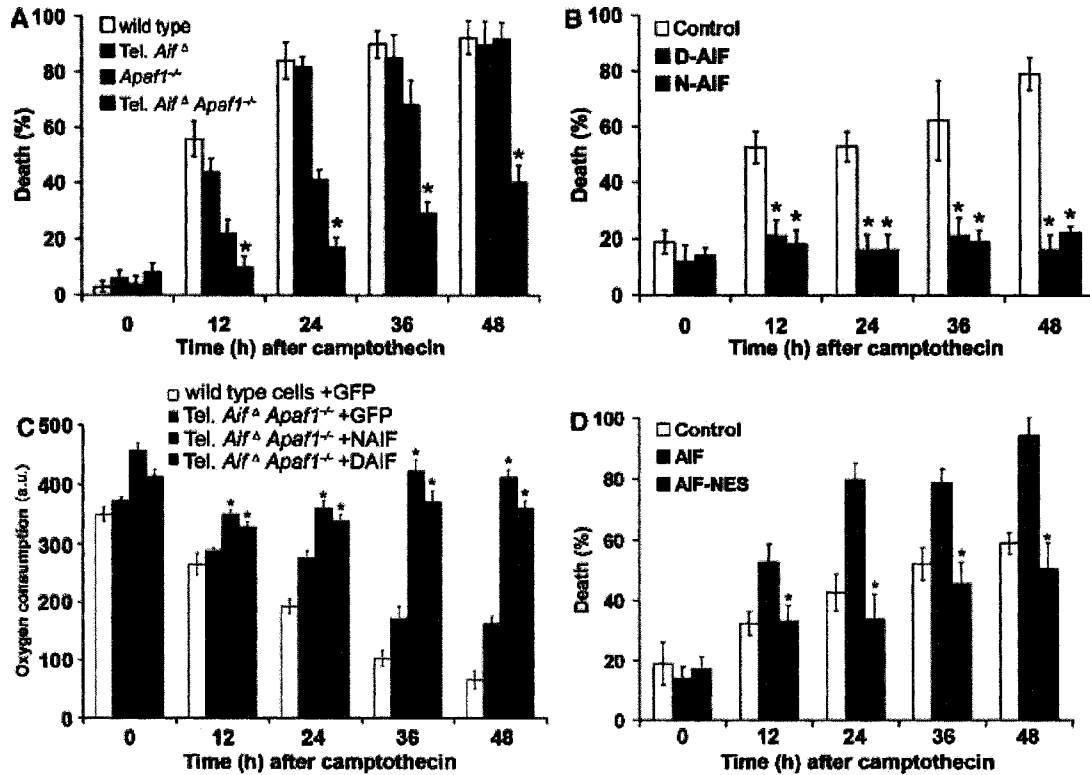


Figure 6 Dissociation of the dual roles of AIF in tel. *Aif* Δ *Apaf1* $^{-/-}$ neurons revealed AIF's proapoptotic role at the nucleus apart from its physiological role in the mitochondria. (A) Cortical neurons cultured from E14.5 wild type, tel. *Aif* Δ , *Apaf1* $^{-/-}$ and tel. *Aif* Δ *Apaf1* $^{-/-}$ double mutant embryos were treated with camptothecin in enriched media and cell death were assessed at the indicated time points ($n=3$). (B) Cortical neurons from E14.5 tel. *Aif* Δ *Apaf1* $^{-/-}$ double mutant embryos were infected at the time of plating with mitochondrially anchored D-AIF and N-AIF and a GFP control virus at 50 MOI in enriched media. Camptothecin was then added and cell death was assessed by Hoechst staining ($n=3$). (C) Oxygen consumption of tel. *Aif* Δ *Apaf1* $^{-/-}$ neurons expressing D-AIF and N-AIF after camptothecin treatment ($n=3$). * $P<0.05$ compared to tel. *Aif* Δ *Apaf1* $^{-/-}$ neurons expressing GFP control. (D) Cortical neurons from tel. *Aif* Δ *Apaf1* $^{-/-}$ double mutant were infected at the time of plating with AIF, NES-AIF or a GFP control at 50 MOI in enriched media. Camptothecin was then added, and cell death was assessed at the indicated time points ($n=3$). * $P<0.05$ compared to GFP control.

wild-type AIF exhibited markedly increased cell death compared to neurons expressing control GFP (Figure 6D). Importantly, expression of AIF-NES failed to restore AIF-mediated cell death, as shown by comparable survival rates between tel. *Aif* Δ *Apaf1* $^{-/-}$ neurons expressing AIF-NES and control GFP (Figure 6D). These studies indicate that a major part of the proapoptotic function of AIF is mediated in the nucleus.

Overexpression of anchored AIF in wild-type cells only transiently delayed cell death after apoptosis induction

Since AIF has dual functions in apoptosis and cell survival, we next asked which of the following is the cause of cell death after apoptosis induction: (a) the loss of AIF from the mitochondria, (b) the proapoptotic action of AIF in the nucleus, or (c) both as equally important. We answer this question first by looking at apoptosis of wild-type neurons expressing anchored AIF constructs. The release and loss of AIF in the mitochondria of wild-type cells during apoptosis, therefore, will be reconstituted by the anchored AIF. At the same time the endogenous wild-type pool of AIF will still translocate to the nucleus. If the loss of AIF from mitochondria is indeed sufficient to induce apoptosis, then replenishing anchored AIF in the mitochondria should rescue cell death in these wild-type cells. At 12 and 24 h after camp-

tothecin treatment, wild-type cells expressing the anchored AIF constructs exhibited less cell death than control cells (Figure 7A). This suggests that at early time points after the induction of apoptosis, loss of AIF from the mitochondria contributes to cell death. At 36 h, however, wild-type cells with anchored AIF constructs exhibited similar rates of apoptosis as cells expressing GFP (Figure 7A). This suggests that at later time points, the apoptotic function of endogenous AIF in the wild-type cells is the major contributor to cell death. At 12 and 24 h, the presence of anchored AIF in the wild-type cells can also retain cytochrome *c* in the mitochondria as revealed by immunocytochemistry and subcellular fractionation followed by Western blot analysis (Figure 7C and D). The mitochondrial membrane potential (Figure 7B), ATP production (Figure 7E) and oxygen consumption (Figure 7F) were also maintained transiently. These suggest that during apoptosis, the presence of AIF in the wild-type mitochondria is able to transiently reduce the release of cytochrome *c* and maintain membrane potential. Caspase activation was also transiently delayed in wildtype cells expressing anchored AIF mutants (Supplementary Figure 6C), possibly due to the transient retention of cytochrome *c* in the mitochondria (Figure 7C and D). To further establish the apoptotic function of endogenous AIF, we expressed anchored AIF mutants in control, *Apaf1* $^{-/-}$, tel. *Aif* Δ , tel.

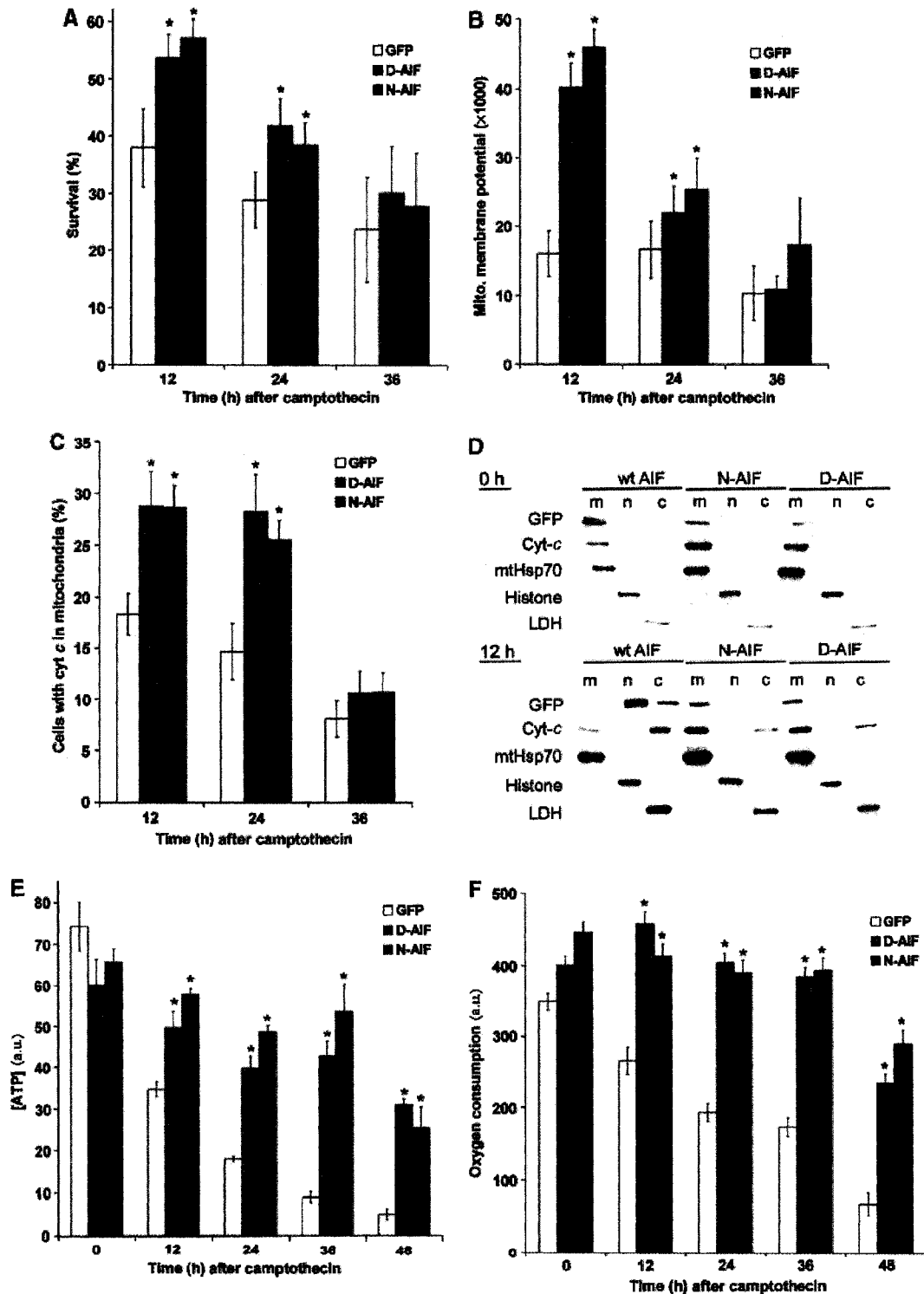


Figure 7 Anchored AIF can transiently protect wild-type neurons against DNA damage induced apoptosis. Cortical neurons from E14.5 wild-type mice were infected at time of plating with the anchored D-AIF and N-AIF constructs and a GFP only control at 50 MOI. Camptothecin were then added. (A) Survival of the cells was measured by nuclear morphology revealed using Hoechst staining ($n=5$), $*P<0.05$. (B) Mitochondrial membrane potential was measured by TMRE intensity ($n=5$), $*P<0.05$. (C) Percentages of cells with cytochrome *c* retained in the mitochondria ($n=5$). Cytochrome *c* retention in mitochondria was determined using anti cyt-*c* immunohistochemistry. $*P<0.05$. (D) Western analysis on subcellular fractionation of neurons infected with N-AIF, D-AIF, and GFP control, to show cytochrome *c* release. Upper panel: no camptothecin, lower panel: 12 h after camptothecin treatment. m = mitochondrial fraction, n = nuclear fraction, and c = cytoplasmic fraction. (E) ATP concentration of the neurons expressing either N-AIF, D-AIF, or GFP as control. $*P<0.05$ compared GFP control. (F) Oxygen consumption of neurons expressing either N-AIF, D-AIF, or GFP as control. $*P<0.05$ compared to GFP control.

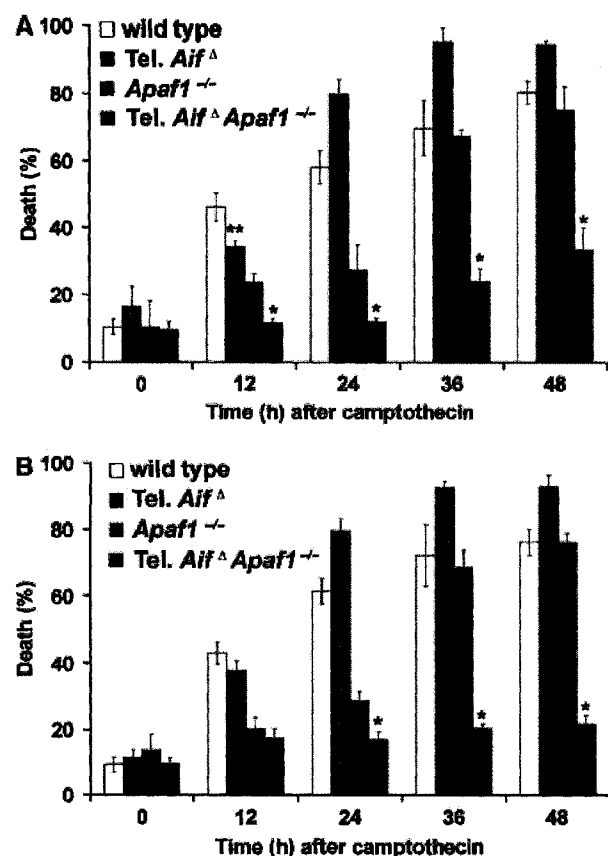


Figure 8 Endogenous AIF can still execute cell death in the presence of anchored AIF mutants in the mitochondria. Cortical neurons cultured (in conventional media) from E14.5 wild type, tel. *Aif* Δ , *Apaf1* $^{-/-}$ and tel. *Aif* Δ *Apaf1* $^{-/-}$ double mutant embryos were infected at the time of plating with the anchored D-AIF and N-AIF constructs. These cells were then treated with camptothecin and cell death was assessed at the indicated time points. (A) N-AIF ($n=3$) and (B) D-AIF ($n=3$). * $P<0.05$; ** $P<0.05$ compared to wildtype at 12 h.

Aif Δ *Apaf1* $^{-/-}$ neurons and induced apoptosis by the addition of camptothecin. Expression of anchored AIF mutants, N-AIF and D-AIF, can provide protection in tel. *Aif* Δ *Apaf1* $^{-/-}$ double null neurons since endogenous AIF is absent. In contrast, *Apaf1* $^{-/-}$ neurons exhibited significant apoptosis (Figure 8A and B), suggesting that the endogenous AIF existing in *Apaf1* $^{-/-}$ single knockout plays a prominent role in the execution of cell death. Together, these studies demonstrate that during cell death, the release and loss of AIF from mitochondria may contribute to the early phase of apoptosis; however, the pro-apoptotic function of AIF in the nucleus is a major contributor to apoptosis signaling. This is demonstrated by wild type and *Apaf1* $^{-/-}$ cells that still succumb to death even in the presence of anchored AIF in the mitochondria (Figures 7A, 8A and B).

Discussion

The anchored AIF constructs that are retained in the mitochondria during cell death provide us the means to dissociate the dual roles of AIF in cell life and death. The results of this study support a number of conclusions. First, we show that

AIF is required for neuronal survival because *Aif* Δ neurons exhibit fragmented mitochondria and abnormal cristae structure and undergo apoptosis during development. Second, anchored AIF expressed in tel. *Aif* Δ *Apaf1* $^{-/-}$ mice can protect against DNA damage-induced cell death over than seen in control tel. *Aif* Δ *Apaf1* $^{-/-}$ neurons. Third, expression of anchored AIF in wild-type cells, however, can only provide transient protection, indicating that loss of AIF from the mitochondria is not a major event in apoptosis signaling. The finding that these cells eventually die indicates that the proapoptotic function of AIF in the nucleus is necessary to execute cell death. The fact that AIF mutants with NES failed to induce cell death in tel. *Aif* Δ *Apaf1* $^{-/-}$ cells supports this conclusion. These studies demonstrate that loss of AIF from the mitochondria is not a key apoptotic stimulus, but rather, that AIF plays an important proapoptotic function following nuclear translocation, which is sufficient to induce neuronal cell death.

Previous studies have shown that apart from its apoptotic role, AIF also has an important physiological role in mitochondria. Studies in *Hq* mice, which have only 20% AIF expression, indicate that AIF may act as a reactive oxygen species (ROS) scavenger (Klein *et al*, 2002). Cells with depleted AIF have reduced electron transport chain complex I expression in the mitochondria and as a result oxidative phosphorylation is compromised (Vahsen *et al*, 2004). The interaction of AIF with complex I, however, has not been found, and its redox partner remains unknown. As such, the exact role of AIF in mitochondria remains elusive and controversial.

In this report, we have identified a novel role of AIF in maintaining mitochondrial structure. Mitochondria in AIF deficient neurons are fragmented and often clustered around the nucleus, and have abnormally dilated cristae. These defects are not due to a secondary effect from reduced survival because they were cultured in enriched media to ensure survival. The abnormal cristae morphology may explain the reduced survival and the respiratory defect in *Aif* $^{-/-}$ cells (Vahsen *et al*, 2004), since mitochondrial cristae structure is important in regulating the respiratory processes (Frey and Mannella, 2000; Mannella, 2006). As AIF may be responsible for maintaining mitochondrial cristae, the loss of proper cristae formation due to AIF deficiency may subsequently induce mitochondrial fragmentation and bioenergetic failure. Following injury, expression of mitochondrially anchored AIF may provide enhanced protection by maintaining mitochondrial integrity. This is supported by our electron microscopic (EM) studies, which reveal a tighter intra cristae cross-sectional distance (Figure 4) that may account for the delay in cytochrome *c* release in cells expressing anchored AIF mutants (Figure 7C and D). This interpretation is consistent with previous studies, which have demonstrated that cristae hold the greatest proportion of cytochrome *c* (Bernardi and Azzone, 1981) and cristae remodeling is required for its release (Scorrano *et al*, 2002; Germain *et al*, 2005).

The importance of AIF's physiological role is further shown in the telencephalon conditional AIF mutant, which displayed abnormal cortical development and premature death by E17. The absence of AIF during neuronal development results in mitochondrial dysfunction, which in turn may trigger multiple apoptotic pathways that may involve the activation of caspases (Narasimhaiah *et al*, 2005), as the

AIF deficient telencephalon showed a higher number of activated caspase 3 *in vivo* during development (Figure 1D), and lack of AIF triggers mitochondrial dysfunction *in vitro* (Figure 2). The enhanced cell death is mainly seen in maturing neurons but not in progenitor cells, suggesting that there is a difference in the sensitivity to the loss of AIF. Previous studies have shown that progenitors have a lower level of ROS compared to mature neurons in the cortex (Tsatmali *et al*, 2005), as well, progenitors have a higher level of telomerase than matured neurons (Mattson and Klapper, 2001), which may provide further protection against cellular stress. It has also been shown that mature neurons may recruit different apoptotic pathways compared to progenitors (D'Sa-Eipper *et al*, 2001). For example, neurons become more sensitive to excitotoxicity as they mature while progenitors are relatively resistant (Fannjiang *et al*, 2003).

That AIF deficient mitochondria exhibit hyperpolarization in the presence of a defect in oxidative phosphorylation is somewhat unexpected; however, hyperpolarization has been previously observed in situations where electron transport is defective (reviewed in Di Lisa and Bernardi, 1998; Skulachev, 2006). For example, after inhibition of the electron transport chain by NO (inhibitor of complex IV), cells respond by a defence mechanism that results in the reversal of ATP synthase to increase mitochondrial membrane potential to protect cells from death (Beltrán *et al*, 2000, 2002). Moreover, in a number of different cell types, including neural cells, where ATP production via oxidative phosphorylation is defective, mitochondrial membrane potential is generated by the reversal of ATP synthase using ATP produced by glycolysis (Rego *et al*, 2001; Peachman *et al*, 2001). Thus, it is possible that AIF mutant mitochondria, which do not generate ATP by oxidative phosphorylation, are using a similar mechanism to generate membrane potential. Future studies, however, are required to fully resolve this issue.

Since AIF has an important physiological role in mitochondria, one may argue that the loss of AIF from the mitochondria is the cause of cell death and the proapoptotic function of AIF in the nucleus is of minor consequence. To clarify this controversy, we constructed AIF anchored mutants, which cannot be released from the mitochondria, to dissociate the apoptotic role and physiological role of AIF. Overexpressing AIF anchored mutants in wild type and *Apaf1*^{-/-} cells could transiently protect against cell death; however, on longer time courses these cells still died. This indicates that although loss of AIF during the initial phase of cell death can partially contribute to the cell's demise, it is the proapoptotic function of the endogenous wild-type AIF in nucleus that ultimately kills the cell. The proapoptotic role of AIF in nucleus is further supported by the use of an AIF mutant construct (AIF-NES) that fails to translocate into the nucleus during cell death. Tel. *Aif*^Δ *Apaf1*^{-/-} cells expressing these AIF mutants had the same death rate than the cells with control construct under apoptotic induction, indicating that the nuclear translocation ability of AIF is required for its apoptotic function. Importantly, expression of anchored AIF in tel. *Aif*^Δ *Apaf1*^{-/-} cells exhibits even greater survival after apoptosis induction than tel. *Aif*^Δ *Apaf1*^{-/-} cells. This indicates apoptosis can be halted in two ways: (1) most importantly by preventing its proapoptotic action in the nucleus, and (2) to a lesser extent by maintaining the physiological role of AIF in mitochondria.

In conclusion, this study demonstrates that AIF has a novel function in maintaining the cristae structure of mitochondria in neurons. Neurons with depleted AIF have reduced viability and defective mitochondrial cristae structure. During the initial state of apoptosis, the release of AIF from the mitochondria can partly contribute to cell death; however, it is the proapoptotic role of AIF in the nucleus that seals the apoptotic fate of the cell. These studies clarify the proapoptotic function of AIF in signaling cell death in the nucleus, and indicate a novel role of AIF in maintenance of mitochondrial structure.

Materials and methods

Mice and primary neuronal cultures

The floxed AIF mice have been previously described (Joza *et al*, 2005). To generate telencephalon-specific AIF conditional mutants, floxed AIF homozygous female mice were bred with Foxg1-cre mice (Hebert and McConnell, 2000), to generate mutant Foxg1-cre:AIF^{flox/Y} or female Foxg1-cre:AIF^{flox/flox} (both indicated as tel. *Aif*^Δ) mice. *Apaf1*^{-/-} mice were obtained from Ceconi *et al* (1998). To detect the presence of cre-mediated recombination, PCR analysis of AIF exon 7 was performed on DNA extracted from the telencephalon of mutant and control embryos. Primers for 1303f (5'-GTAGATCAGGTTGGCCAGAACTC-3'), 1903r (5'-GGATTAAGGCATGTGCCA ACACG-3') and 659r (5'-GAATCTGGAATATGGCACAGAGG-3') yielded 700 and 600 bp products for the unrecombined floxed and wild-type alleles, respectively, and a 350 bp band for the recombined floxed allele. Western blot analysis was performed as described (Cregan *et al*, 1999), with antibodies against AIF (D-20, 1:500, Santa Cruz Biotechnology) and the 39 kDa subunit of complex I (A21344, 1:500, Molecular Probes). Mice were maintained on FVB/N and C57/BL6 mixed genetic backgrounds and littermates were used in all experiments. Cortical neurons were cultured as described previously (Fortin *et al*, 2001).

ATP production and oxygen consumption assays

At indicated time points, ATP levels were determined using a luciferase-based CellTiter-Glo assay kit (Promega) with a PolarStar plate reader (BMG). Data were collected from multiple replicate wells in each of the three experiments (*n*=3). For oxygen consumption measurements, cells were plated in the fluorescent dye-embedded 96-well microplate of the BD oxygen biosensor system (BD Biosciences). Results were read at indicated times with a fluorescent microplate reader. The data were normalized according to the manufacturer's protocol.

Subcellular fractionation

Subcellular fractionation of neurons was performed as described previously (Yu *et al*, 2002). Antibodies against histone (US Biological H5110-10, 1:500), mtHsp70 (Affinity BioReagents MA3-028, 1:500) and lactate dehydrogenase (Sigma L7016, 1:500) were used to detect nuclear, mitochondrial and cytoplasmic fractions, respectively. GFP and cytochrome c were detected using antibodies against GFP (Abcam Ab6556, 1:500) and cytochrome c (BD Pharmingen 556433, 1:500), respectively. The experiments were repeated at least three times with similar results.

Tissue fixation, cryoprotection and immunohistochemistry

Tissue fixation, cryoprotection and immunohistochemistry of cortical tissues using active caspase 3 (BD Pharmingen, 559565, 1:100) and PH3 (Upstate Biotechnology, 06-570, 1:500) antibodies were performed as described previously (Ferguson *et al*, 2002).

AIF constructs

Anchored AIF constructs (N-AIF, D-AIF) and AIF with a NES (AIF-NES) were generated by standard subcloning procedures. Briefly, for N-AIF, the MLS of the protein pOSA-14114, an inner membrane anchored protein (Steenart and Shore, 1997), was cloned in frame to mouse AIF as follows. The DFHR moiety was removed and two restriction sites (*Pst*I and *Kpn*I) and a stop codon were introduced. A second pOCT cleavage site was introduced into the encoded protein so that MPP will process the protein such that only the

amino acids SQVAR will remain N-terminal to the transmembrane domain after import into the mitochondrial inner membrane. For D-AIF, the MLS domain of D-lactate dehydrogenase (Rojo *et al*, 1998; Flick and Konieczny, 2002) was inserted at the N-terminus of Δ MLS AIF-GFP (Δ 1–120), with the proper in frame start codon. AIF-NES was constructed by adding the NES of HIV Rev (LPPLERLTL) (Fischer *et al*, 1995) to the N terminal of AIF-GFP. Constructs were confirmed by DNA sequencing. Recombinant adenoviral vectors carrying these constructs were then prepared and used as described (Cregan *et al*, 2002).

Digitonin permeabilization

Immunocytochemical analysis on digitonin permeabilized neurons was performed as described previously (Otera *et al*, 2005). Western analysis on digitonin permeabilized isolated mitochondria was performed as follows. Briefly, cells expressing GFP tagged wild-type AIF and GFP tagged N-AIF were collected and mitochondria were isolated in isolation buffer (220 mM mannitol, 68 mM sucrose, 80 mM KCl, 0.5 mM EGTA, 2 mM magnesium acetate, 1 \times protease inhibitor and 10 mM HEPES at pH7.4). The mitochondria were resuspended in succinate buffer (1 mM ATP, 5 mM sodium succinate, 0.08 mM ADP, 2 mM K₂HPO₄, pH 7.4). A gradient of digitonin (0–2 mg digitonin/mg mitochondrial protein) was then added with trypsin. One percent Triton X-100 plus trypsin was used as a positive control. After 30 min on ice, the reaction was stopped by adding soybean trypsin inhibitor for 10 min. The samples were then subjected to Western blot analysis.

Camptothecin treatment, cell viability assays and caspase activity assay

Camptothecin treatment (10 μ M), caspase activity assay, and AIF immunocytochemistry were performed as described previously (Cregan *et al*, 2002). Cell death was determined by the characteristic nuclear morphology of chromatin condensation revealed by Hoechst staining.

Mitochondrial membrane potential and length measurements

For live mitochondrial imaging and electrochemical potential determination, neurons were plated on poly-D-lysine coated glass coverslips. At 36 h after seeding, cells were incubated with 50 nM TMRE at 37°C for 20 min and the coverslips were mounted in live-cell chambers and visualized as described (Neuspiel *et al*, 2005). Total fluorescence arbitrary units were recorded for the whole field. The total fluorescence intensity was quantified as the sum of the values of each pixel within the field minus the average background

signal per pixel. The average intensity per cell was calculated by dividing the total fluorescence intensity by the number of cells in that field. Mitochondrial length was measured by tracing mitochondria using Northern Eclipse software.

Electron microscopy and intra cristae cross-sectional distance measurements

Electron microscopy was performed as described (Neuspiel *et al*, 2005). Briefly, after 2 days of culture, neurons were isolated, washed with PBS, fixed in 1.6% glutaraldehyde and embedded in SPURR resin (Mariva, Québec). Thin sections were cut with a Leica Ultracut E ultramicrotome and counterstained with lead citrate and uranyl acetate. Digital images were taken using a JEOL 1230 TEM at 60 kV adapted with a 2K \times 2K bottom mount CCD digital camera (Hamamatsu, Japan) and AMT software. Intra cristae cross sectional distance was measured using Northern Eclipse software.

Quantifications and statistical analysis

For cell death studies, a minimum of 500 cells per field was scored for each treatment at the indicated time points. For mitochondrial membrane potential measurements, a minimum of 100 cells for each treatment was scored. For mitochondrial length measurements, a minimum of 1000 mitochondria for each treatment was scored. For intracristal cross-sectional distance measurements, a minimum of 100 mitochondria for each treatment was measured. The data represent mean values \pm s.d. from three independent experiments ($n = 3$) unless otherwise noted. *P*-values were obtained using two-way ANOVA and Fisher's *post hoc* tests.

Supplementary data

Supplementary data are available at *The EMBO Journal* Online (<http://www.embojournal.org>).

Acknowledgements

We would like to thank Drs Valina Dawson and Seong Woon Yu for advice in subcellular fractionation, Dr Mary-Ellen Harper for discussion, and Carl McIntosh for assistance in the *in vivo* studies. This work was supported by grants from the Canadian Institutes of Health Research (CIHR) to RSS; Marie Curie Excellence Grant and the Austrian National Bank to JMP. The viral vector facility is supported by a grant from Canadian Stroke Network (RSS and DSP). ECC and KAM are supported by a CIHR studentship.

References

- Arnould D, Gaume B, Karbowski M, Sharpe JC, Cecconi F, Youle RJ (2003) Mitochondrial release of AIF and EndoG requires caspase activation downstream of Bax/Bak-mediated permeabilization. *EMBO J* **22**: 4385–4399
- Beltrán B, Mathur A, Duchon MR, Erusalimsky JD, Moncada S (2000) The effect of nitric oxide on cell respiration: a key to understanding its role in cell survival or death. *Proc Natl Acad Sci* **97**: 14602–14607
- Beltrán B, Quintero M, García-Zaragoza E, O'Connor E, Esplugues JV, Moncada S (2002) Inhibition of mitochondrial respiration by endogenous nitric oxide: a critical step in Fas signalling. *Proc Natl Acad Sci* **99**: 8892–8897
- Bernardi P, Azzone GF (1981) Cytochrome C as an electron shuttle between outer and inner mitochondrial membranes. *J Biol Chem* **256**: 7187–7192
- Cande C, Vahsen N, Kouranti I, Schmitt E, Daugas E, Spahr C, Luban J, Kroemer RT, Giordanetto F, Garrido C, Penninger JM, Kroemer G (2004) AIF and cyclophilin A cooperate in apoptosis-associated chromatinolysis. *Oncogene* **23**: 1514–1521
- Cao G, Clark RS, Pei W, Yin W, Zhang F, Sun FY, Graham SH, Chen J (2003) Translocation of apoptosis-inducing factor in vulnerable neurons after transient cerebral ischemia and in neuronal cultures after oxygen–glucose deprivation. *J Cereb Blood Flow Metab* **23**: 1137–1150
- Cecconi F, Alvarez-Bolado G, Meyer BI, Roth KA, Gruss P (1998) Apaf1 (CED-4 homolog) regulates programmed cell death in mammalian development. *Cell* **94**: 727–737
- Cheung EC, Melanson-Drapeau L, Cregan SP, Vanderluit JL, Ferguson KL, McIntosh WC, Park DS, Bennett SA, Slack RS (2005) Apoptosis-inducing factor is a key factor in neuronal cell death propagated by BAX-dependent and BAX-independent mechanisms. *J Neurosci* **25**: 1324–1334
- Colgan J, Asmal M, Luban J (2000) Isolation, characterization and targeted disruption of mouse ppia: cyclophilin A is not essential for mammalian cell viability. *Genomics* **68**: 167–178
- Cozzolino M, Ferraro E, Ferri A, Rigamonti D, Quondamatteo F, Ding H, Xu ZS, Ferrari F, Angelini DF, Rotilio G, Cattaneo E, Carri MT, Cecconi F (2004) Apoptosome inactivation rescues proneural and neural cells from neurodegeneration. *Cell Death Differ* **11**: 1179–1191
- Cregan SP, Dawson VL, Slack RS (2004) Role of AIF in caspase-dependent and caspase-independent cell death. *Oncogene* **23**: 2785–2796
- Cregan SP, Fortin A, MacLaurin JG, Callaghan SM, Cecconi F, Yu SW, Dawson TM, Dawson VL, Park DS, Kroemer G, Slack RS (2002) Apoptosis-inducing factor is involved in the regulation of caspase-independent neuronal cell death. *J Cell Biol* **158**: 507–517
- Cregan SP, MacLaurin JG, Craig CG, Robertson GS, Nicholson DW, Park DS, Slack RS (1999) Bax-dependent caspase-3 activation is a key determinant in p53-induced apoptosis in neurons. *J Neurosci* **19**: 7860–7869
- D'Sa-Eipper C, Leonard JR, Putcha G, Zheng TS, Flavell RA, Rakic P, Kuida K, Roth KA (2001) DNA damage-induced neural precursor cell apoptosis requires p53 and caspase 9 but neither Bax nor caspase 3. *Development* **128**: 137–146